Mathematical Concepts for DTI and High-Angular Resolution Diffusion Imaging

Christophe Lenglet
Siemens Corporate Research - Princeton, NJ

Mathematics in Brain Imaging
IPAM - UCLA
July 16, 2008

Outline of the Presentation

- Basics of diffusion MRI & local diffusion models
- Mathematical concepts for Tensors/ODFs processing
- Reconstruction of local diffusion models
- DTI tractography
- Combining DTI and fMRI: Cortico-striatal circuits
- DTI & HARDI segmentation
- HARDI mapping of white matter complexity

Organization of the White Matter

- Composed of axonal nerve fibers, protected by a myelin sheath
- Found in inner layer of cortex, optic nerves, central & lower areas of the brain and the spinal cord.
- Axons can be distributed diffusely or concentrated in bundles:
  - Projection tracts: connections cerebral cortex / subcortical areas
  - Association tracts: cortico-cortical connections in given hemisphere
  - Commissural tracts: connections of homologous areas

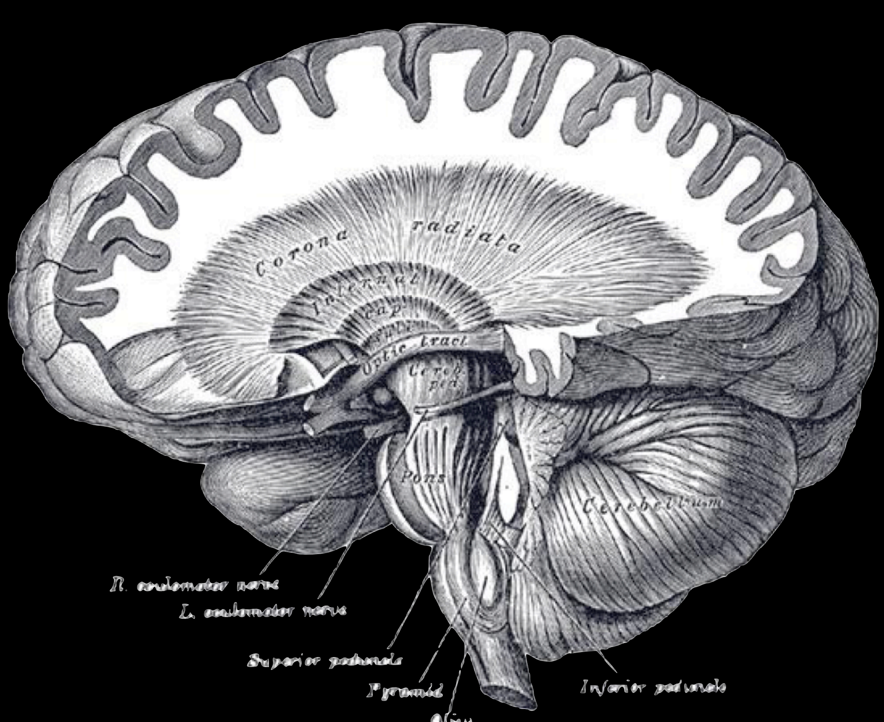

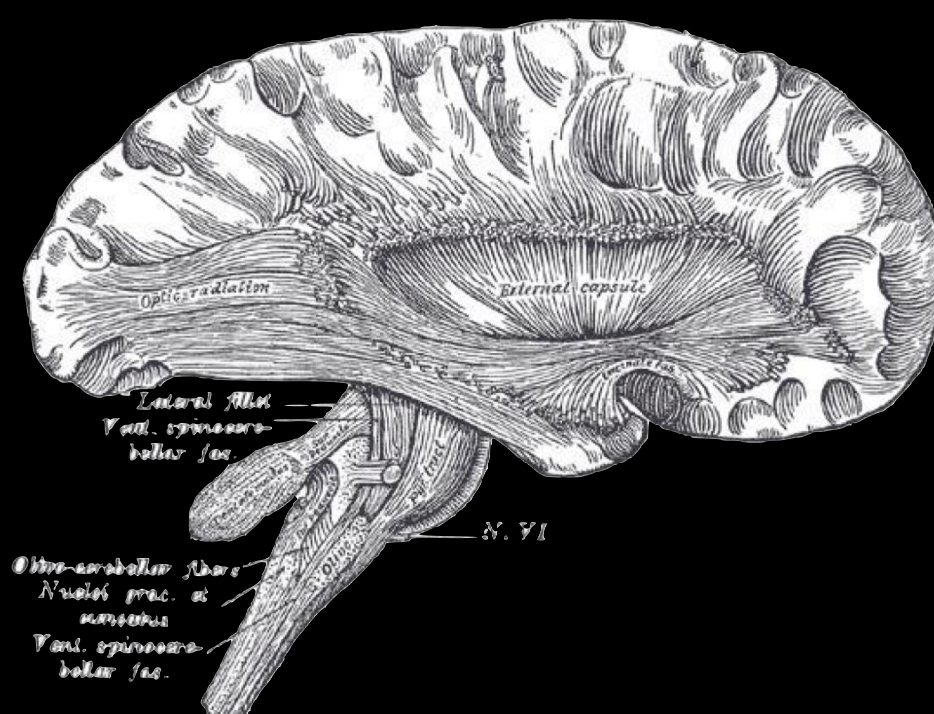

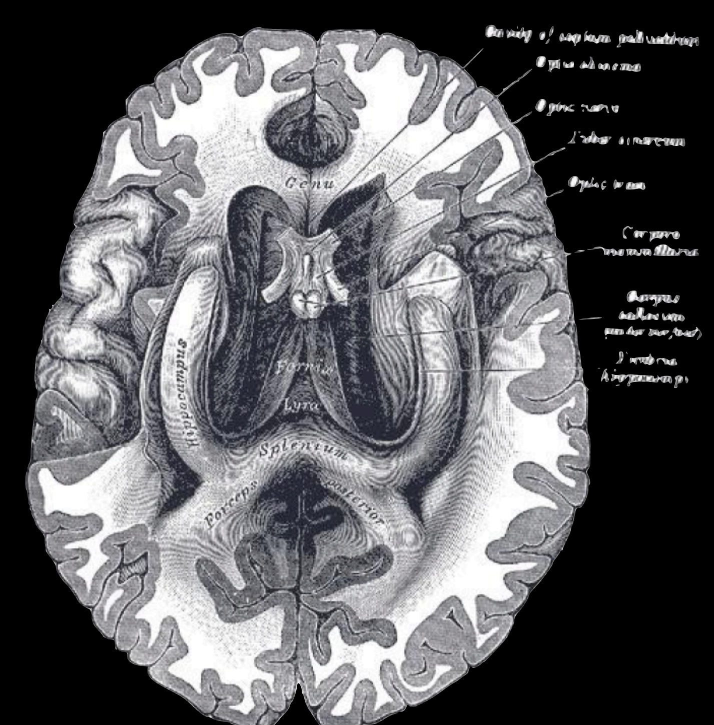

20th U.S. edition of Gray's Anatomy of the Human Body (public domain)

Association Tracts

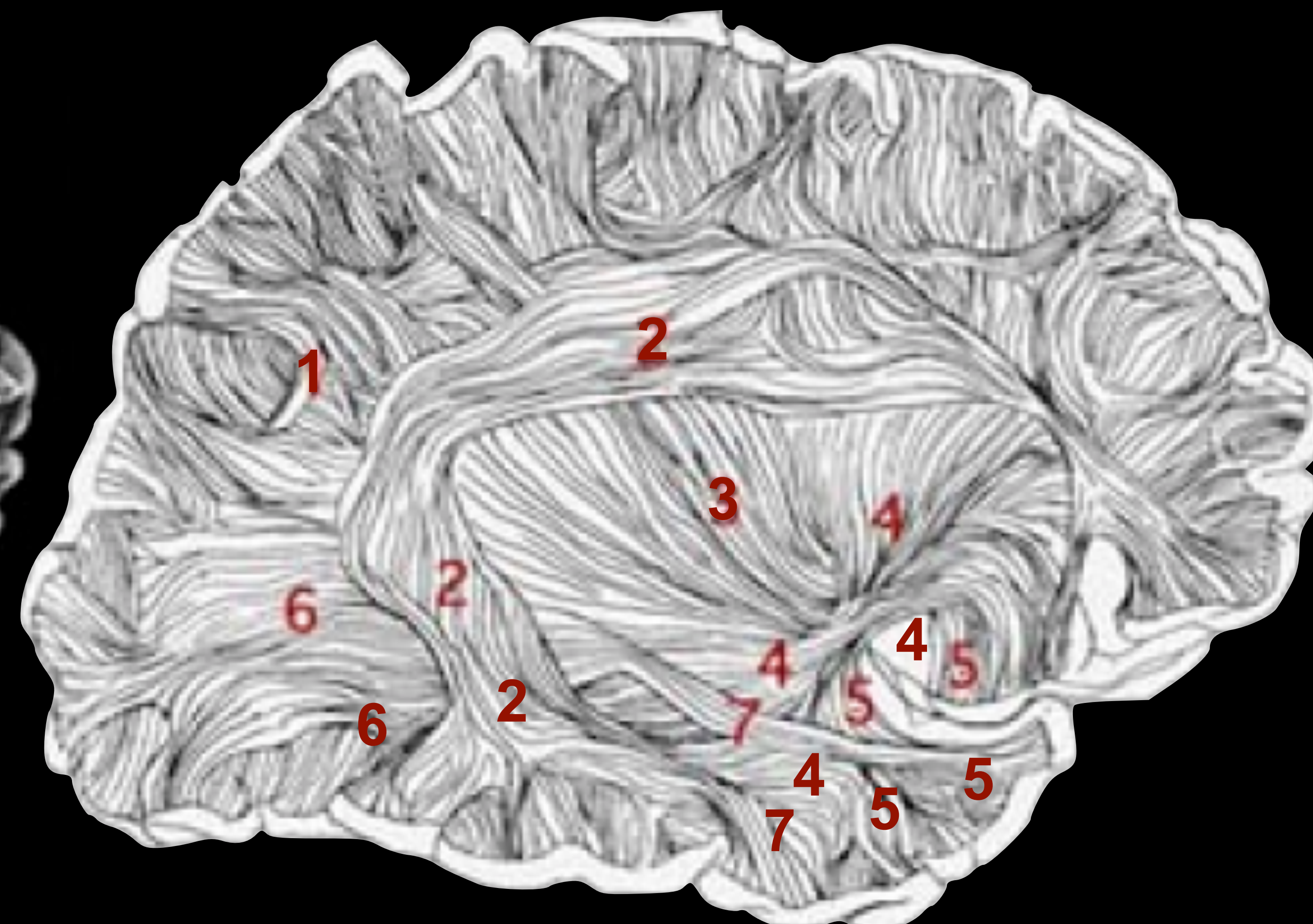

Images from [Williams-etal97]

1. *Short arcuate bundles,* ***2.*** *Superior longitudinal fasciculus,* ***3.*** *External capsule,* ***4.*** *Inferior occipitofrontal fasciculus,* ***5.*** *Uncinate fasciculus,* ***6.*** *Sagittal stratum,* ***7.*** *Inferior longitudinal fasciculus*

Association Tracts

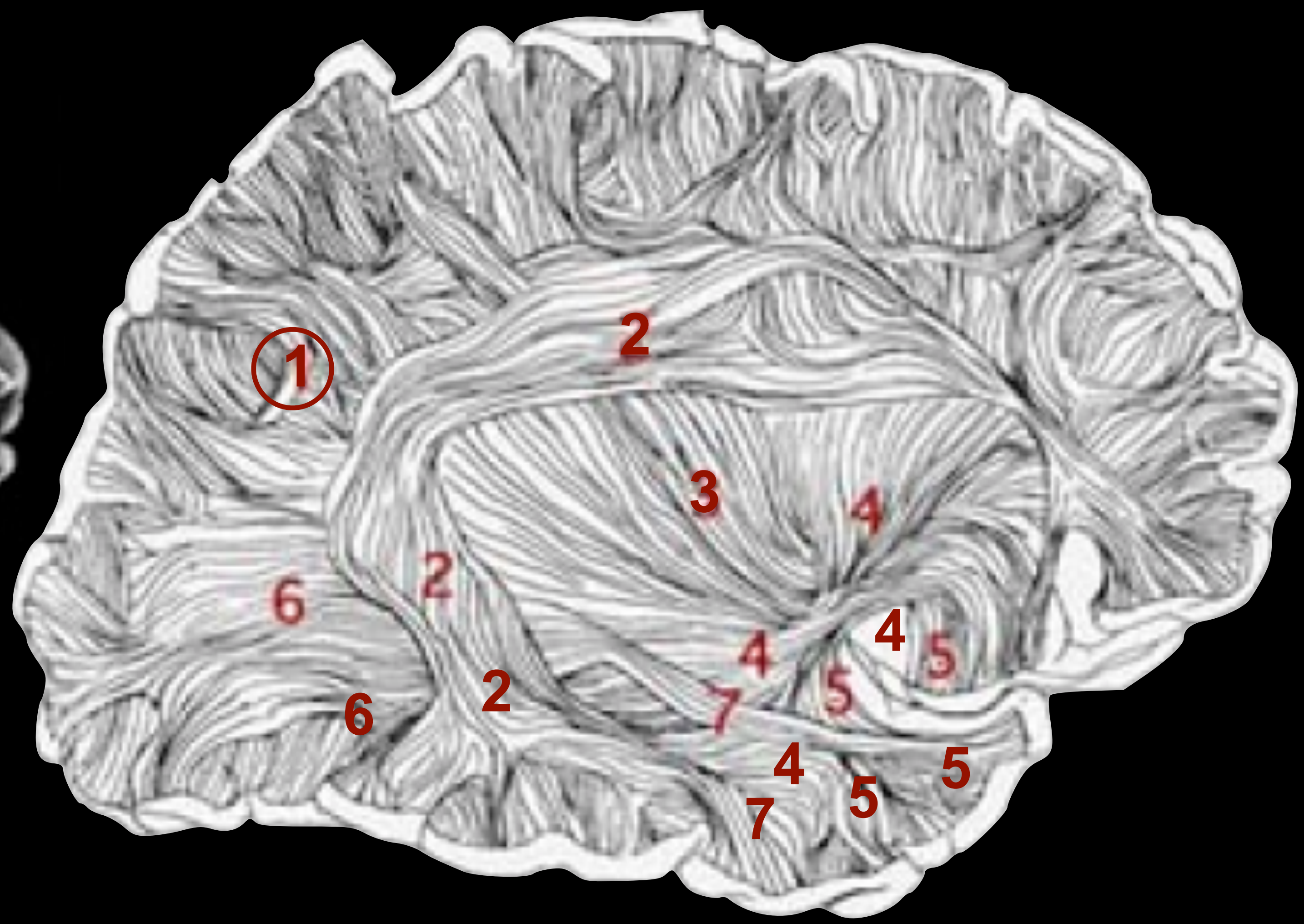

Images from [Williams-etal97]

1. Short arcuate bundles, 2. Superior longitudinal fasciculus, 3. External capsule, 4. Inferior occipitofrontal fasciculus, 5. Uncinate fasciculus, 6. Sagittal stratum, 7. Inferior longitudinal fasciculus

Association Tracts

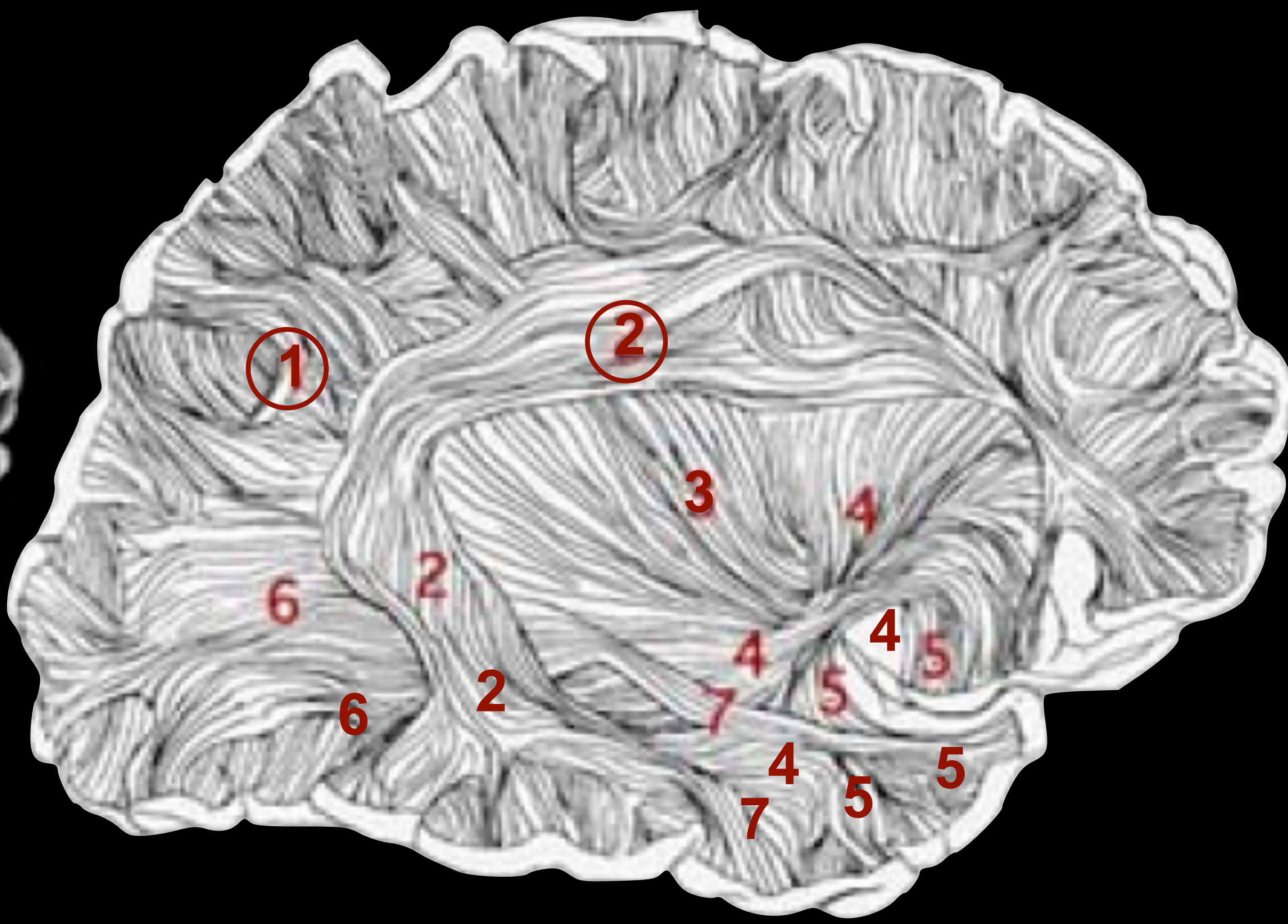

Images from [Williams-etal97]

1. *Short arcuate bundles,* **2.** *Superior longitudinal fasciculus,* **3.** *External capsule,* **4.** *Inferior occipitofrontal fasciculus,* **5.** *Uncinate fasciculus,* **6.** *Sagittal stratum,* **7.** *Inferior longitudinal fasciculus*

Association Tracts

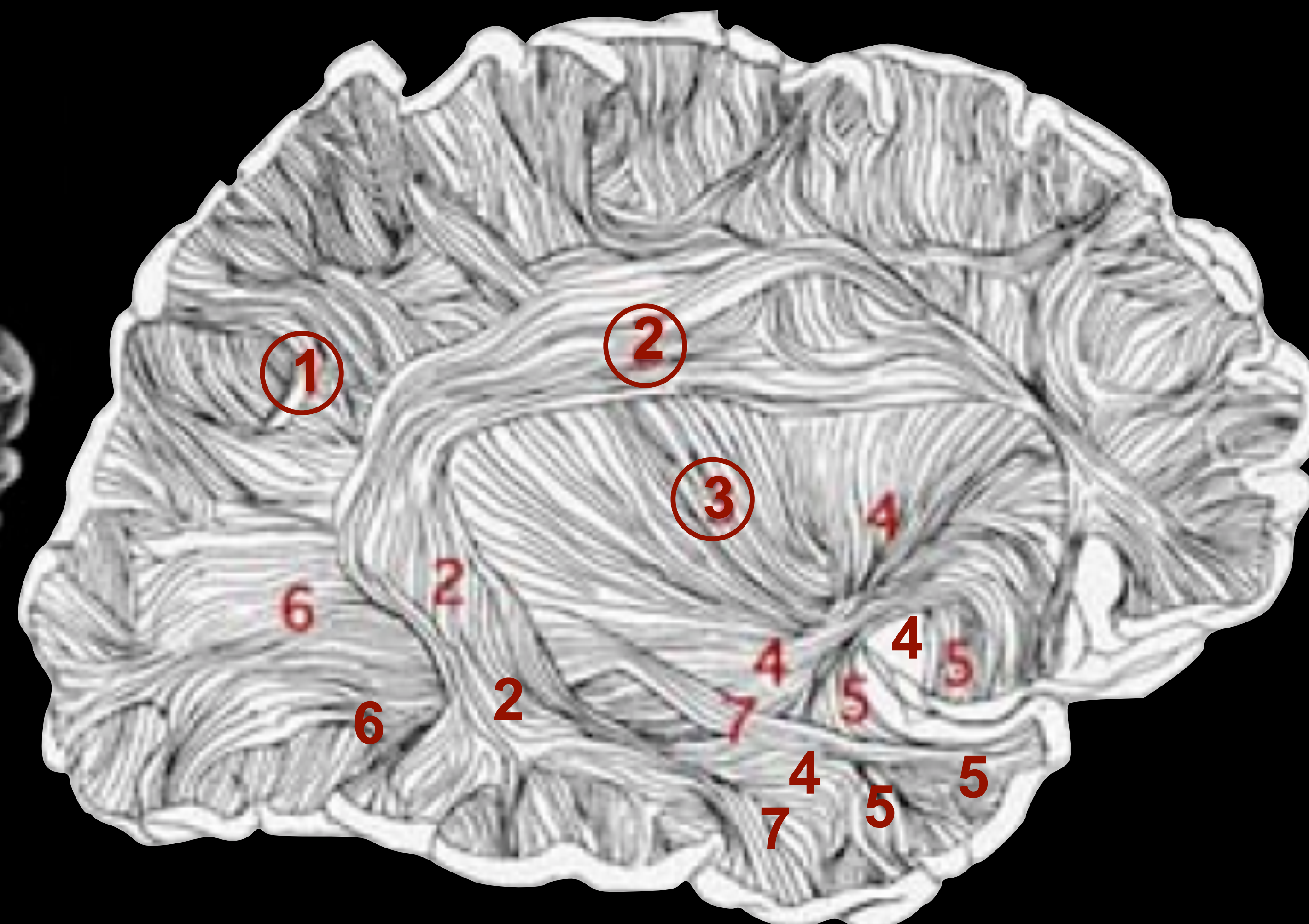

Images from [Williams-etal97]

1. *Short arcuate bundles,* 2. *Superior longitudinal fasciculus,* 3. *External capsule,* 4. *Inferior occipitofrontal fasciculus,* 5. *Uncinate fasciculus,* 6. *Sagittal stratum,* 7. *Inferior longitudinal fasciculus*

Basics of Diffusion MRI & Local Diffusion Models

Anisotropic Water Diffusion

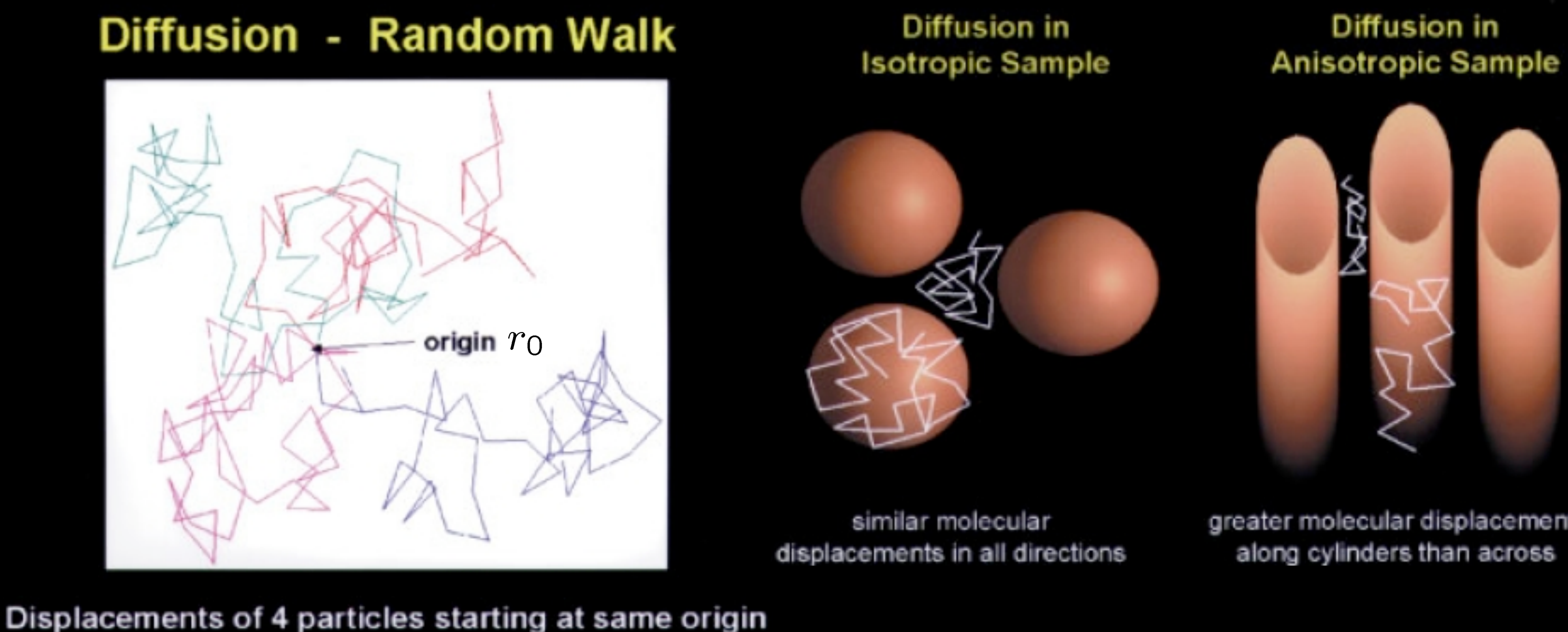

Images from [Beaulieu-etal02]

Anisotropic Water Diffusion

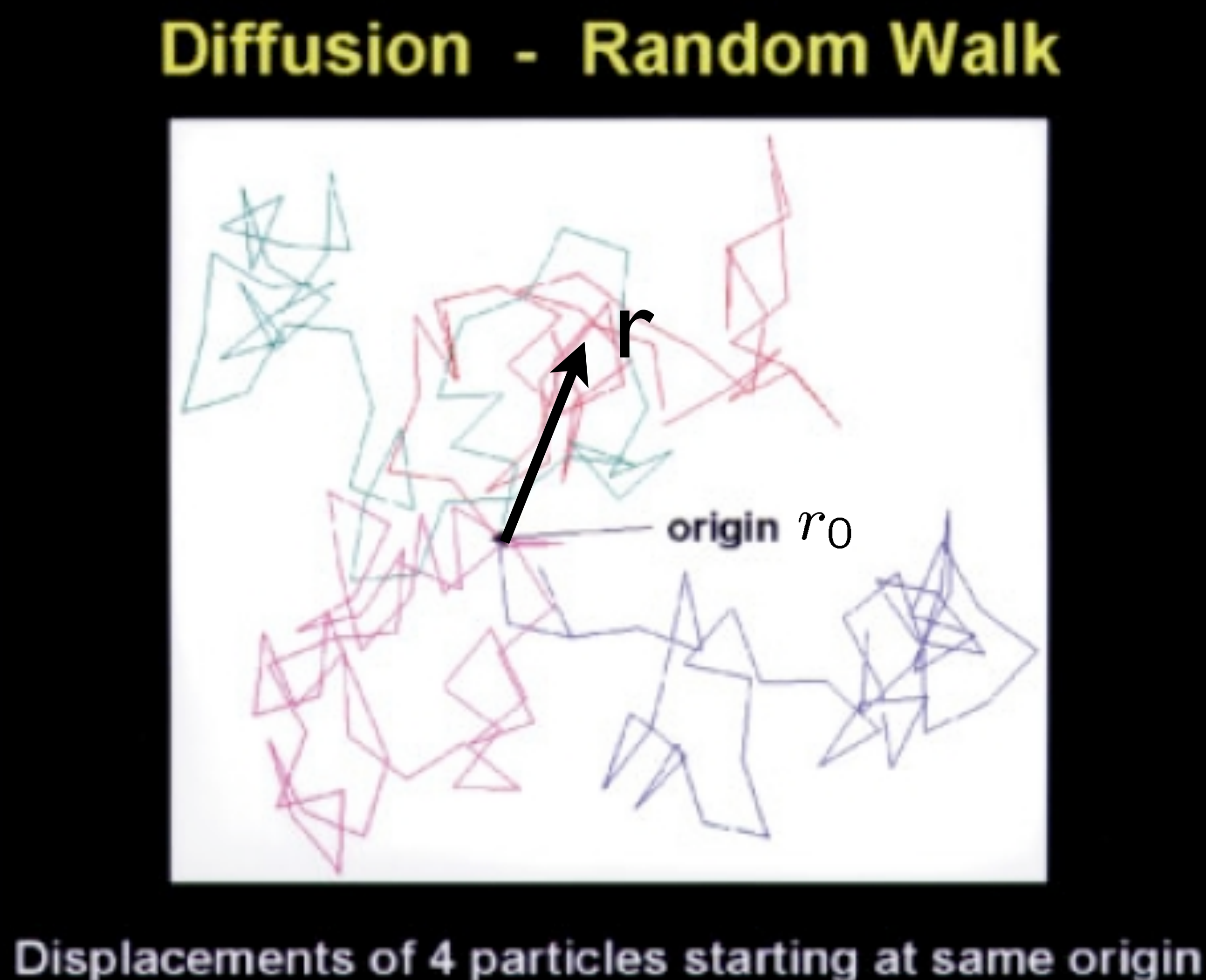

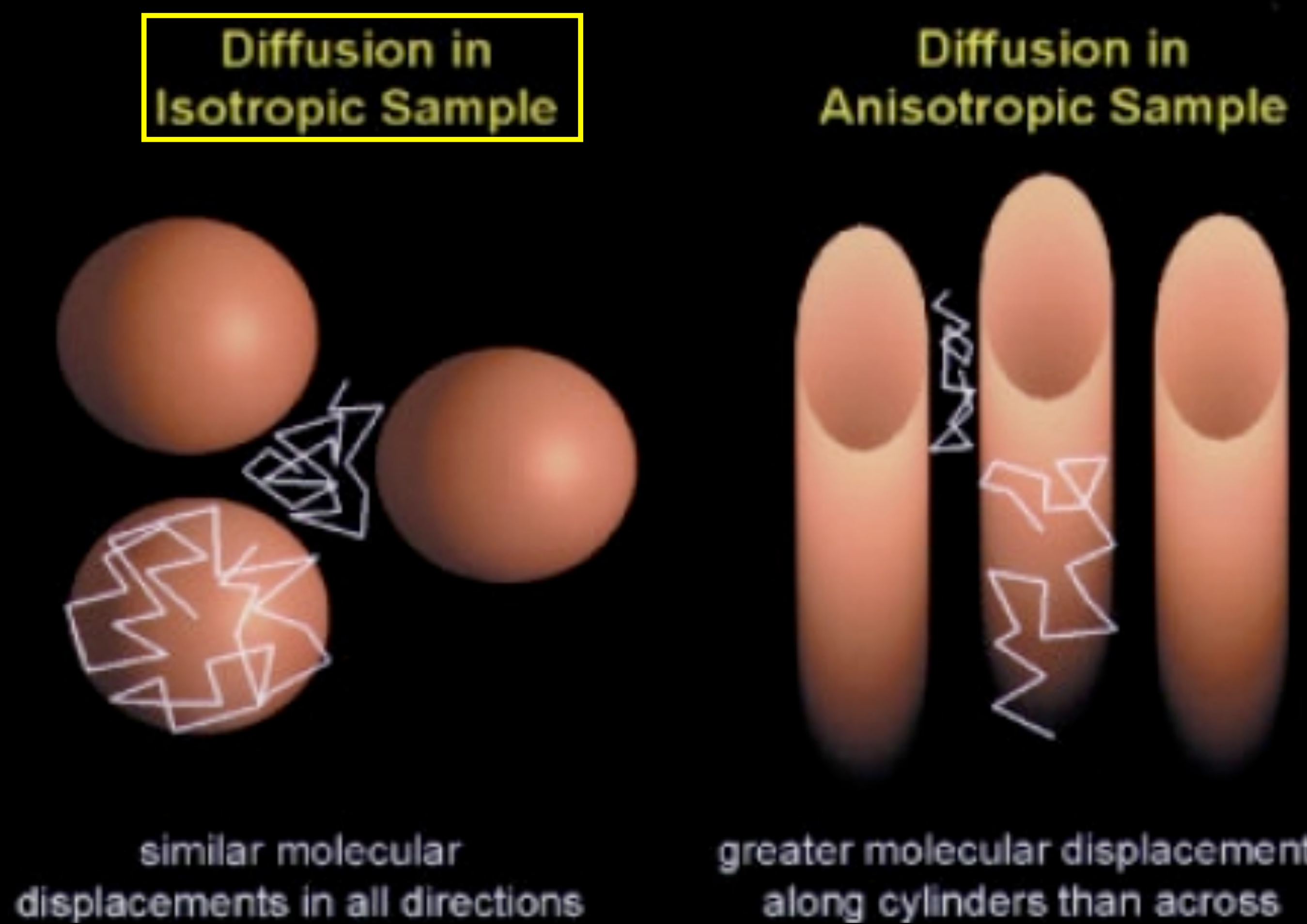

Images from [Beaulieu-etal02]

$$D = \frac{1}{6\tau}\langle r^T r \rangle$$

[Einstein-1905]

Anisotropic Water Diffusion

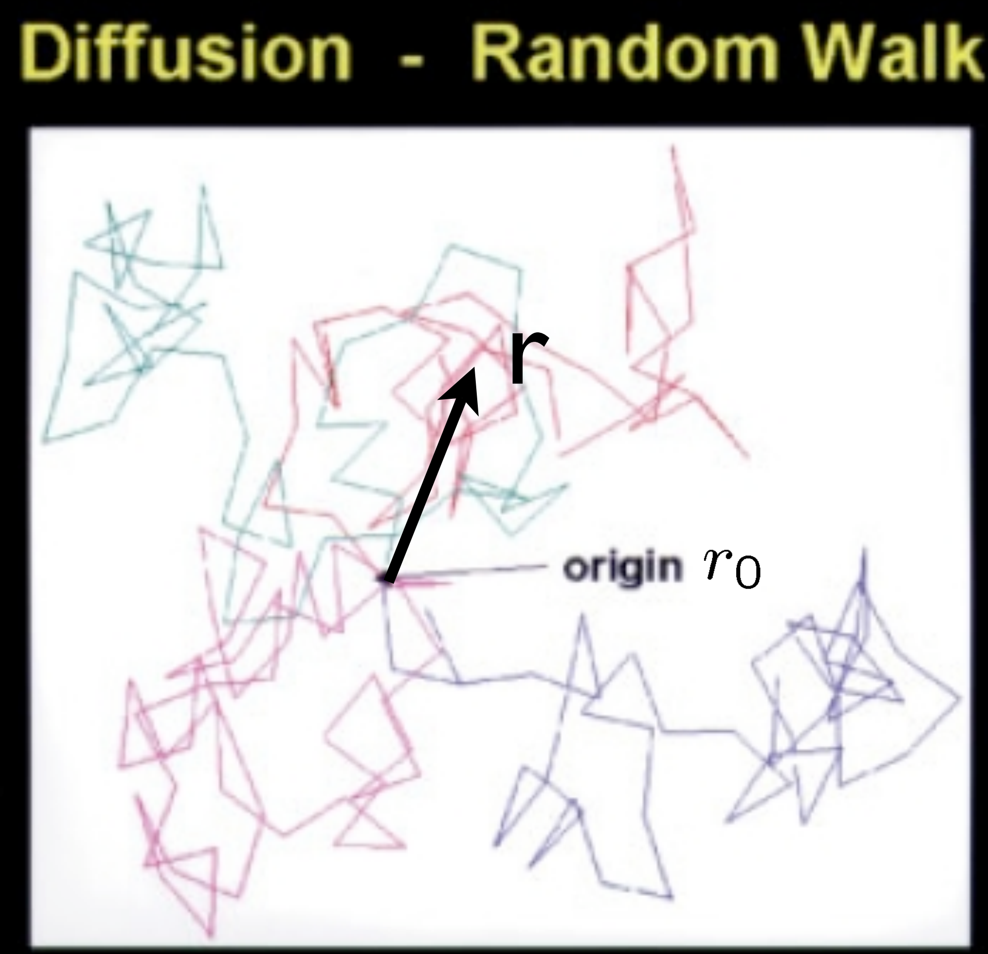

Displacements of 4 particles starting at same origin

Images from [Beaulieu-etal02]

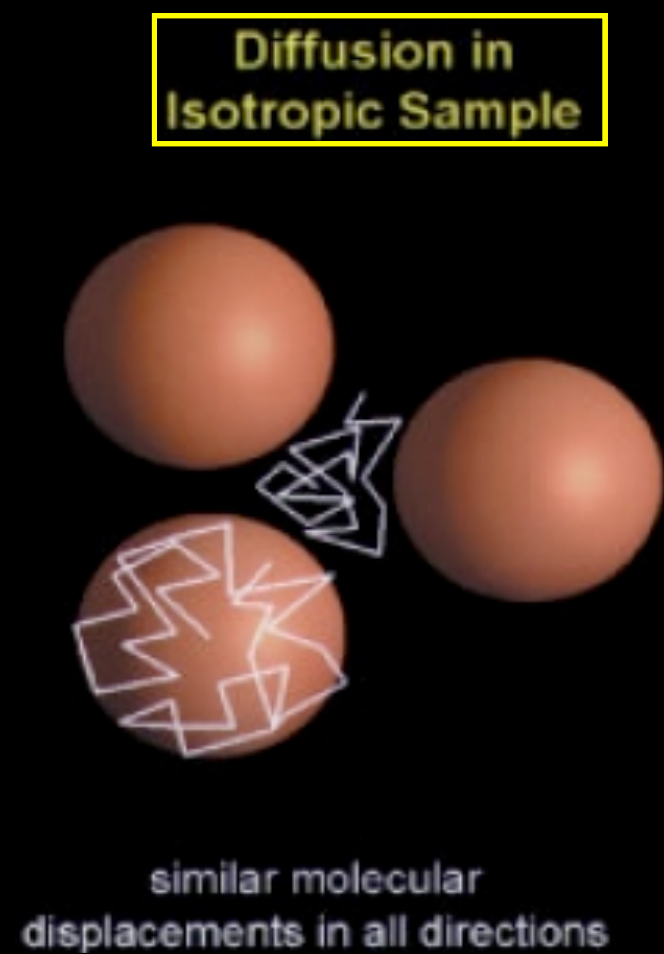

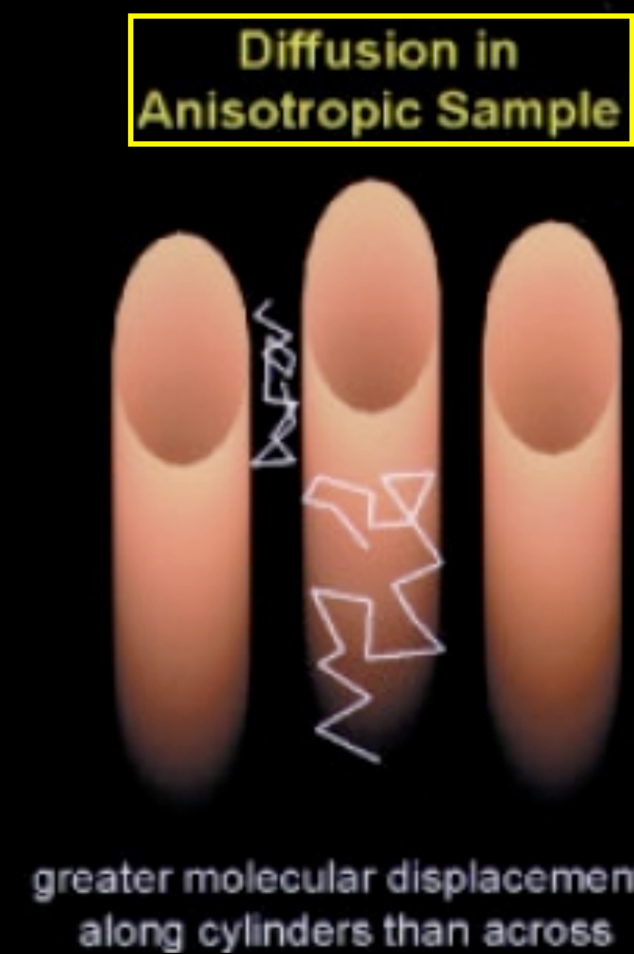

$$\mathbf{D} = \begin{pmatrix} D_{xx} & D_{xy} & D_{xz} \\ D_{xy} & D_{yy} & D_{yz} \\ D_{xz} & D_{yz} & D_{zz} \end{pmatrix} = \frac{1}{6\tau}\langle rr^T \rangle$$

[Einstein-1905]

Anisotropic Water Diffusion

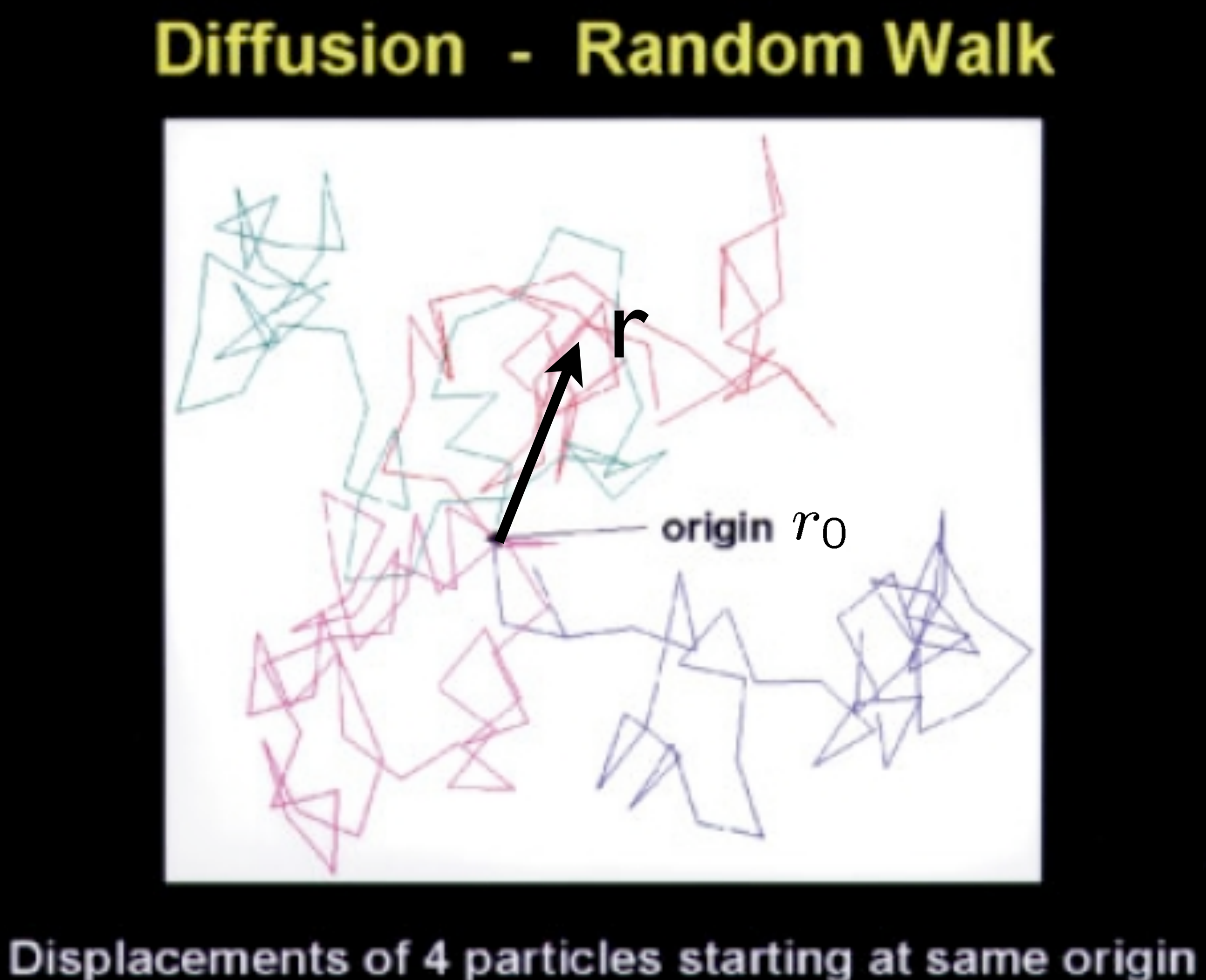

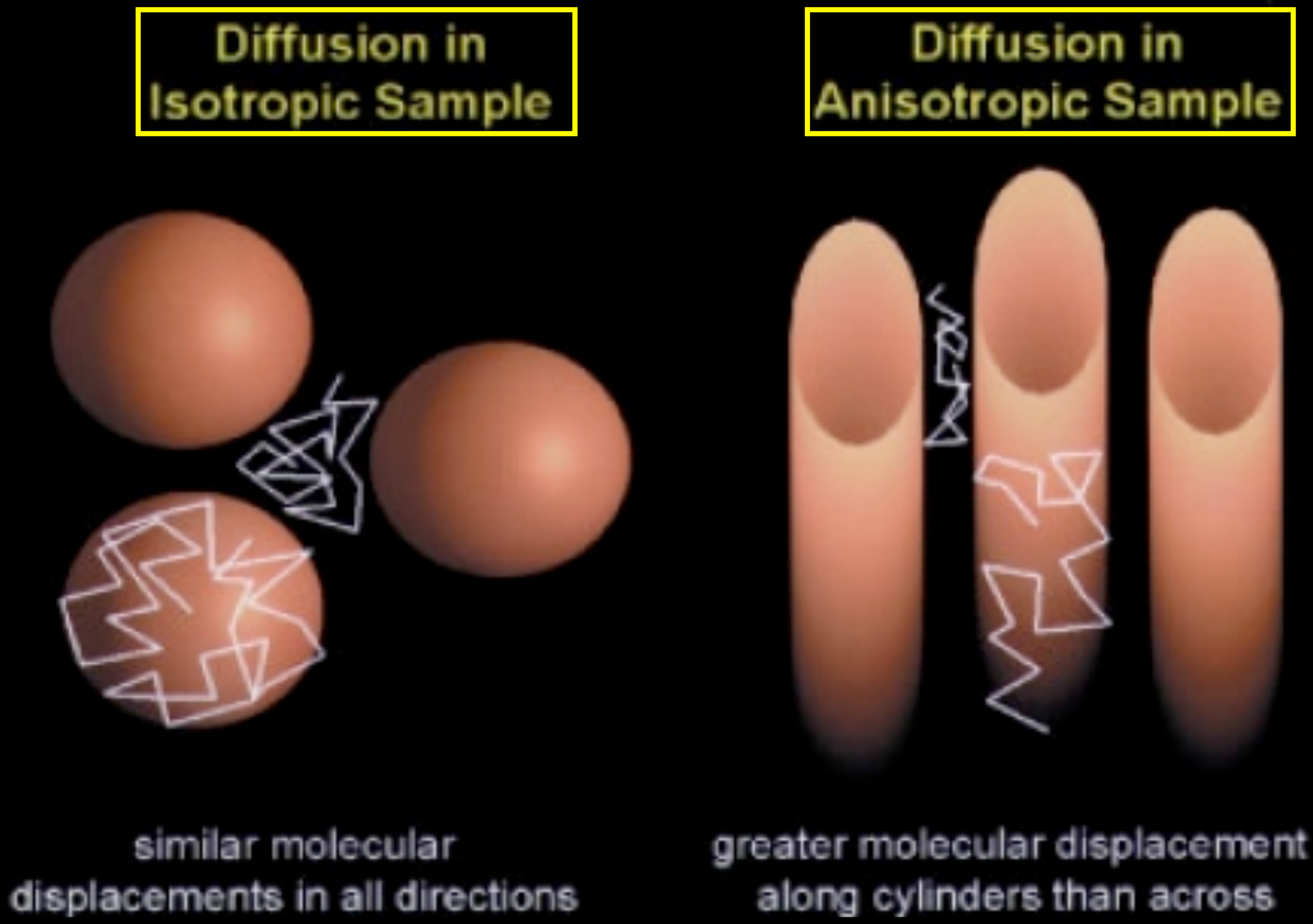

Images from [Beaulieu-etal02]

$$\mathbf{D} = \begin{pmatrix} D_{xx} & D_{xy} & D_{xz} \\ D_{xy} & D_{yy} & D_{yz} \\ D_{xz} & D_{yz} & D_{zz} \end{pmatrix} = \frac{1}{6\tau}\langle rr^T \rangle$$

[Einstein-1905]

Water diffusion is sensitive to the underlying tissue microstructure and provides a unique means to assess its orientation and integrity.

Anisotropic Water Diffusion in the Brain

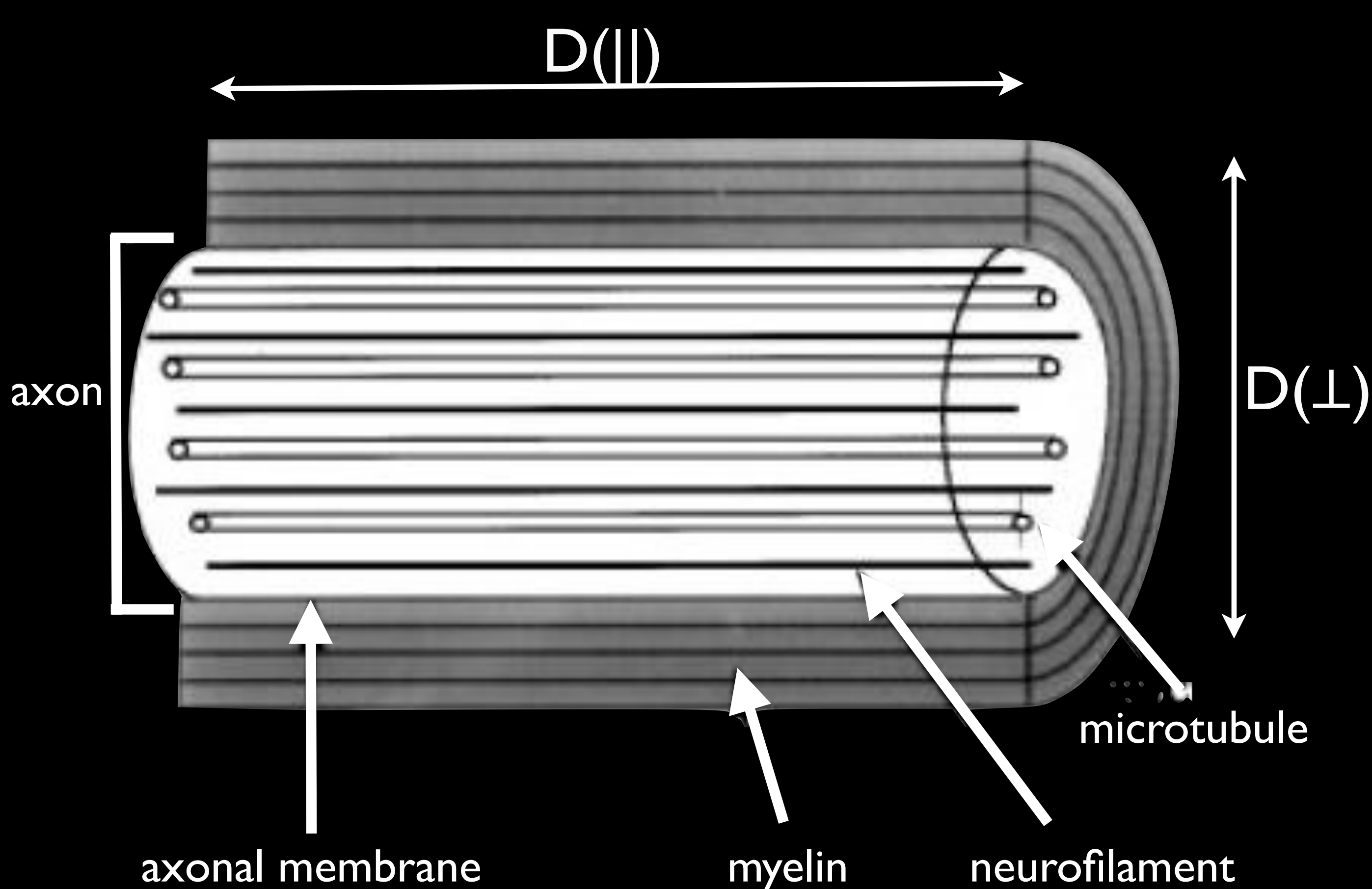

Adapted from [Beaulieu-etal02]

A simple schematic of the longitudinal view of a myelinated axon.

- First systematic study in [Moseley-etal1991]:

  $D(||) = 1.3 \times 10\text{-}5\ cm^2.s^{-1}$
  $D(\perp) = 0.4 \times 10\text{-}5\ cm^2.s^{-1}$

  Ratio of 2 to 4 for Δ=30ms

- Sources of anisotropy:
  - ✓ Axonal membrane
  - ✓ Myelination can modulate it
  - ✗ Neurofibrils do not affect it

- Anisotropy also found in kidney, skeletal muscles and myocardium.

MR Quantification of Water Diffusion

- Signal attenuation:

$$S(q_k, \tau) = S_0 \int_{\mathbb{R}^3} p(r|\tau) e^{2\pi i q_k^T r} dr$$
$$= \mathcal{F}[p(r|\tau)]$$

with $q_k = \gamma \delta g_k / 2\pi$ reciprocal displacement vector (*q*-space imaging)

and $g_k = q_k / \|q_k\|$

- Fourier transform of the Ensemble Average Propagator (EAP) $p(r|r_0, \tau)$

- DTI (Assumption of Gaussian diffusion)

$$p(r|\tau) = \frac{1}{\sqrt{(4\pi)^3 |\mathbf{D}|}} e^{\frac{r^T \mathbf{D}^{-1} r}{4\tau}}$$

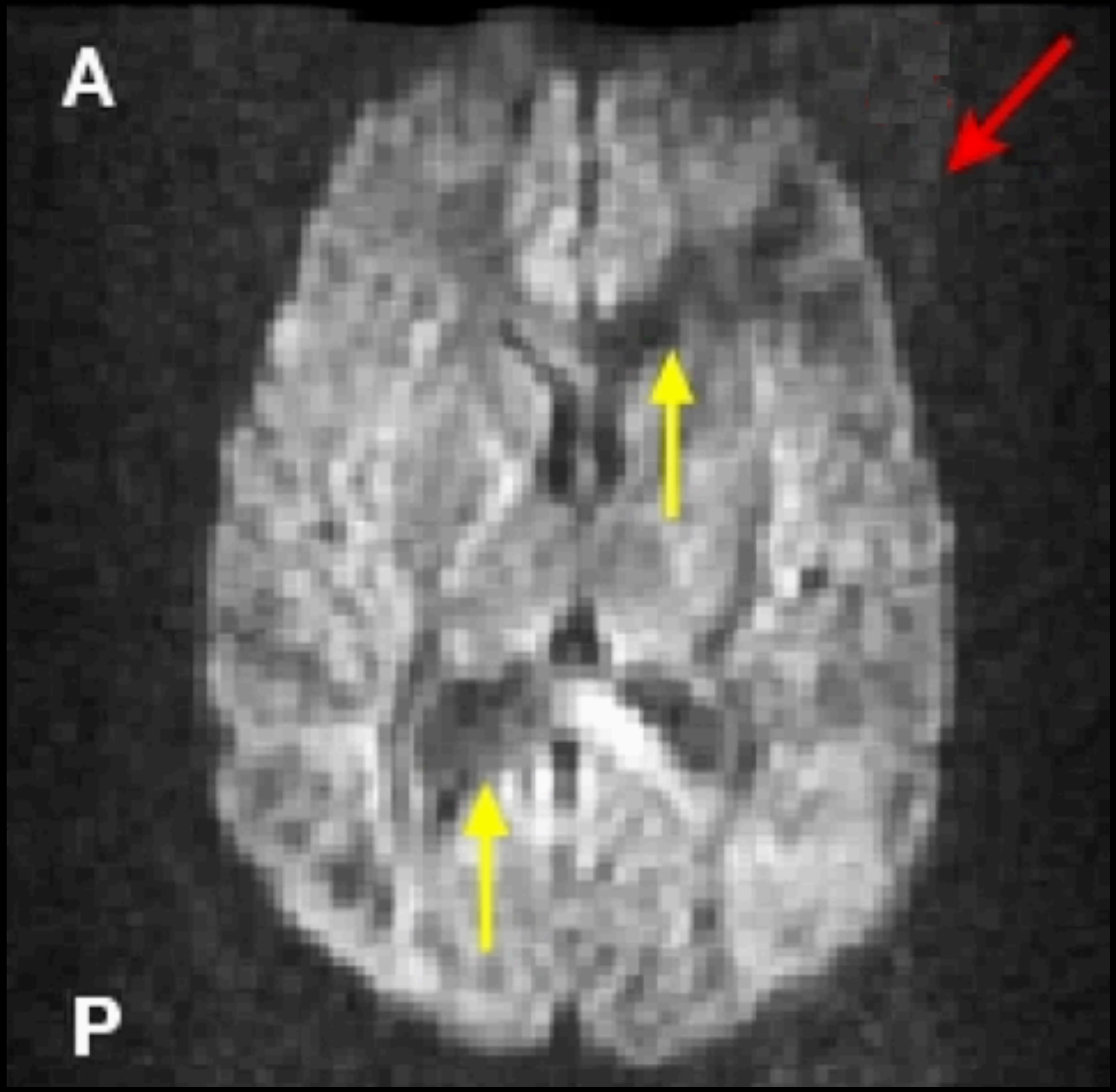

Examples of DWI for 2 gradients

Data: Centre IRMf, CHU La Timone, Marseille, FRANCE

[Stejskal-Tanner65], [Hashemi-Bradley04], [Karger-Heink83], [Tuch02]

MR Quantification of Water Diffusion

- Signal attenuation:

$$S(q_k,\tau) = S_0 \int_{\mathbb{R}^3} p(r|\tau) e^{2\pi i q_k^T r} dr$$
$$= \mathcal{F}[p(r|\tau)]$$

with $q_k = \gamma \delta g_k / 2\pi$ reciprocal displacement vector (*q*-space imaging)

and $g_k = q_k / ||q_k||$

- Fourier transform of the Ensemble Average Propagator (EAP) $p(r|r_0,\tau)$

- DTI (Assumption of Gaussian diffusion)

$$p(r|\tau) = \frac{1}{\sqrt{(4\pi)^3 |\mathbf{D}|}} e^{\frac{r^T \mathbf{D}^{-1} r}{4\tau}}$$

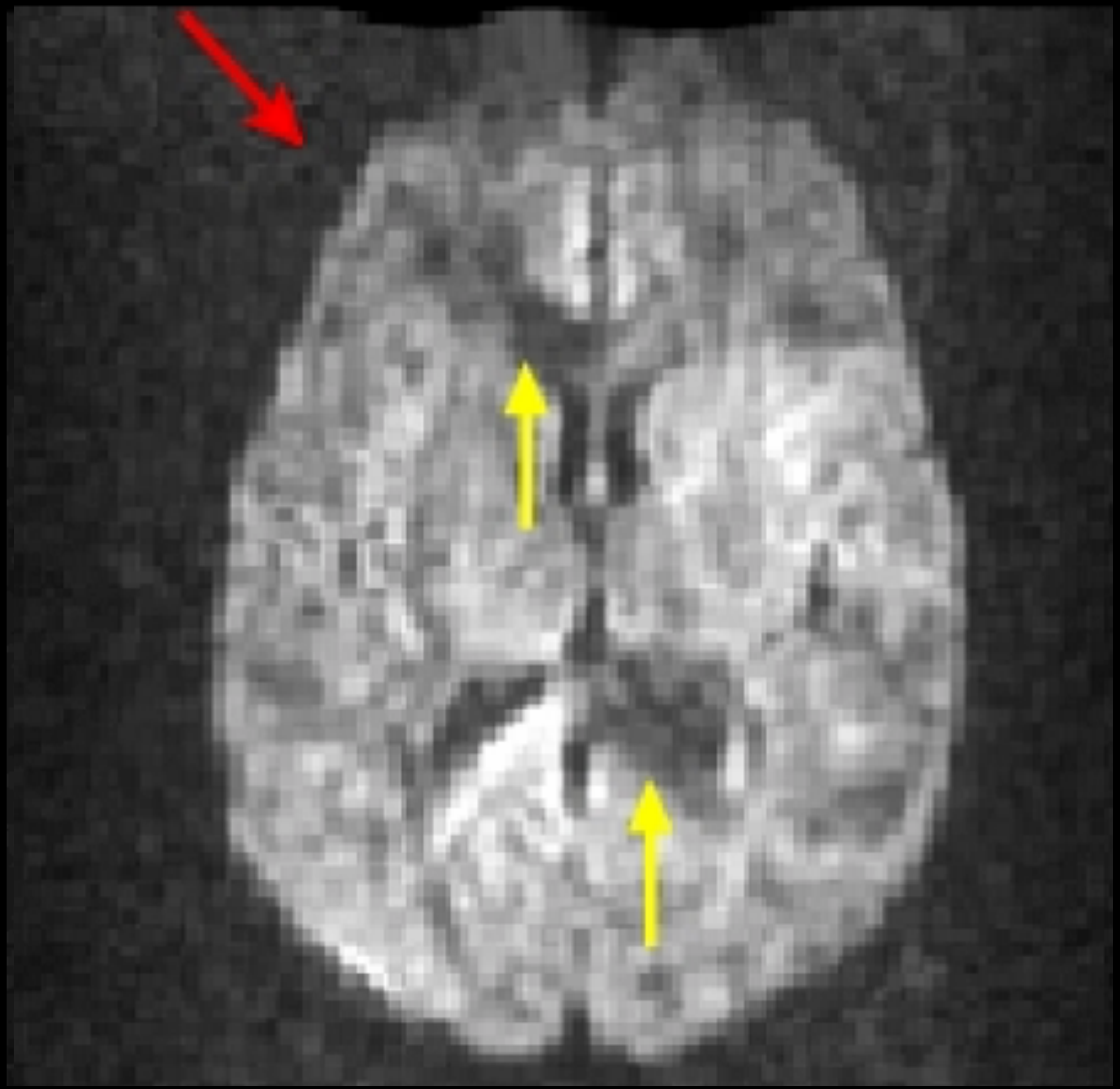

Examples of DWI for 2 gradients

Data: Centre IRMf, CHU La Timone, Marseille, FRANCE

[Stejskal-Tanner65], [Hashemi-Bradley04], [Karger-Heink83], [Tuch02]

The Diffusion Tensor Model

- Pulsed Gradient Spin Echo (SPGE) imaging sequence:

$$S(q_k, \tau) = S_0 e^{-\gamma^2 \delta^2 |g_k|^2 \left(\Delta - \frac{\delta}{3}\right) g_k^T \mathbf{D} g_k}$$

$S(q_k, \tau)$: Diffusion weighted images

γ : Spin gyromagnetic ratio

g_k : Unit diffusion gradient

δ : Gradient pulses duration

Δ : Time between 2 gradient pulses

$g_k^T \mathbf{D} g_k$: Apparent Diffusion Coefficient

- Diffusion tensor $\mathbf{D}$: 3 x 3 symmetric, positive definite matrix characterizing the covariance of the local Gaussian diffusion process of water molecules

[LeBihan-etal86], [Basser-etal94], [Stejskal-Tanner65]

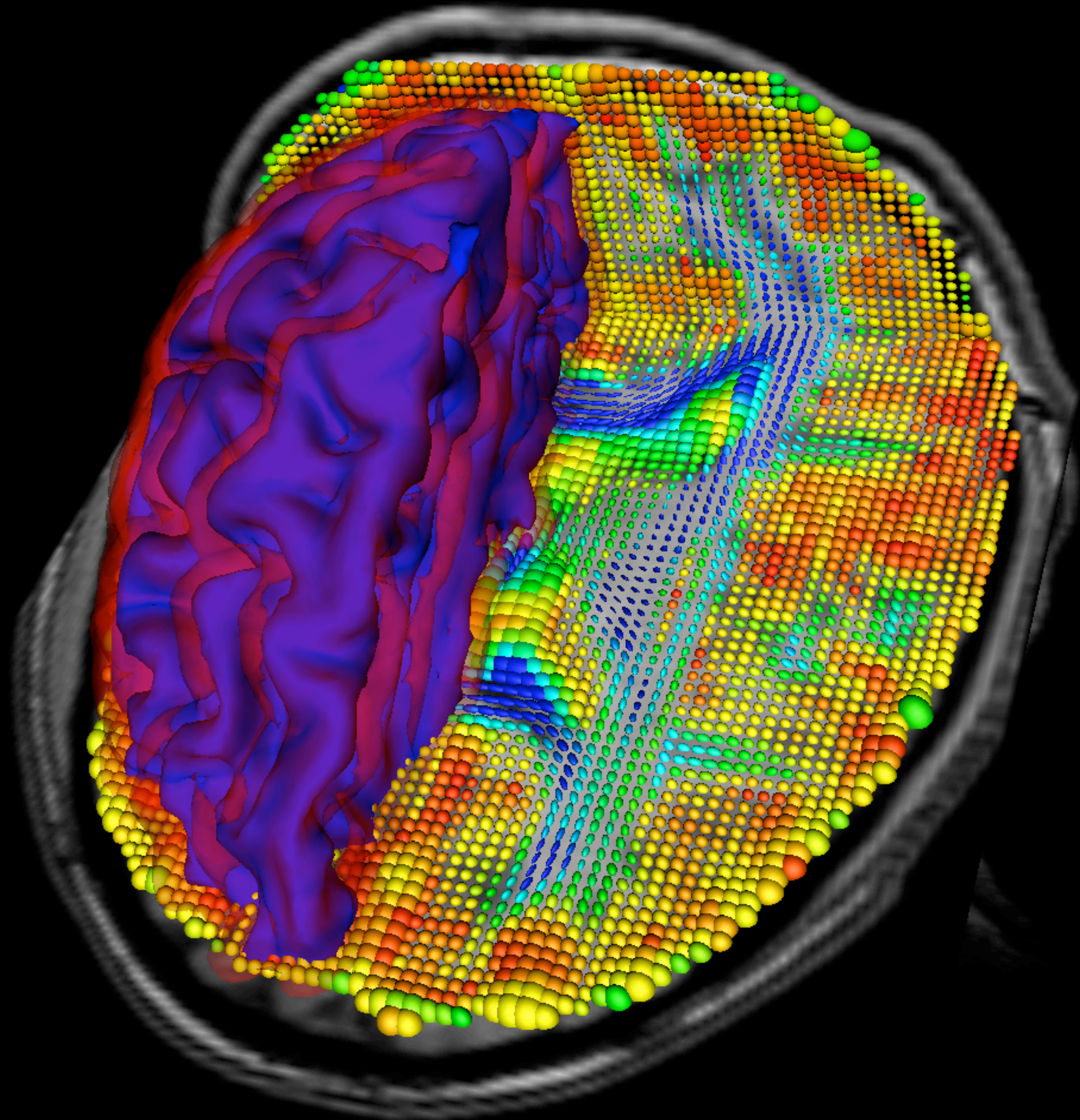

Characterizing Tissue Microstructure

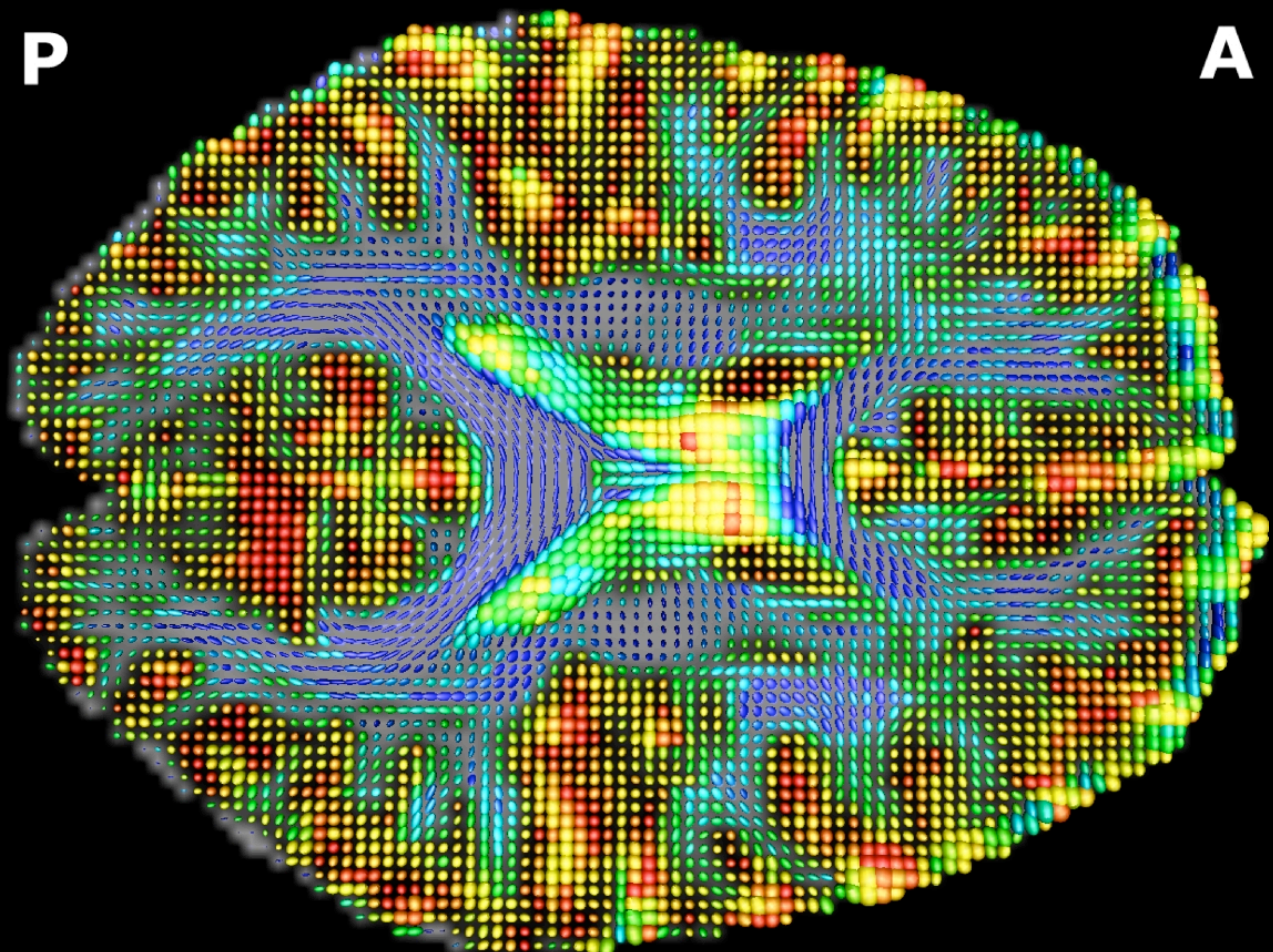

Data: Center for Magnetic Resonance Research, University of Minnesota

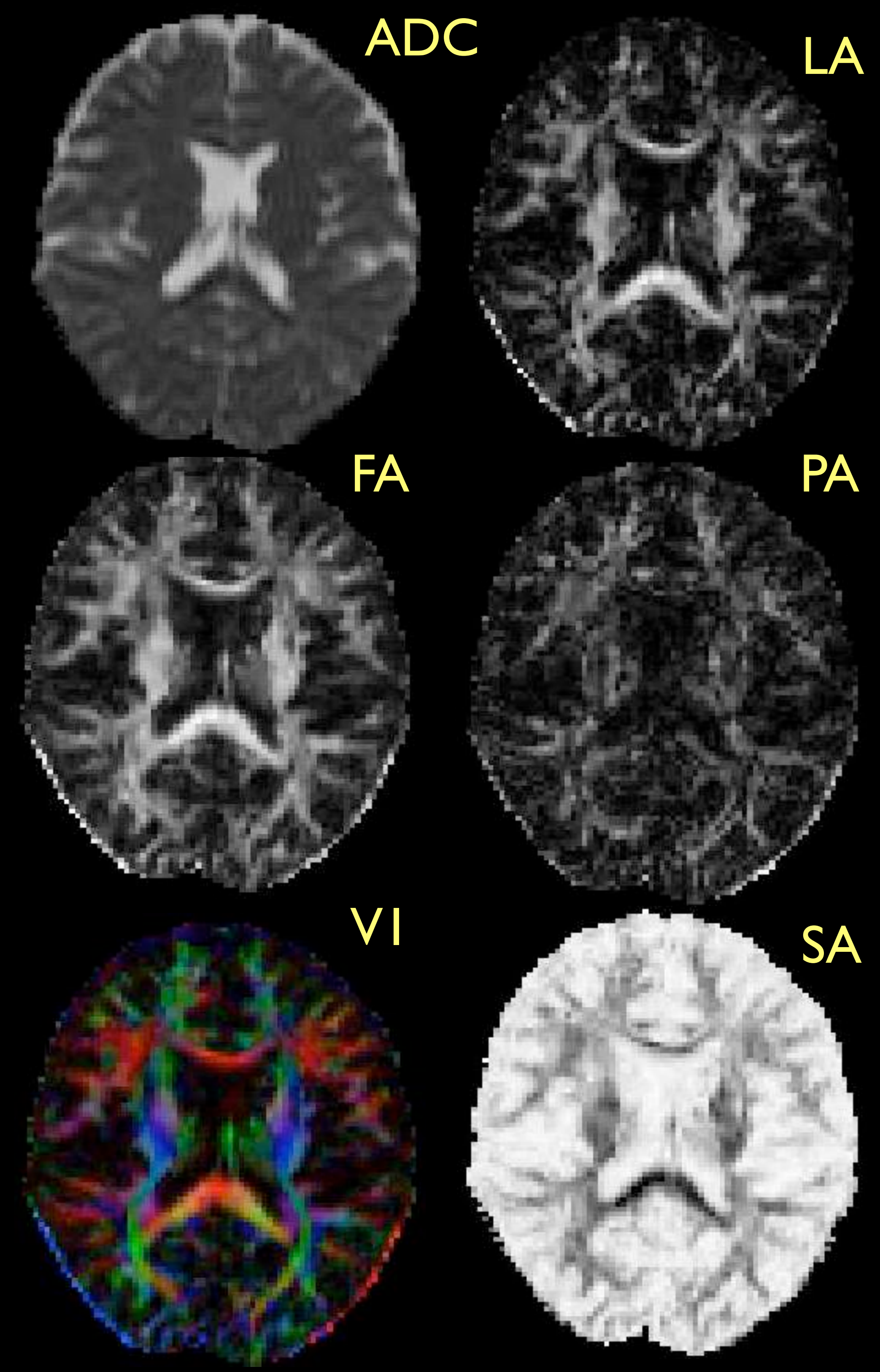

- **Applications:** Cerebro-vascular diseases, multiple sclerosis, Alzheimer's and Parkinson's disease, schizophrenia, brain development, effects of aging ...etc

[Pierpaoli-Basser96], [Westin-Maier-etal02]

Limitations of the Diffusion Tensor Model

- Unable to resolve fiber crossing
- Limited information in curving areas

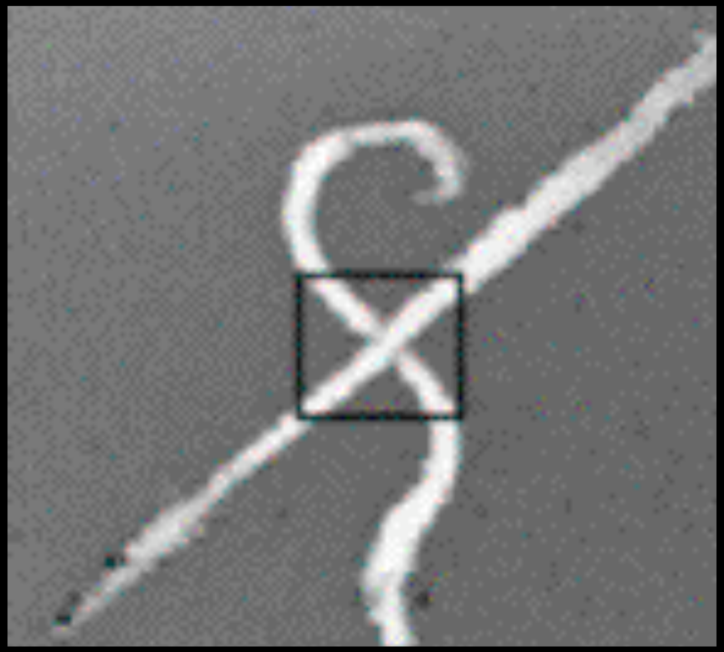

Biological phantom from
rat spinal cords

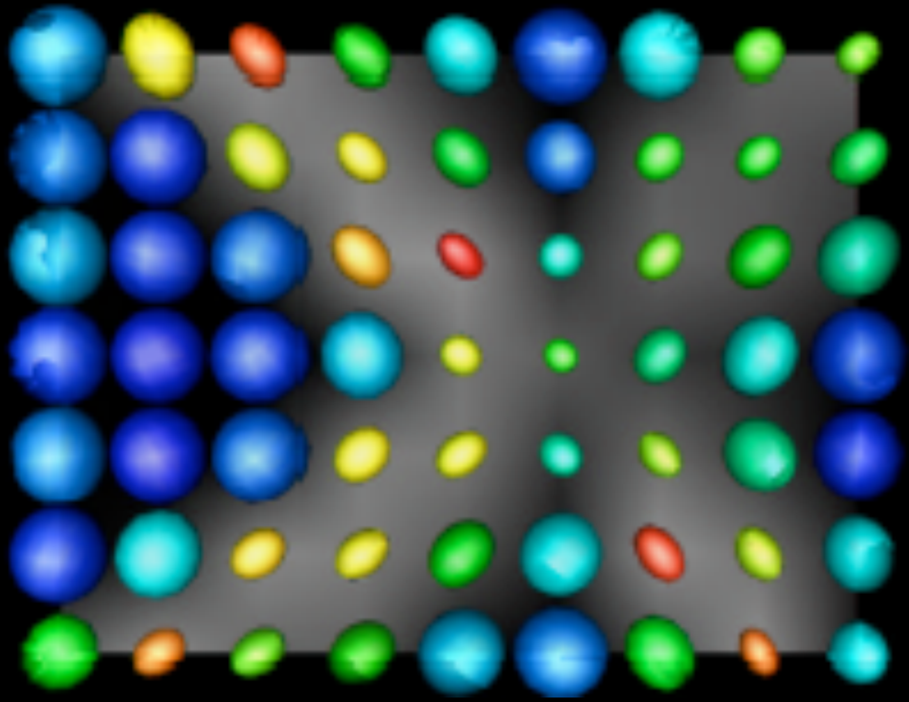

Diffusion tensors in crossing

[J. Campbell, McGill University, PhD thesis, 2004 & Neuroimage 2005]

Q-Space Imaging / Diffusion Spectrum Imaging

- Measure signal on a 3D Cartesian grid in *q*-space
- Compute 3D inverse Fourier transform to get EAP

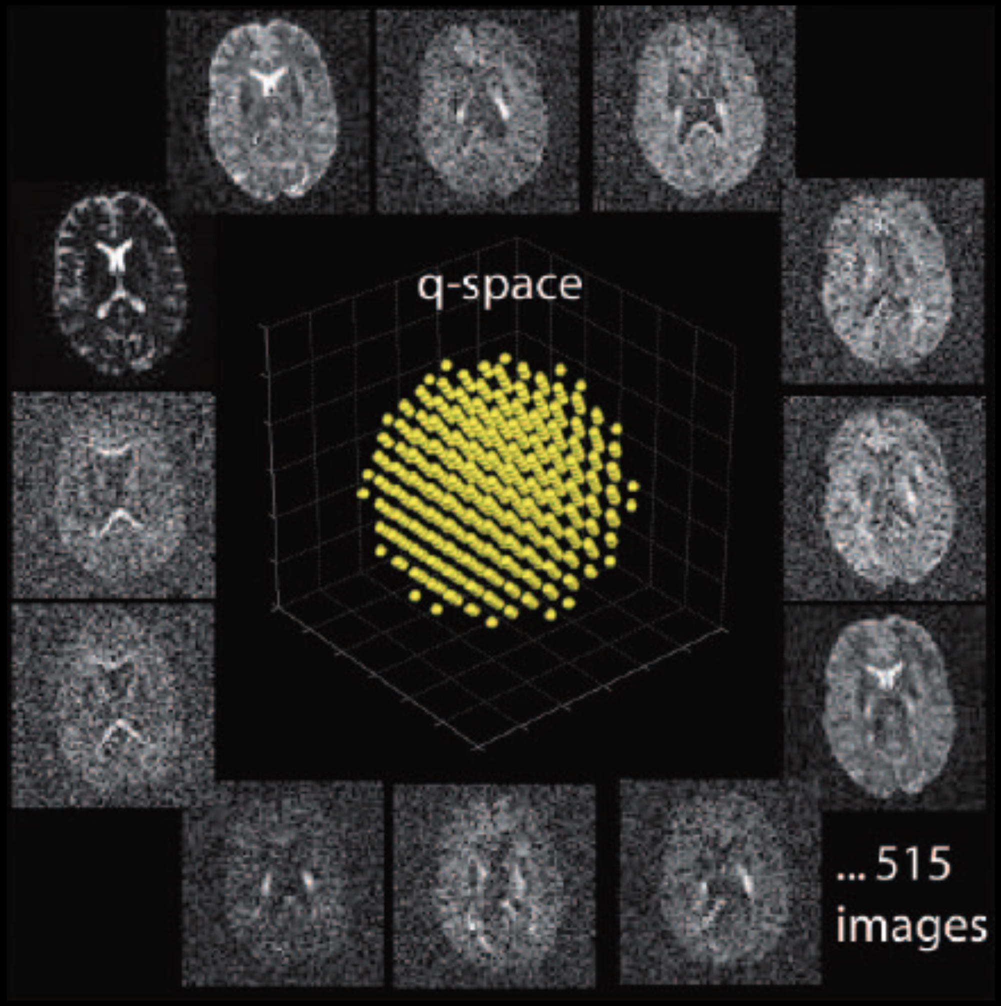

Image from [Hagmann et al, Eurographics, 2006]

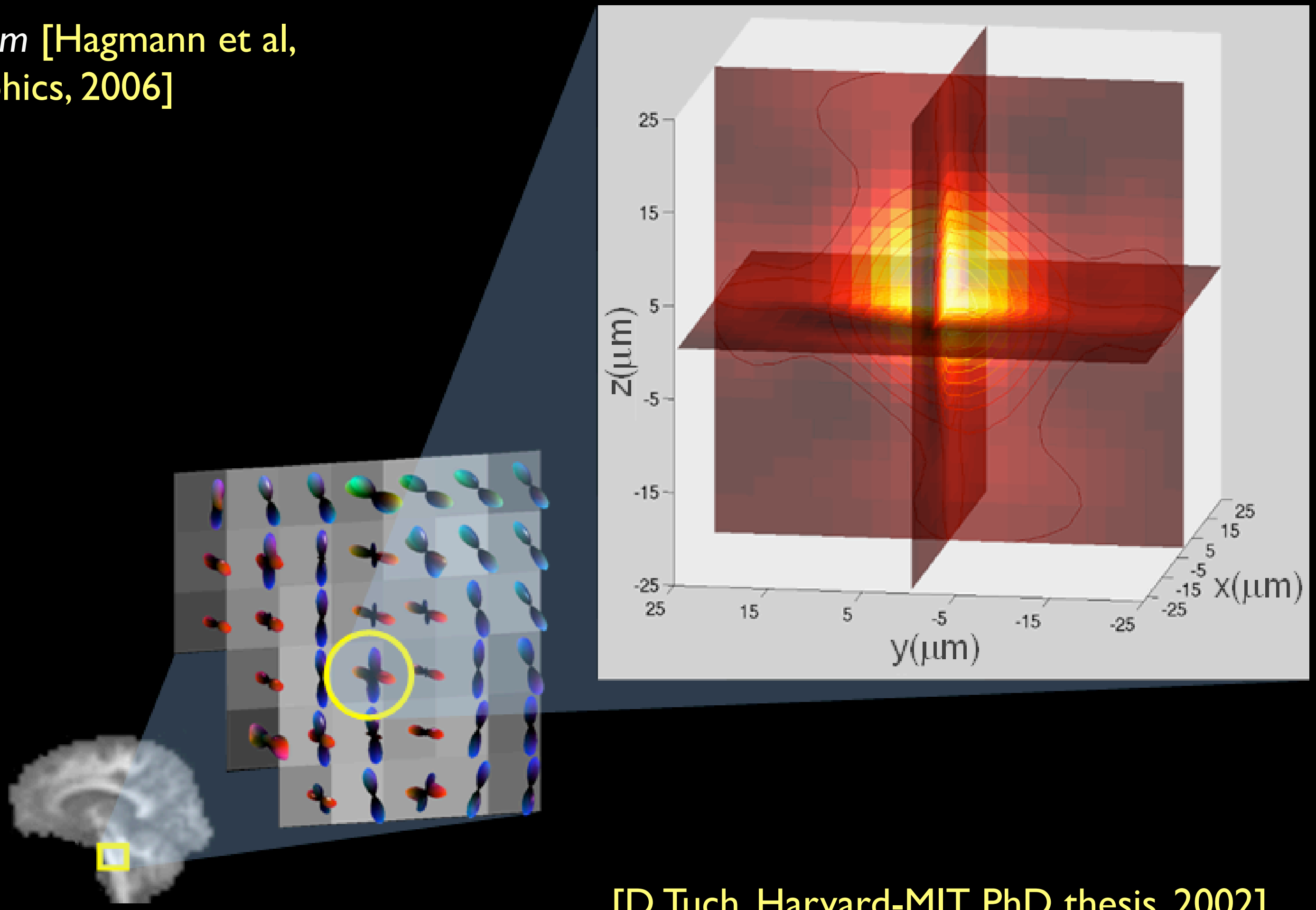

[D. Tuch, Harvard-MIT PhD thesis, 2002]

but...

- Requires many (~500) measurements
- Requires large b-values / strong gradients
- Long imaging time

Diffusion Orientation Distribution Function

- Radial integration of the 3D EAP $\psi(u) = \int_0^\infty p(\alpha u|\tau)d\alpha$

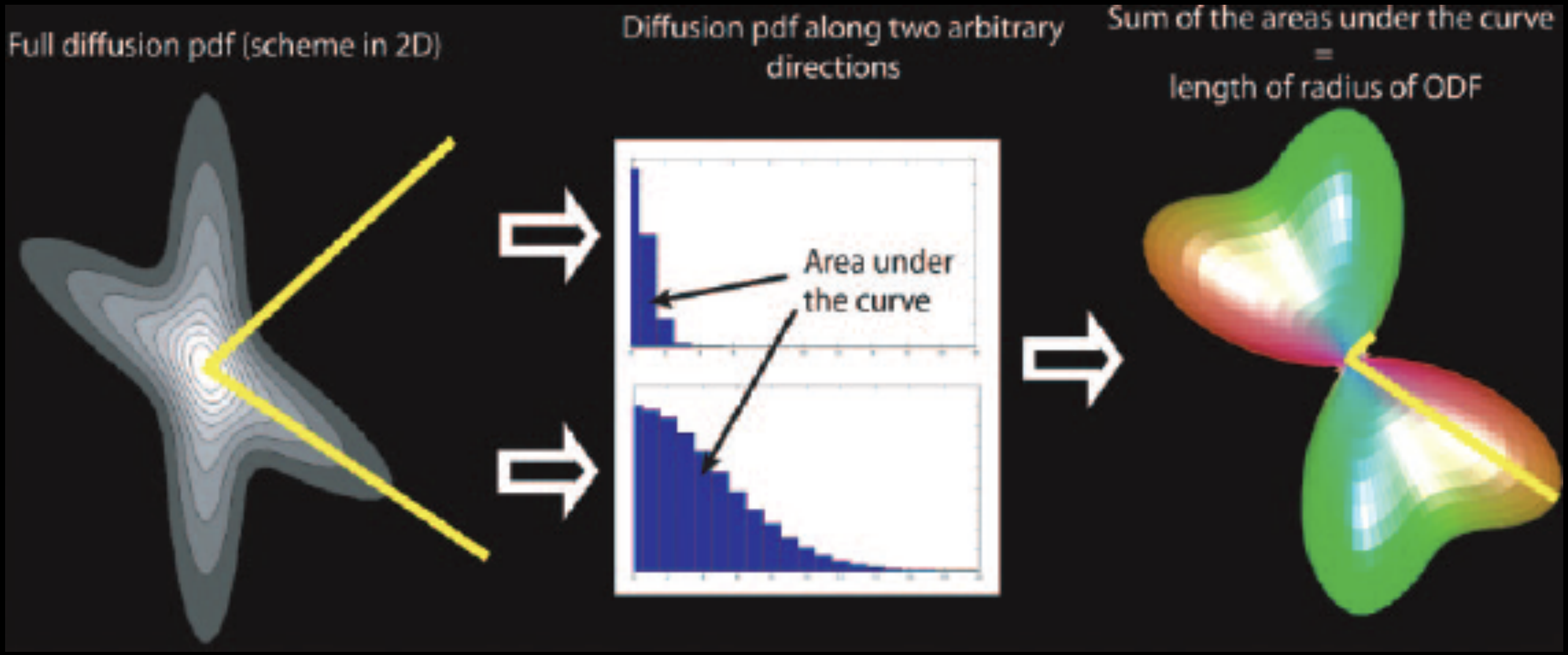

Image from [Hagmann et al, Eurographics, 2006]

Fiber distribution | *True diffusion profile (with Stejskal-Tanner Eq.)* | *Diffusion Tensor PDF* | *Orientation Distribution Function*

Q-Ball Imaging

- Goal: Directly recover angular information of fibers distribution
- QBI achieves this by just sampling a **single** shell in *q*-space

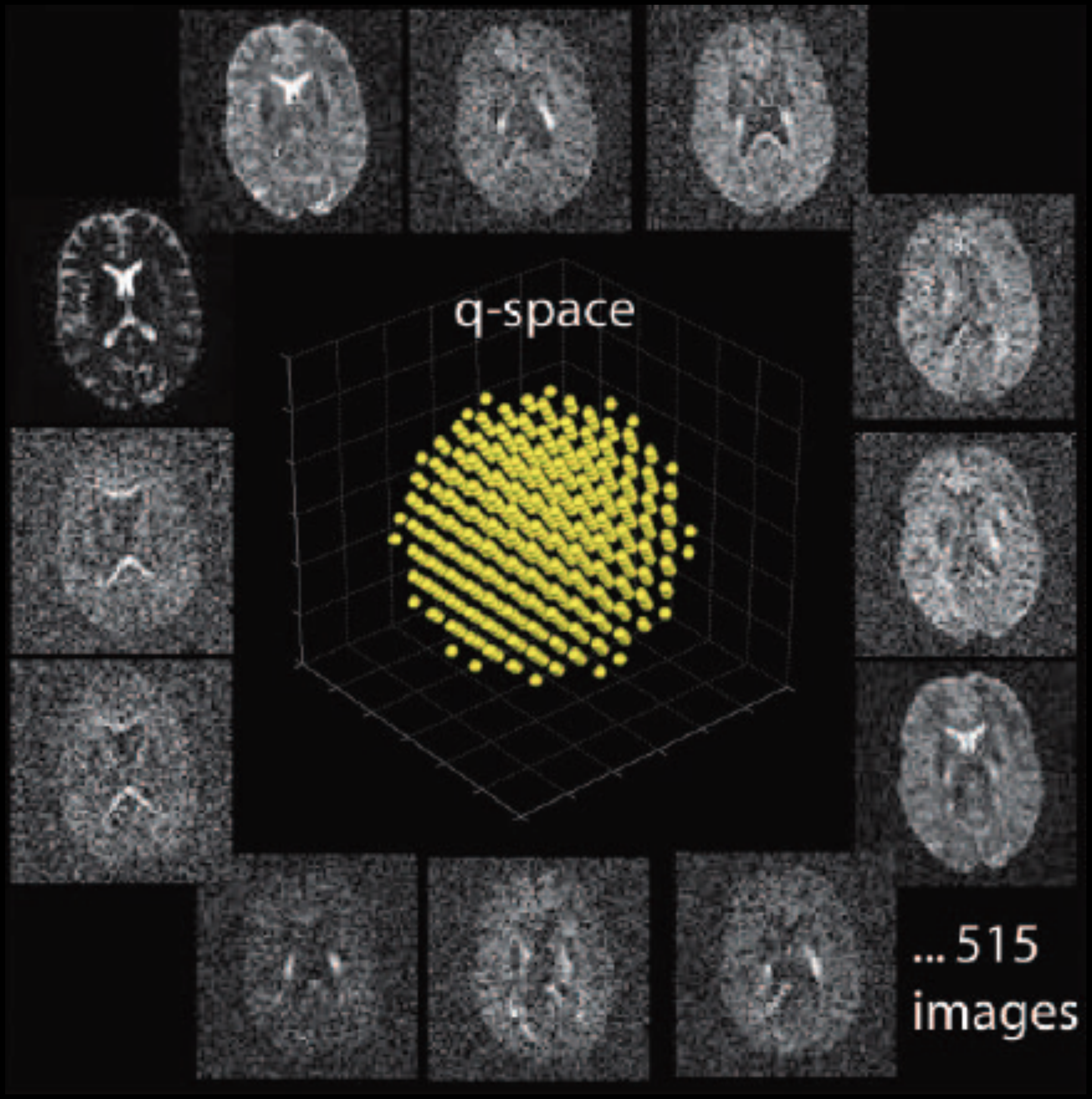

Image from [Hagmann et al, Eurographics, 2006]

$$\psi(u) = \frac{1}{2}\int_{-\infty}^{\infty} p(\alpha u)d\alpha$$

$$\propto \int_{-\infty}^{\infty} p(0,0,z)dz$$

$$\propto \int_{-\infty}^{\infty}\int_{0}^{2\pi}\int_{0}^{\infty} p(r,\theta,z)\delta(r,\theta)rdrd\theta dz$$

This can be approximated by the Funk-Radon Transform (FRT)

[D. Tuch, Harvard-MIT PhD thesis, 2002]

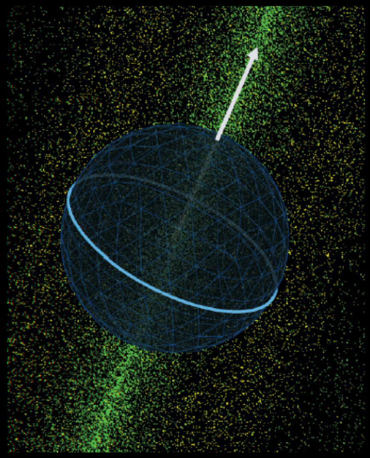

$$\psi(u) \simeq \mathcal{G}_{q'}[S(q)](u) = \int \delta(u^T q)S(q)dq$$

Q-Ball Imaging

- Goal: Directly recover angular information of fibers distribution
- QBI achieves this by just sampling a **single** shell in *q*-space

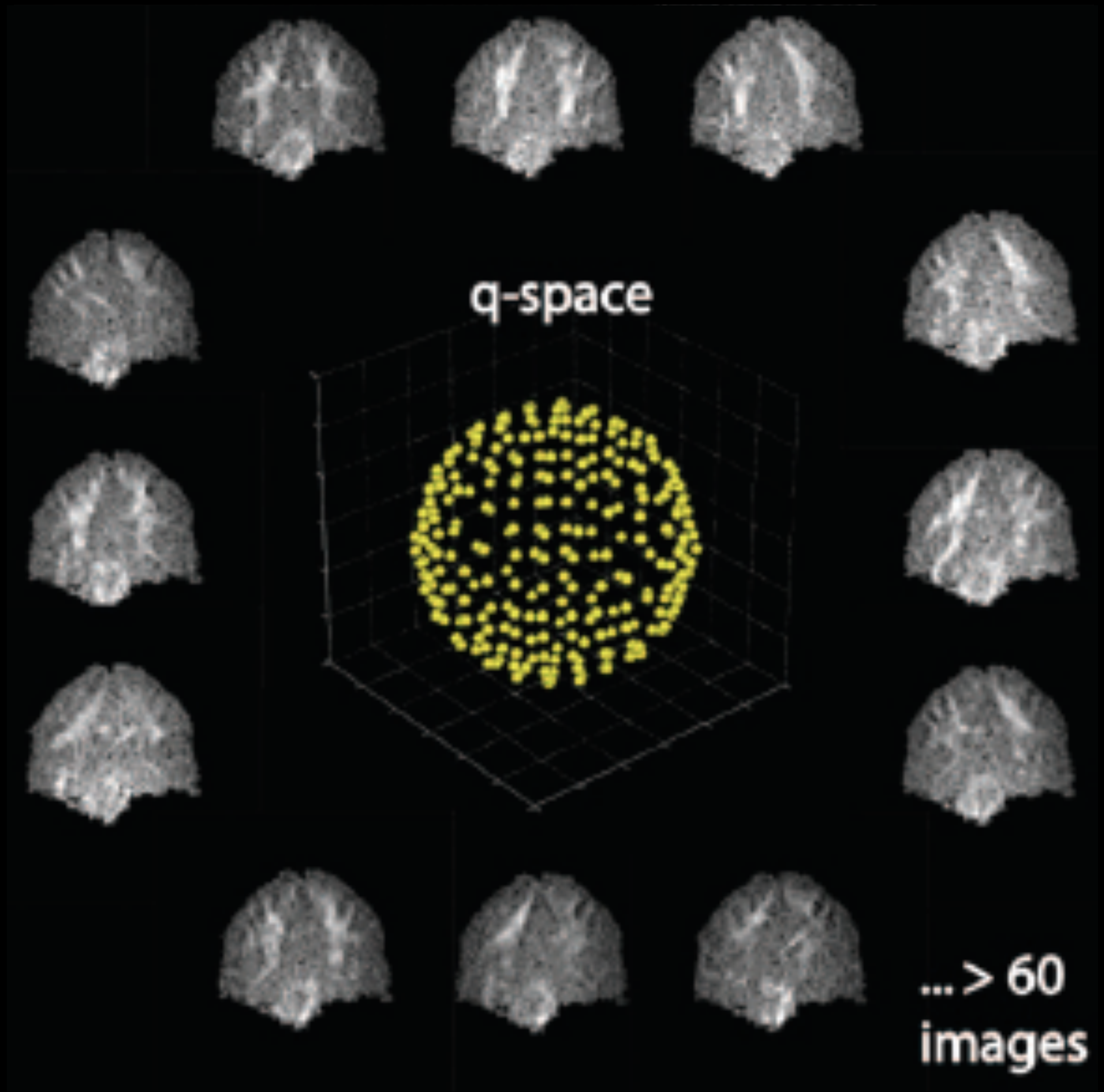

Image from [Hagmann et al, Eurographics, 2006]

$$\psi(u) = \frac{1}{2}\int_{-\infty}^{\infty} p(\alpha u) d\alpha$$

$$\propto \int_{-\infty}^{\infty} p(0,0,z)dz$$

$$\propto \int_{-\infty}^{\infty}\int_{0}^{2\pi}\int_{0}^{\infty} p(r,\theta,z)\delta(r,\theta) r dr d\theta dz$$

This can be approximated by the Funk-Radon Transform (FRT)

[D. Tuch, Harvard-MIT PhD thesis, 2002]

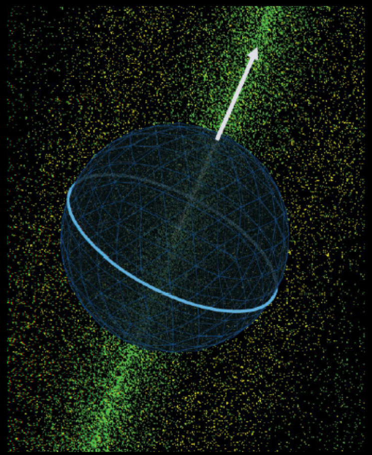

$$\psi(u) \simeq \mathcal{G}_{q'}[S(q)](u) = \int \delta(u^T q) S(q) dq$$

ODF Approximation by FRT

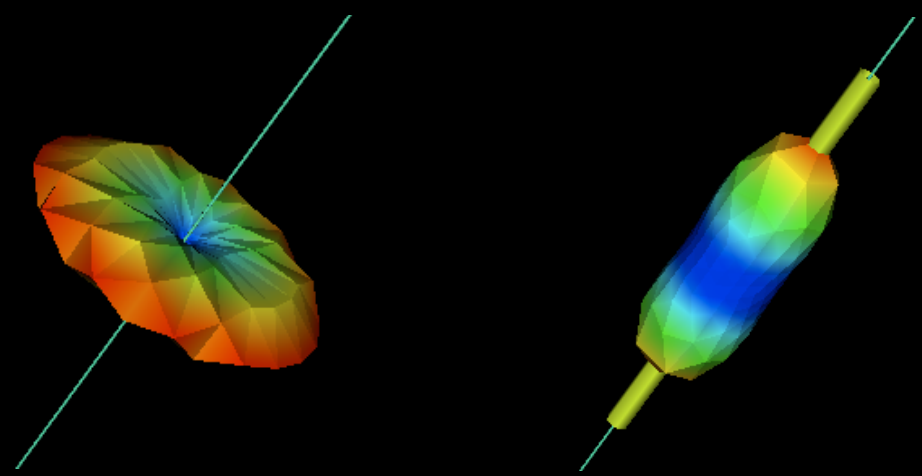

Signal *ODF*

Funk-Radon Transform Example 1

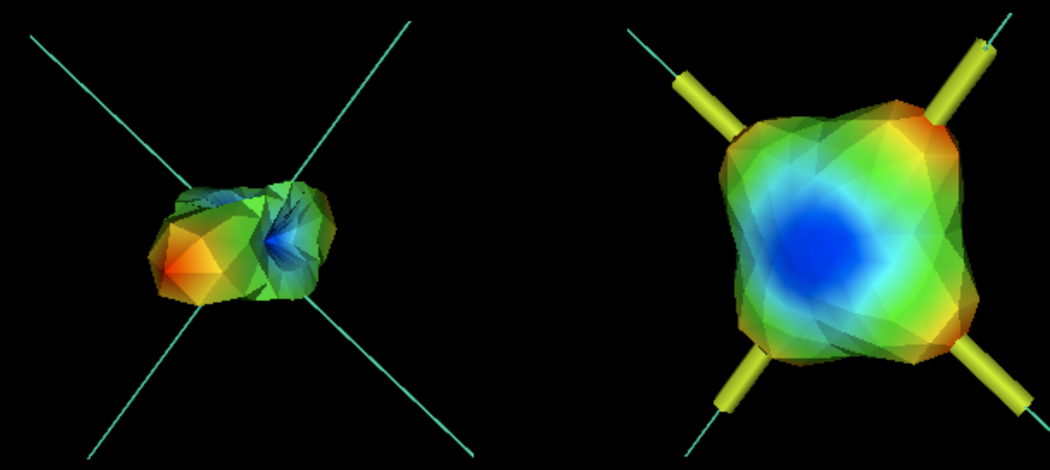

Signal *ODF*

Funk-Radon Transform Example 2

$$\mathcal{G}_{q'}[S(q)](u) = \int_0^{2\pi} S(q', q_\theta, 0)\,dq\theta$$

FRT at *q'* in direction *u* (z here) is integral over great circle in *xy*-plane

$$= \int_0^{2\pi}\int_0^{\infty} S(q', q_\theta, 0)\,\delta(q_r - q')\,q_r\,dq_r\,dq_\theta$$

$$= \int_0^{2\pi}\int_0^{\infty} \mathcal{F}_{2D}[S(q', q_\theta, 0)]\,\mathcal{F}_{2D}[\delta(q_r - q')]\,r\,dr\,d\theta$$

Using Parseval-Plancherel theorem:

$$\int_{-\infty}^{\infty} f(x)\overline{g}(x)\,dx = \int_{-\infty}^{\infty} \mathcal{F}[f(x)](k)\overline{\mathcal{F}[g(x)]}(k)\,dk$$

ODF Approximation by FRT

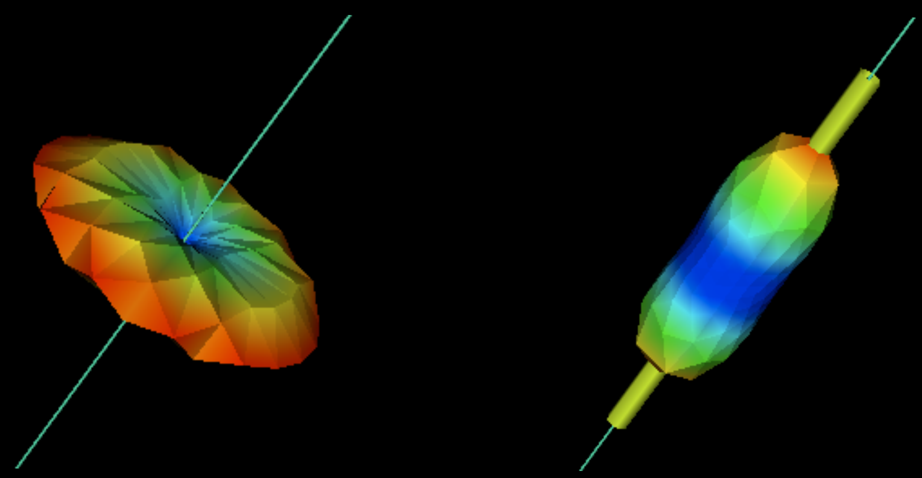

Signal *ODF*

Funk-Radon Transform Example 1

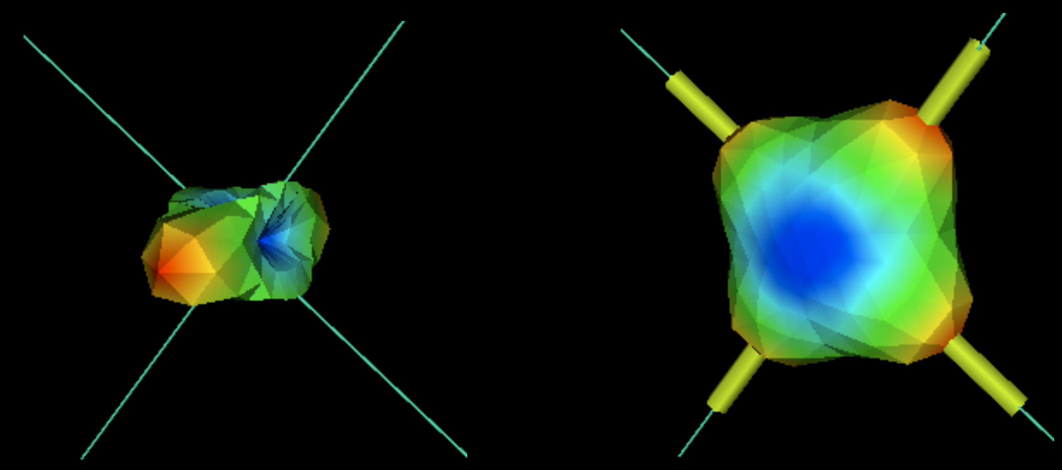

Signal *ODF*

Funk-Radon Transform Example 2

$$\mathcal{G}_{q'}[S(q)](u) = \int_0^{2\pi} S(q', q_\theta, 0) dq\theta$$

FRT at *q'* in direction *u* (z here) is integral over great circle in *xy*-plane

$$= \int_0^{2\pi} \int_0^{\infty} S(q', q_\theta, 0)\delta(q_r - q') q_r dq_r dq_\theta$$

$$= \int_0^{2\pi} \int_0^{\infty} \boxed{\mathcal{F}_{2D}[S(q', q_\theta, 0)]}\boxed{\mathcal{F}_{2D}[\delta(q_r - q')]} r dr d\theta$$

Using Parseval-Plancherel theorem:

$$\int_{-\infty}^{\infty} f(x)\bar{g}(x)dx = \int_{-\infty}^{\infty} \mathcal{F}[f(x)](k)\overline{\mathcal{F}[g(x)]}(k)dk$$

ODF Approximation by FRT

- **Central slice theorem:** $\mathcal{F}_{2D}[\mathcal{L}[f(x)](u)] = \mathcal{I}[\mathcal{F}_{3D}[f(x)]](u)$

with $\mathcal{L}[f(x)](u) = \int_{-\infty}^{\infty} f(x + \alpha u) d\alpha$ *(projection)*

$\mathcal{I}[f(x)](u) = f(x)\delta(x^T u)$ *(intersection)*

- **Hankel transform** (2D Fourier transform with no angular dependence)

$$\mathcal{F}_{2D}[f(x)] = \mathcal{F}_{2D}[f(r)] = 2\pi \int_0^{\infty} f(r) J_0(2\pi q r) r dr$$

hence

$$\boxed{\mathcal{F}_{2D}[S(q', q_\theta, 0)]} = \mathcal{F}_{2D}[\mathcal{I}[\mathcal{F}_{3D}[p(r,\theta,z)]](u)] = \mathcal{L}[p(r,\theta,z)](u) = \int_{-\infty}^{\infty} p(r,\theta,z) dz$$

$$\boxed{\mathcal{F}_{2D}[\delta(q_r - q')]} = 2\pi \int_0^{\infty} \delta(q_r - q') J_0(2\pi q_r r) q_r dq_r = 2\pi q' J_0(2\pi q' r)$$

ODF Approximation by FRT

- Putting everything together

$$\mathcal{G}_{q'}[S(q)](u) = 2\pi q' \int_{-\infty}^{\infty} \int_{0}^{2\pi} \int_{0}^{\infty} p(r,\theta,z) J_0(2\pi q' r) r dr d\theta dz$$

- We recall that

$$\psi(u) = \int_{-\infty}^{\infty} \int_{0}^{2\pi} \int_{0}^{\infty} p(r,\theta,z) \delta(r,\theta) r dr d\theta dz$$

- If the zeroth-order Bessel function is close to a Dirac, the FRT approximates well the ODF. Hence the need for high b-values...

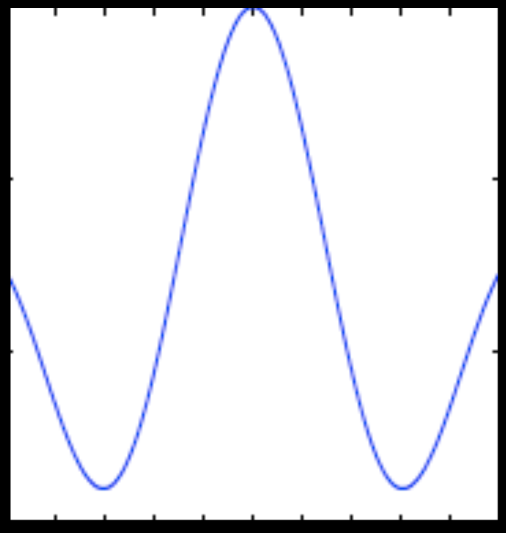

b=1

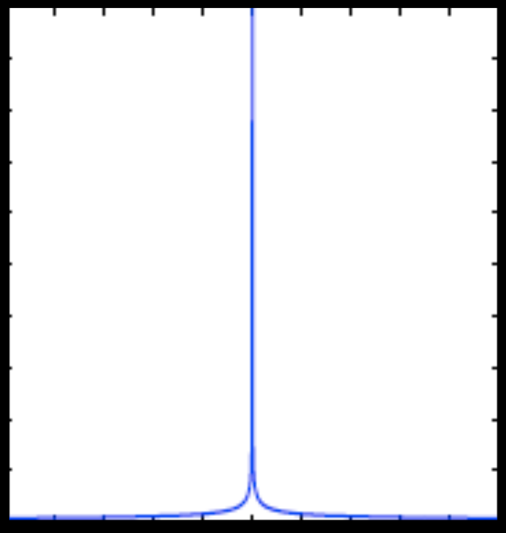

b=1000

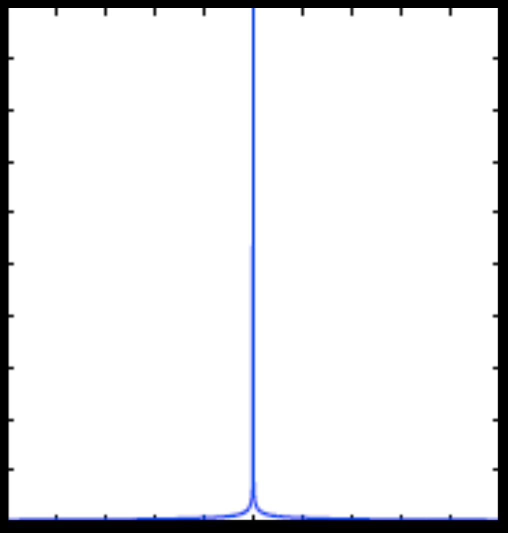

b=4000

[D. Tuch, Harvard-MIT PhD thesis, 2002], [M. Descoteaux INRIA PhD thesis 2008]

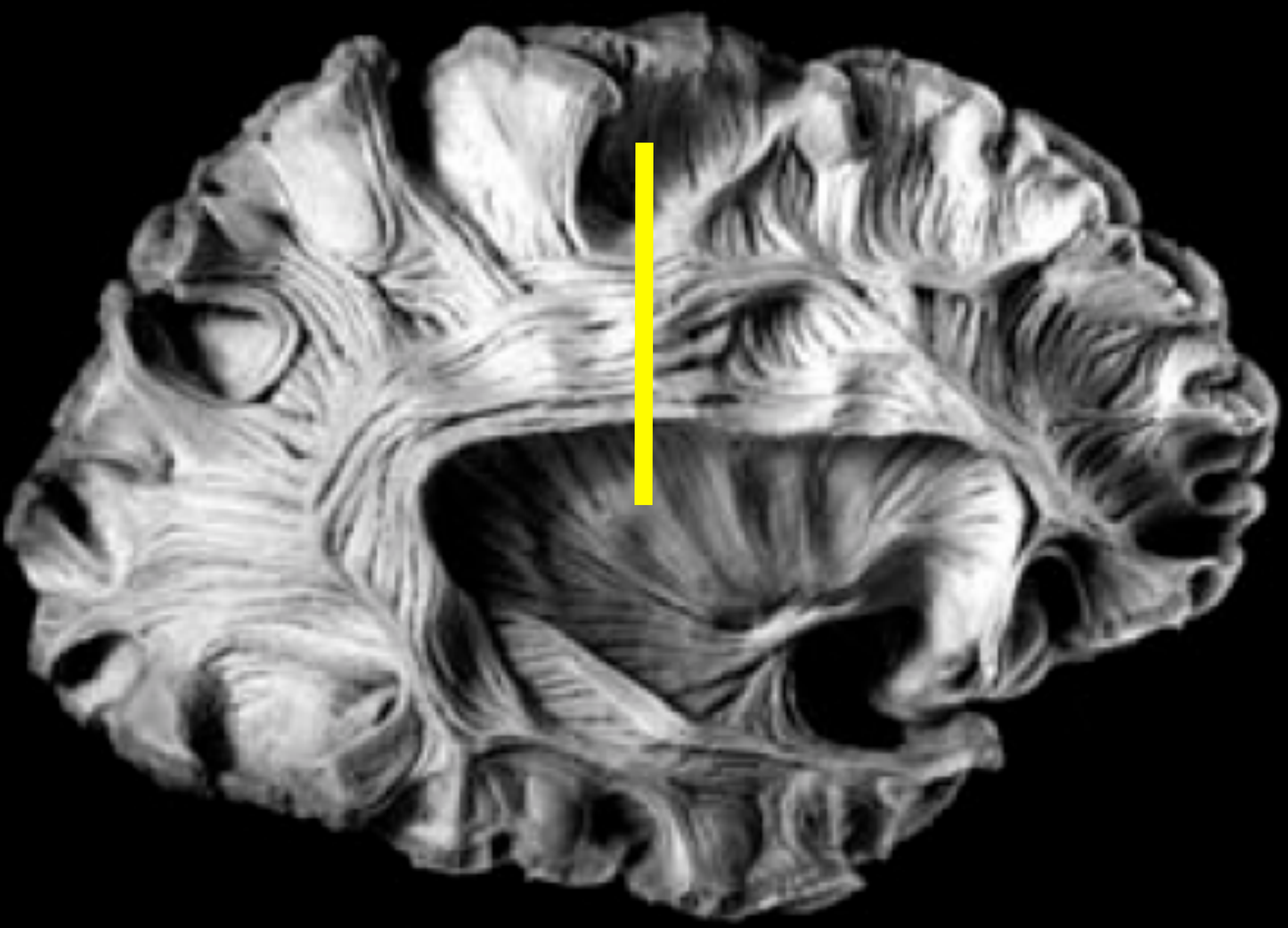

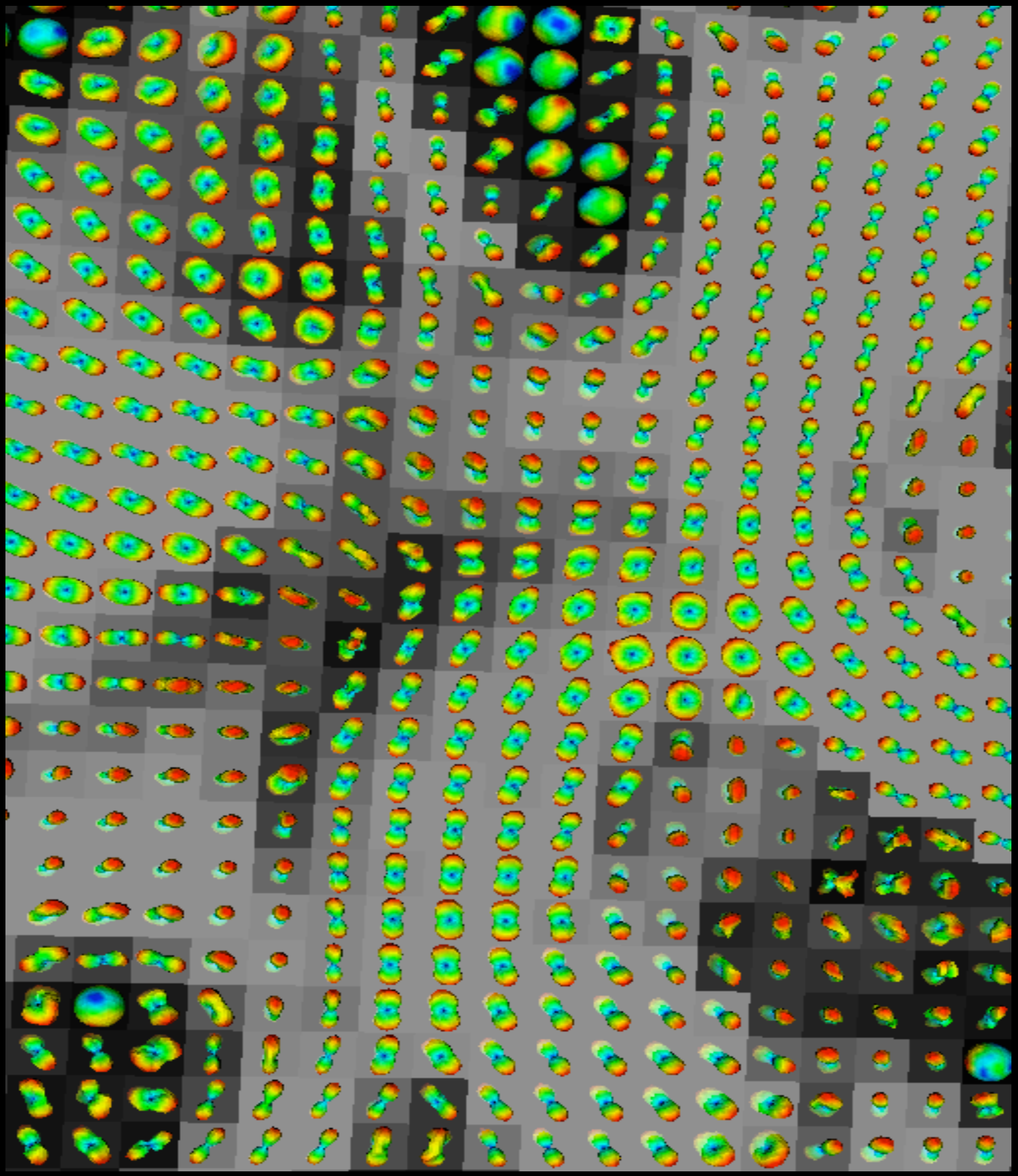

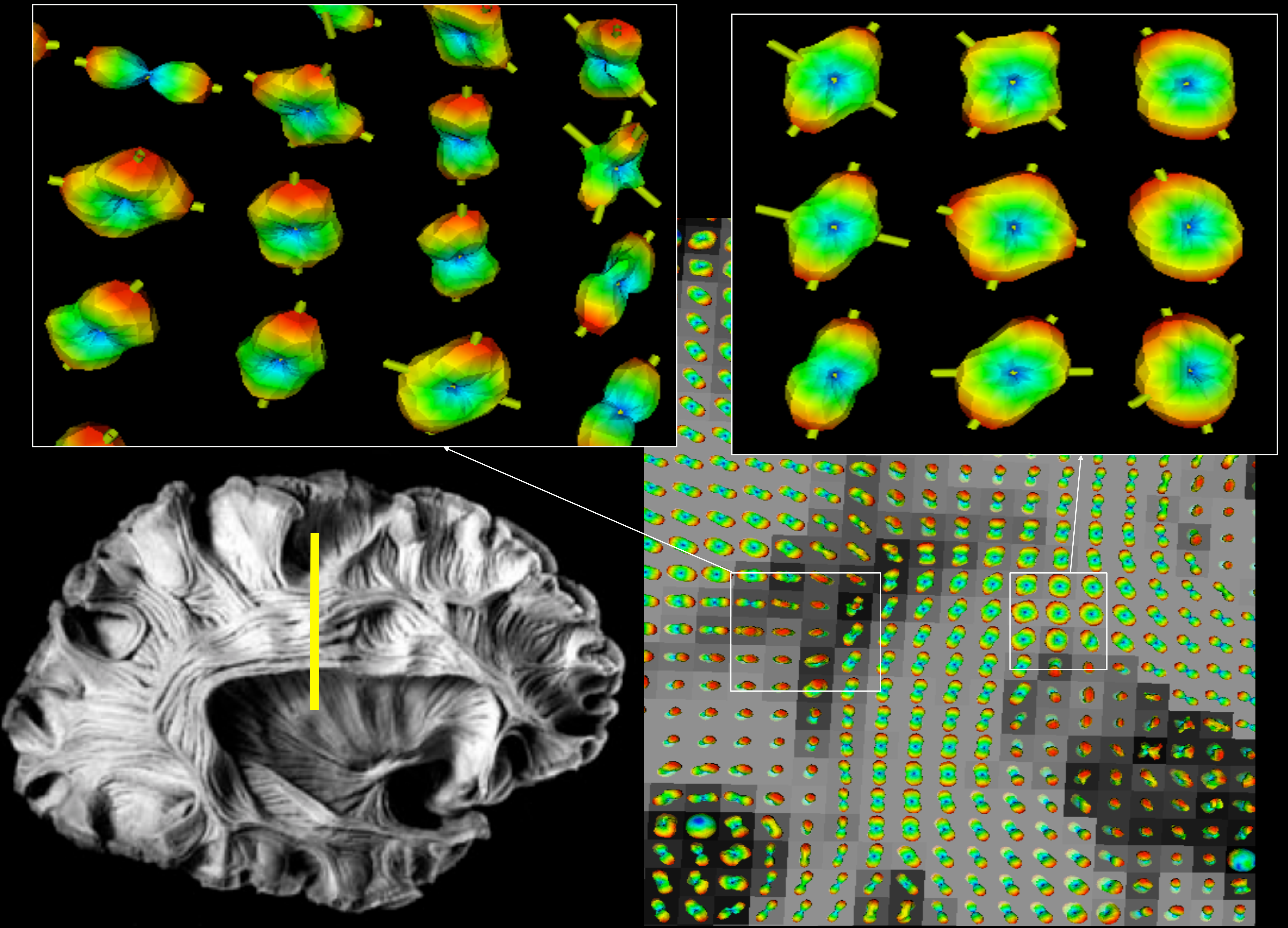

Mathematical Concepts for Tensors & ODFs Processing

- *Symmetric Positive Definite Matrices*
- *Spherical Harmonics*

Riemannian Geometry 101

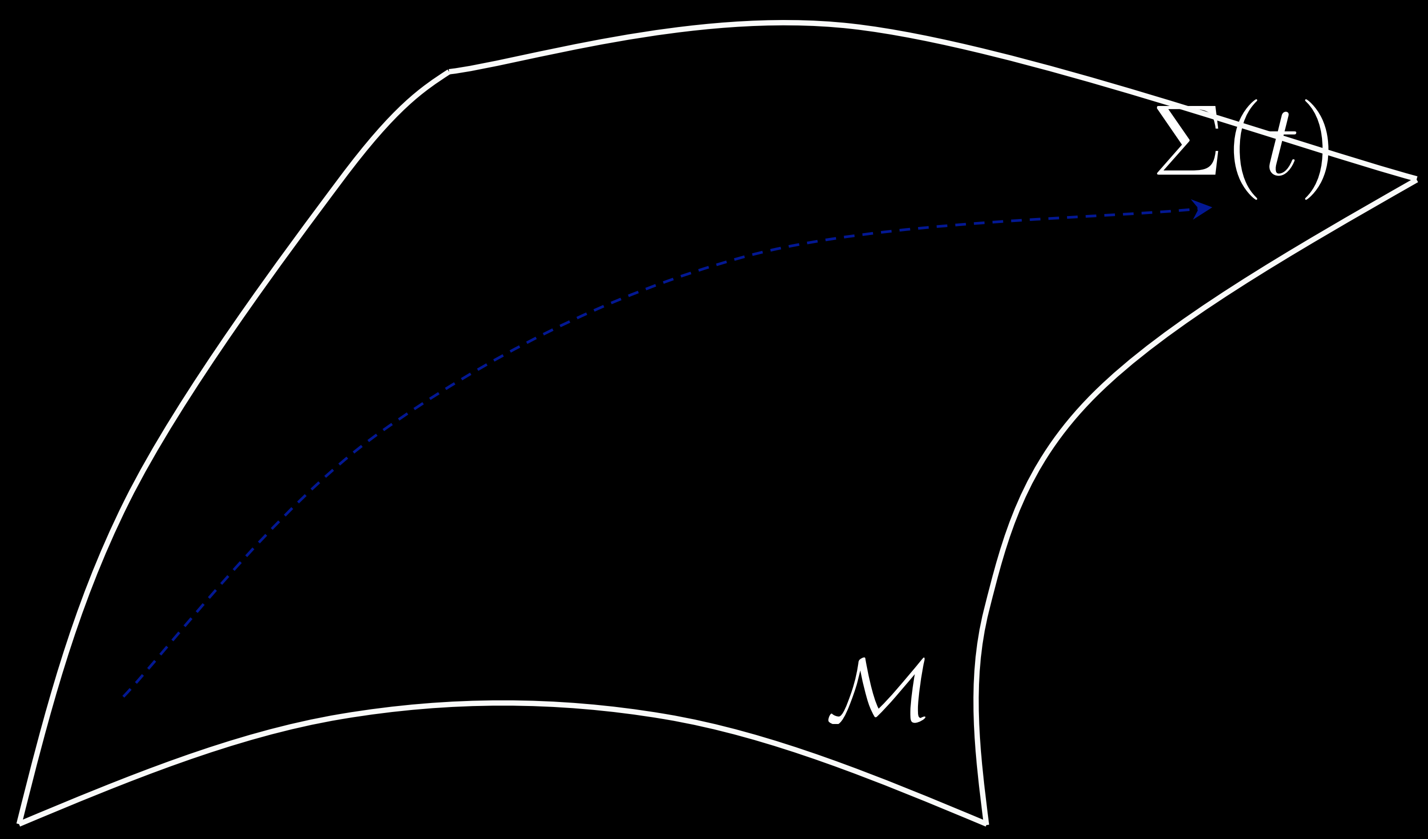

n-dimensional Riemannian manifold $\mathcal{M}$
locally looks like $\mathbb{R}^n$

[Do Carmo92]

Riemannian Geometry 101

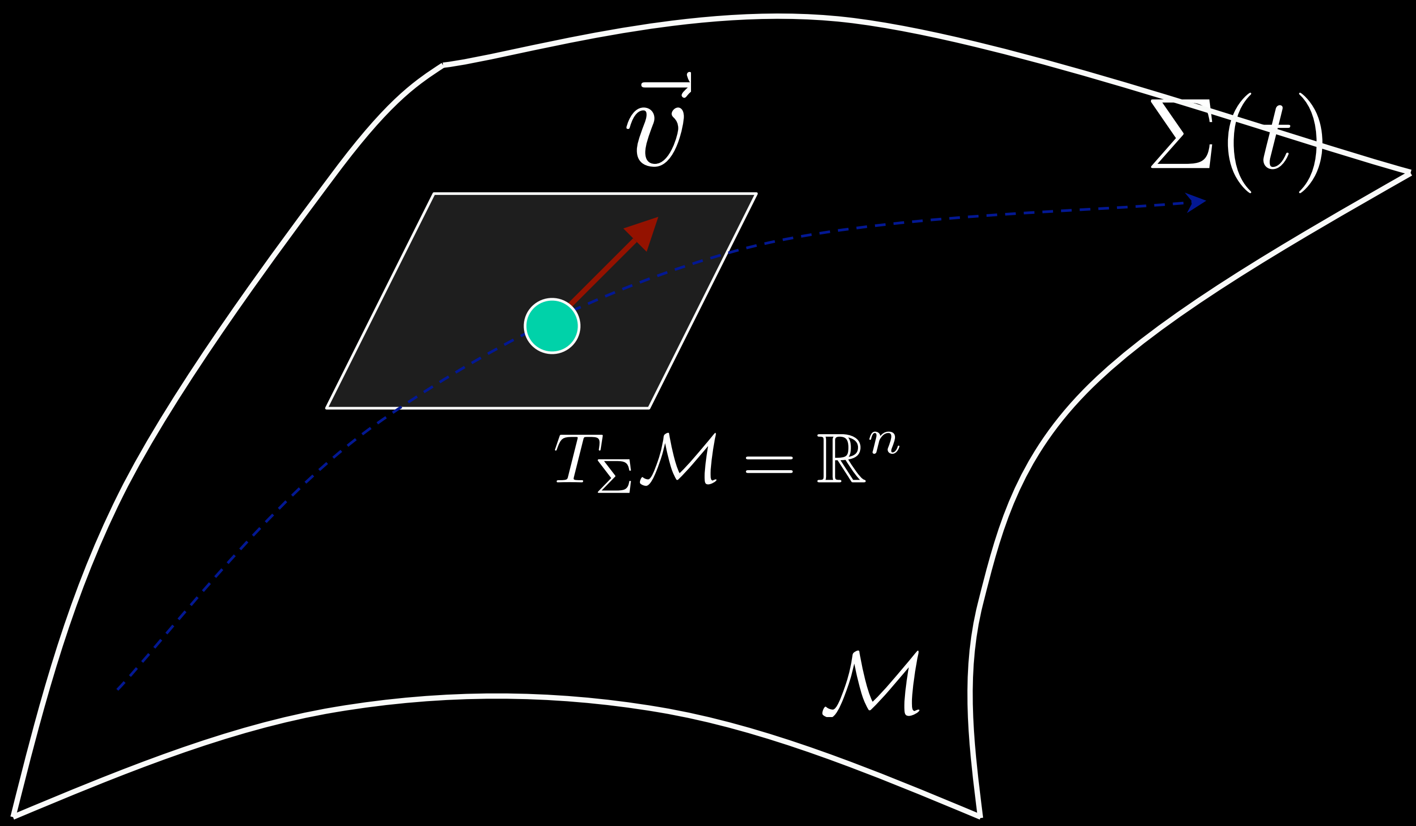

n-dimensional Riemannian manifold $\mathcal{M}$
locally looks like $\mathbb{R}^n$

⇓

Collection of inner products $\langle .,. \rangle_\Sigma$
associated to each tangent space $T_\Sigma \mathcal{M}$

[Do Carmo92]

Riemannian Geometry 101

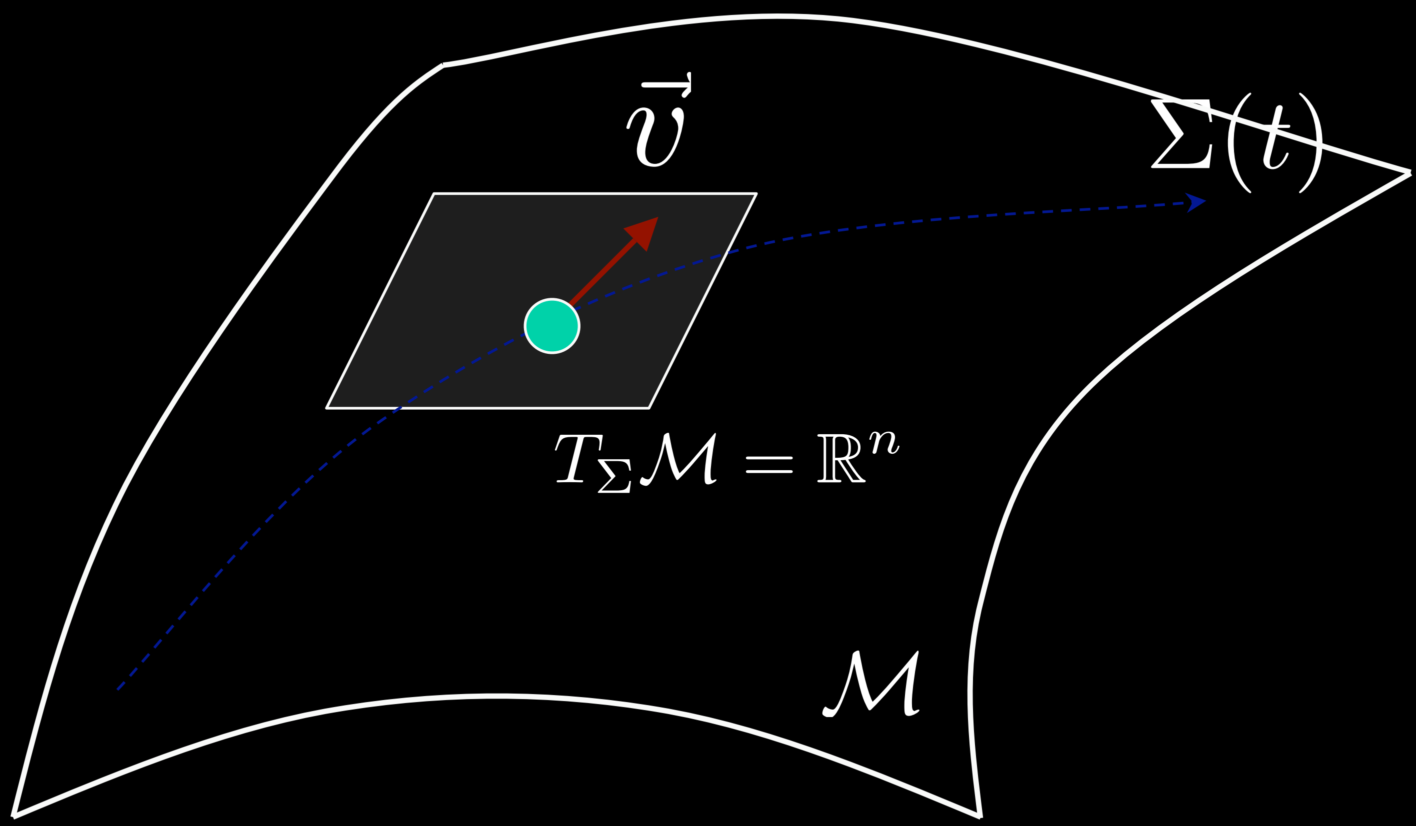

n-dimensional Riemannian manifold $\mathcal{M}$
locally looks like $\mathbb{R}^n$

⬇

Collection of inner products $\langle .,. \rangle_\Sigma$
associated to each tangent space $T_\Sigma\mathcal{M}$

⬇

Magnitude of a tangent vector depends on the tangent space it is attached to:

$$\|v\|_\Sigma^2 = \langle v, v\rangle_\Sigma = v^T G v$$

[Do Carmo92]

Riemannian Geometry 101

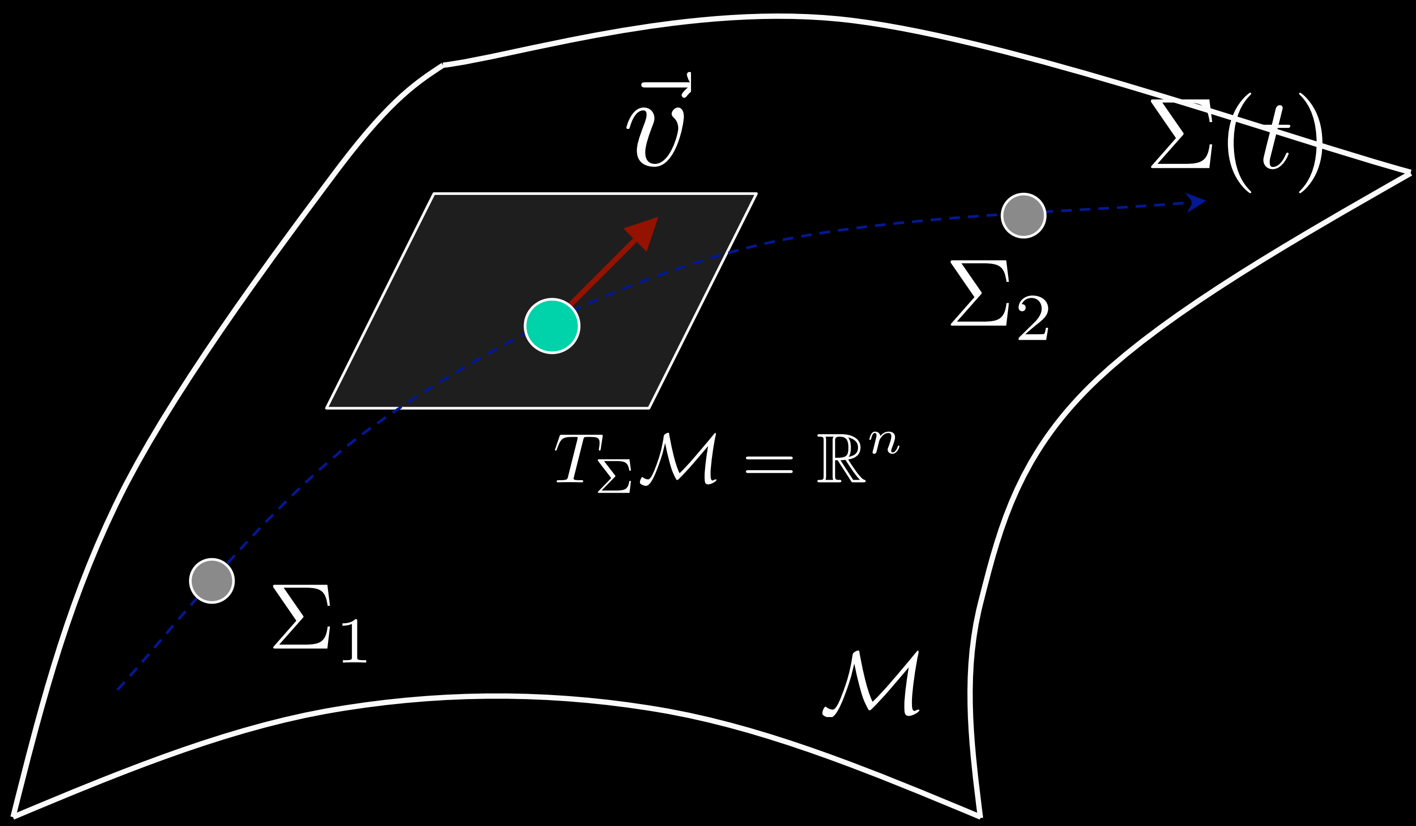

n-dimensional Riemannian manifold $\mathcal{M}$
locally looks like $\mathbb{R}^n$

Collection of inner products $\langle ., . \rangle_\Sigma$
associated to each tangent space $T_\Sigma \mathcal{M}$

Magnitude of a tangent vector depends on the tangent space it is attached to:

$$\|v\|_\Sigma^2 = \langle v, v \rangle_\Sigma = v^T G v$$

Notion of distance:

$$\mathcal{D}(\Sigma_1, \Sigma_2) = \int_{t_1}^{t_2} \|\dot{\Sigma}(t)\|_{\Sigma(t)} dt$$

[Do Carmo92]

Statistics on Riemannian Manifolds

- Empirical mean of a set of N random elements $\{\Sigma_i\} \quad i = 1, ..., N$ is the minimizer $\Sigma = \overline{\Sigma}$ of the variance:

$$\sigma^2\left(\{\Sigma_i\}\right) = \frac{1}{N-1}\sum_{i=1}^{N}\mathcal{D}^2(\Sigma, \Sigma_i)$$

- Empirical covariance matrix:

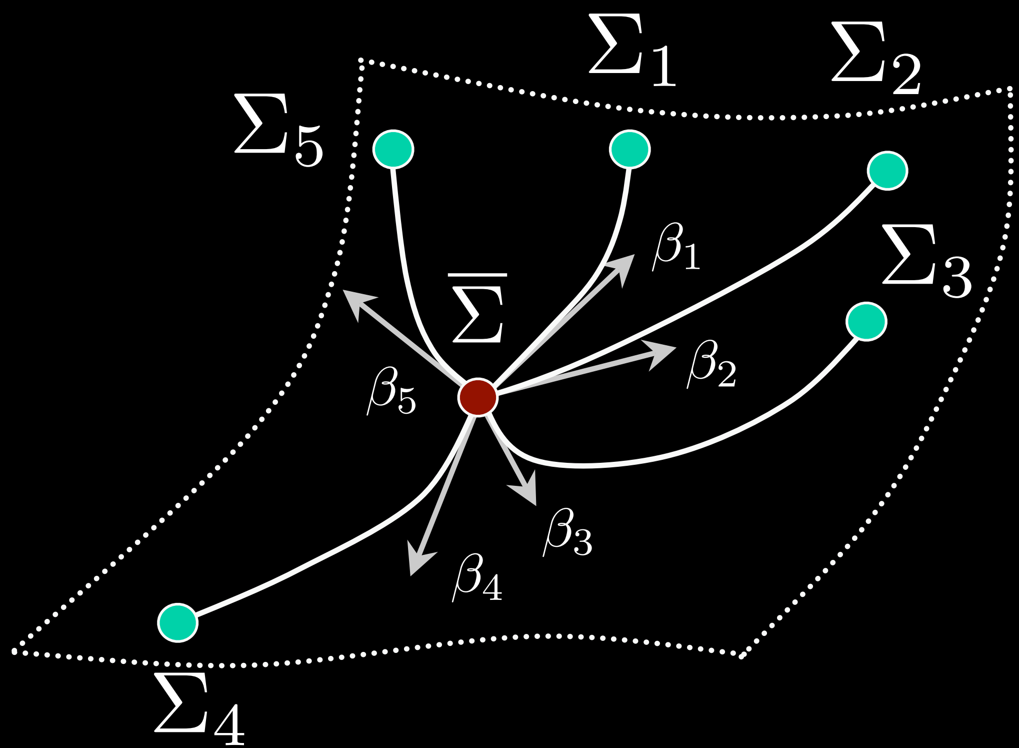

$$\Lambda = \frac{1}{N-1}\sum_{i=1}^{N}\varphi(\beta_i)\varphi(\beta_i)^T$$

$$\beta_i = -\nabla_{\overline{\Sigma}}\mathcal{D}^2(\overline{\Sigma, \Sigma_i})$$

[Fréchet48], [Pennec-etal, IJCV/JMIV'06]

The Manifold of Multivariate Normal PDFs

- $\mathcal{P}(r|\Sigma)$: normal distribution for $r \in \mathbb{R}^3$ with fixed mean

- Parameterized by the 6 independent elements of its covariance matrice:

$$\Sigma = \begin{bmatrix} \Sigma^1 & \Sigma^2 & \Sigma^3 \\ \Sigma^2 & \Sigma^4 & \Sigma^5 \\ \Sigma^3 & \Sigma^5 & \Sigma^6 \end{bmatrix}$$

- When $\mathcal{P}(r|\Sigma)$ is sufficiently smooth in the $\Sigma^i,\ i = 1, ..., 6$, it is natural to introduce a structure of sub-manifold $S^+(3) \subset \mathbb{R}^6$

[Rao45], [Burbea-Rao82], [Amari90]

The Manifold of Multivariate Normal PDFs

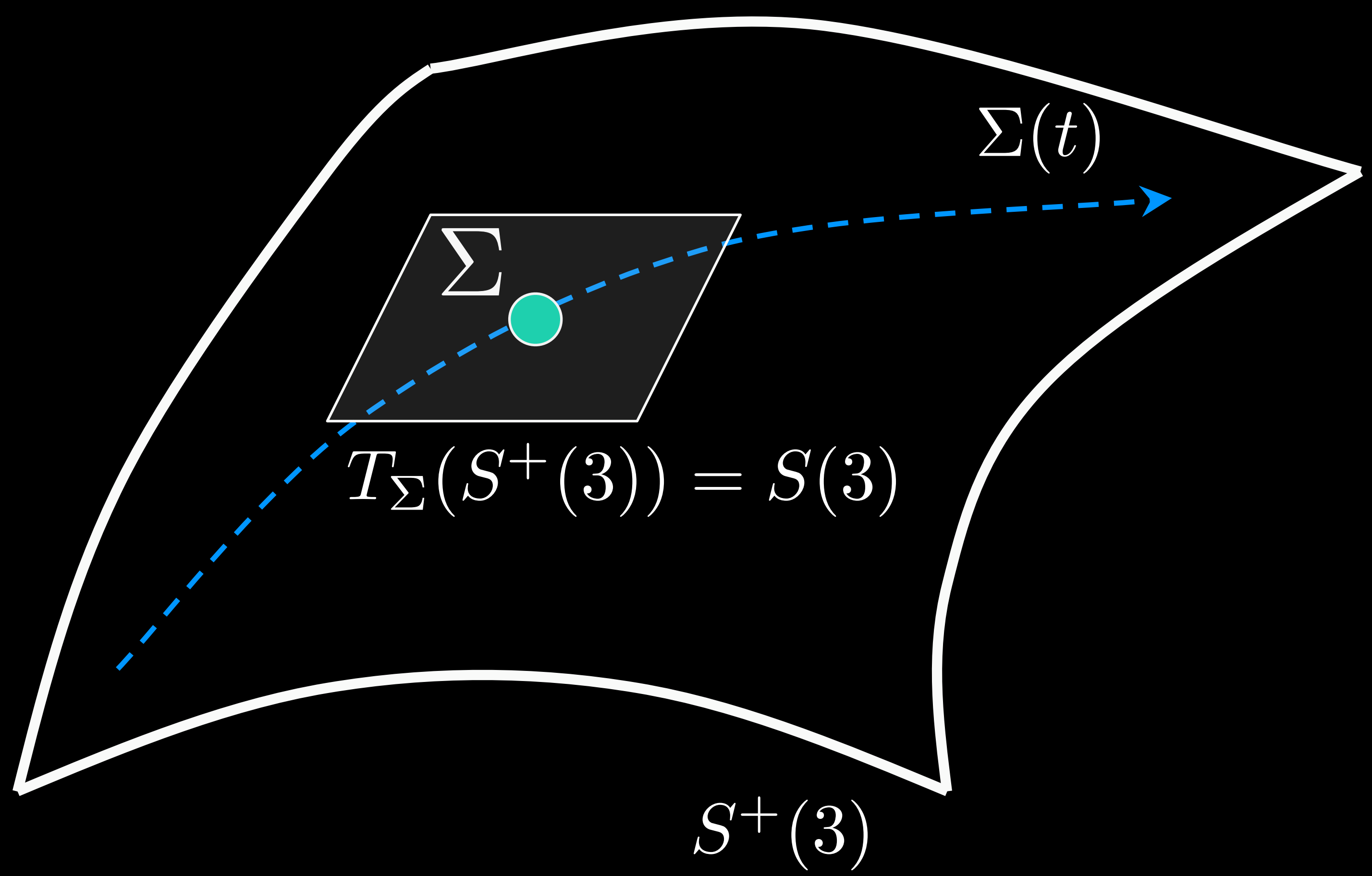

[Rao45], [Burbea-Rao82], [Amari90]

The Manifold of Multivariate Normal PDFs

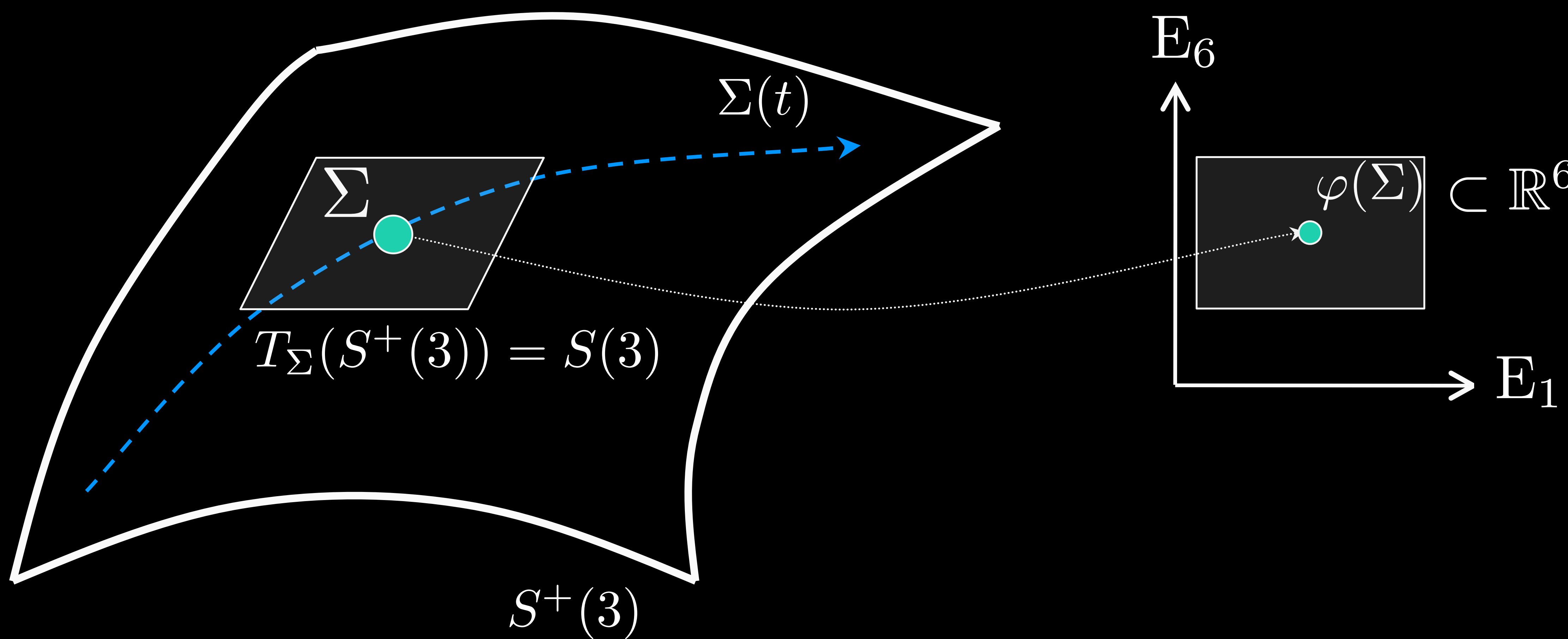

[Rao45], [Burbea-Rao82], [Amari90]

The Manifold of Multivariate Normal PDFs

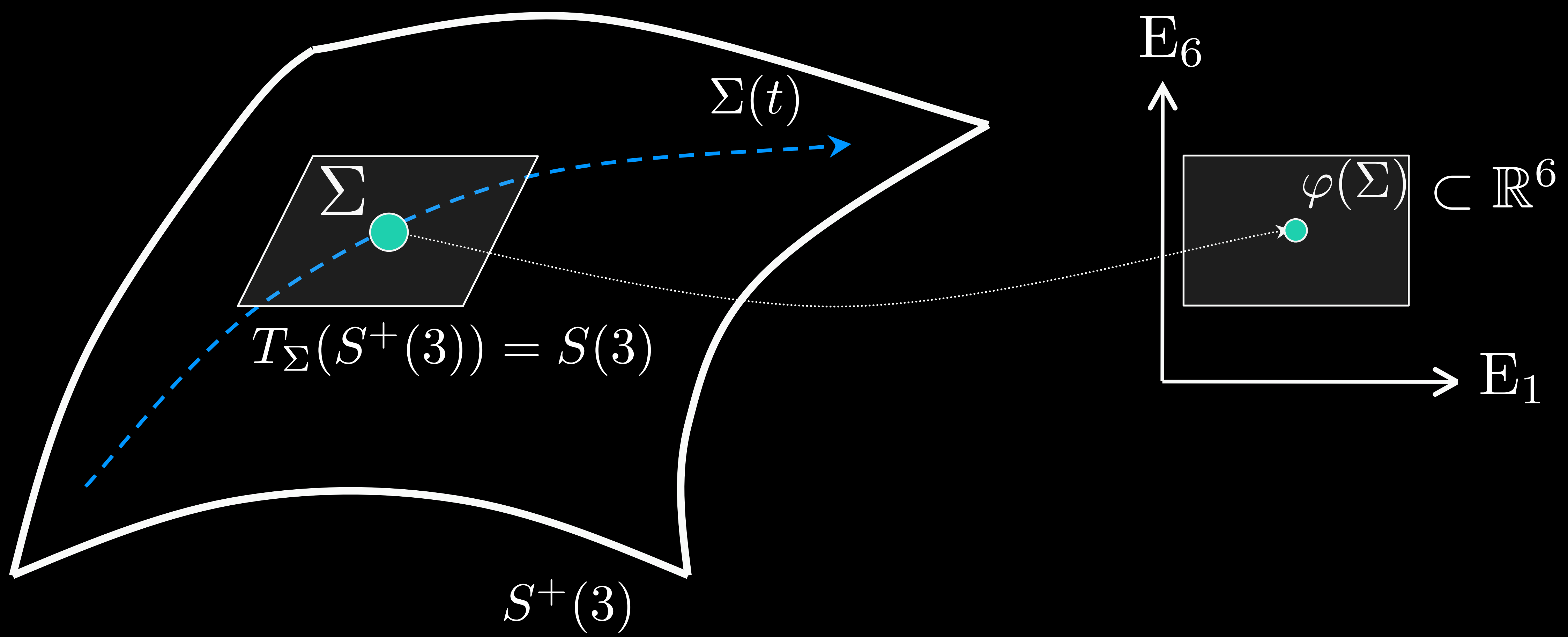

- But, there are many possible metrics between parameterized densities: Euclidean, J-divergence, Riemannian (more than one in fact!), Log-Euclidean... which one should we use and for what?

[Rao45], [Burbea-Rao82], [Amari90]

J-divergence (Kullback-Leibler)

- Distance: $$\mathcal{D}_j(A,B) = \sqrt{\frac{1}{2}\mathcal{D}_{kl}(A,B) + \mathcal{D}_{kl}(B,A)}$$

  where $$\mathcal{D}_{kl}(A,B) = \int_{\mathbb{R}^3} \mathcal{P}(r|A) \log \frac{\mathcal{P}(r|A)}{\mathcal{P}(r|B)} dr$$

- Invariance by congruence transformation:

$$\mathcal{D}_{kl}(A,B) = \mathcal{D}_{kl}(XAX^T, XBX^T) \quad \forall A,B \in S^+(3), X \in GL(3)$$

- For 3D Gaussian densities:

$$\mathcal{D}_j(A,B) = \sqrt{\frac{1}{4}(A^{-1}B + B^{-1}A) - 6}$$

$$\nabla_A \mathcal{D}_j^2(A,B) = \frac{1}{4}(B^{-1} - A^{-1}BA^{-1})$$

[Lenglet-etal04], [Wang-Vemuri04/05], [Lenglet-etal06]

Riemannian Metric

- The Fisher information matrix is a measure of the amount of information carried by realizations of a random variable about the unknown parameters of the underlying distribution:

$$g_{ij} = \int_{\mathbb{R}^3} \frac{\partial \mathcal{P}(r|\Sigma)}{\partial \Sigma^i} \frac{\partial \mathcal{P}(r|\Sigma)}{\partial \Sigma^j} \mathcal{P}(r|\Sigma) dr \quad i, j = 1, ..., 6$$

- Riemannian metric for Gaussian densities

$$\langle A, B \rangle_\Sigma = \frac{1}{2} \mathrm{trace} \left(\Sigma^{-1} A \Sigma^{-1} B \right) \quad \forall A, B \in S(3)$$

Riemannian Metric

- The Fisher information matrix is a measure of the amount of information carried by realizations of a random variable about the unknown parameters of the underlying distribution:

$$g_{ij} = \int_{\mathbb{R}^3} \frac{\partial \mathcal{P}(r|\Sigma)}{\partial \Sigma^i} \frac{\partial \mathcal{P}(r|\Sigma)}{\partial \Sigma^j} \mathcal{P}(r|\Sigma) dr \quad i, j = 1, \ldots, 6$$

- Riemannian metric for Gaussian densities

$$\langle A, B \rangle_\Sigma = \frac{1}{2} \mathrm{trace} \left(\Sigma^{-1} A \Sigma^{-1} B \right) \quad \forall A, B \in S(3)$$

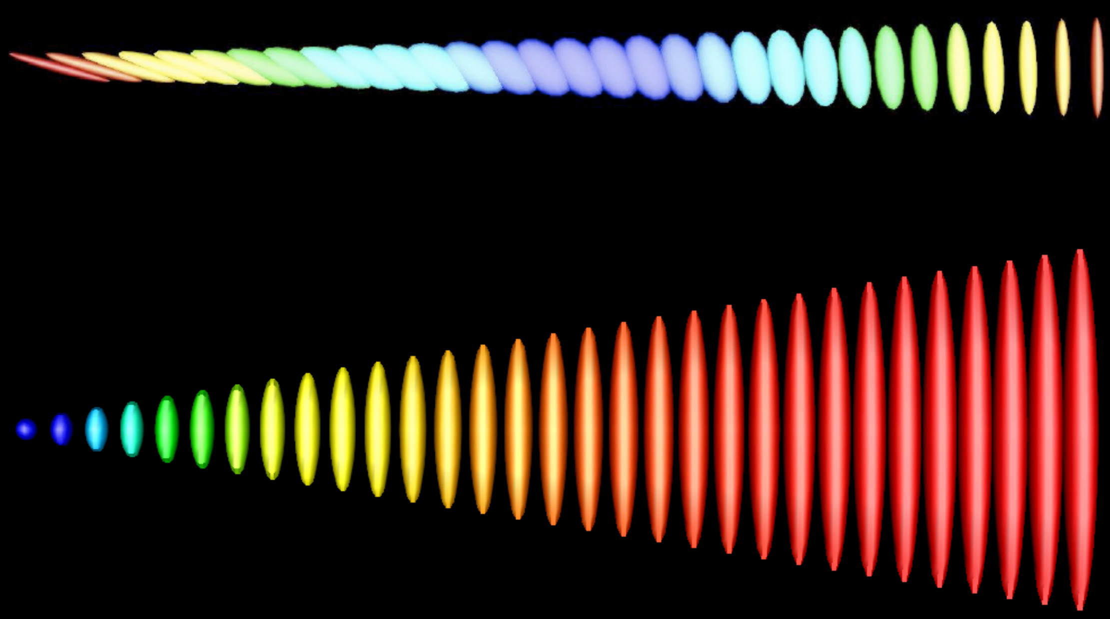

Euclidean metric

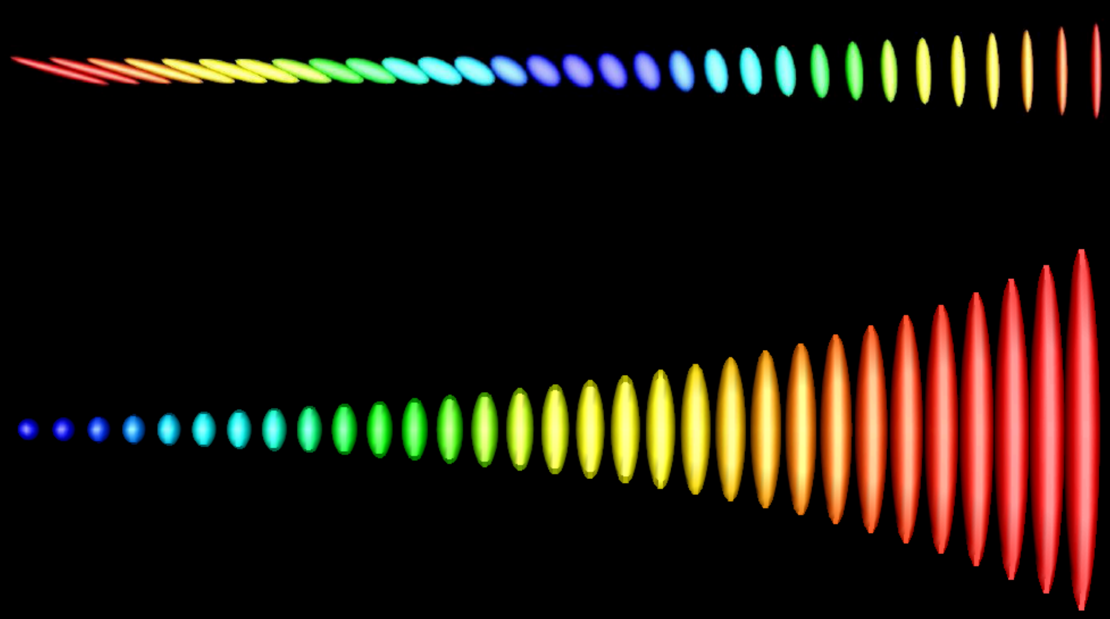

Riemannian metric

Riemannian Metric, Geodesics

- Geodesic equations:

$$\frac{d^2\Sigma^k(t)}{dt^2} + \Gamma^k_{ij}\frac{d\Sigma^i(t)}{dt}\frac{d\Sigma^j(t)}{dt} = 0\,\forall k = 1, ..., n$$

have a closed-form solution:

$$\Sigma(t) = \Sigma_0^{1/2}\exp\left(t\Sigma_0^{-1/2}\dot{\Sigma}_0\Sigma_0^{-1/2}\right)\Sigma_0^{1/2}\,\forall t \in [0,1]$$

- Geodesic distance (Jensen, 1976)

$$\mathcal{D}_g(\Sigma_1, \Sigma_2) = \sqrt{\tfrac{1}{2}\mathrm{trace}\left(\log^2\left(\Sigma_1^{-1/2}\Sigma_2\Sigma_1^{-1/2}\right)\right)}$$

[Atkinson-Mitchell81], [Skovgaard84], [Calvo-Oller92]

Riemannian Statistics

- The mean of set of tensors can be computed as the minimizer of the variance with

$$\beta_i = -\nabla \mathcal{D}_g^2(\overline{\Sigma}_g, \Sigma_i) = \overline{\Sigma}_g \log(\overline{\Sigma}_g^{-1} \Sigma_i) \in S_{\overline{\Sigma}_g}(3)$$

Geodesic gradient descent:

$$\overline{\Sigma}_{t+1} = \overline{\Sigma}_t^{1/2} \exp\left(-dt \overline{\Sigma}_t^{-1/2} \left(\frac{1}{N}\sum_{i=1}^{N} \beta_i\right) \overline{\Sigma}_t^{-1/2}\right) \overline{\Sigma}_t^{1/2}$$

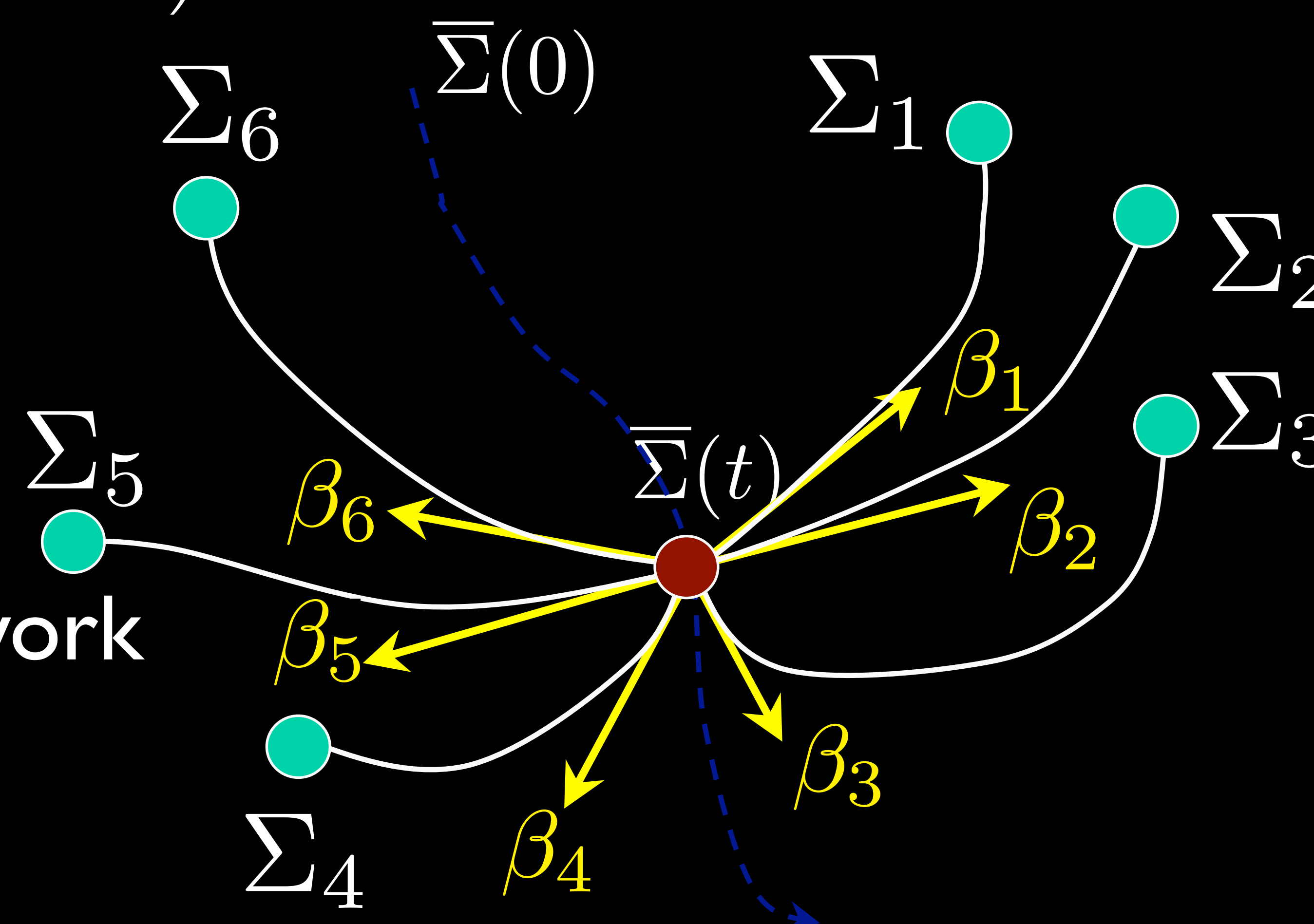

- Covariance matrix:

$$\Lambda_g = \frac{1}{N-1}\sum_{i=1}^{N} \beta_i \beta_i^T$$

- Recent Log-Euclidean framework

[Fletcher-etal04], [Lenglet-etal04/06], [Pennec-etal04/06], [Arsigny-etal05/06], [Schwartzmann06], [Moakher05], [Kindlmann07]

Spherical Harmonics

- Basis for complex functions on the unit sphere
- Analogous to Fourier transform: SH series of any function
- Even order SH are antipodally symmetric
- Satisfy the angular part of the Laplace equation:

$$\underbrace{\frac{1}{\sin\theta}\frac{\partial}{\partial\theta}\left(\sin\theta\frac{\partial Y_l^m}{\partial\theta}\right)+\frac{1}{\sin^2\theta}\frac{\partial^2 Y_l^m}{\partial\phi^2}}_{\Delta_b Y_l^m}+l(l+1)Y_l^m=0$$

- SH of order *l* and degree *m* are:

$$Y_l^m(\theta,\phi)=\sqrt{\frac{2l+1}{4\pi}\frac{(l-m)!}{(l+m)!}}P_l^m(\cos\theta)e^{im\phi}$$

- SH series fit of discrete data

$$X=BC$$

$$\Rightarrow C=(B^TB)^{-1}B^TX$$

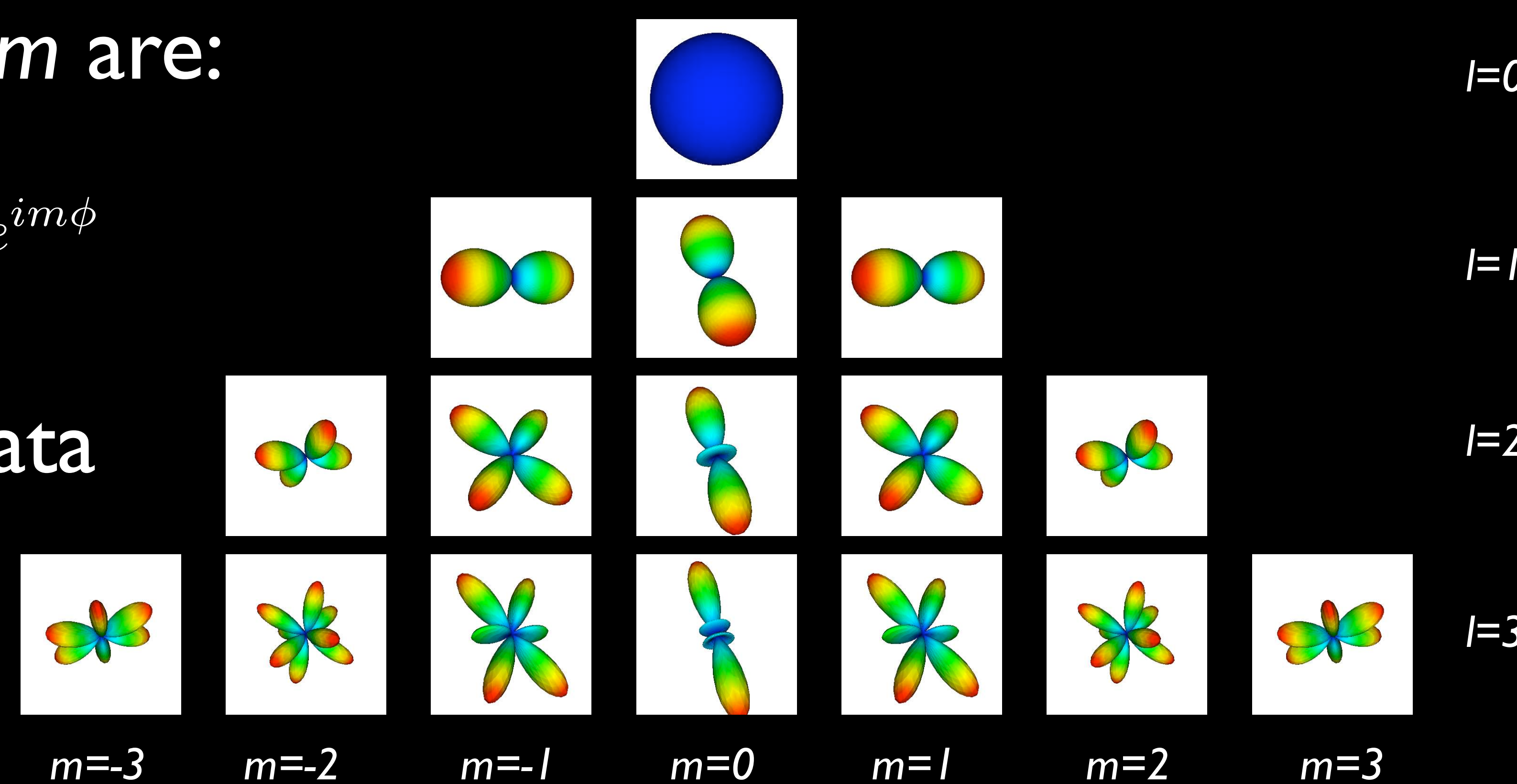

Reconstruction Methods for Local Diffusion Models

(with contributions from M. Descoteaux)

Tensors Estimation

- Linearize the Stejskal-Tanner equation: $-\frac{1}{b}\ln\left(\frac{S(q_k)}{S_0}\right) = g_k^T \mathbf{D} g_k$
- For N diffusion gradients and with

$$G_k = (g_k^1 g_k^1,\ 2g_k^1 g_k^2,\ 2g_k^1 g_k^3,\ g_k^2 g_k^2,\ 2g_k^2 g_k^3,\ g_k^3 g_k^3)^T \in \mathbb{R}^6$$

and $\varphi(\mathbf{D}) = (D_{xx},\ D_{xy},\ D_{xz},\ D_{yy},\ D_{yz},\ D_{zz})^T \in \mathbb{R}^6$

- We end up with the linear system:

$$\underbrace{\begin{bmatrix} G_1^T \\ \vdots \\ G_N^T \end{bmatrix}}_{\mathbf{G}} \varphi(\mathbf{D}) = \underbrace{\begin{bmatrix} -\frac{1}{b}\ln\left(\frac{S_1}{S_0}\right) \\ \vdots \\ -\frac{1}{b}\ln\left(\frac{S_N}{S_0}\right) \end{bmatrix}}_{\mathbf{Y}} \Rightarrow \varphi(\mathbf{D}) = \left(\left(\mathbf{G}^T\mathbf{G}\right)^{-1}\mathbf{G}^T\right)\mathbf{Y}$$

- Simple and fast but no positivity constraint...

[Westin-etal02], [Mangin-etal02], [Tschumperlé-etal03], [Wang-etal04], [Niethammer-etal06], [Koay-etal06] [Fillard-etal05/07]

Constrained Tensors Estimation

- Minimize the energy: $$\mathscr{E}(S_0, ..., S_N) = \sum_{k=1}^{N} \psi \underbrace{\left(\frac{1}{b} \ln \left(\frac{S_k}{S_0} \right) + g_k^T \mathbf{D} g_k \right)}_{r_k(\mathbf{D})}$$
- Intrinsic gradient: $$\nabla \mathscr{E} = \sum_{k=1}^{N} \psi'(r_k(\mathbf{D}))\mathbf{D} g_k \left(\mathbf{D} g_k\right)^T$$ (ψ *M*-estimator)
- Intrinsic gradient descent:

$$\mathbf{D}_{l+1} = \mathbf{D}_l^{1/2} \exp \left(-dt\, \mathbf{D}_l^{-1/2} \left(\sum_{k=1}^{N} \psi'(r_k(\mathbf{D}_l))\mathbf{D}_l g_k \left(\mathbf{D}_l g_k\right)^T \right) \mathbf{D}_l^{-1/2} \right) \mathbf{D}_l^{1/2}$$

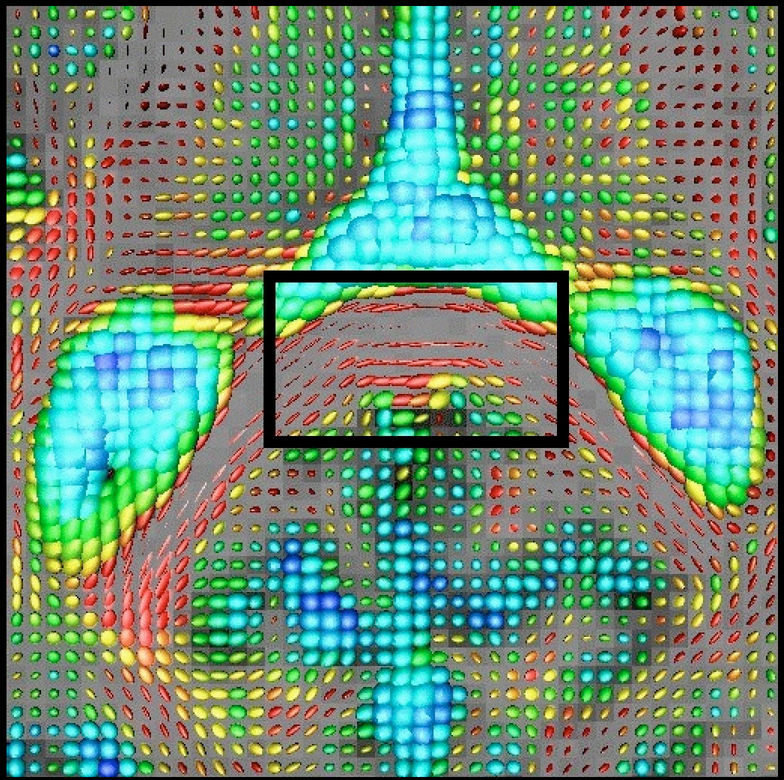

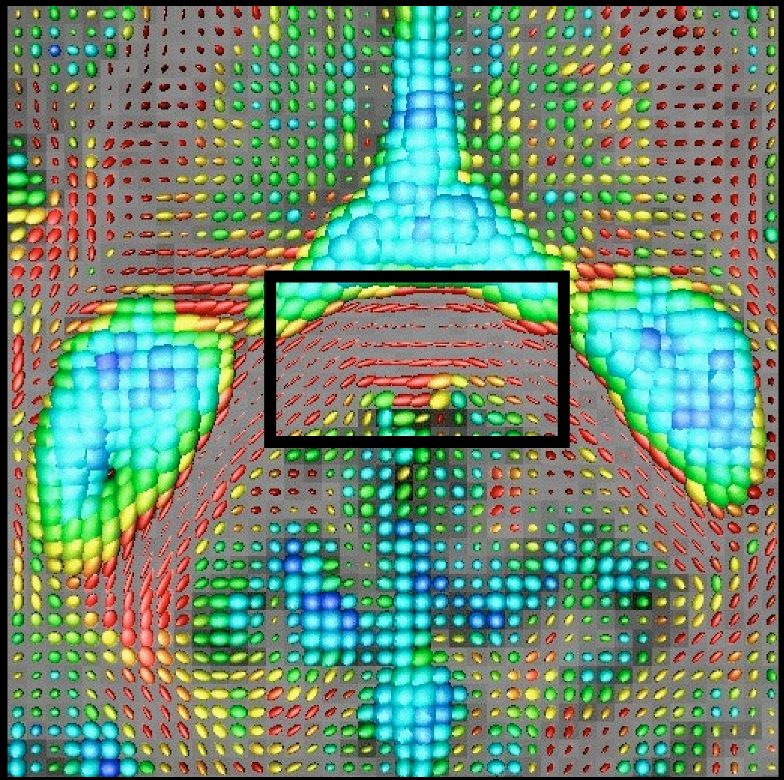

Constrained Tensors Estimation

- Minimize the energy: $$\mathscr{E}(S_0, ..., S_N) = \sum_{k=1}^{N} \psi \underbrace{\left(\frac{1}{b} \ln \left(\frac{S_k}{S_0} \right) + g_k^T \mathbf{D} g_k \right)}_{r_k(\mathbf{D})}$$
- Intrinsic gradient: $$\nabla \mathscr{E} = \sum_{k=1}^{N} \psi'(r_k(\mathbf{D})) \mathbf{D} g_k \left(\mathbf{D} g_k \right)^T$$ (ψ M-estimator)
- Intrinsic gradient descent:

$$\mathbf{D}_{l+1} = \mathbf{D}_l^{1/2} \exp \left(-dt\, \mathbf{D}_l^{-1/2} \left(\sum_{k=1}^{N} \psi'(r_k(\mathbf{D}_l)) \mathbf{D}_l g_k \left(\mathbf{D}_l g_k \right)^T \right) \mathbf{D}_l^{-1/2} \right) \mathbf{D}_l^{1/2}$$

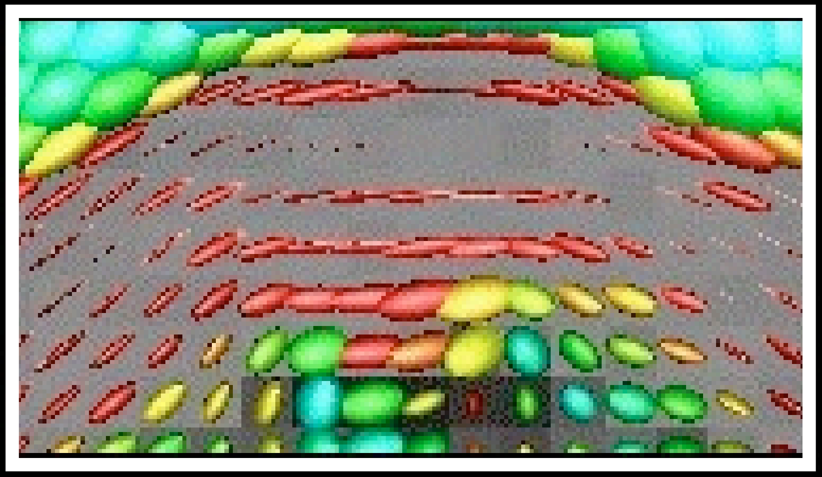

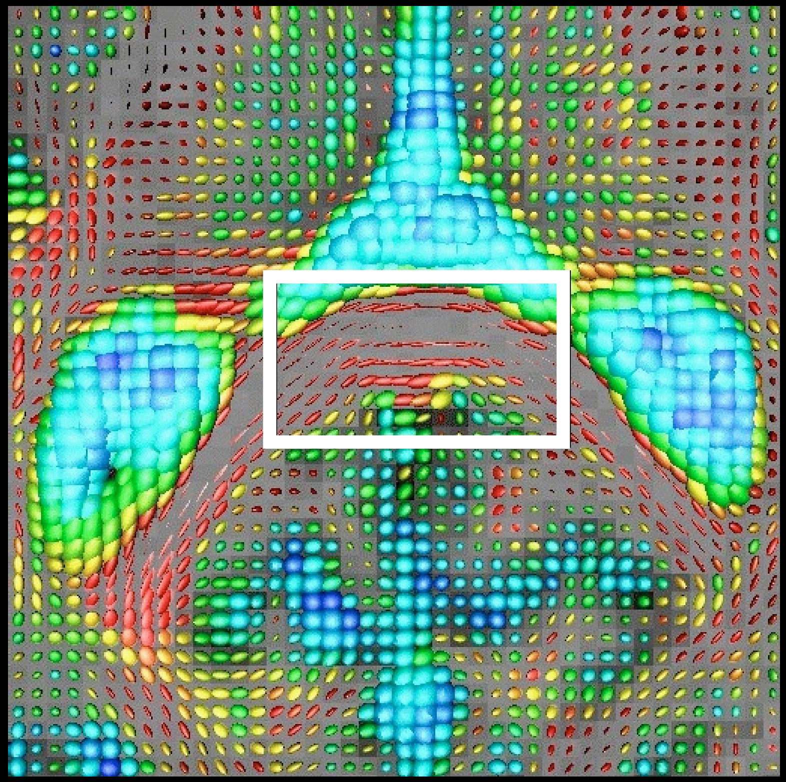

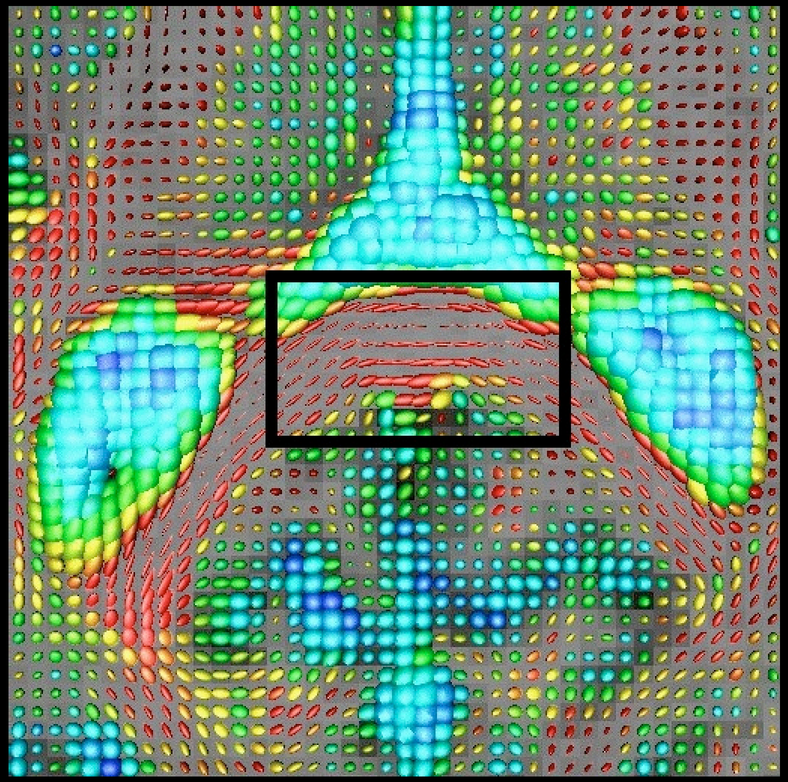

Constrained Tensors Estimation

- Minimize the energy: $\mathscr{E}(S_0, ..., S_N) = \sum_{k=1}^{N} \psi \underbrace{\left(\frac{1}{b} \ln \left(\frac{S_k}{S_0} \right) + g_k^T \mathbf{D} g_k \right)}_{r_k(\mathbf{D})}$
- Intrinsic gradient: $\nabla \mathscr{E} = \sum_{k=1}^{N} \psi'(r_k(\mathbf{D})) \mathbf{D} g_k \left(\mathbf{D} g_k \right)^T$ (ψ M-estimator)
- Intrinsic gradient descent:

$$\mathbf{D}_{l+1} = \mathbf{D}_l^{1/2} \exp \left(-dt \, \mathbf{D}_l^{-1/2} \left(\sum_{k=1}^{N} \psi'(r_k(\mathbf{D}_l)) \mathbf{D}_l g_k \left(\mathbf{D}_l g_k \right)^T \right) \mathbf{D}_l^{-1/2} \right) \mathbf{D}_l^{1/2}$$

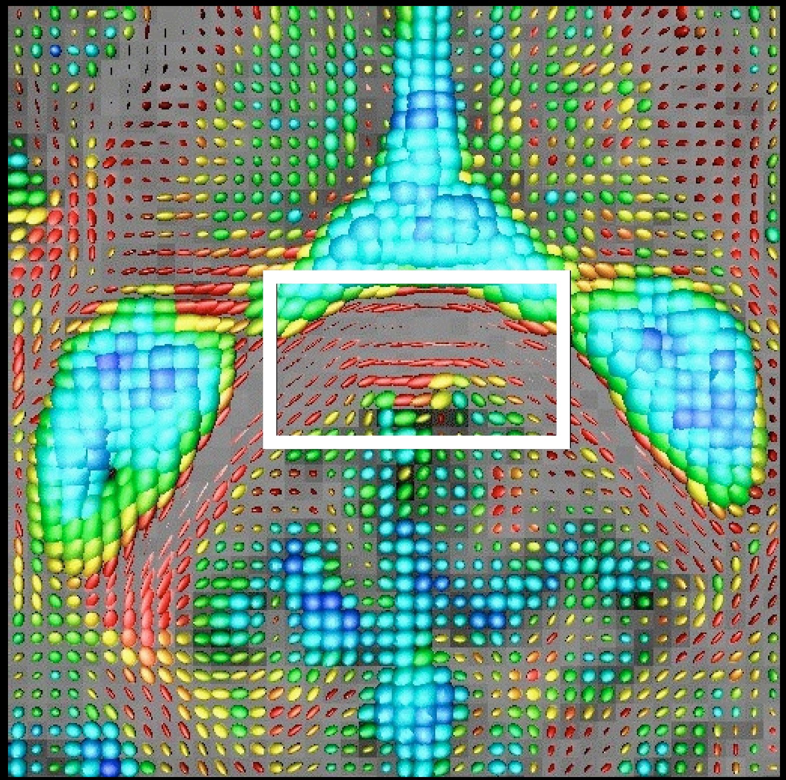

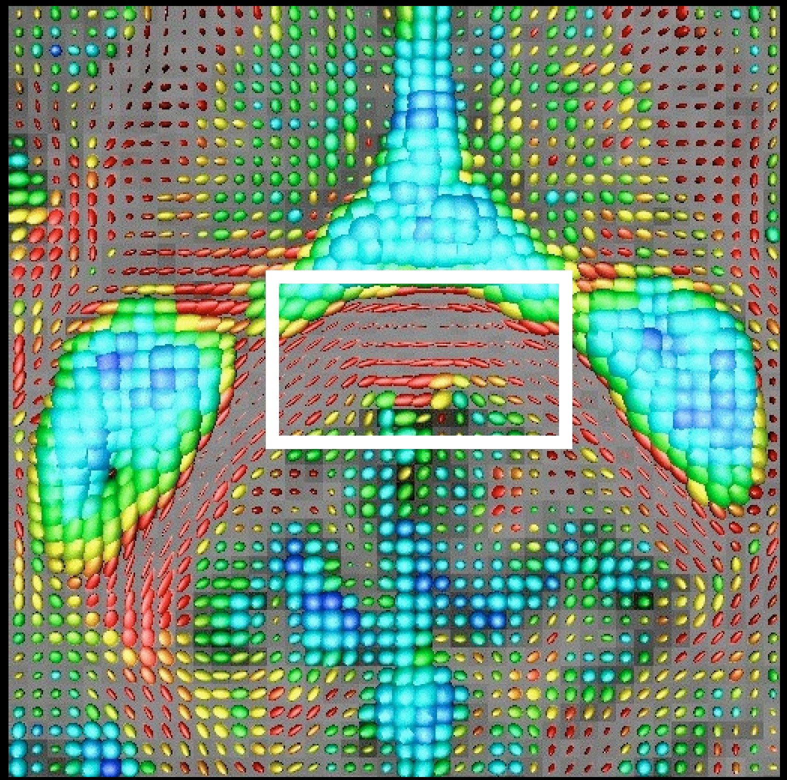

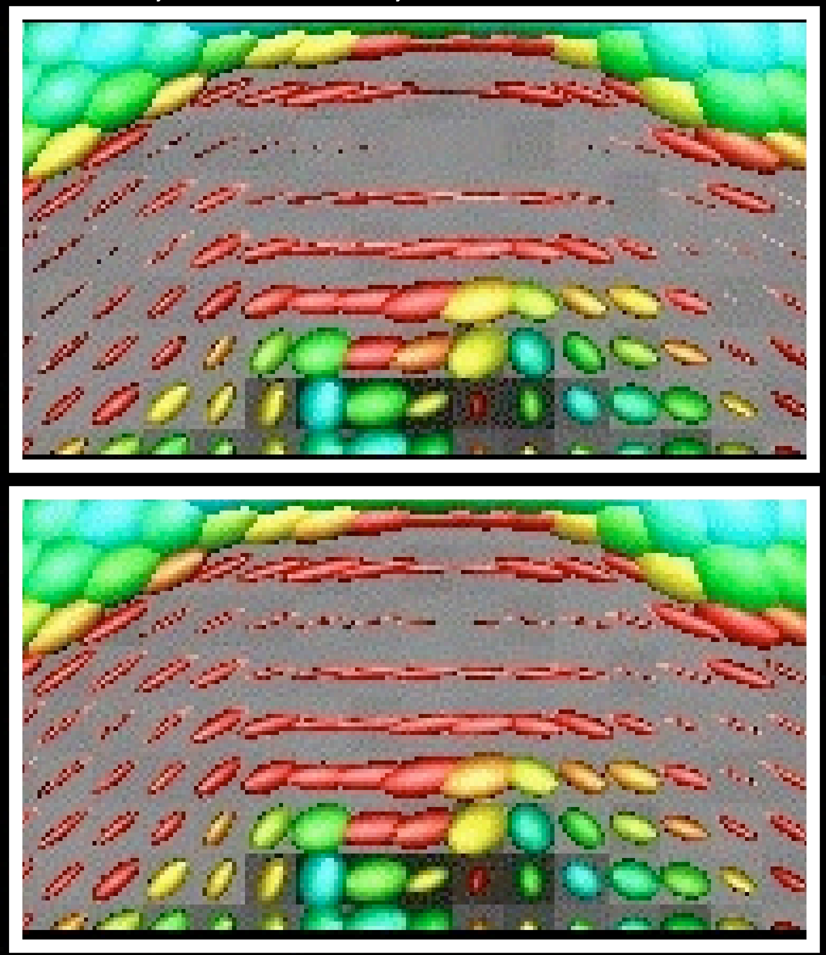

Diffusion ODFs Estimation

- Fast analytic ODF computation:

$$\psi(u) \simeq \mathcal{G}_{q'}[S(q)](u) = \int \delta(u^T q) S(q) dq$$

$$= \sum_{j=1}^{N} c_j \int_{|q|=1} \delta(u^T q) Y_j(q) dq \qquad \text{with} \quad S(q) = \sum_{j=1}^{N} c_j Y_j(q)$$

- The Funk-Radon transform is linear!

Funk-Hecke Theorem: Let f be a continuous function on $[-1, 1]$ and H_l any spherical harmonic of order l. Then, given a unit vector u

$$\int_{|v|=1} f(u^T v) H_l(v) dv = \lambda(l) H_l(u)$$

where

$$\lambda(l) = \frac{2\pi}{p_l(1)} \int_{-1}^{1} P_l(t) f(t) dt$$

with P_l the Legendre polynomial of degree l.

[Descoteaux *et al.* 2006], [Hess *et al.* *2006*]

Diffusion ODFs Estimation

- Fast analytic ODF computation:

$$\psi(u) \simeq \mathcal{G}_{q'}[S(q)](u) = \int \delta(u^T q) S(q) dq$$

$$= \sum_{j=1}^{N} c_j \int_{|q|=1} \delta(u^T q) Y_j(q) dq \qquad \text{with} \quad S(q) = \sum_{j=1}^{N} c_j Y_j(q)$$

- The Funk-Radon transform is linear!

with $\delta_n(x) = \frac{n}{\sqrt{\pi}} e^{-n^2 x^2}$ s.t. $\lim_{n\to\infty} \delta_n(x) = \delta(x)$, $\lim_{n\to\infty} \int_{\mathbb{R}} \delta_n(x) f(x) = f(0)$

$$\int \delta(u^T q) Y_j(q) dq = \int \lim_{n\to\infty} \delta_n(u^T q) Y_j(q) dq = 2\pi \frac{P_{l(j)}(0)}{P_{l(j)}(1)} Y_j(q)$$

and so $\quad \mathcal{G}_{q'}[S(q)](u) = \sum_j 2\pi \frac{P_{l(j)}(0)}{P_{l(j)}(1)} c_j Y_j(q)$

[Descoteaux *et al.* 2006], [Hess *et al.* 2006]

Brain Anatomical Connectivity Mapping

Neural fibers as shortest paths

(Joint work with E. Prados & J.P. Pons)

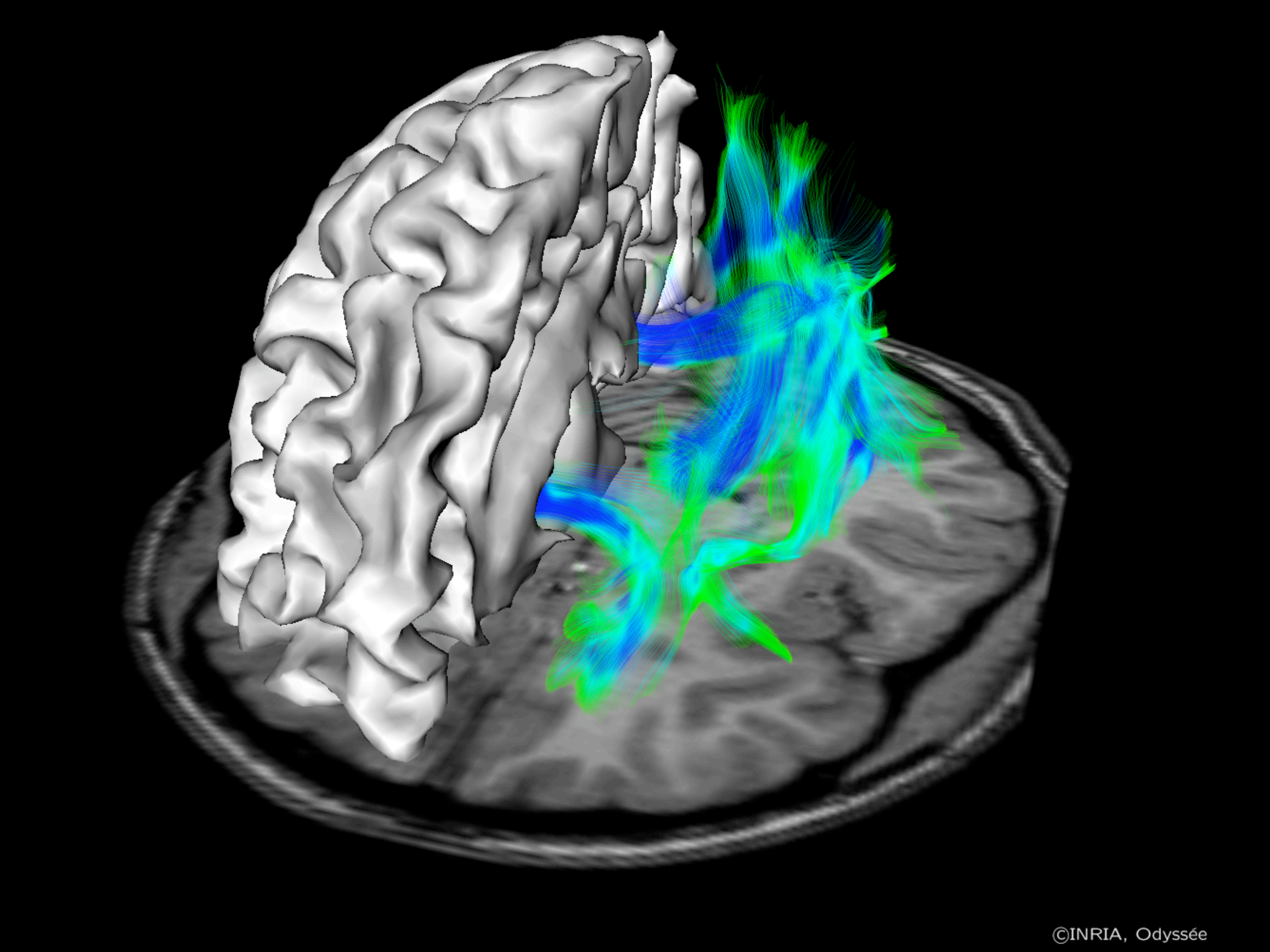
©INRIA, Odyssée

Fiber Tracts as Geodesic Paths

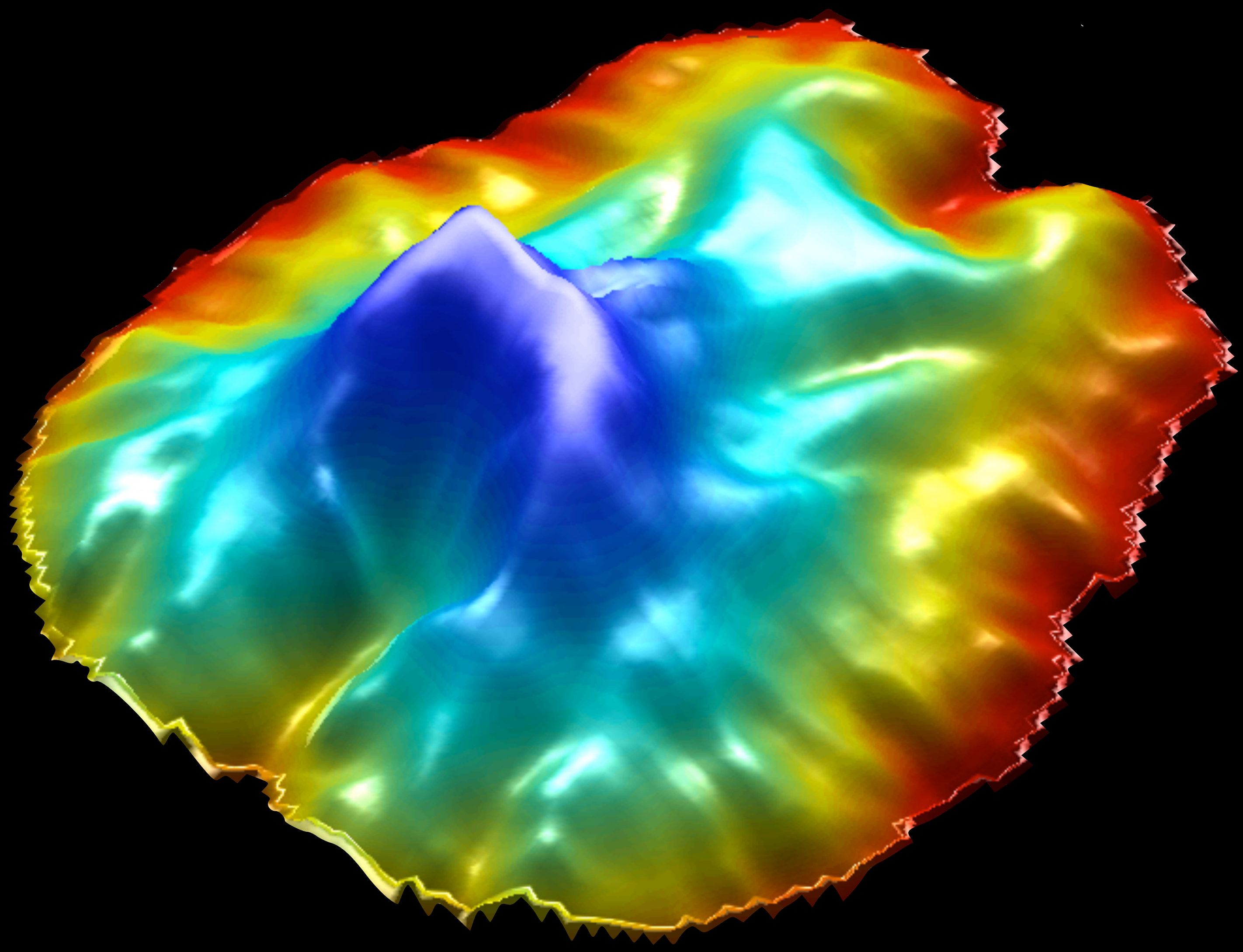

Distance function

Geodesics

Data: CEA-SHFJ, Orsay

Fiber Tracts as Geodesic Paths

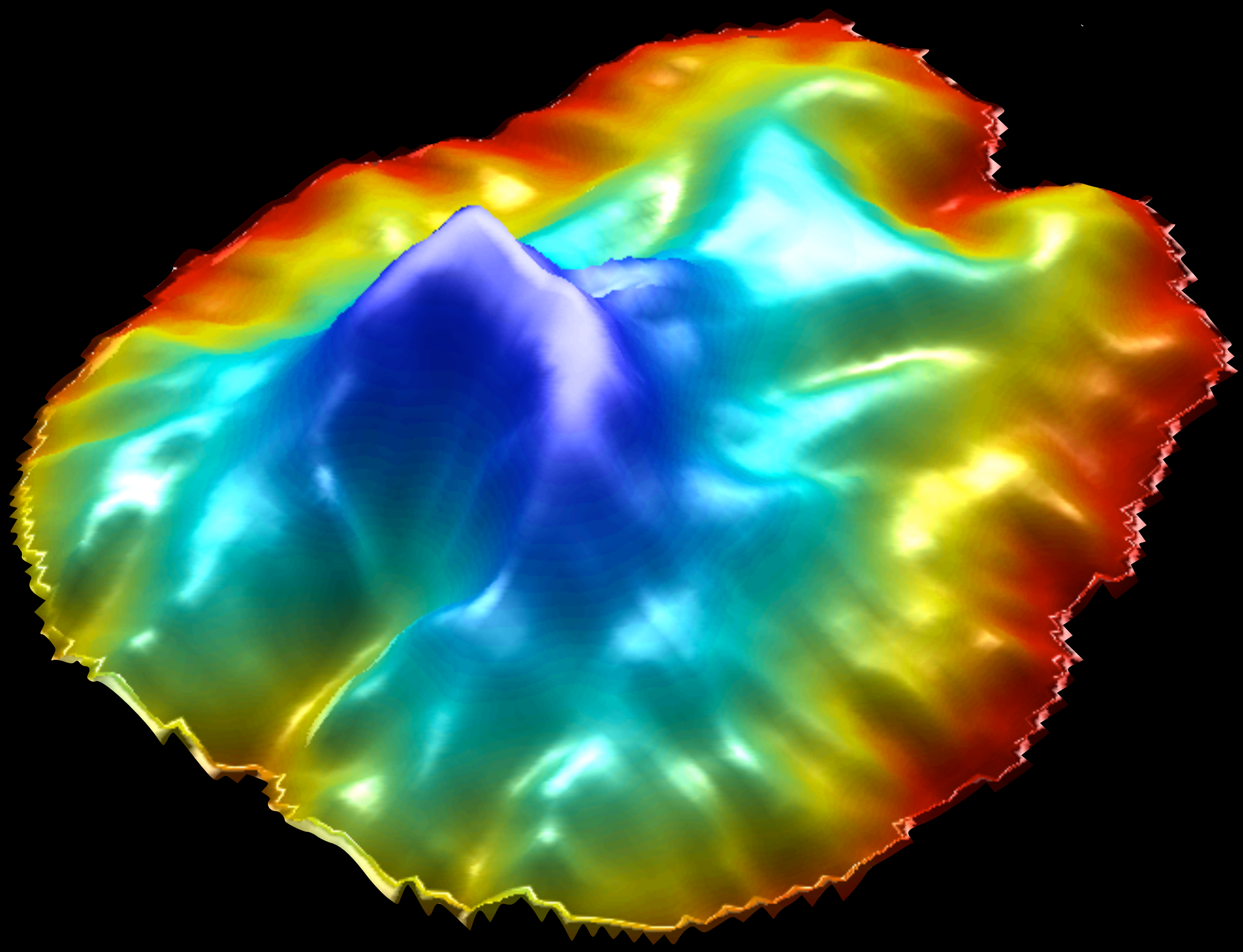

Distance function

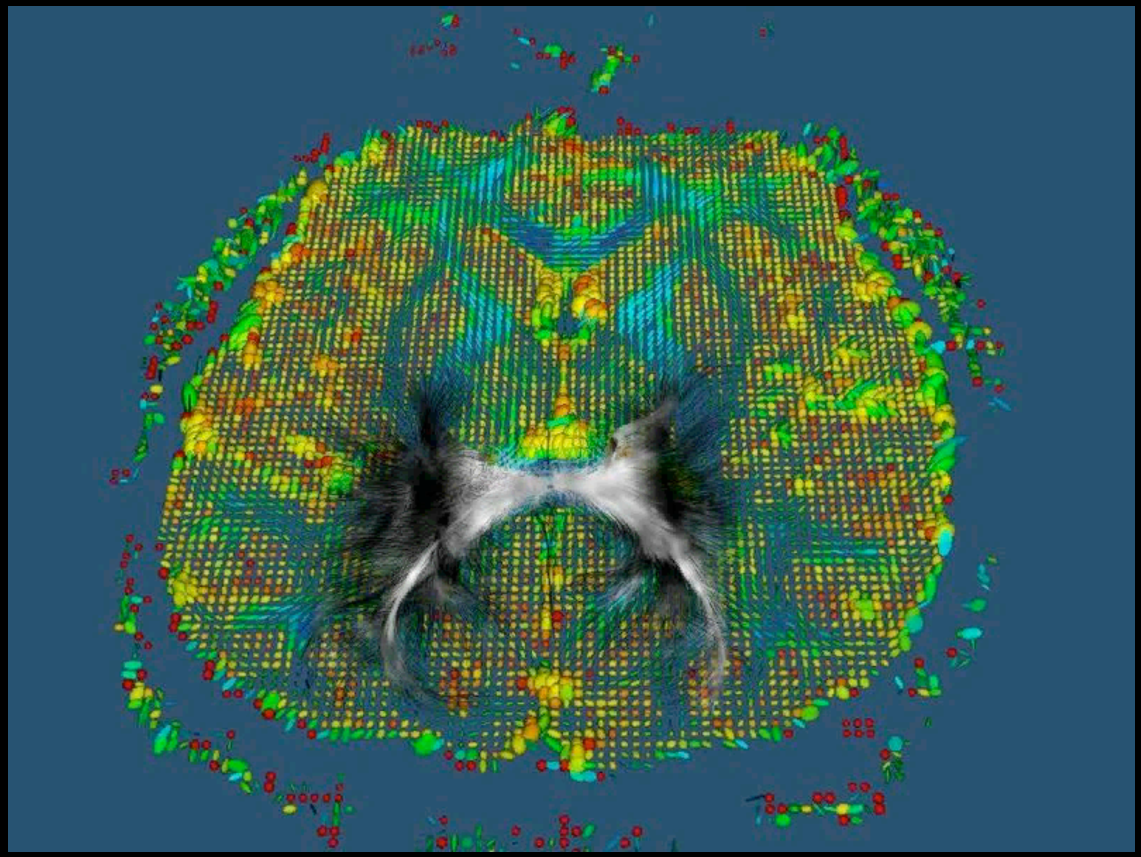

Geodesics

Data: CEA-SHFJ, Orsay

Geometry Induced by a Diffusion Process

Notion of diffusion variance metric: $G = \mathbf{D}^{-1}$

$\lambda_2 = 1$

$\mathrm{v} = (\mathrm{v}_1, v_2)^T \in \mathbb{R}^2$

$\|v\|\,?$

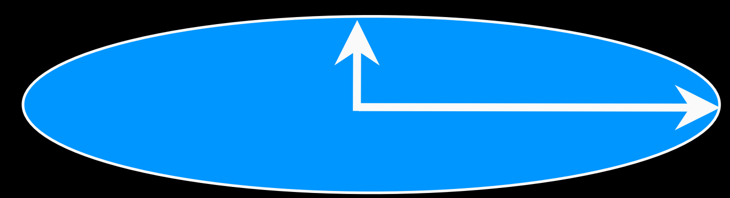

$\lambda_1 = 3 \Rightarrow \|v\|^2 = \frac{1}{3}v_1^2 + v_2^2$

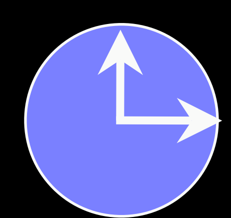

$\lambda_1 = 1 \Rightarrow \|v\|^2 = v_1^2 + v_2^2$

[Darling98], [de Lara95]

Geometry Induced by a Diffusion Process

Notion of diffusion variance metric: $G = \mathbf{D}^{-1}$

$\lambda_2 = 1$

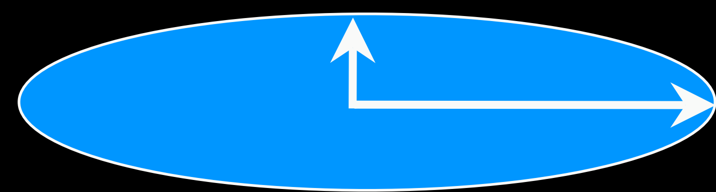

$\lambda_1 = 3 \Rightarrow \|v\|^2 = \frac{1}{3}v_1^2 + v_2^2$

$\mathrm{v} = (\mathrm{v}_1, v_2)^T \in \mathbb{R}^2$

$\|v\|\,?$

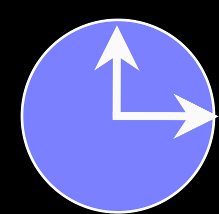

$\lambda_1 = 1 \Rightarrow \|v\|^2 = v_1^2 + v_2^2$

- Use the complete information provided by diffusion tensors
- How do we:
  - compute the geodesic distance?
  - compute the shortest paths (= fiber tracts?)
  - assess the likelihood of connection?

[Darling98], [de Lara95]

Intrinsic Distance Computation: 2 *perspectives*

The distance function ϕ is the unique solution of the anisotropic eikonal equation:

$$\|\mathrm{grad}\phi\| = \left(\frac{\partial\phi}{\partial \mathrm{x}^{\mathrm{i}}}\frac{\partial\phi}{\partial \mathrm{x}^{\mathrm{j}}}\mathrm{g}^{\mathrm{ij}}\right)^{1/2} = 1 \quad \text{in } \mathcal{M}\backslash \mathrm{x}_0$$

with $$\phi(x_0) = 0$$

Boundary value formulation

$$\|\mathrm{grad}\phi\| = 1$$

Front:

$$\mathcal{S}(t) = \{x \in \mathcal{M} : \phi(x) = t\}$$

Initial value formulation

$$\frac{\partial\psi}{\partial t} + \|\mathrm{grad}\psi\| = 0$$

Front:

$$\mathcal{S}(t) = \{x \in \mathcal{M} : \psi(x,t) = 0\}$$

[Crandall-Evans-Lions84], [Osher93], [Kimmel-etal95], [Mantegazza02]

Intrinsic Distance Computation: 2 *perspectives*

The distance function ϕ is the unique solution of the anisotropic eikonal equation:

$$\|\mathrm{grad}\phi\| = \left(\frac{\partial\phi}{\partial \mathrm{x}^{\mathrm{i}}}\frac{\partial\phi}{\partial \mathrm{x}^{\mathrm{j}}}\mathrm{g}^{\mathrm{ij}}\right)^{1/2} = 1 \quad \text{in } \mathcal{M}\backslash \mathrm{x}_0$$

with $$\phi(x_0) = 0$$

Boundary value formulation

$$\|\mathrm{grad}\phi\| = 1$$

Front:

$$\mathcal{S}(t) = \{x \in \mathcal{M} : \phi(x) = t\}$$

Initial value formulation

$$\frac{\partial\psi}{\partial t} + \|\mathrm{grad}\psi\| = 0$$

Front:

$$\mathcal{S}(t) = \{x \in \mathcal{M} : \psi(x,t) = 0\}$$

[Crandall-Evans-Lions84], [Osher93], [Kimmel-etal95], [Mantegazza02]

Boundary Value Formulation (Fast Marching)

- FMM constructs solution by propagating information one way: From small to large values.

- Key point: Approximation of the differential $\mathrm{d}\phi \in T_x^*\mathcal{M}$ in the Hamiltonian :

$$\mathrm{H}(\mathrm{x},\mathrm{d}\phi) = d\phi^T G(x) d\phi - 1$$

Boundary Value Formulation (Fast Marching)

- FMM constructs solution by propagating information one way: From small to large values.

- Key point: Approximation of the differential $\mathrm{d}\phi \in T_x^*\mathcal{M}$ in the Hamiltonian :

$$\mathrm{H}(\mathrm{x},\mathrm{d}\phi) = d\phi^T G(x) d\phi - 1$$

- Choose optimal combination of neighbors (optimal simplex) that yields the smallest value of ϕ

- Used to compute, on the fly, geodesics' velocity $\gamma'(x)$ and statistics of a *connectivity measure*

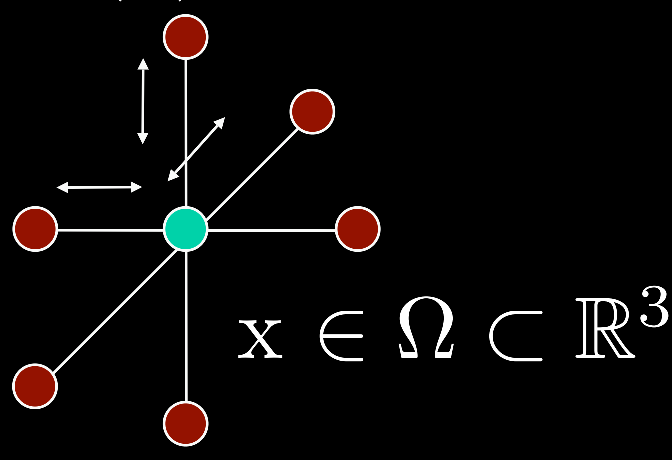

Boundary Value Formulation (Fast Marching)

- FMM constructs solution by propagating information one way: From small to large values.

- Key point: Approximation of the differential $\mathrm{d}\phi \in T_x^*\mathcal{M}$ in the Hamiltonian :

$$\mathrm{H}(\mathrm{x},\mathrm{d}\phi) = d\phi^T G(x) d\phi - 1$$

- Choose optimal combination of neighbors (optimal simplex) that yields the smallest value of ϕ

- Used to compute, on the fly, geodesics' velocity $\gamma'(x)$ and statistics of a *connectivity measure*

$$\mathrm{C}(\mathrm{x}) = \sqrt{\gamma'(x) D(x)^\alpha \gamma'(x)}$$

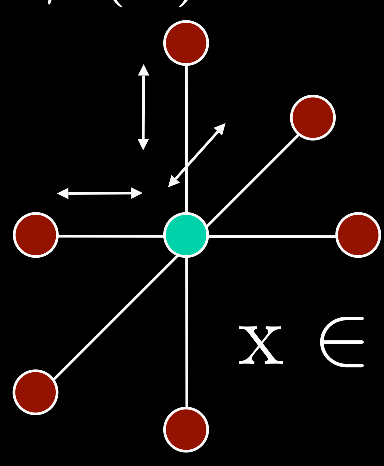

$\mathrm{x} \in \Omega \subset \mathbb{R}^3$

Boundary Value Formulation (Fast Marching)

1. Boundary value

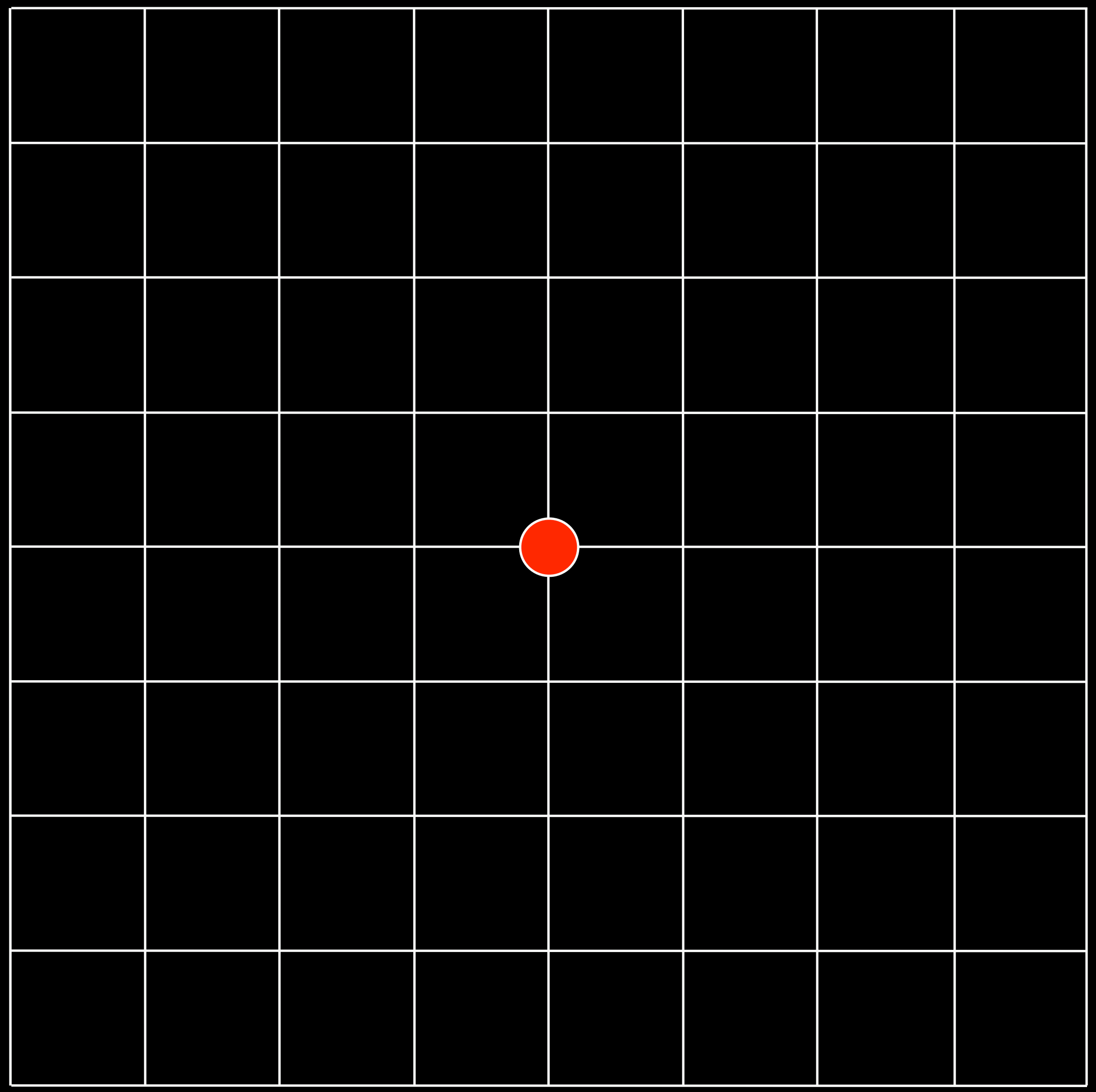

Boundary Value Formulation (Fast Marching)

1. Boundary value

2. Update “downwind”

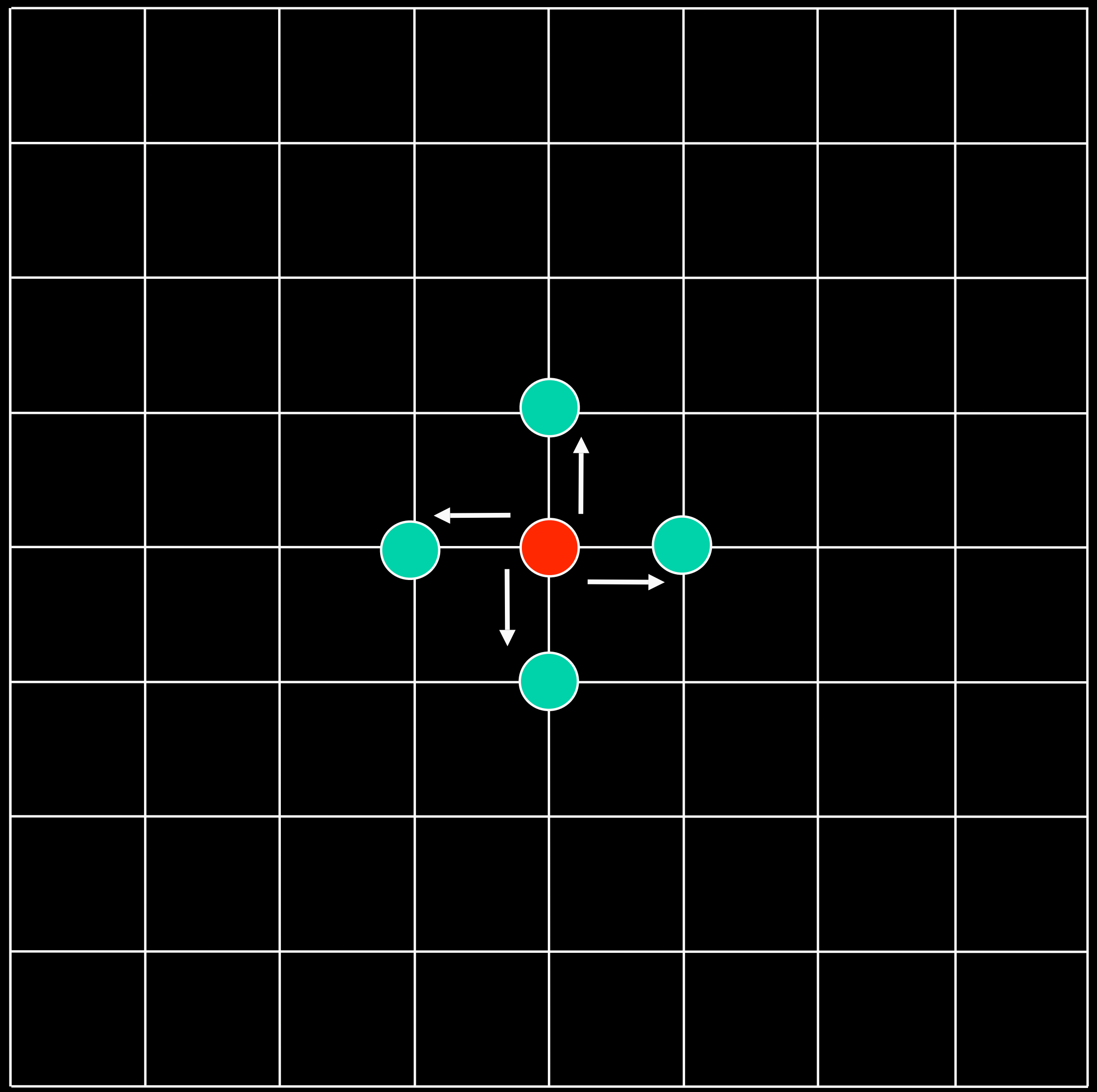

Boundary Value Formulation (Fast Marching)

1. Boundary value

2. Update "downwind"

3. Compute new possible values

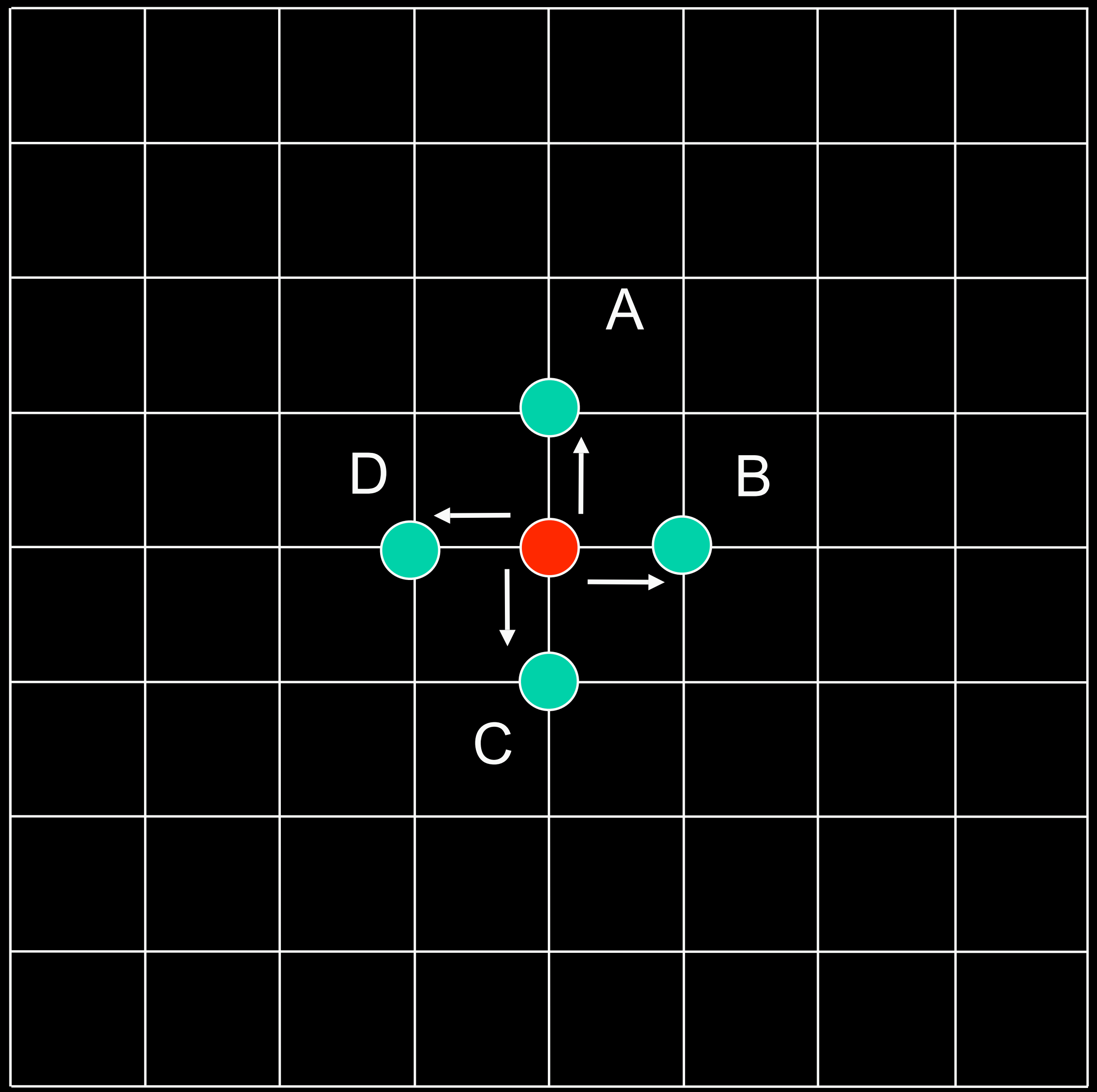

Boundary Value Formulation (Fast Marching)

1. Boundary value

2. Update "downwind"

3. Compute new possible values

4. Choose smallest green sphere (for example A)

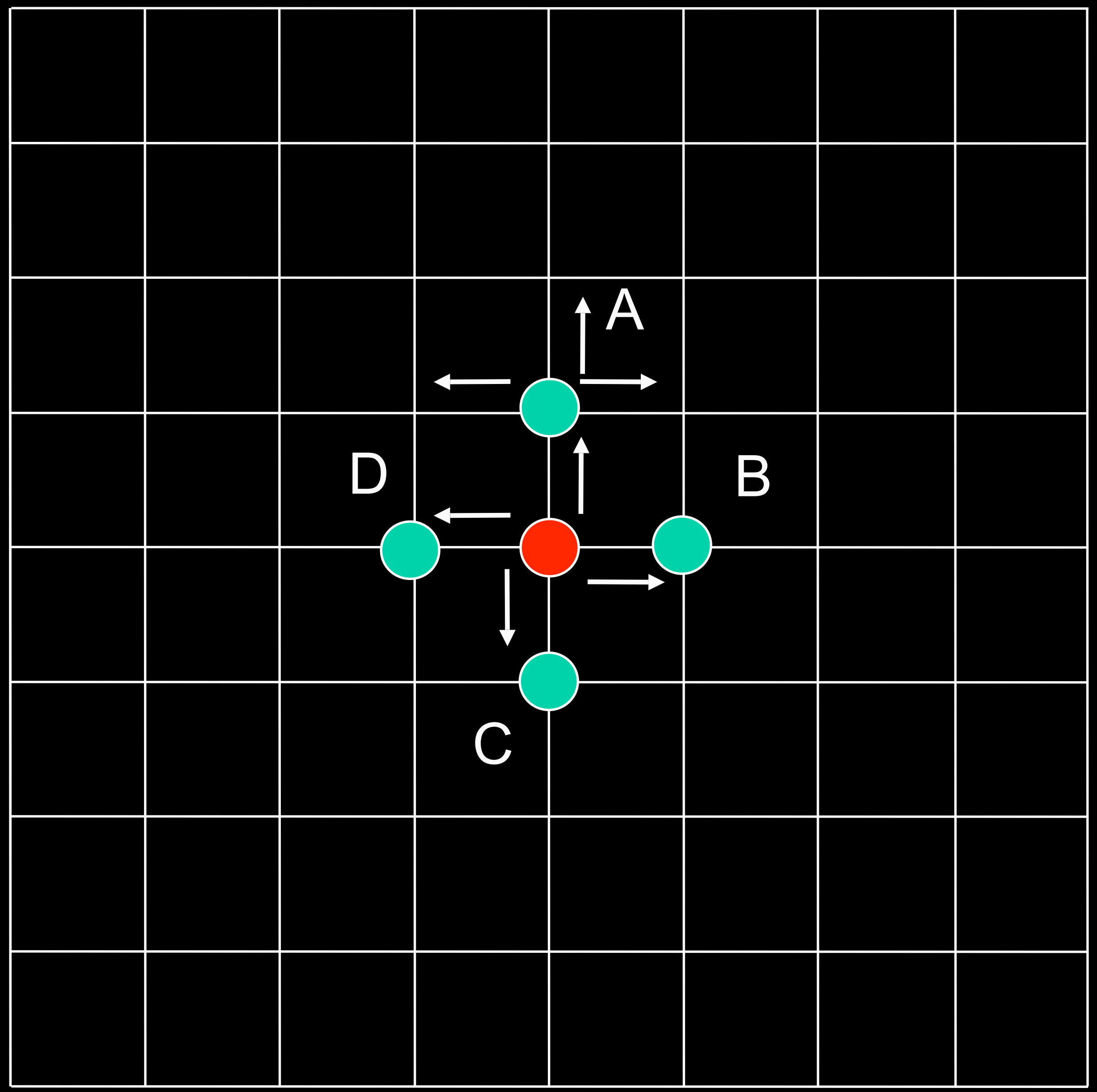

Boundary Value Formulation (Fast Marching)

1. Boundary value

2. Update “downwind”

3. Compute new possible values

4. Choose smallest green sphere (for example A)

5. Freeze value A, update neighboring “downwind” points

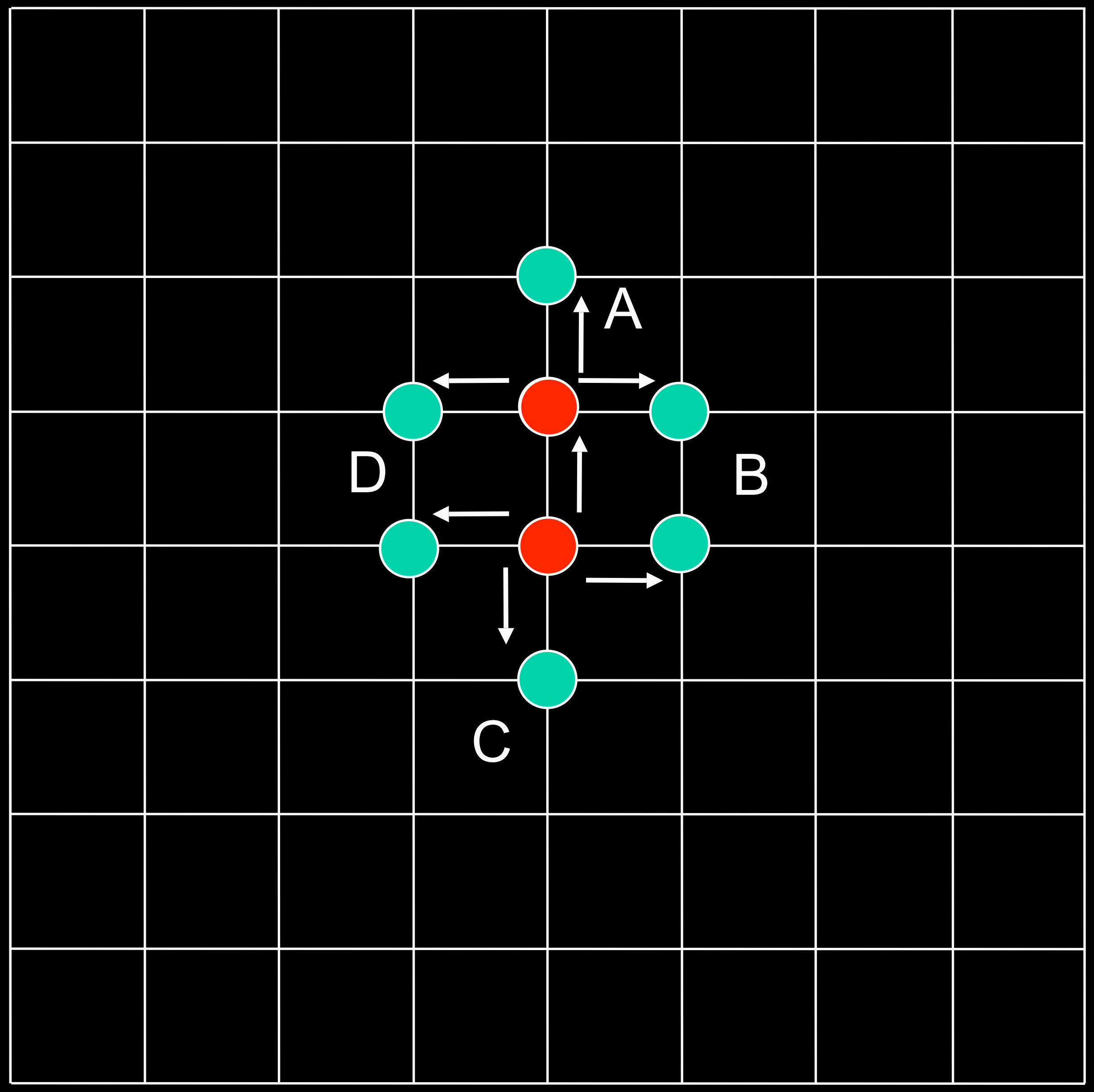

Boundary Value Formulation (Fast Marching)

1. Boundary value

2. Update “downwind”

3. Compute new possible values

4. Choose smallest green sphere (for example A)

5. Freeze value A, update neighboring “downwind” points

4. Choose smallest green sphere (for example B)

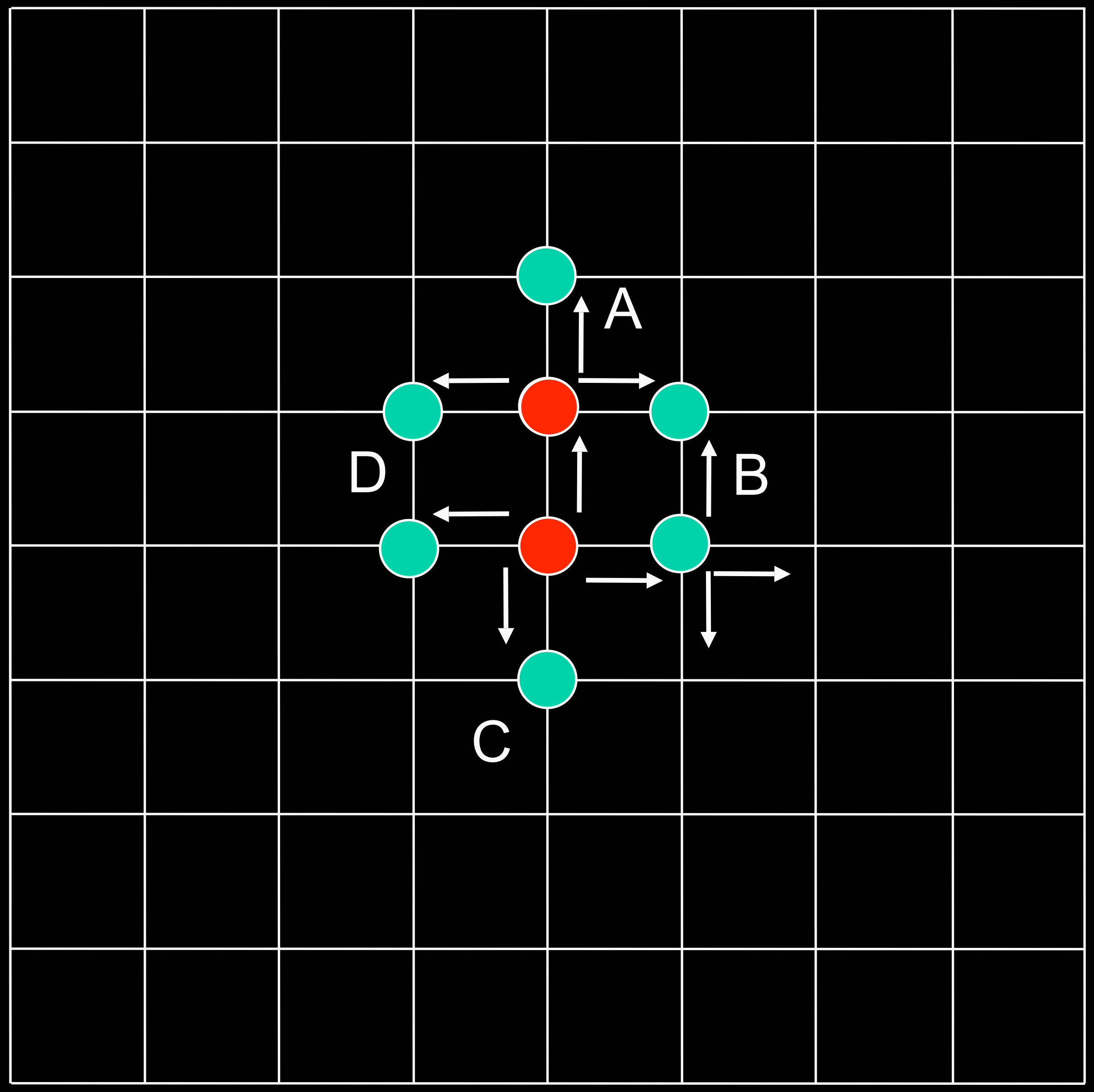

Boundary Value Formulation (Fast Marching)

1. Boundary value

2. Update “downwind”

3. Compute new possible values

4. Choose smallest green sphere (for example A)

5. Freeze value A, update neighboring “downwind” points

4. Choose smallest green sphere (for example B)

6. Freeze value B, update Neighboring “downwind” points

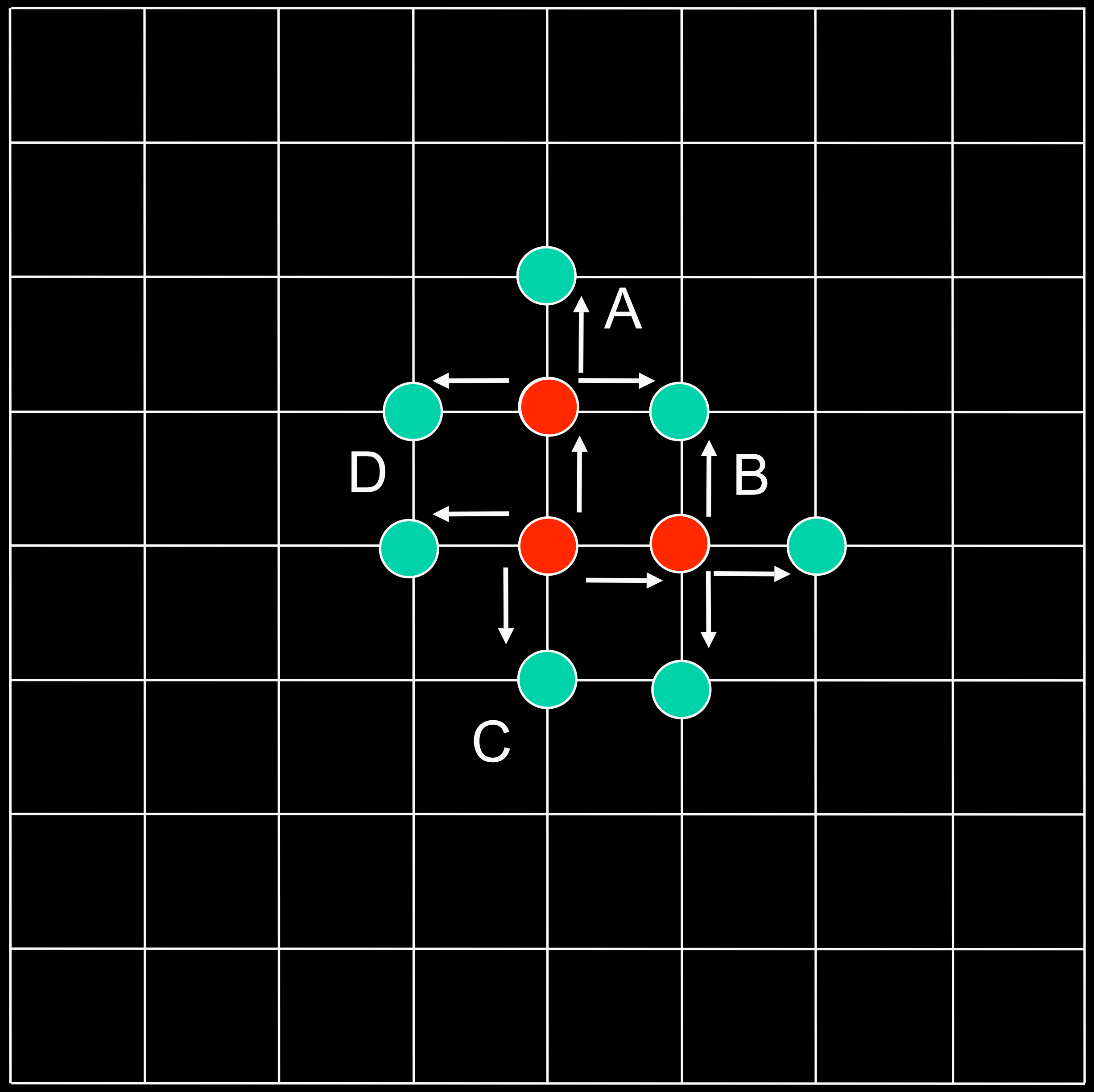

Boundary Value Formulation (Fast Marching)

1. Boundary value

2. Update “downwind”

3. Compute new possible values

4. Choose smallest green sphere
(for example A)

5. Freeze value A, update
neighboring “downwind” points

4. Choose smallest green sphere
(for example B)

6. Freeze value B, update
Neighboring “downwind” points

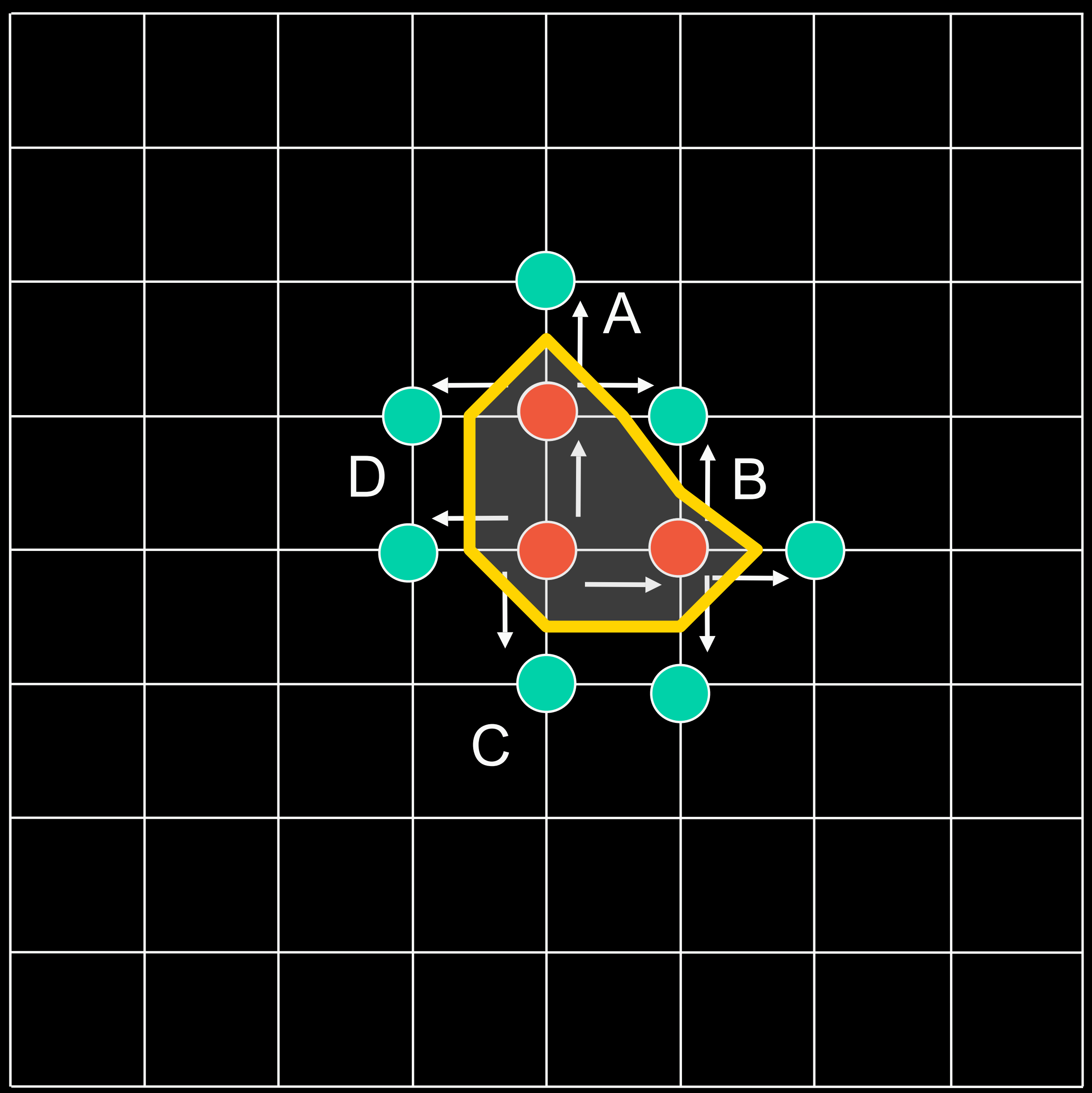

Upwind side

Boundary Value Formulation (Fast Marching)

1. Boundary value

2. Update “downwind”

3. Compute new possible values

4. Choose smallest green sphere (for example A)

5. Freeze value A, update neighboring “downwind” points

4. Choose smallest green sphere (for example B)

6. Freeze value B, update Neighboring “downwind” points

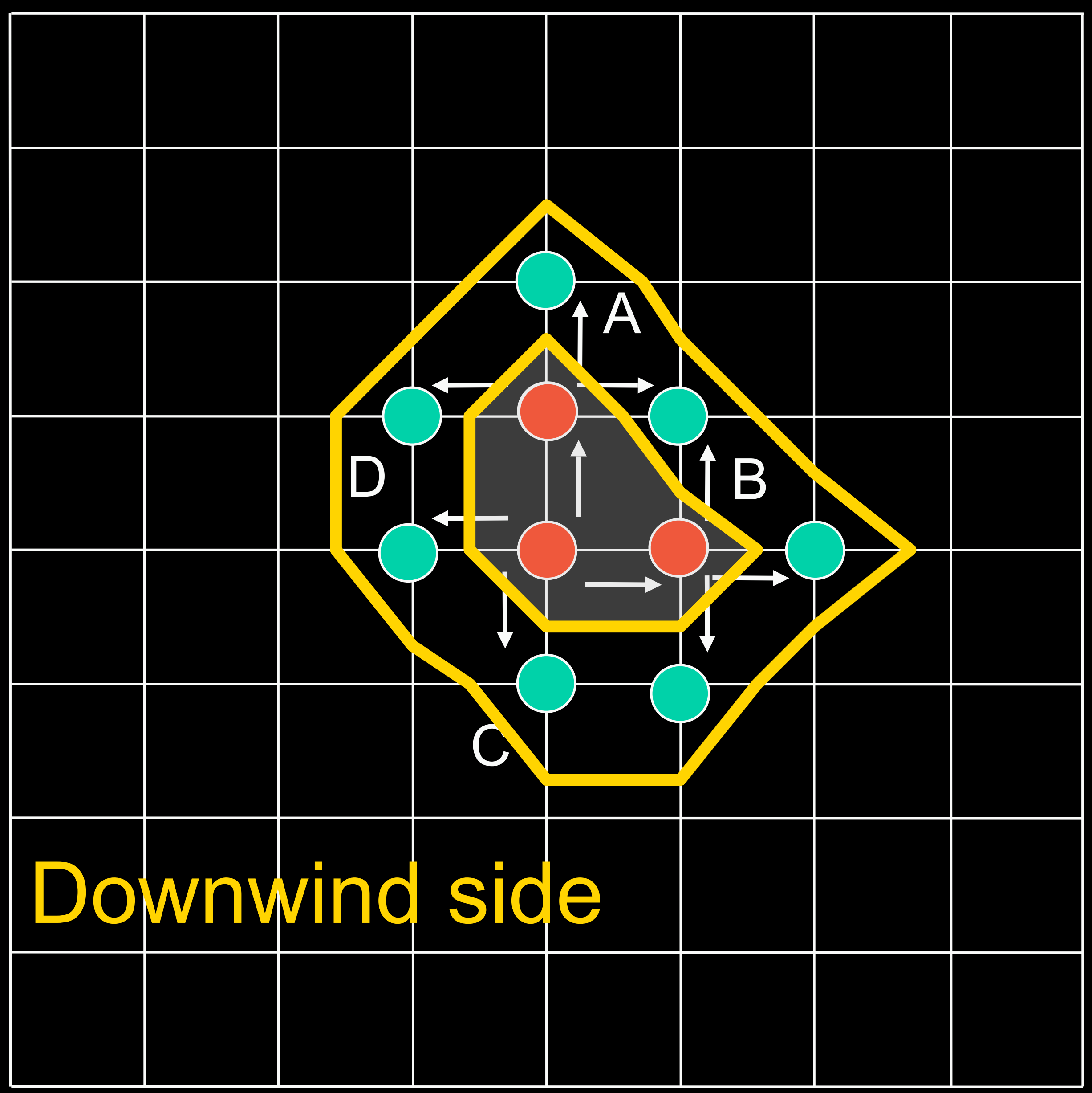

Upwind side

Boundary Value Formulation (Fast Marching)

1. Boundary value

2. Update "downwind"

3. Compute new possible values

4. Choose smallest green sphere (for example A)

5. Freeze value A, update neighboring "downwind" points

4. Choose smallest green sphere (for example B)

6. Freeze value B, update Neighboring "downwind" points

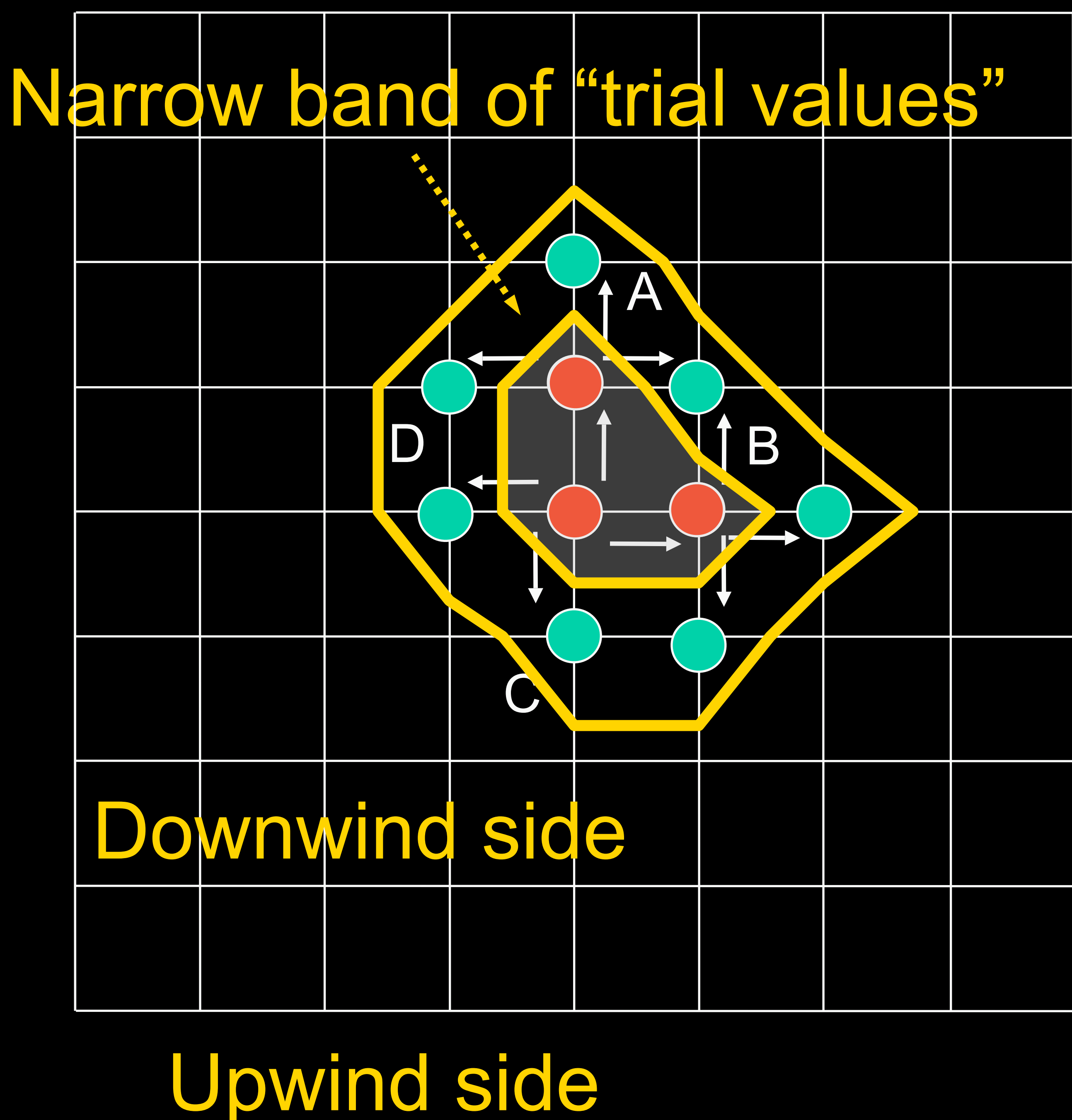

Boundary Value Formulation (Update Scheme)

- At each location $x \in \mathcal{M}$, test the 2^3 possible approximations:

$$[d\phi]_i = \frac{\phi(x) - \phi(x + s_i h_i e_i)}{-s_i h_i}$$

$\mathrm{i} = 1{,}2{,}3$

$\mathrm{s}_i = \pm 1$

e_i canonical basis of $\mathbb{R}^3$

h_i voxel size

- Optimal dynamics: $\mathrm{f}^*(x) = \mathrm{grad}\phi(x) = D(x)d\phi(x)$

has to verify $\mathrm{sign}(\mathrm{f}^*(x))_i = s_i \ \forall i = 1, 2, 3$

This automatically yields the minimum update value for ϕ

Computational Efficiency

Top 10% connections to the CC splenium

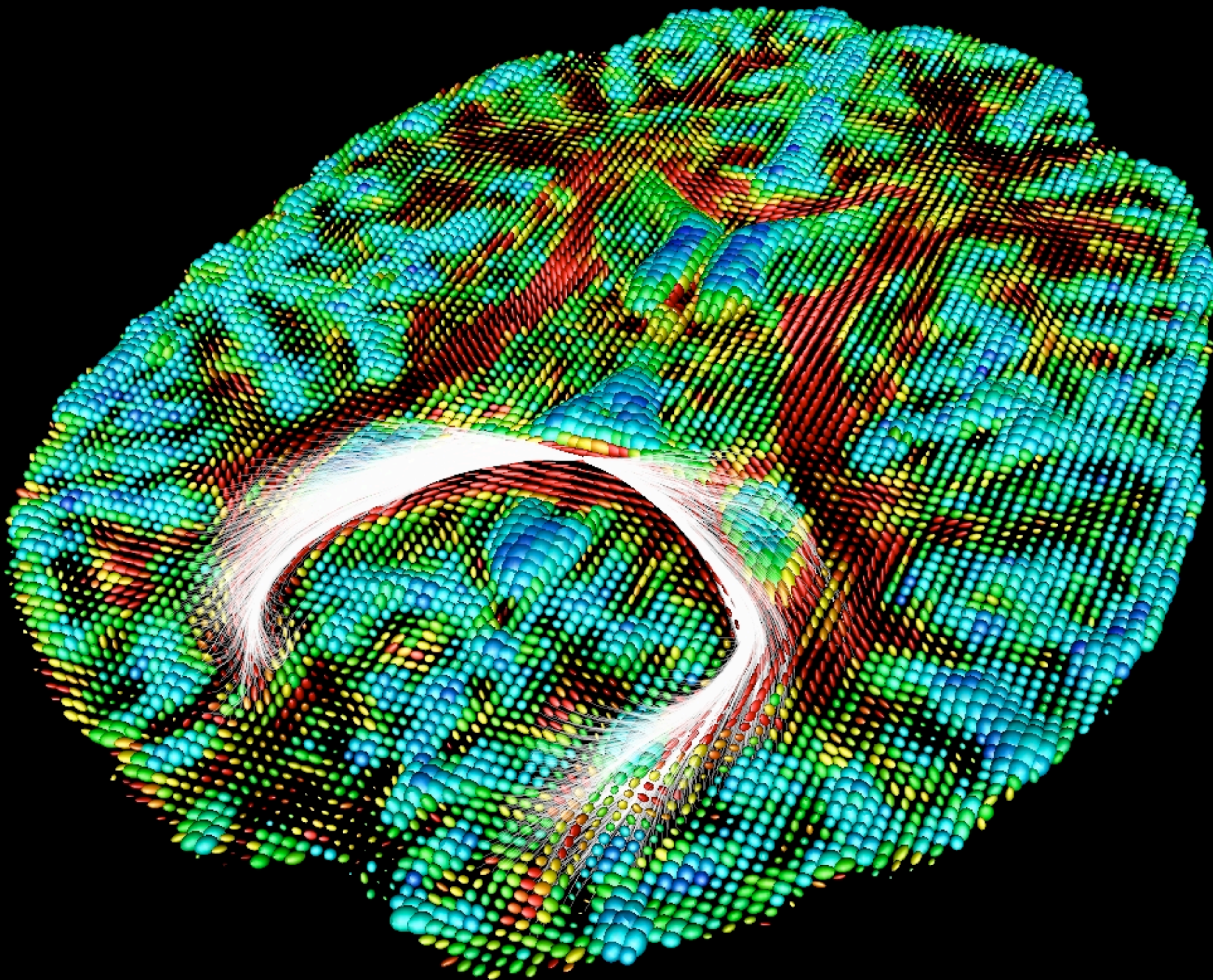

Data: CMRR, University of Minnesota

Geodesic distance:

[Jackowski-etal05]: 7 min

[Lenglet-etal04]: 20 min

Geodesics:

About 3 min / 15,000 fibers

Our FM Algorithm:

7 seconds

Data: 128x128x60

PC: 1.7 GHz / 1.5 Gb RAM

Computational Efficiency

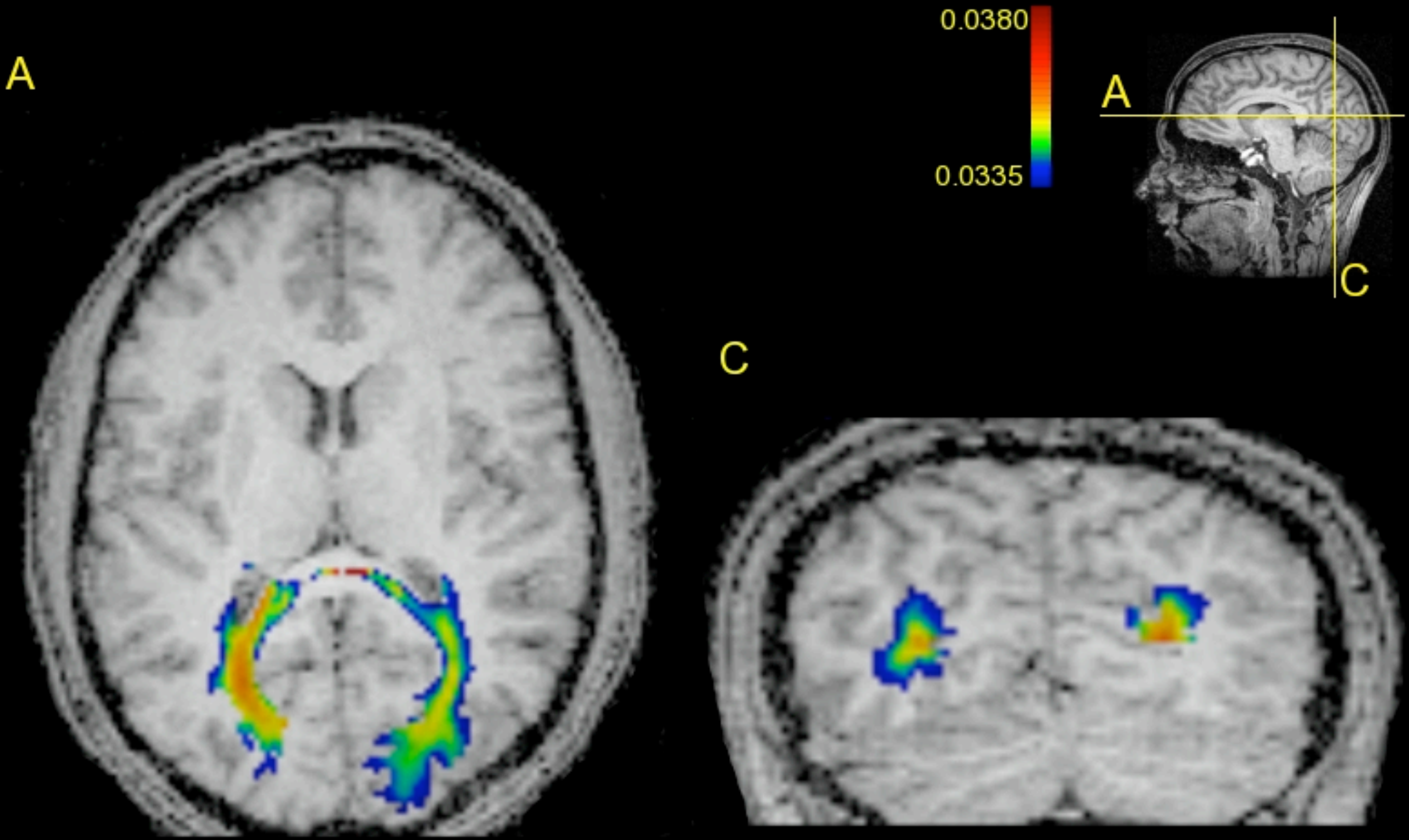

Brain Anatomical Connectivity Mapping

Diffusion Tensor Sharpening

(Joint work with M. Descoteaux)

Tensor Sharpening “improves” Tractography

- Using the full diffusion tensor is good but...

- Front propagation / stochastic tractography techniques are sensitive to the intrinsic “smoothness” of the DT

- Tracts may leak into unexpected regions

Tensor Sharpening "improves" Tractography

- Using the full diffusion tensor is good but...

- Front propagation / stochastic tractography techniques are sensitive to the intrinsic "smoothness" of the DT

- Tracts may leak into unexpected regions

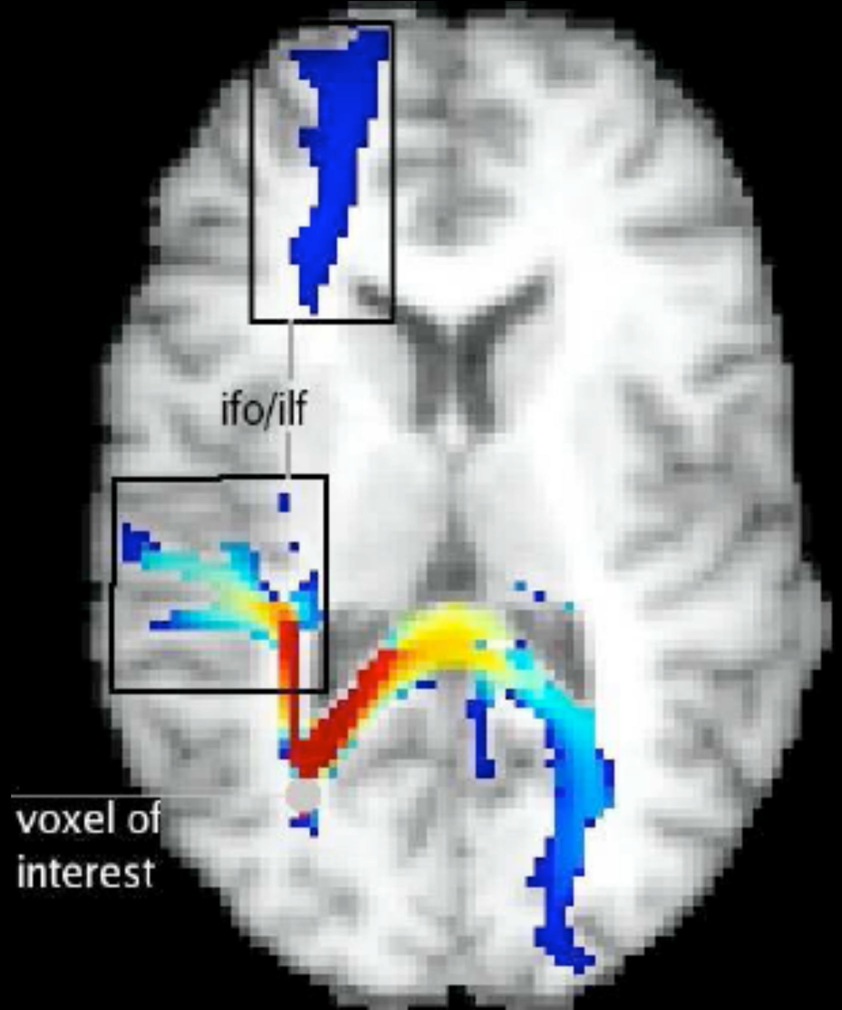

Tensor Sharpening “improves” Tractography

- Using the full diffusion tensor is good but...

- Front propagation / stochastic tractography techniques are sensitive to the intrinsic “smoothness” of the DT

- Tracts may leak into unexpected regions

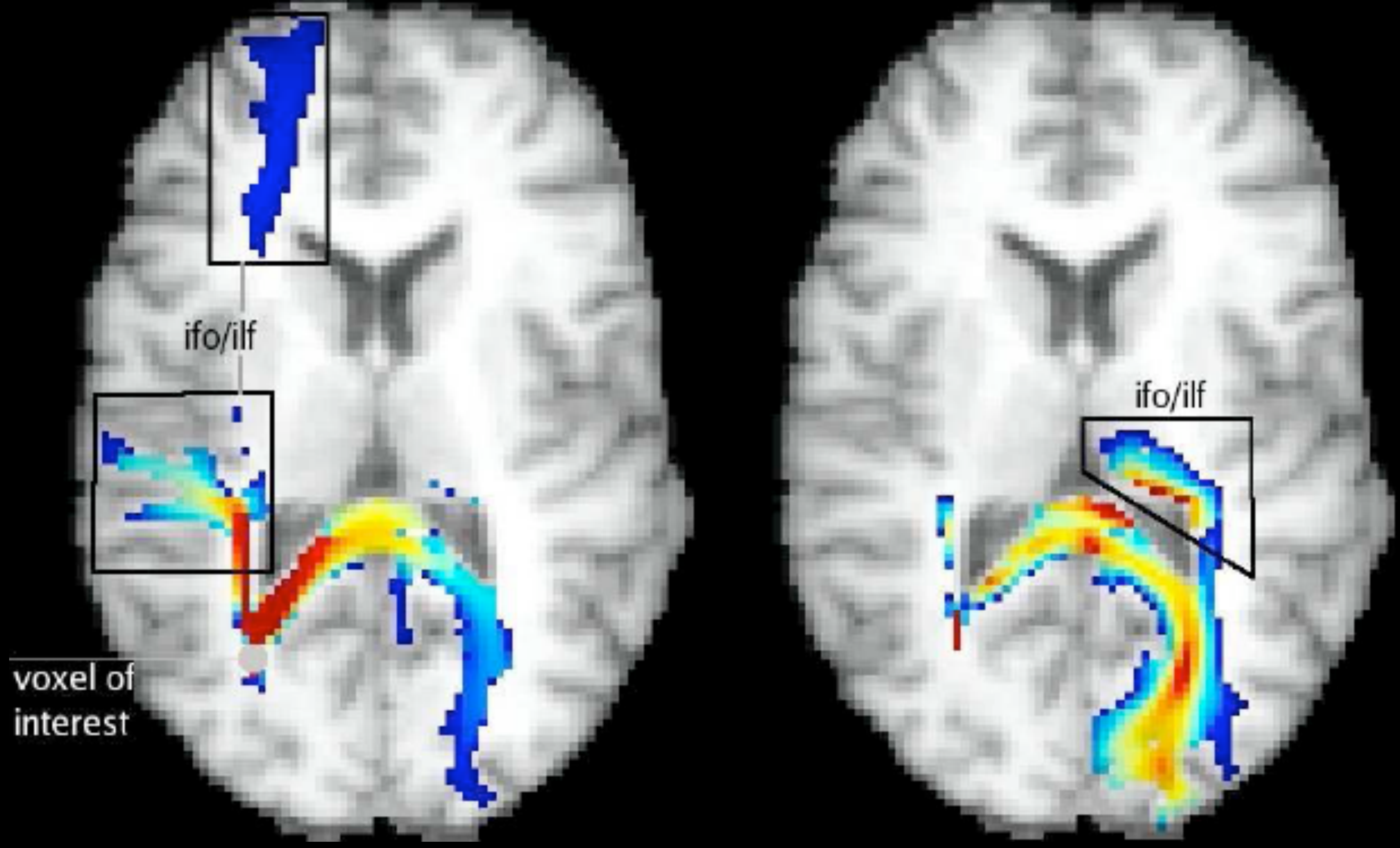

HARDI & Fiber Orientation Estimation: Sharpening

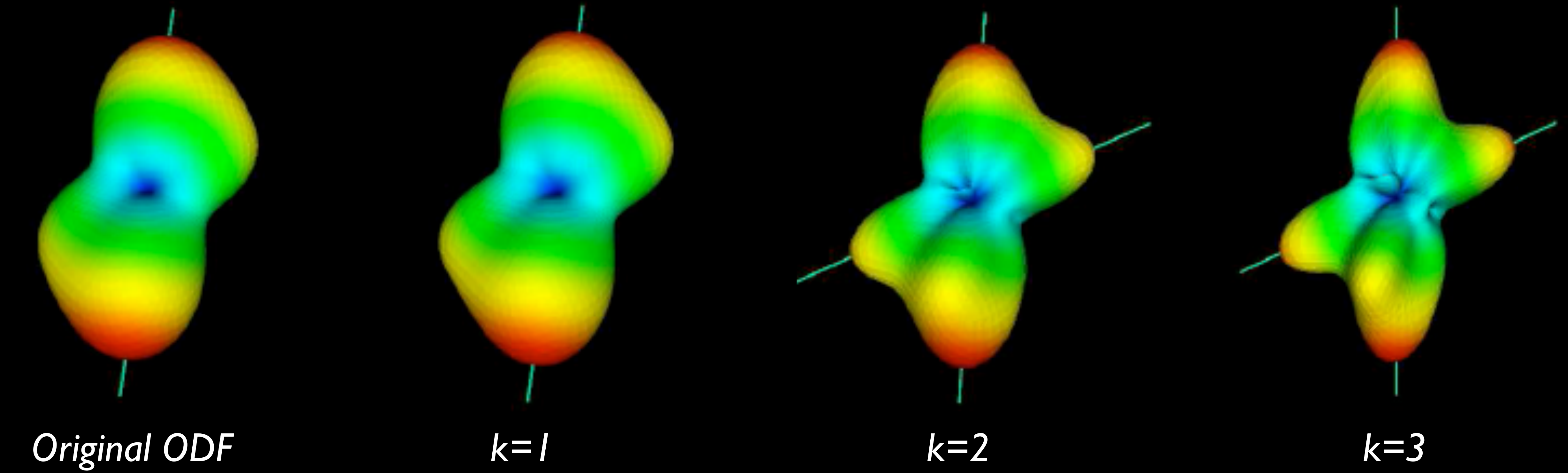

- Goal: Enhance the different fiber compartments
- Go from diffusion ODF to fiber ODF
- Model: Diffusion ODF is the spherical convolution of an axially symmetric single fiber response with a fiber ODF

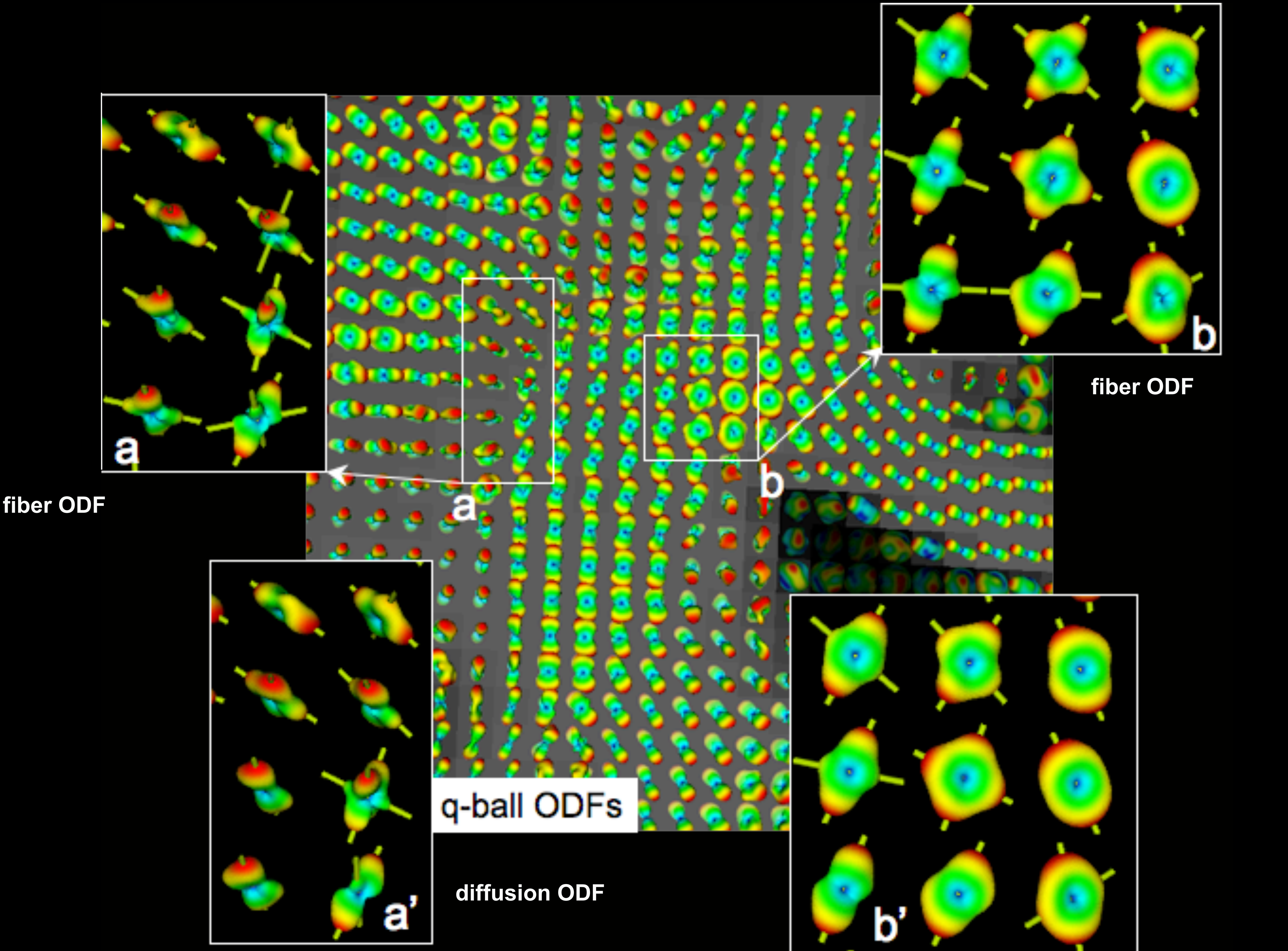
fiber ODF
a
fiber ODF
b
q-ball ODFs
a'
diffusion ODF
b'

Outline of the Tensor Sharpening Procedure

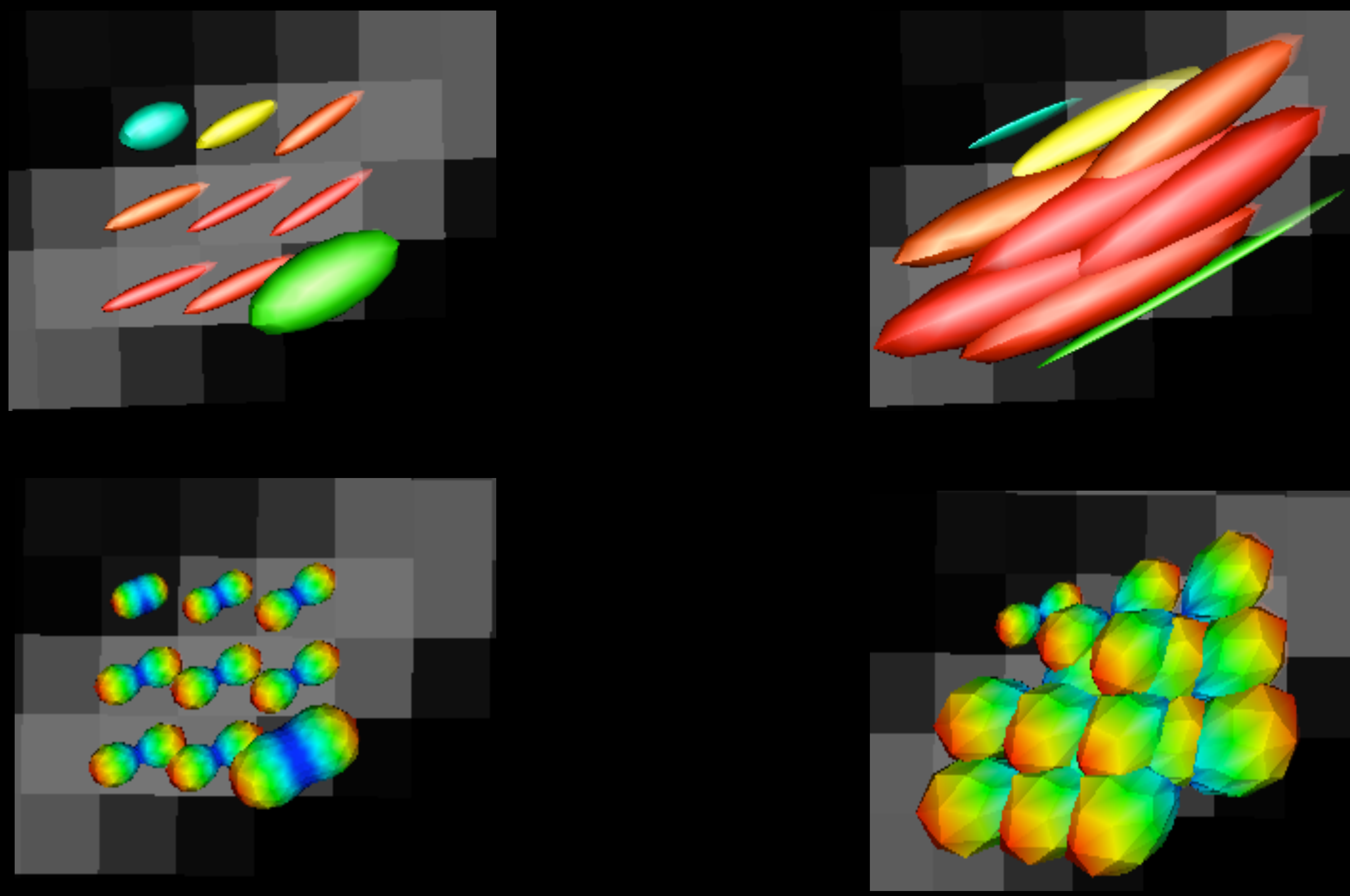

Outline of the Tensor Sharpening Procedure

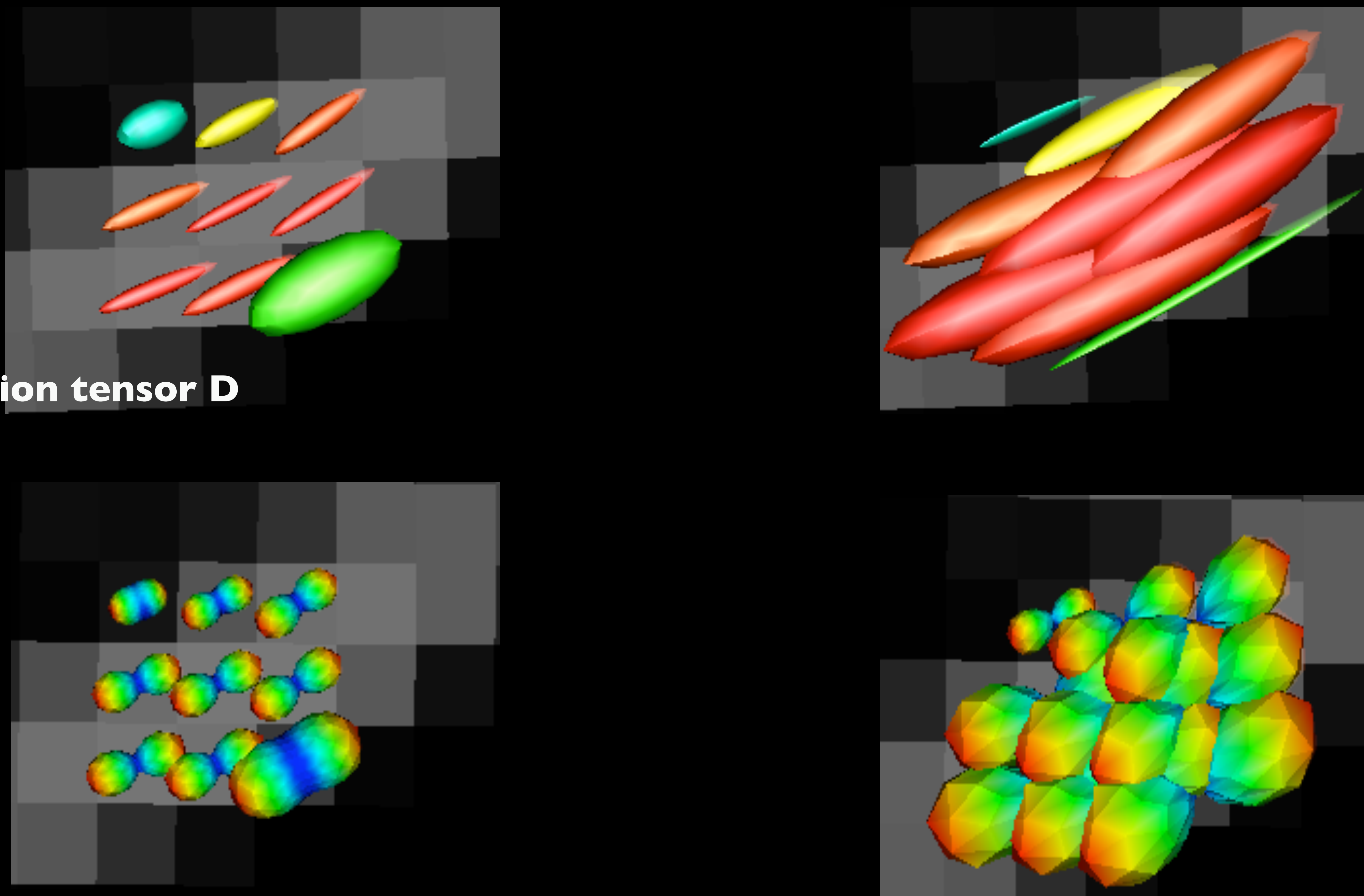

Diffusion tensor D

Outline of the Tensor Sharpening Procedure

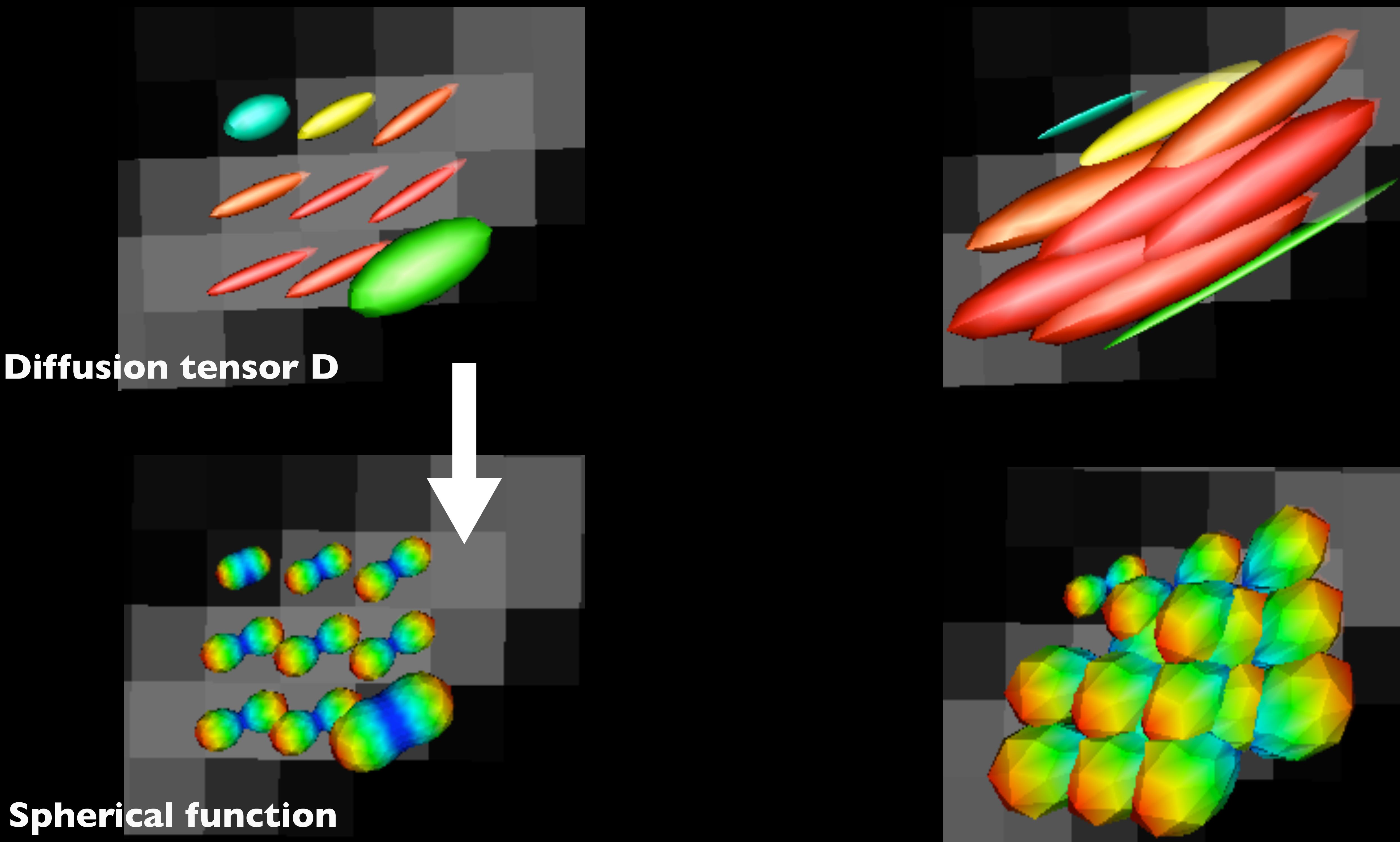

Outline of the Tensor Sharpening Procedure

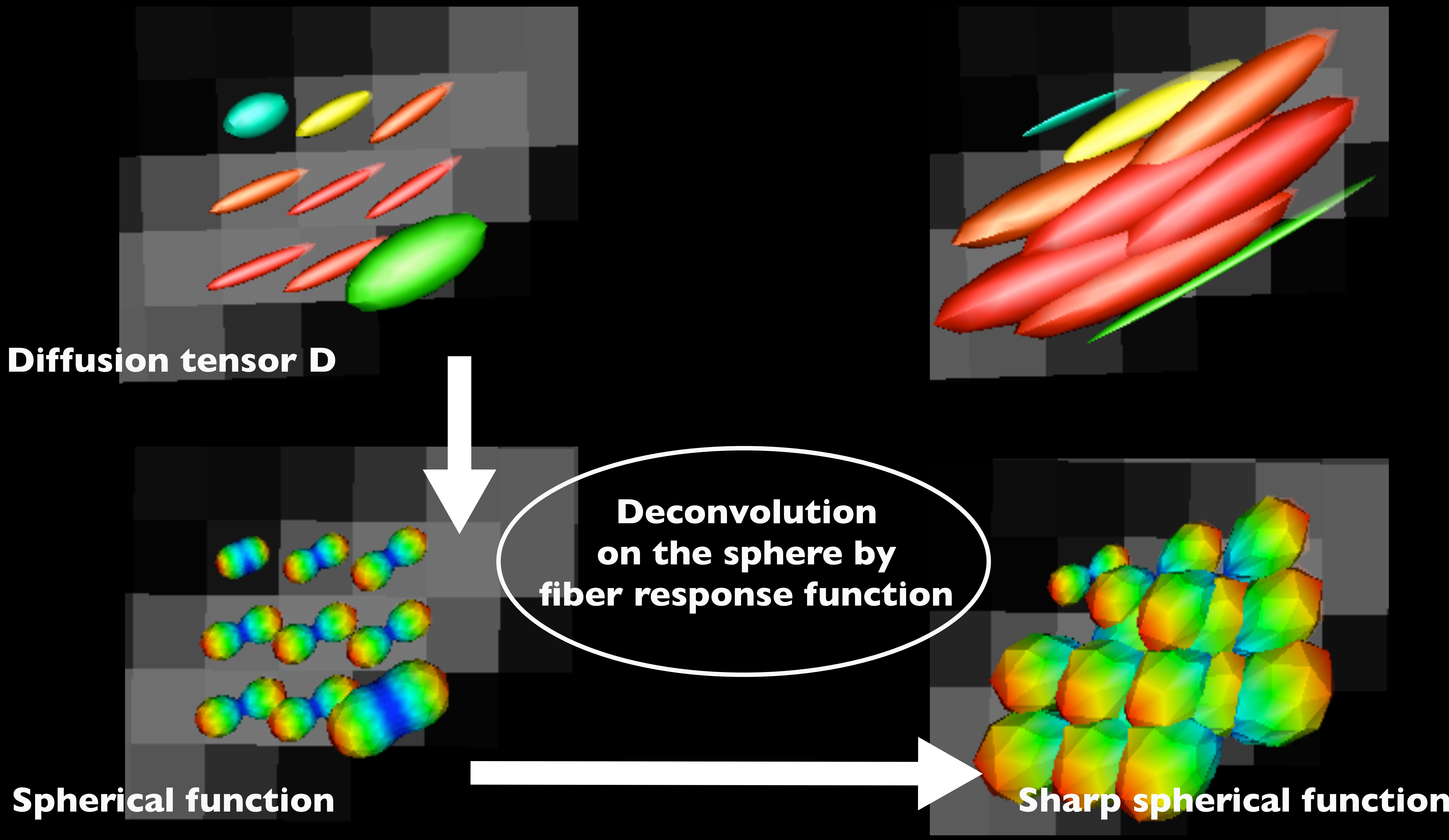

Outline of the Tensor Sharpening Procedure

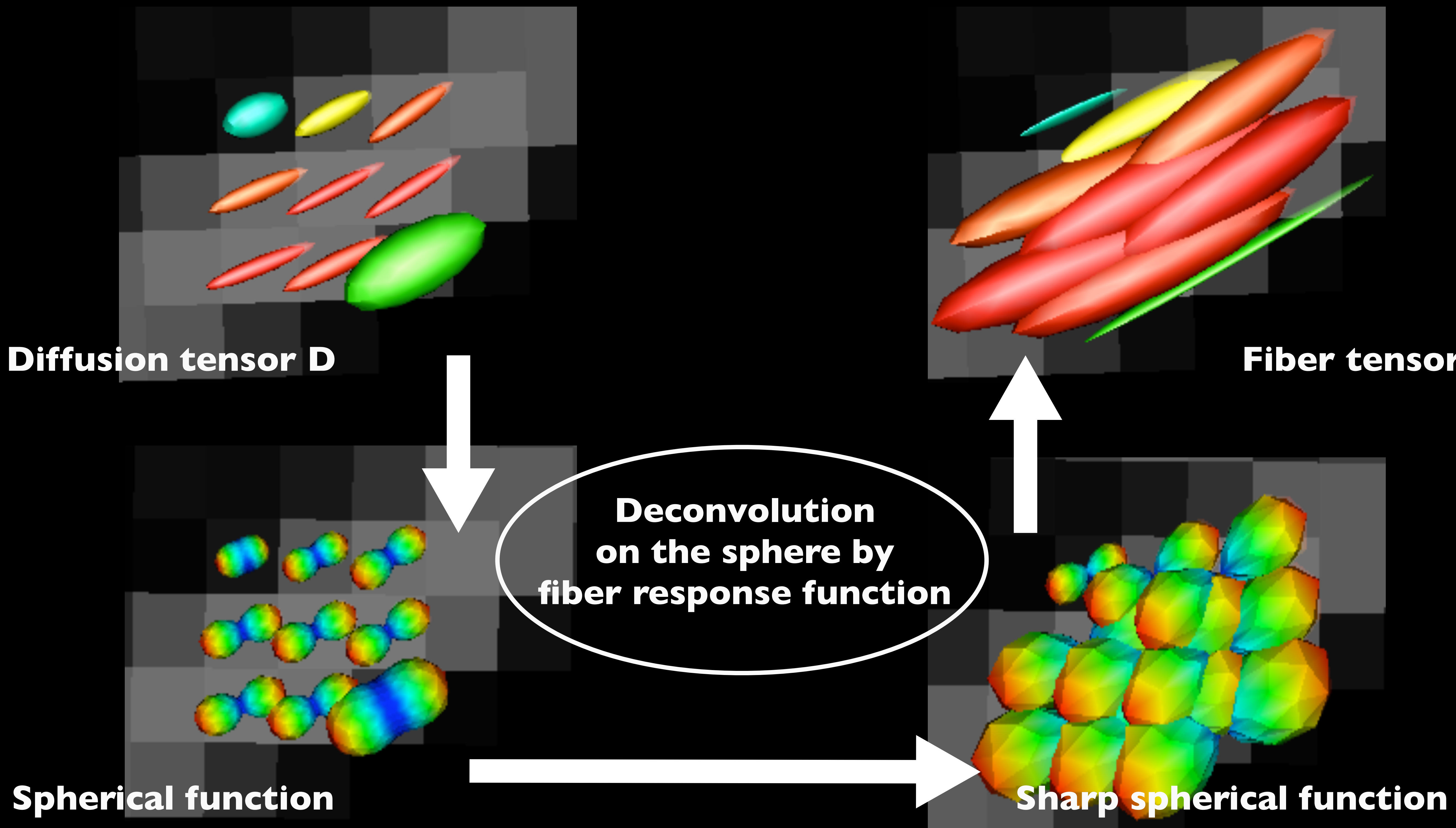

Step 2: Sharpening as a Deconvolution

- Inspired by Tournier *et al.* (Neuroimage 2004)
- Diffusion ODF *S* is a *smoothed* version of the fiber ODF *F*

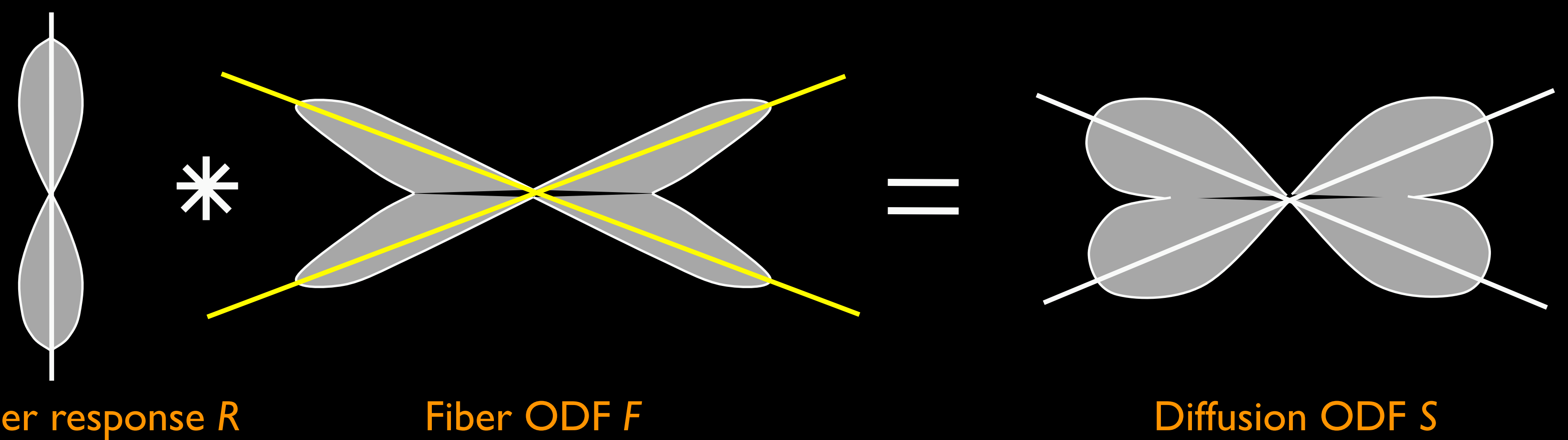

Step 2: Sharpening as a Deconvolution

- Inspired by Tournier *et al.* (Neuroimage 2004)
- Diffusion ODF *S* is a *smoothed* version of the fiber ODF *F*

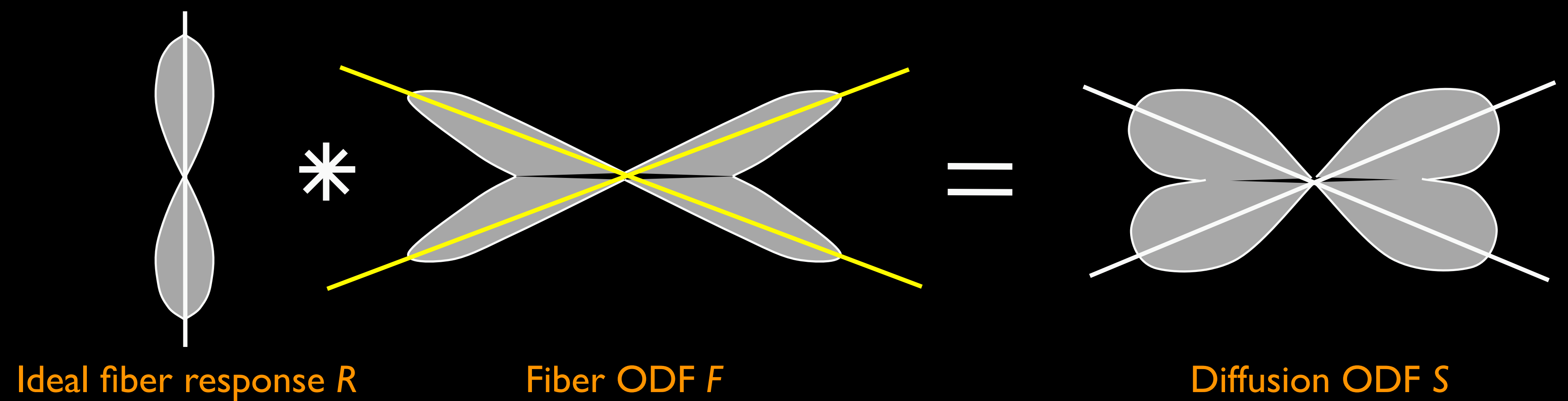

- Need to define a "good" fiber response function *R*
- Assumption of Gaussian profile $R(u) = e^{-bu^T Du}$

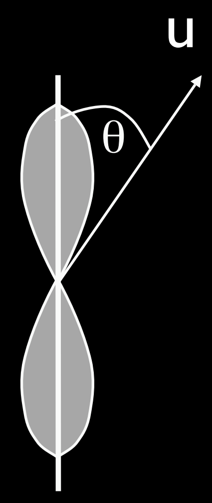

With $D = \begin{pmatrix} a & 0 & 0 \\ 0 & a & 0 \\ 0 & 0 & c \end{pmatrix} \rightarrow R(\theta) \propto e^{-((c-a)\cos^2\theta + a)}$

With *k*, the sharpening factor and $t := \cos(\theta)$

$$R_{\text{sharp}}(t) = e^{(t^2(c^{1/k} - a^{1/k}) + a^{1/k})}$$

Step 2: Deconvolution

- Choice of parameters *a*, *c* and *k*:
  - One can fix *(a,a,c)* and vary *k* to obtain various FA
  - One can fix *k* and vary the ratio *a/c*
  - We choose to fix *(a,a,c)* and vary *k* to achieve realistic FA

$$(a, a, c) = (300^{1/k}, 300^{1/k}, 1700^{1/k}) \times 10^{-6} mm^2/s$$ (FA = 0.5 for k =2)

- Deconvolution is done using the Funk-Hecke theorem:

$$S(u) = \int_{|v|=1} R(\langle u, v\rangle)F(v)dv$$ (Convolution of *F* with *R*)

$$\sum_j c_j Y_j(u) = \sum_j c'_j \int_{|v|=1} R(\langle u, v\rangle)Y_j(v)dv = \sum_j c'_j \lambda(j) Y_j(u)$$ (Funk-Hecke)

$$c'_j = c_j/\lambda(j) \quad \text{with} \quad \lambda(j) = 2\pi \int_{-1}^{1} P_{l(j)}(t)R(t)dt$$

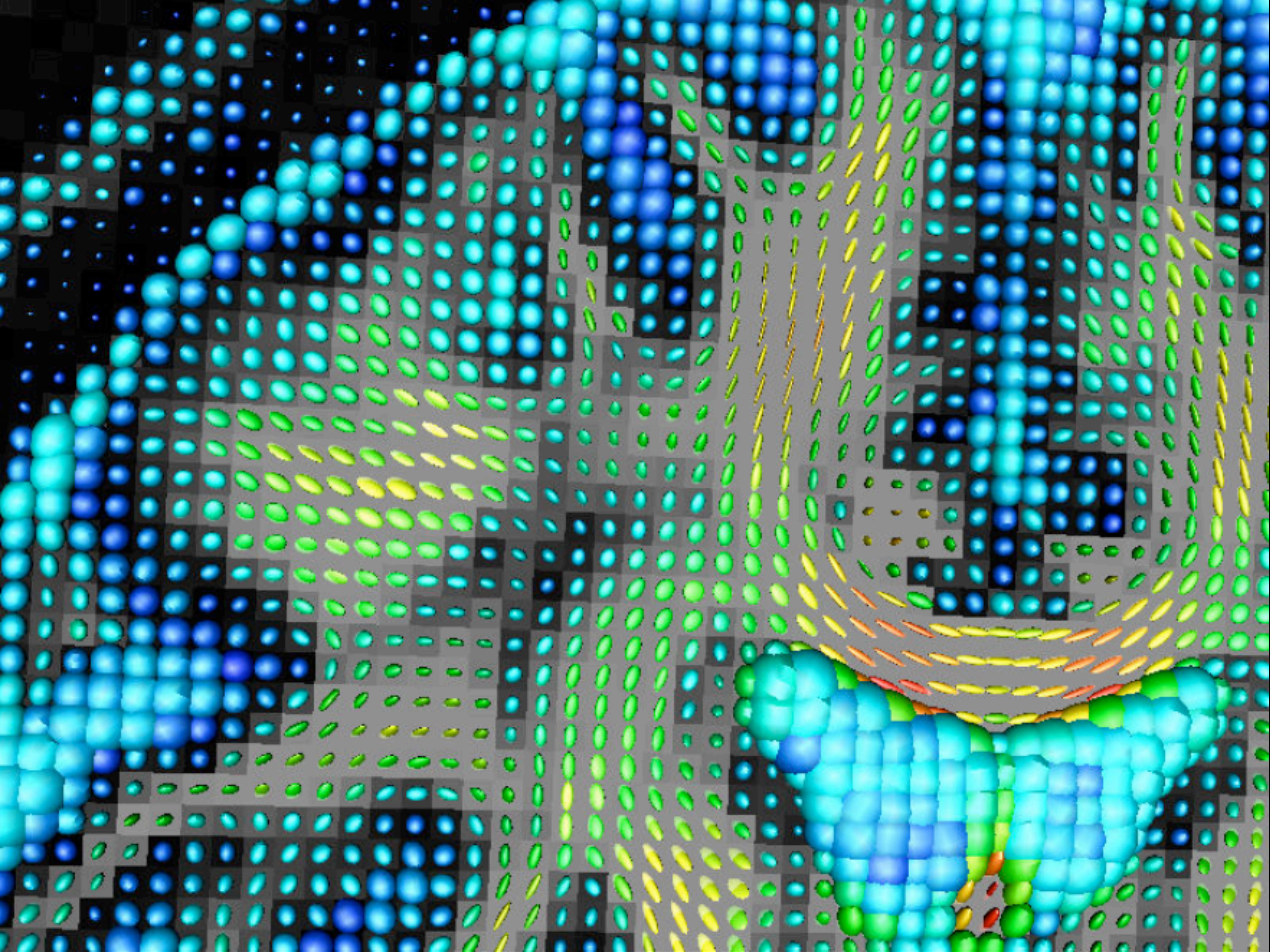

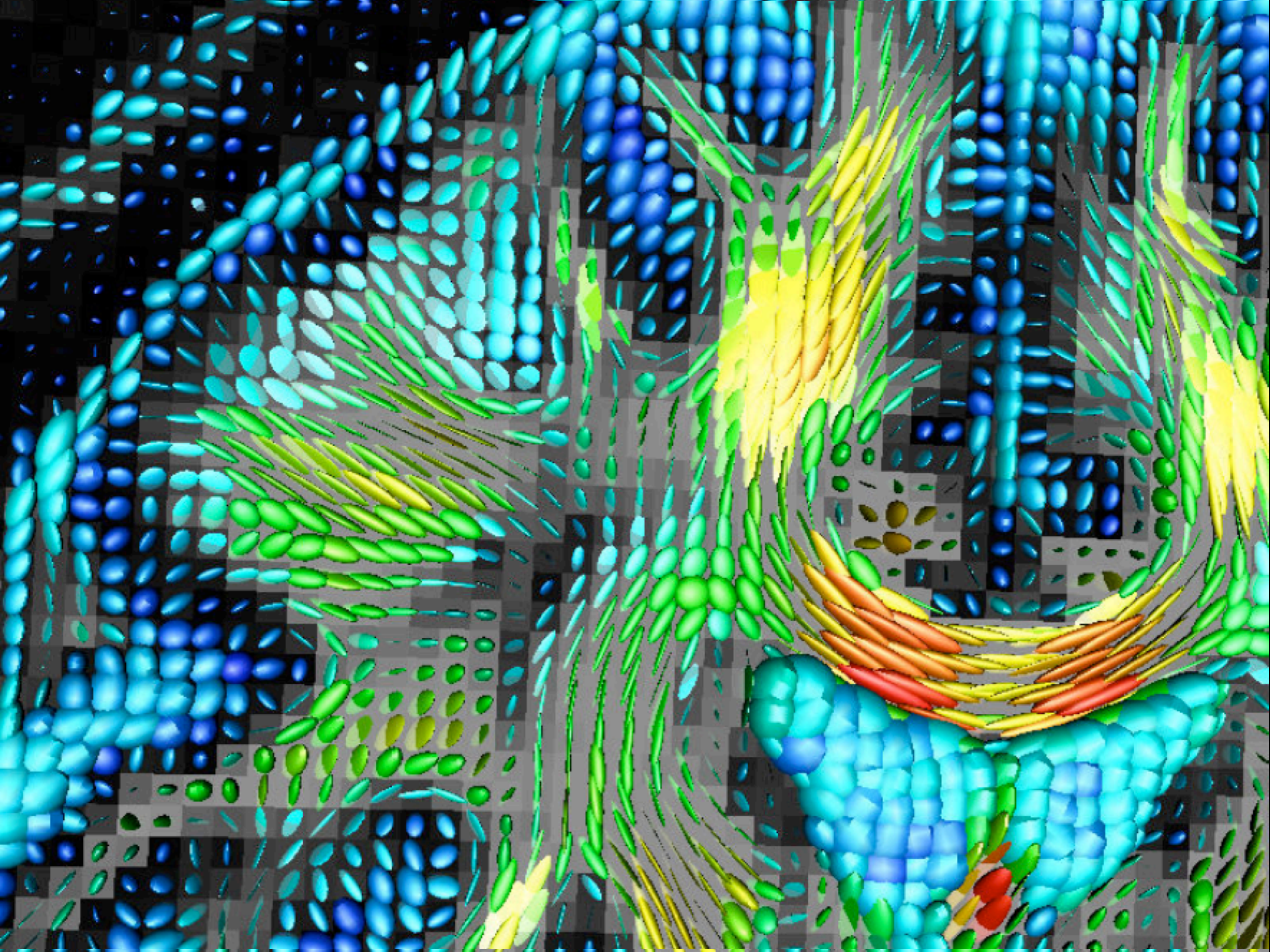

Splenium of the Corpus Callosum

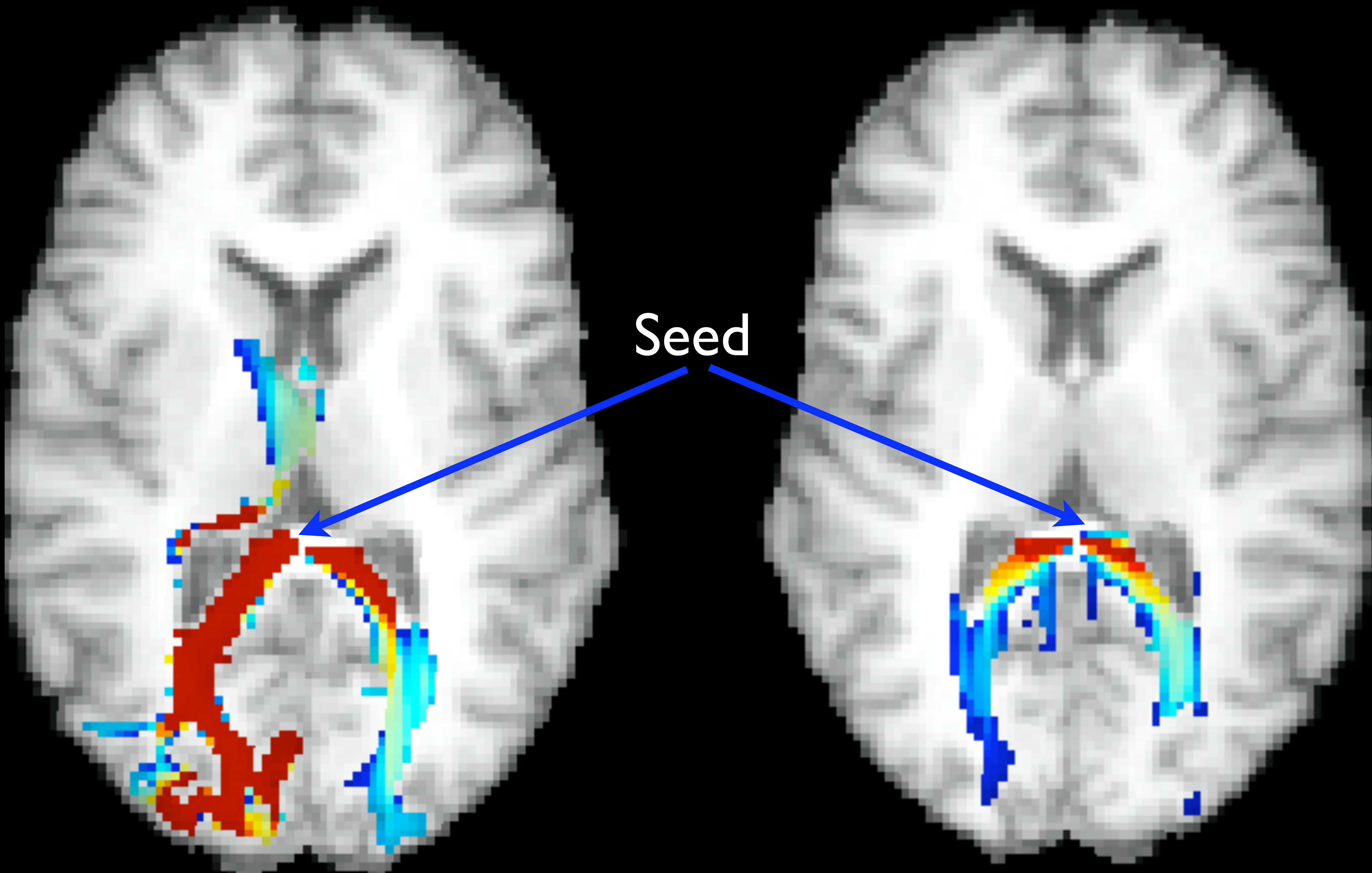

Diffusion tensor *Fiber tensor*

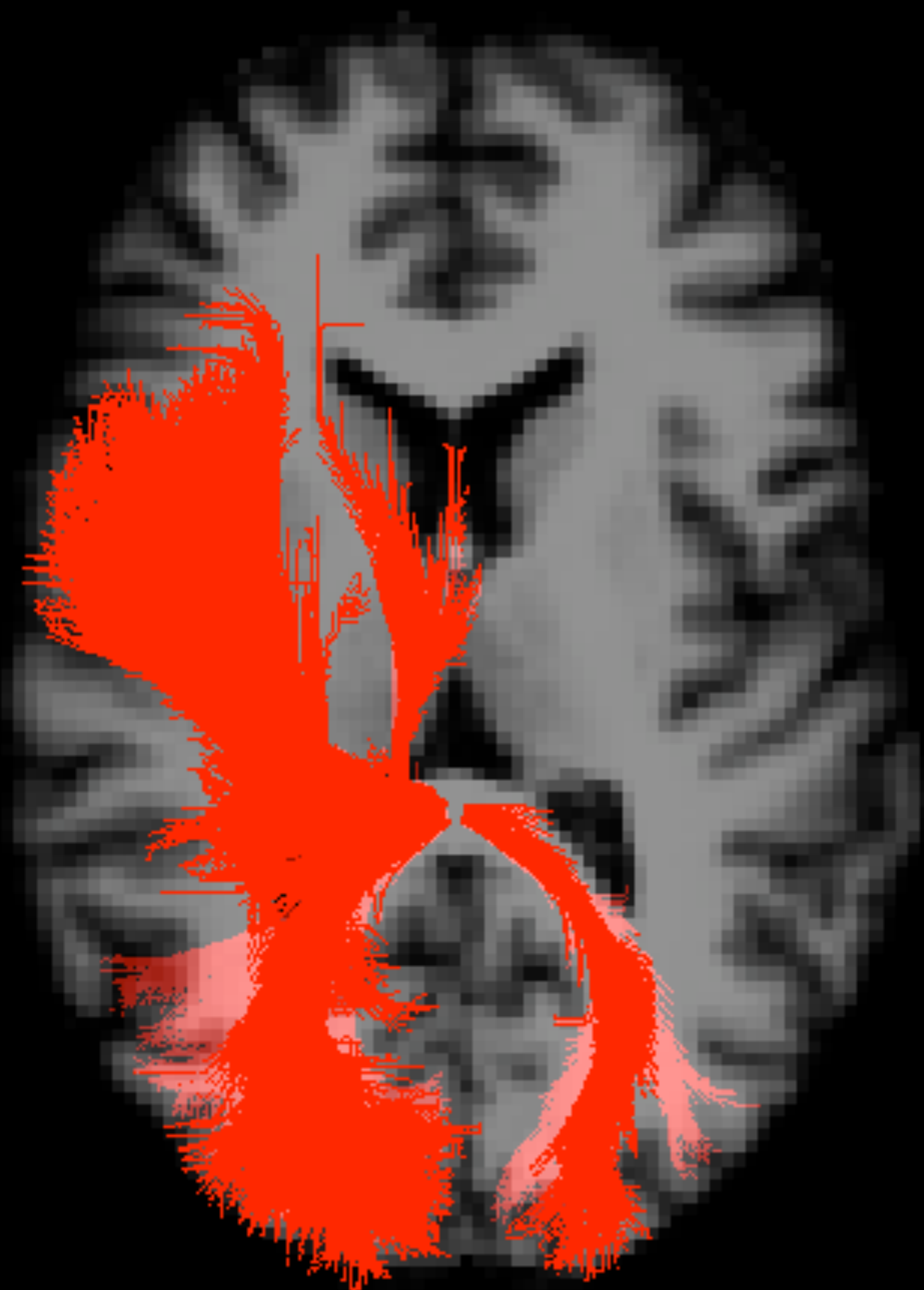

Diffusion tensor

Fiber tensor

Anterior Thalamic Radiation

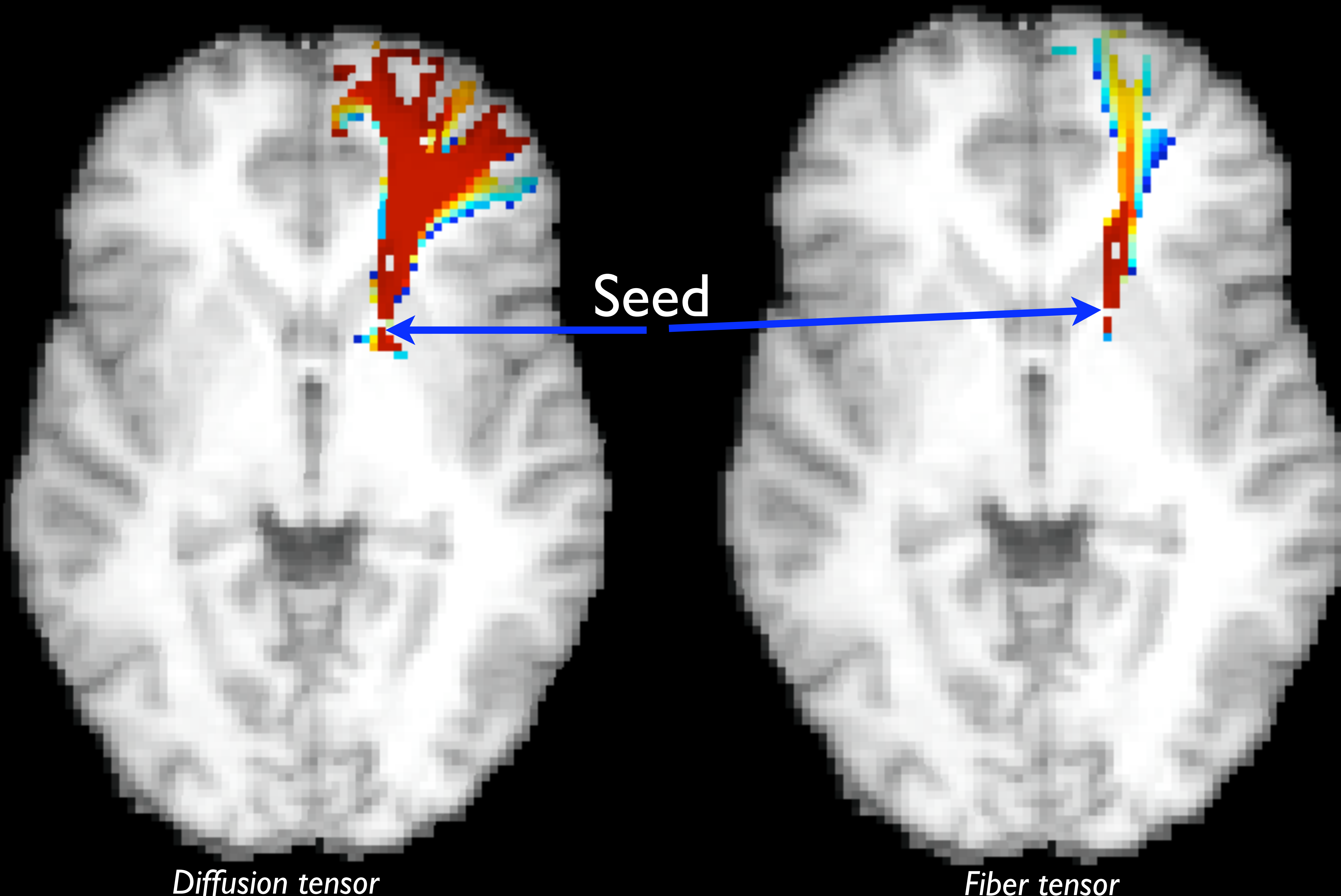

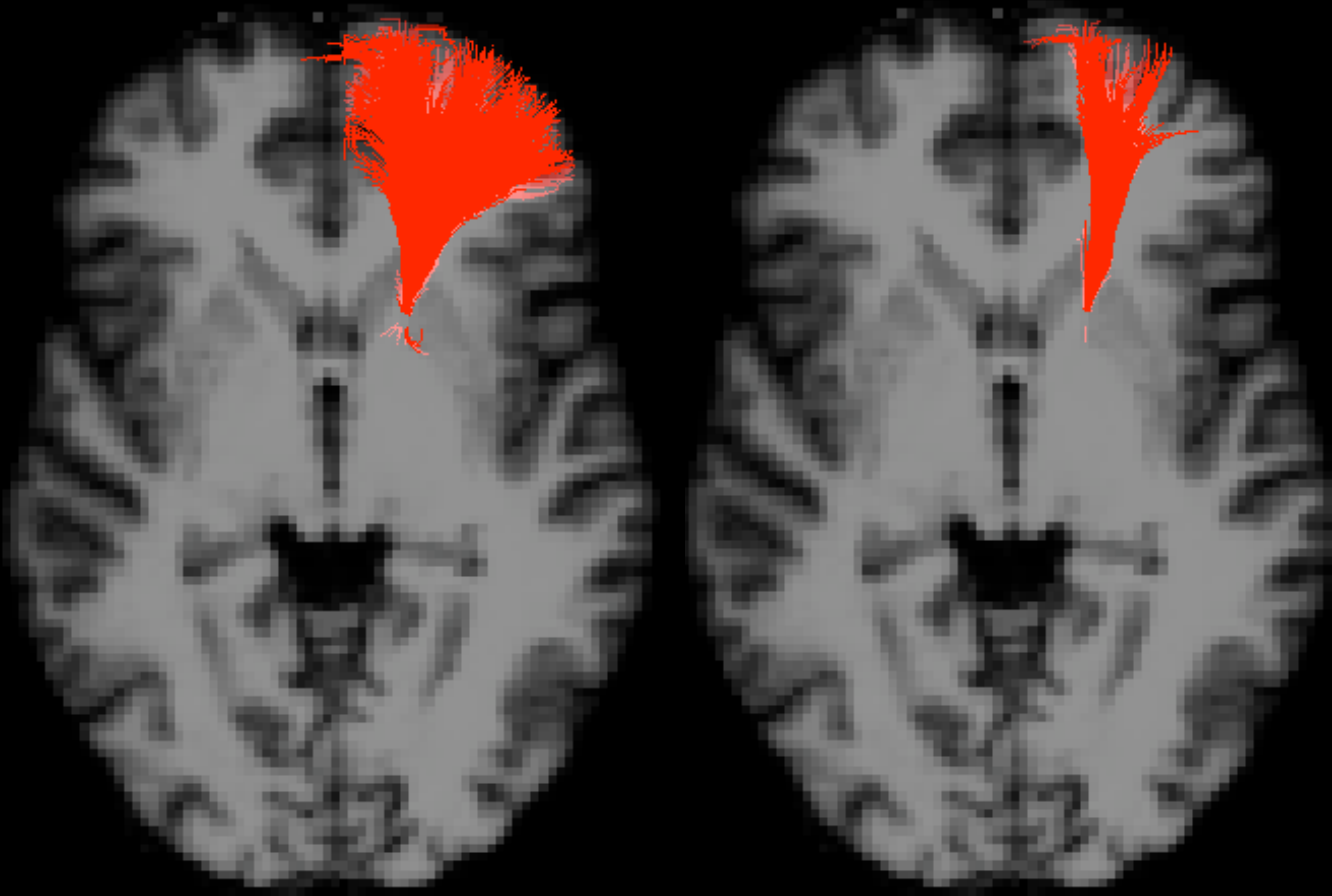

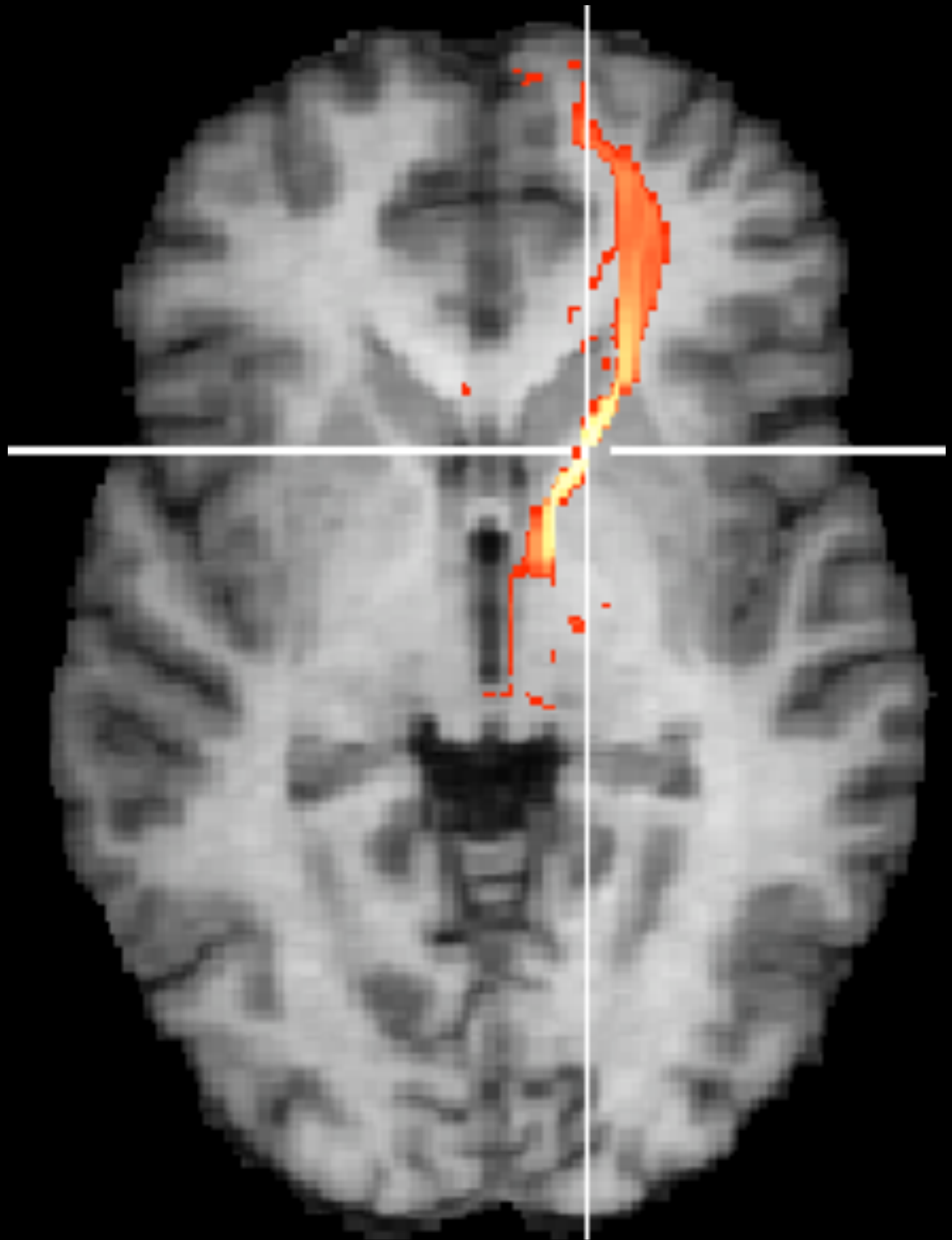

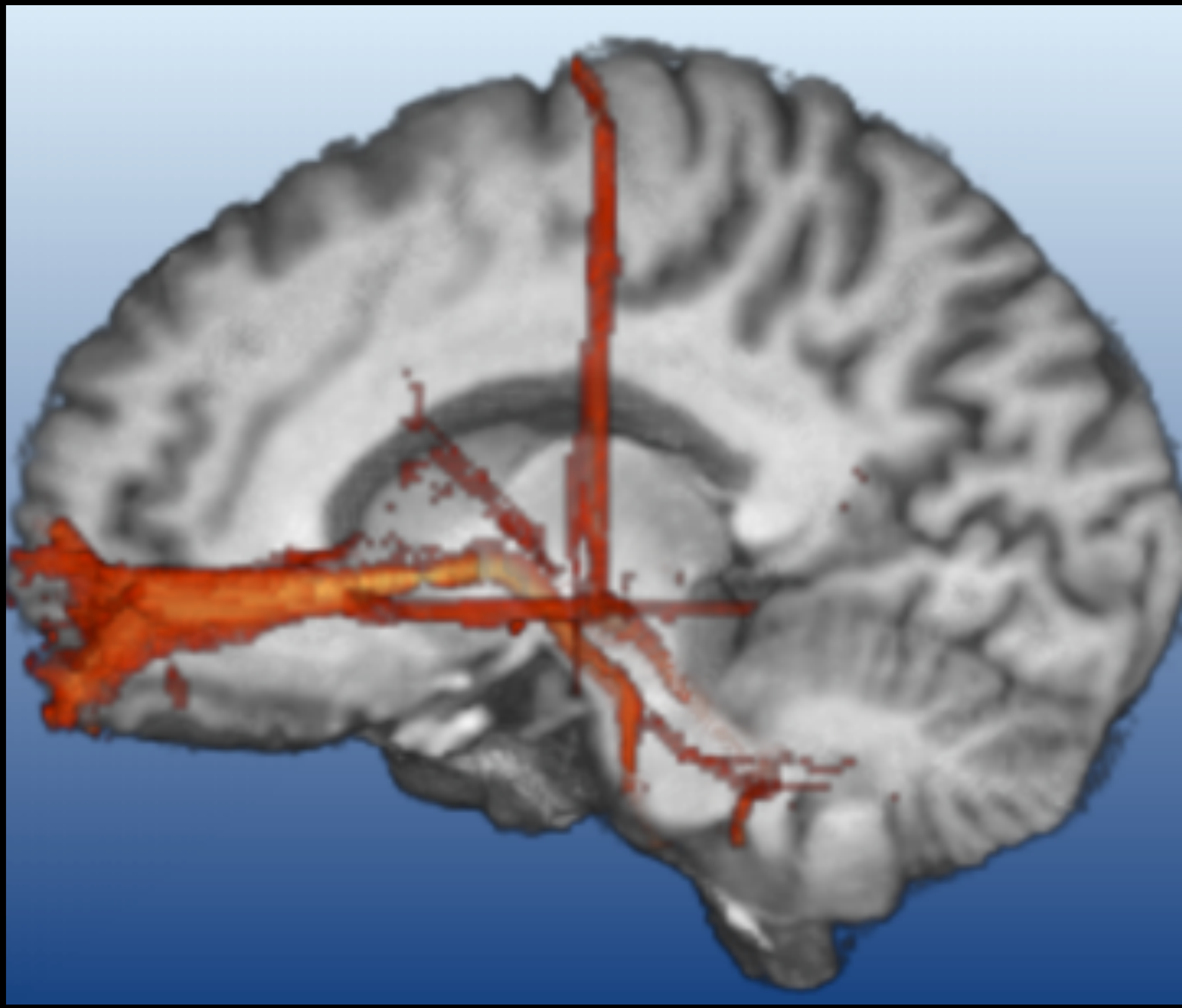

Images from [Koch et al, NeuroImage 2002, Anwander et al, Cerebral Cortex 2007]

Cortico-spinal Tract

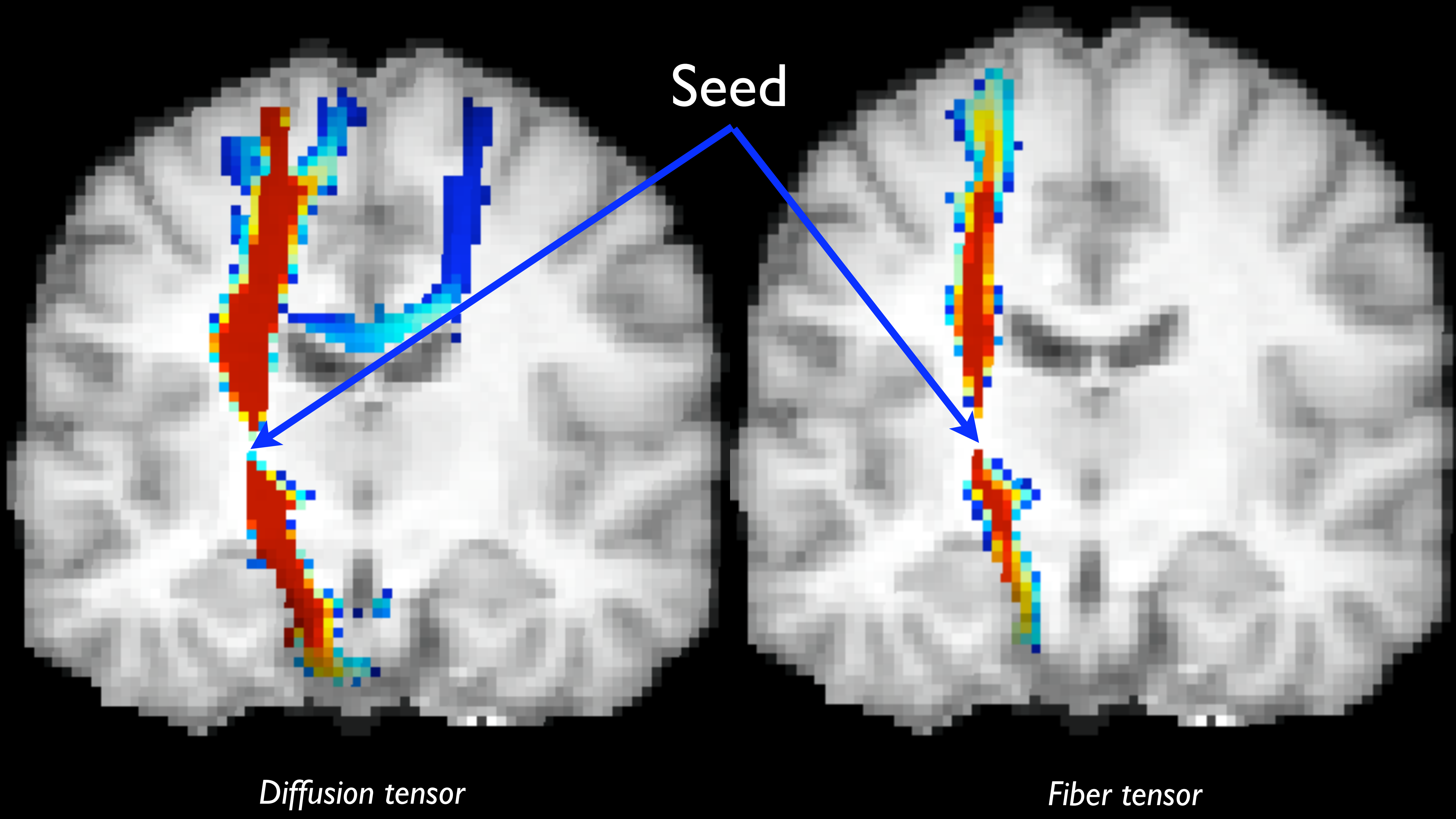

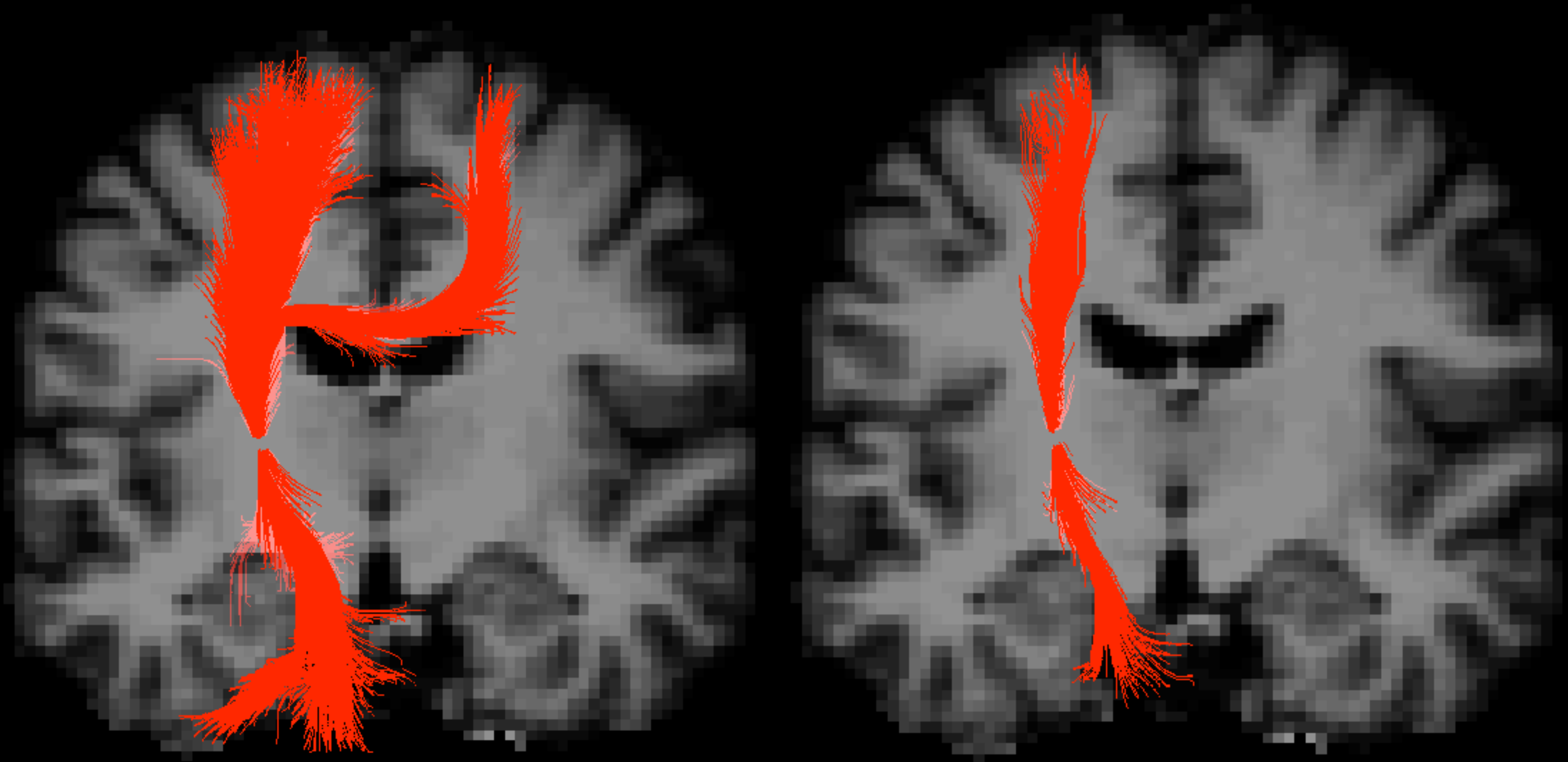

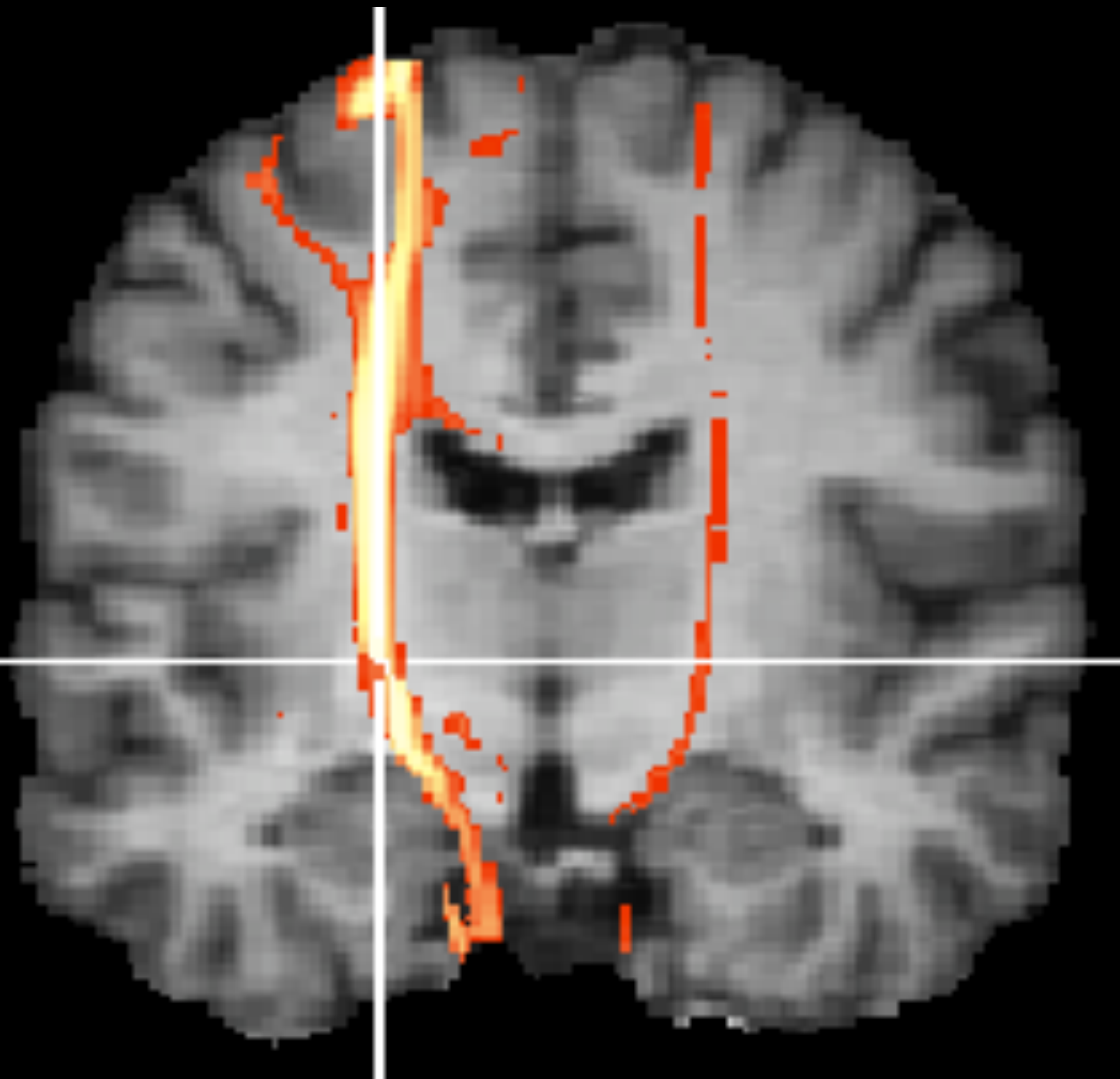

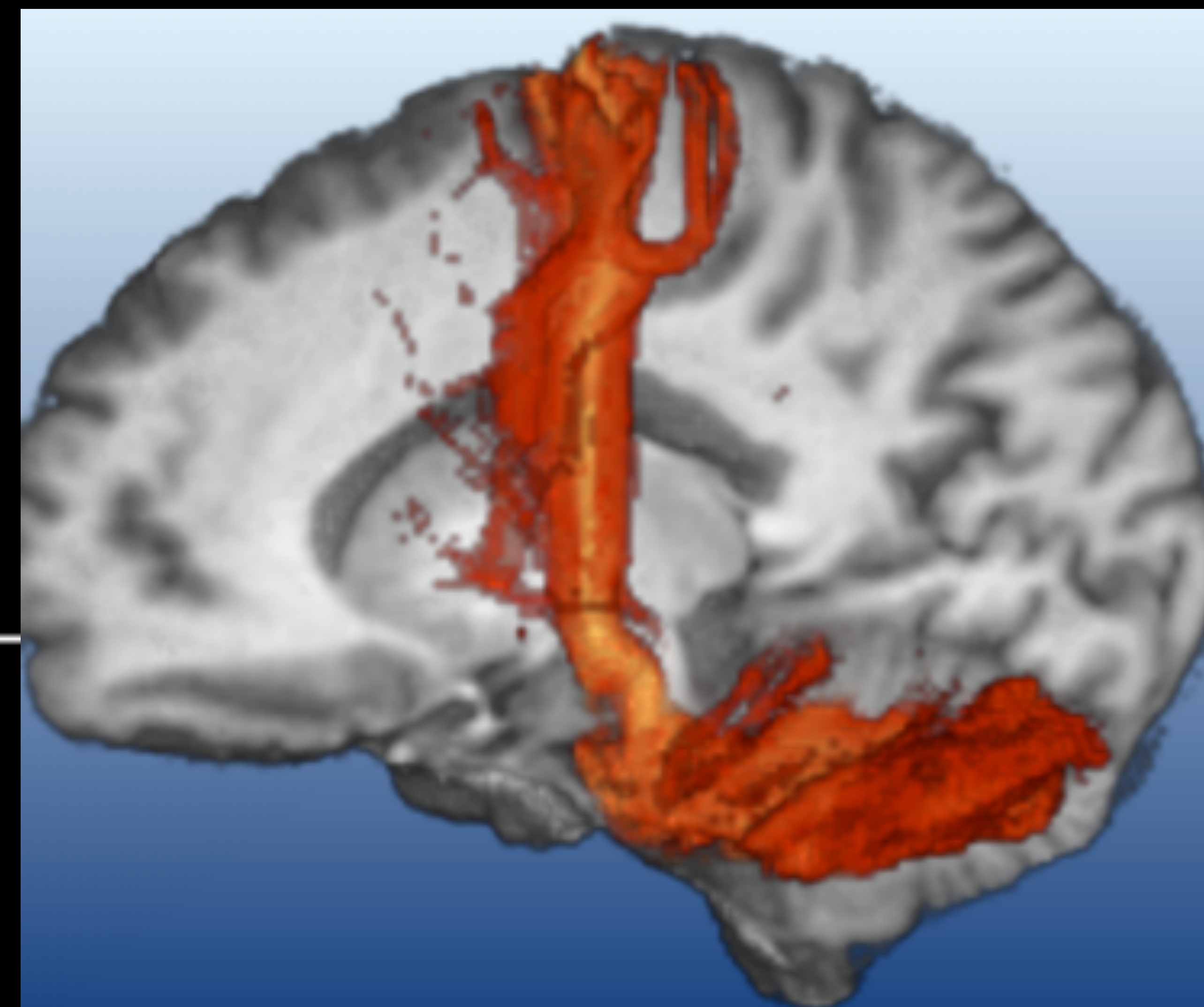

Images from [Koch et al, NeuroImage 2002, Anwander et al, Cerebral Cortex 2007]

Combining DTI & fMRI

Architecture of the cortico-striatal connections

(Joint work with S. Lehéricy)

Overview

- Anatomical connections of the human striatum can be parceled by DTI deterministic tractography.

- Invasive animal studies showed that cortico-striatal fibers are organized in a set of discrete circuits.

- Each circuit is related to distinct behavioral functions:
  - Movement preparation and execution
  - Planning and decision making
  - Learning

- We investigate the connectivity patterns of 2 regions of the striatum.

[Lehericy-Ducros-etal04], [Alexander-DeLong-etal86]

Architecture of the Cortico-Striatal Connections

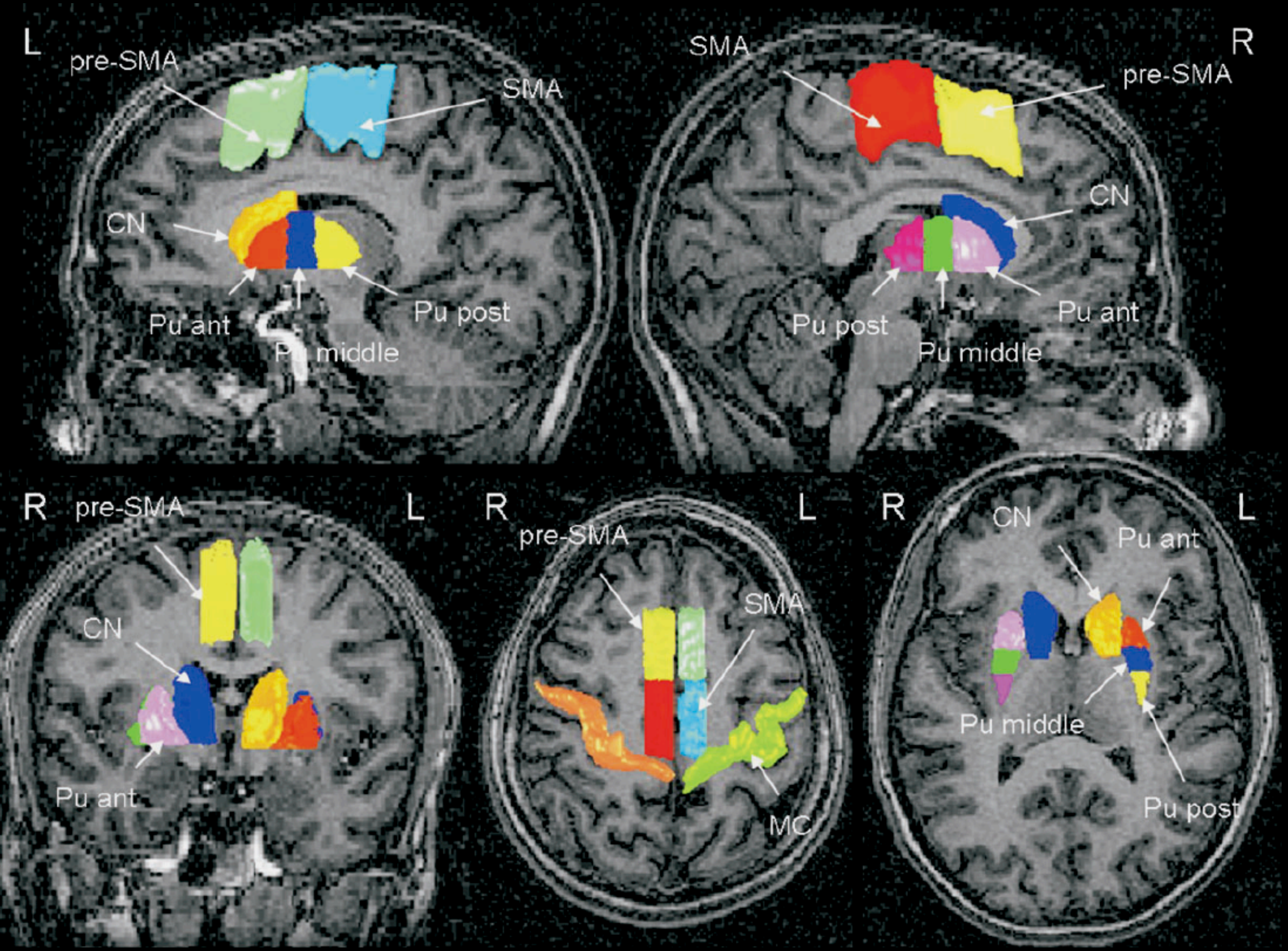

Image from [Lehericy-Ducros-etal04]

[Graybiel95], [Lehericy-Benali-etal03], [Lehericy-etal05]

Architecture of the Cortico-Striatal Connections

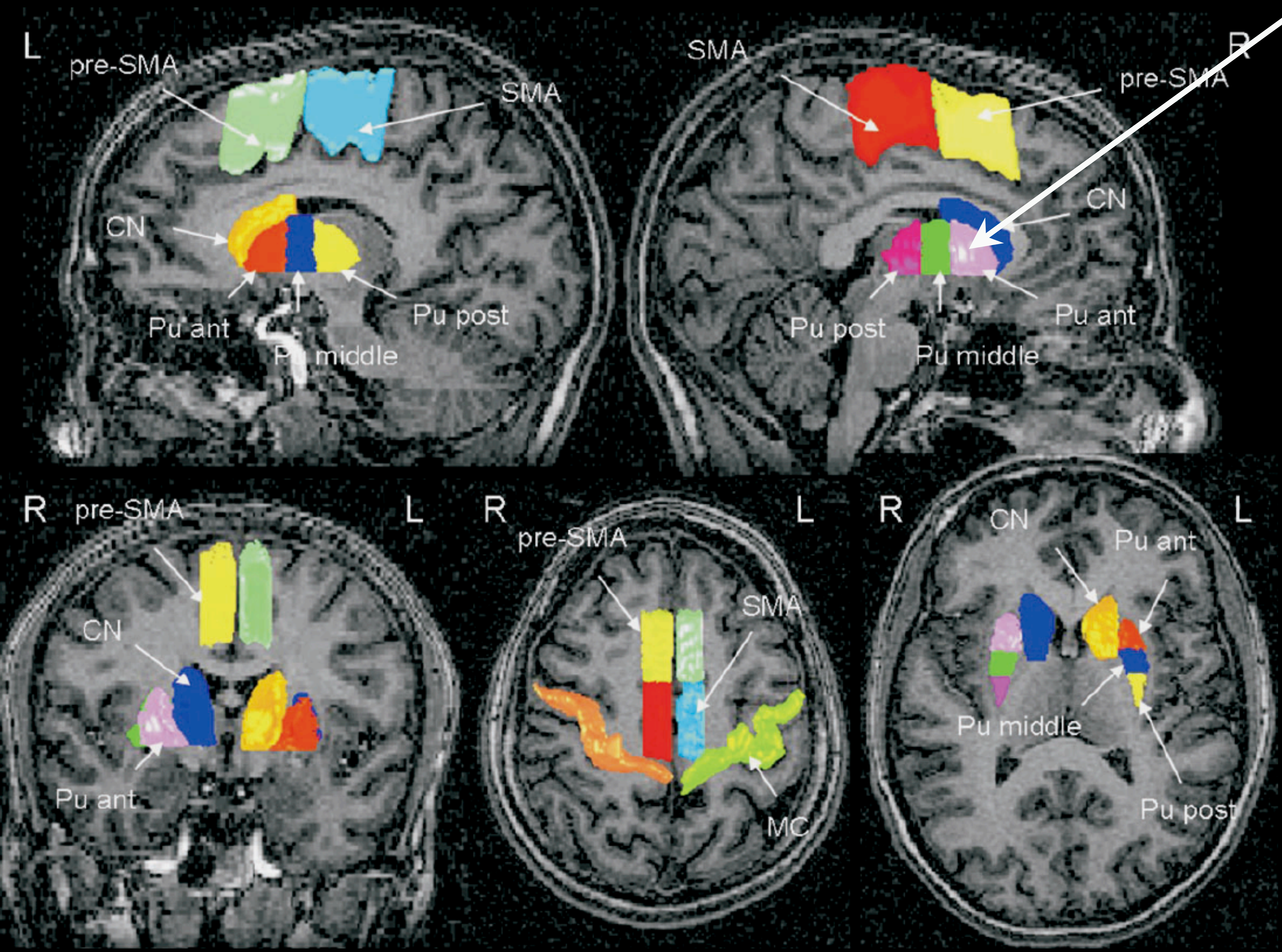

Associative striatal regions are implicated in movement selection / decision, mental simulation of grasping, task planning and learning of new motor skills
>> Anterior compartment

Image from [Lehericy-Ducros-etal04]

[Graybiel95], [Lehericy-Benali-etal03], [Lehericy-etal05]

Architecture of the Cortico-Striatal Connections

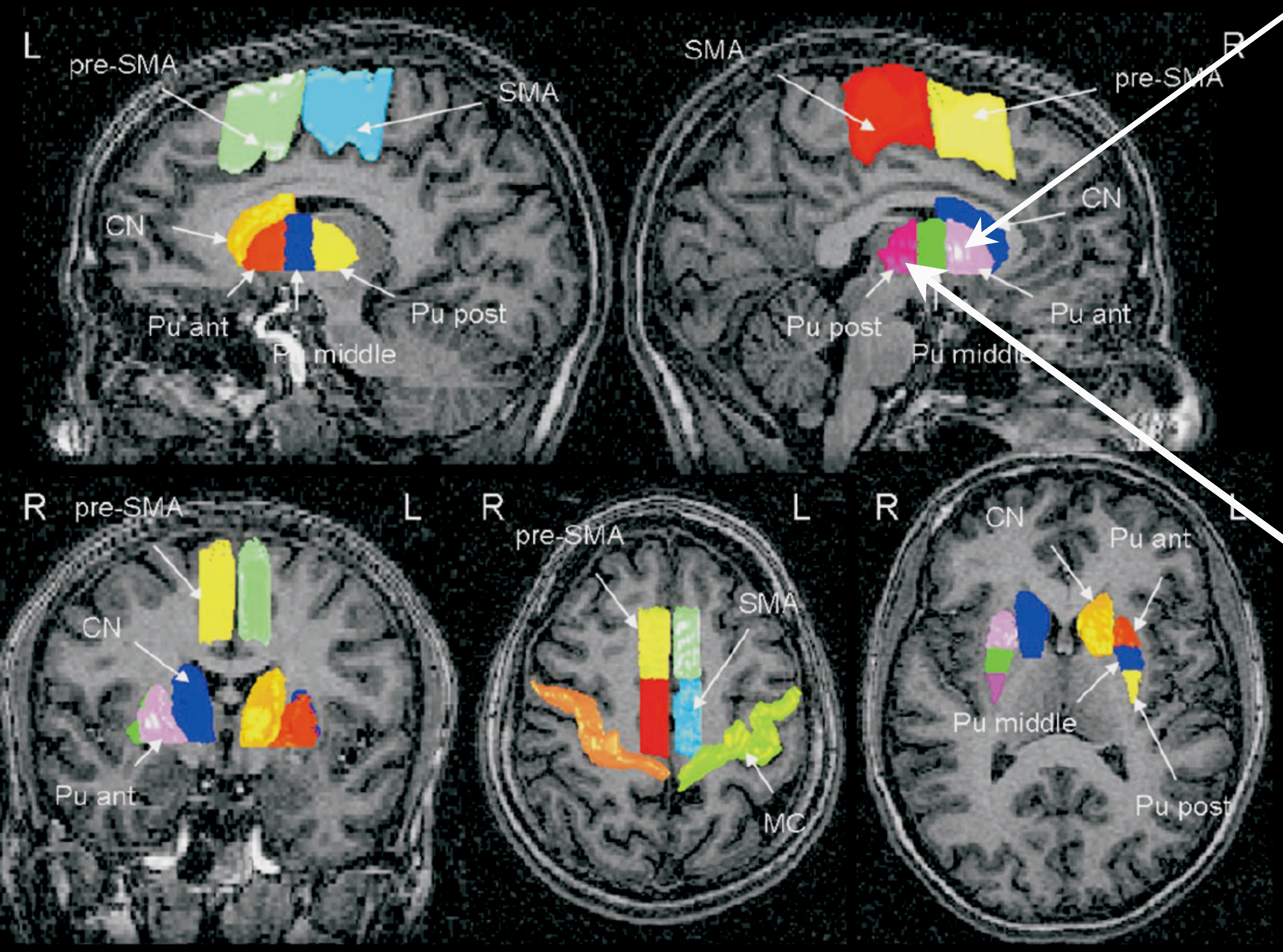

Associative striatal regions are implicated in movement selection / decision, mental simulation of grasping, task planning and learning of new motor skills
>> Anterior compartment

Sensorimotor striatal regions important for movement execution and skills storage (maintain speedy representation and automaticity)
>> Posterior compartment

Image from [Lehericy-Ducros-etal04]

[Graybiel95], [Lehericy-Benali-etal03], [Lehericy-etal05]

Architecture of the Cortico-Striatal Connections

- In [Lehericy-etal05], 13 right-handed subjects followed over 4 weeks
- Subjects asked to practice sequence of 8 moves with fingers 2 and 5

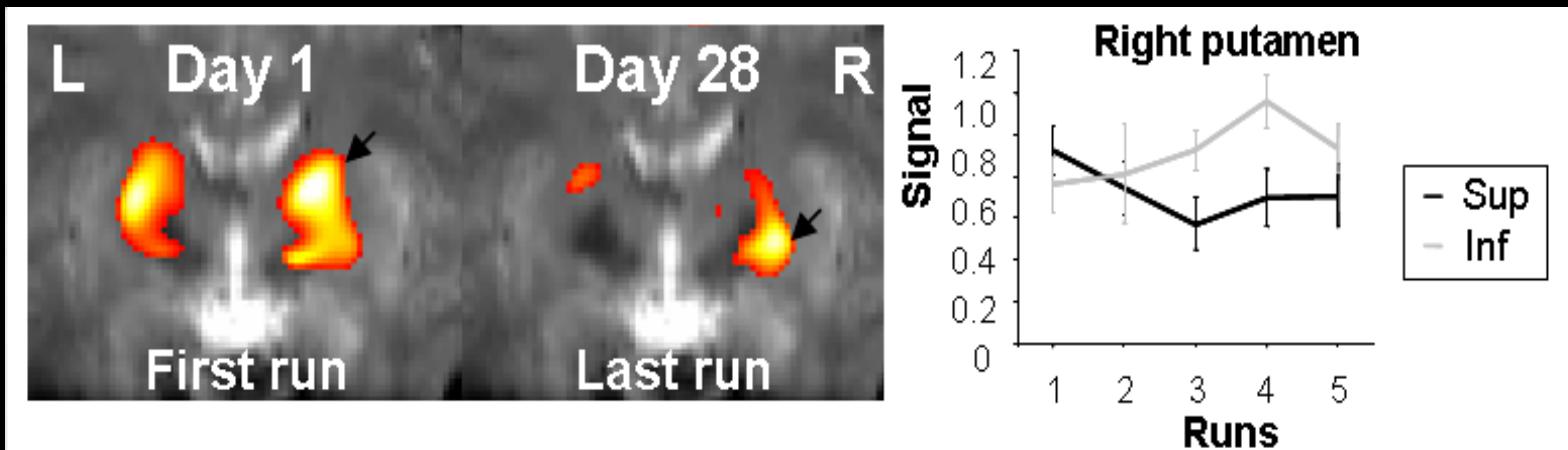

Image from [Lehericy-etal05]

- 2 main foci of activation in the putamen: Anterodorsal (day 1, black) / Posteroventral (day 28, gray).
- Regression analysis on pecentage signal increase:
  - Activation decreases with practice in anterodorsal putamen (bilateral)
  - Activation increases with practice in posteroventral putamen (bilateral)

Architecture of the Cortico-Striatal Connections

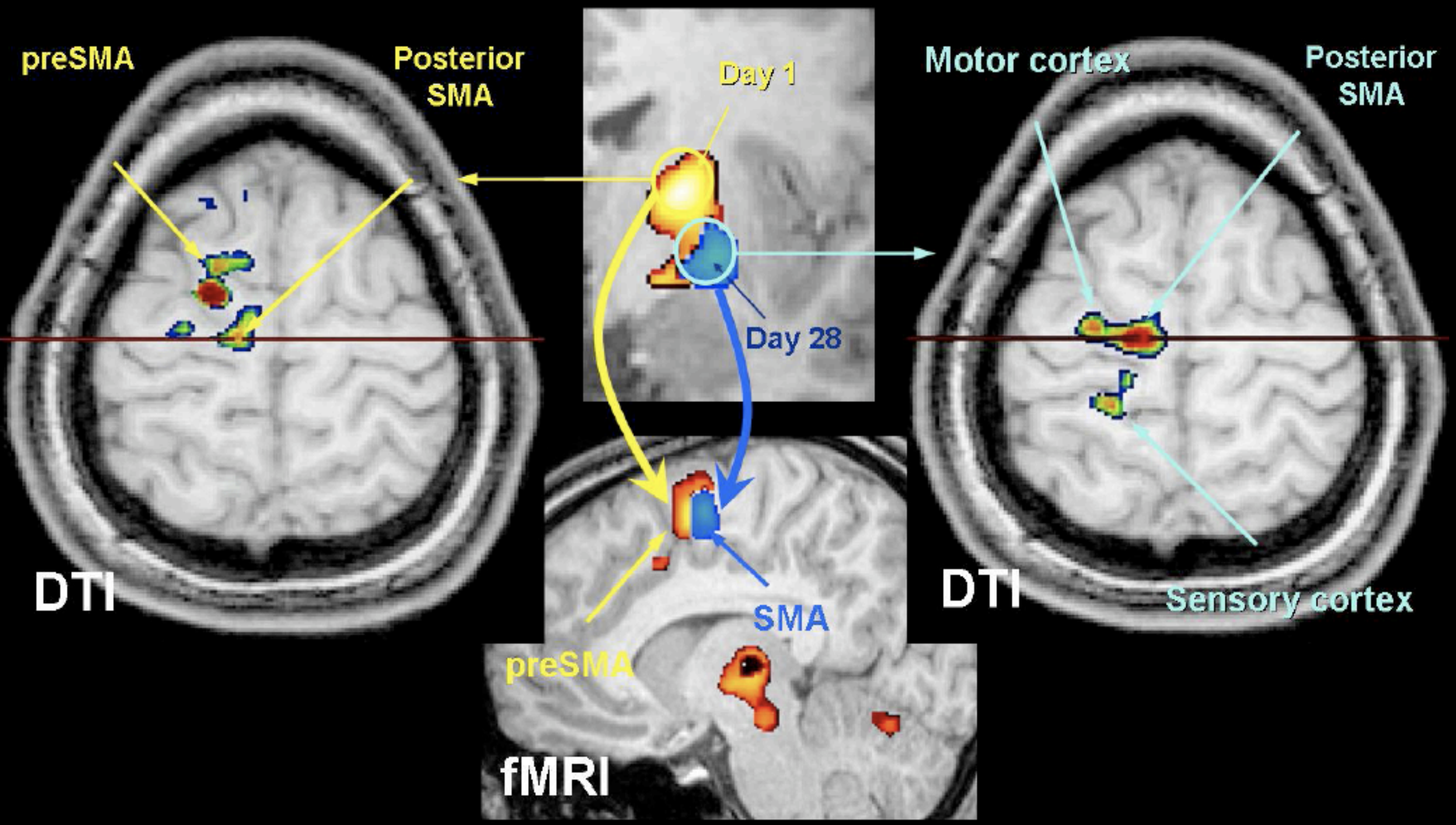

Architecture of the Cortico-Striatal Connections

Native Individual maps
(13 subjects)

Normalized
Individual maps

Average of Normalized
Individual maps

Before learning

After learning

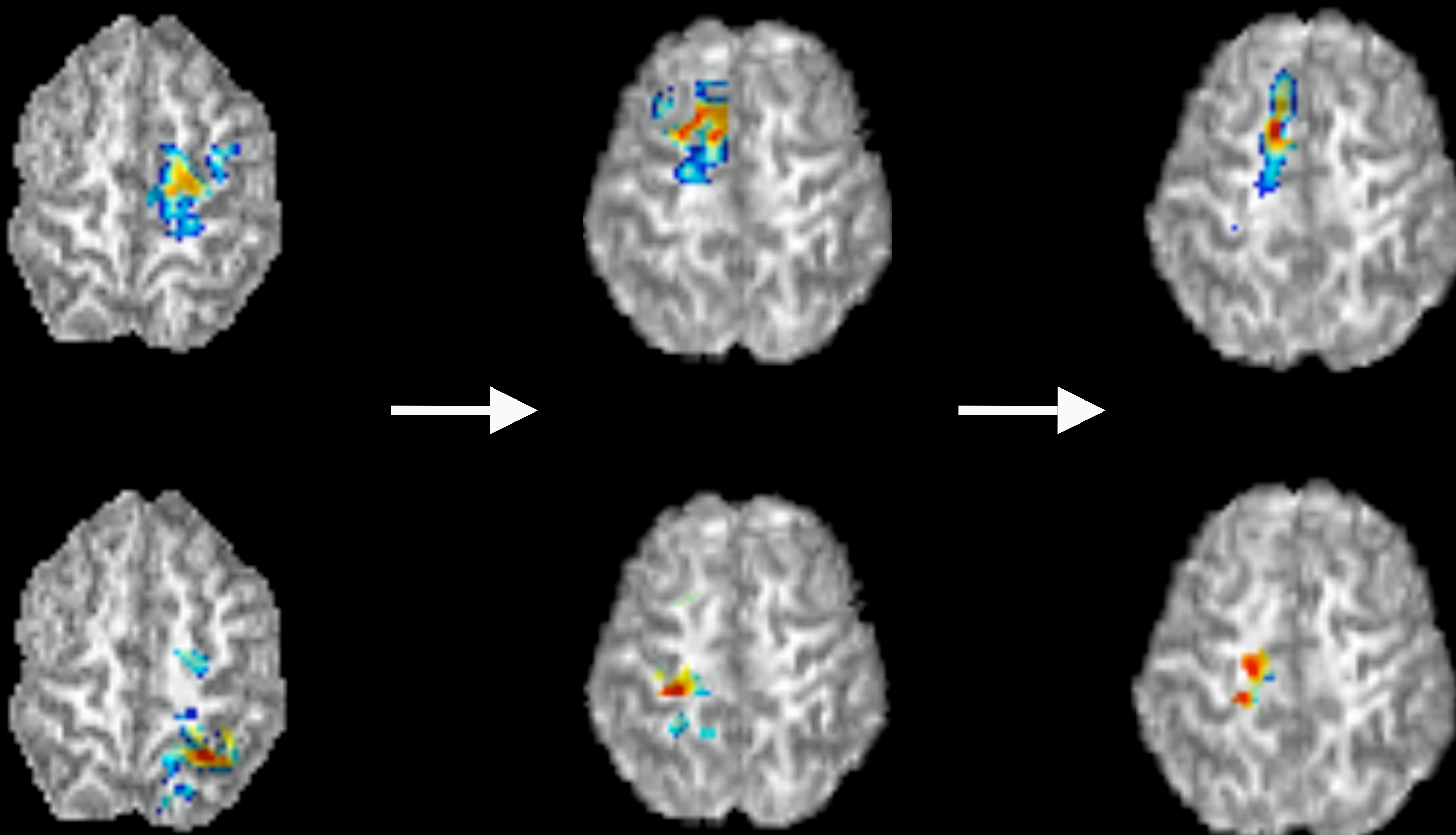

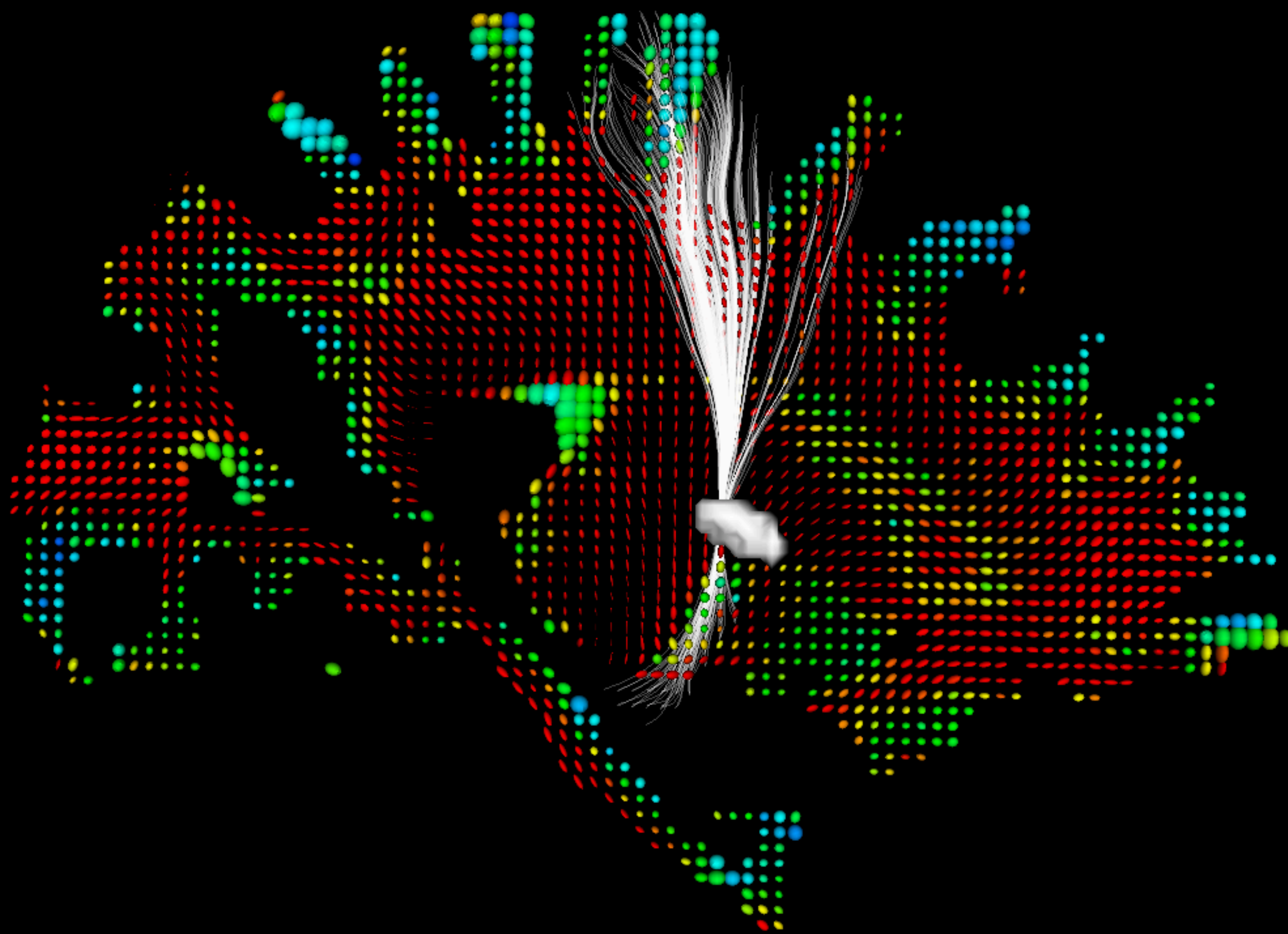

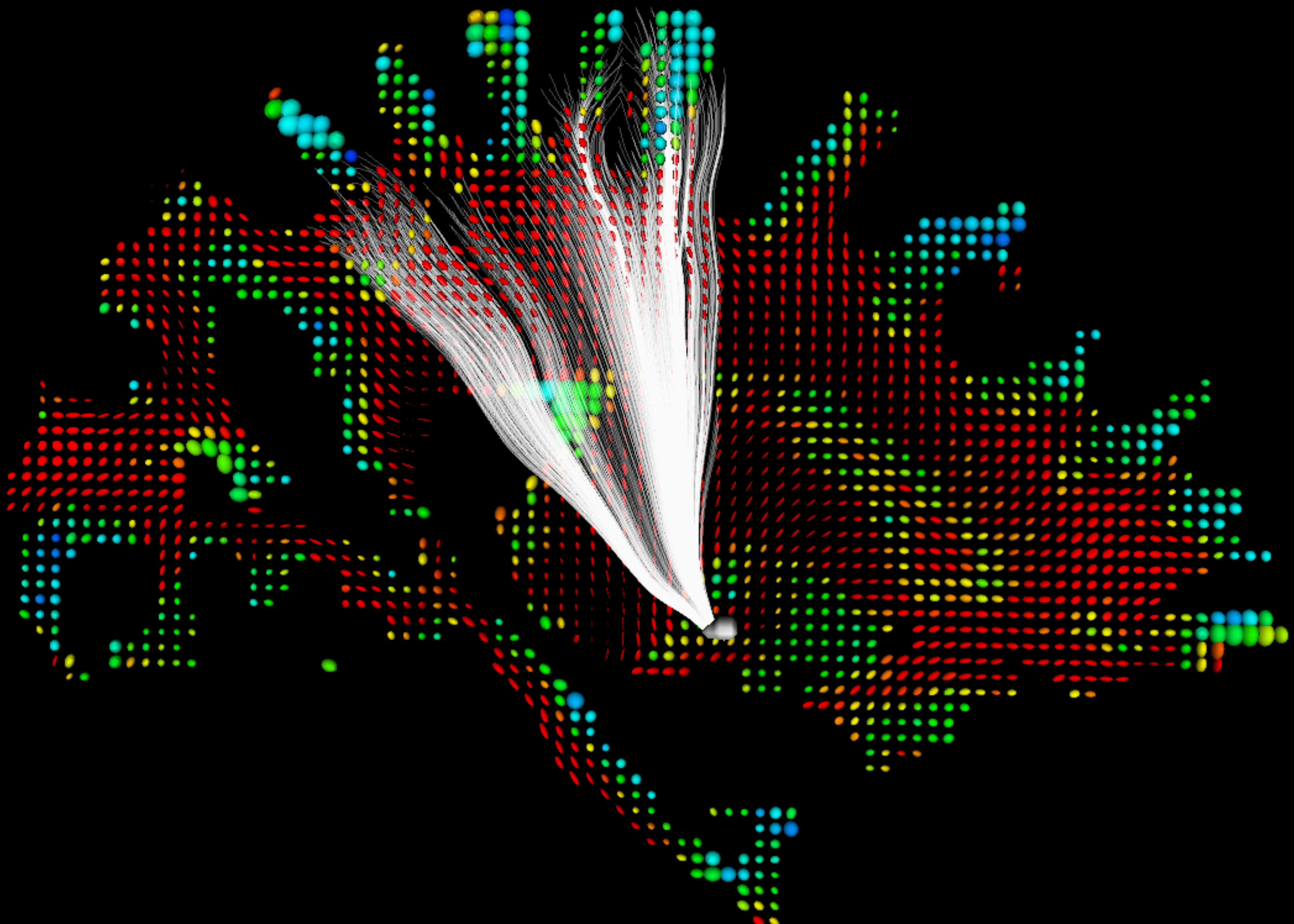

DTI / HARDI Segmentation

Variational formulation

(Joint work with M. Rousson, with contributions from M. Descoteaux)

Fiber Bundles Segmentation by Statistical Surface Evolution

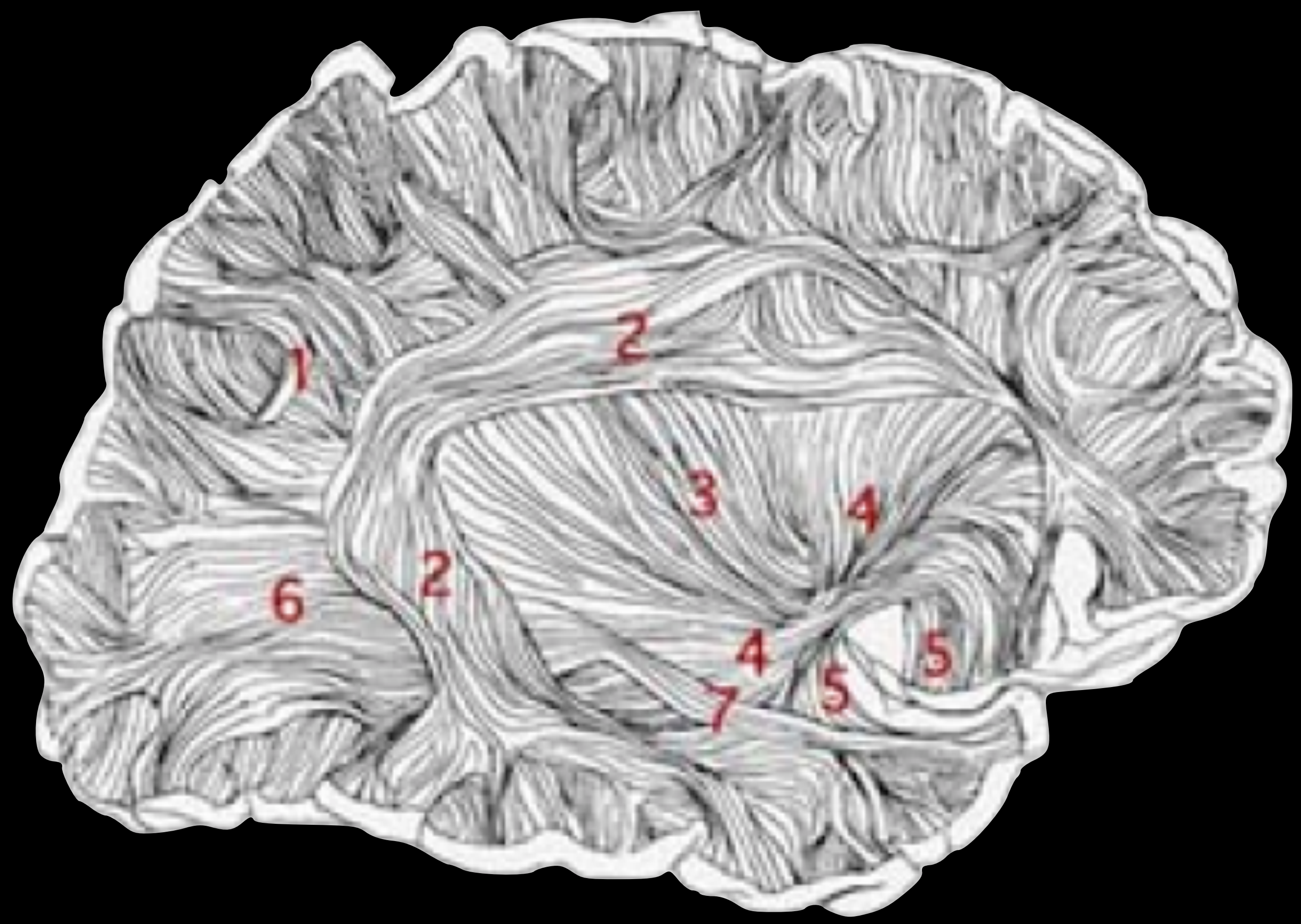

Images from [Williams-etal97]

Fiber Bundles Segmentation by Statistical Surface Evolution

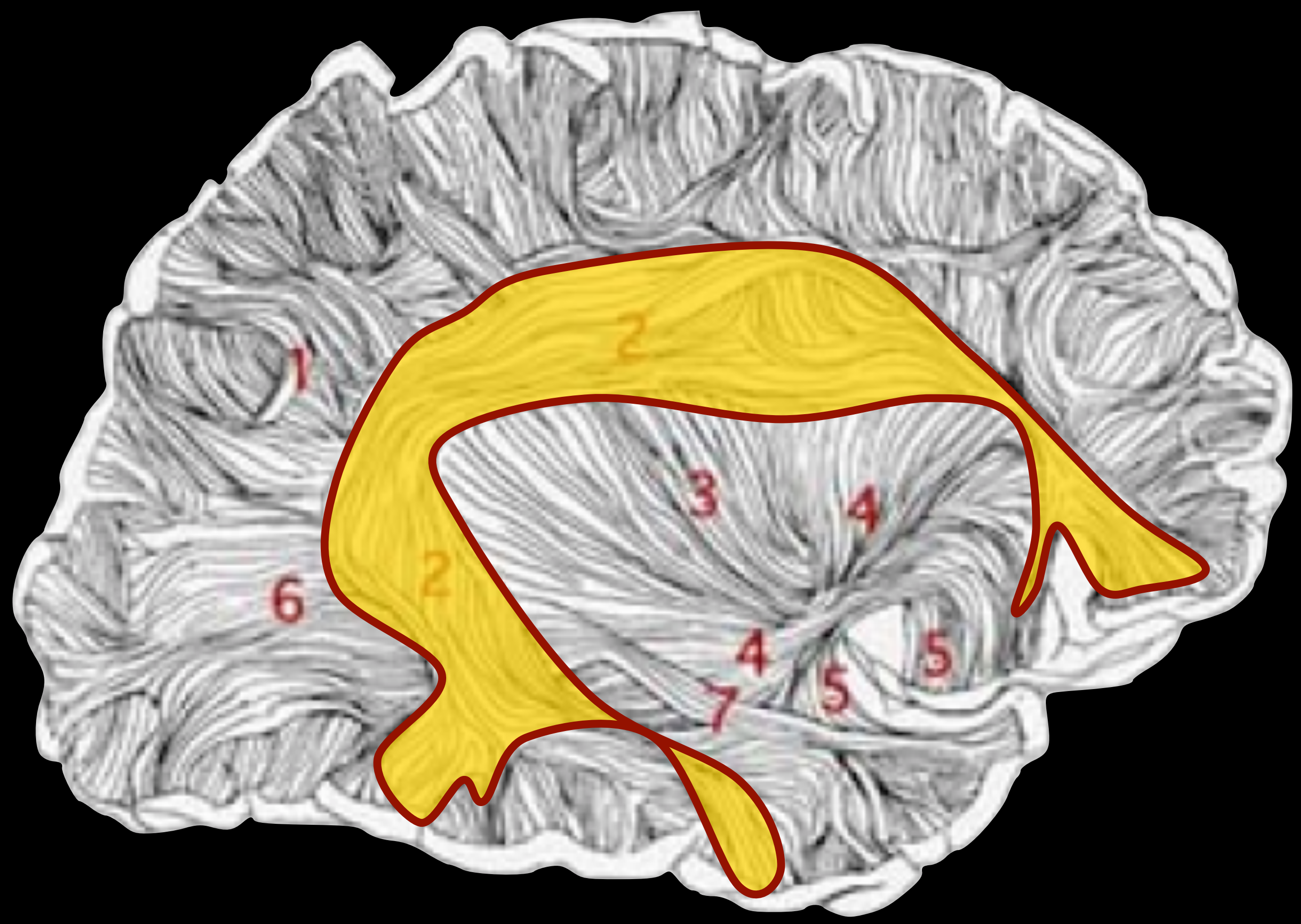

Images from [Williams-etal97]

Fiber Bundles Segmentation by Statistical Surface Evolution

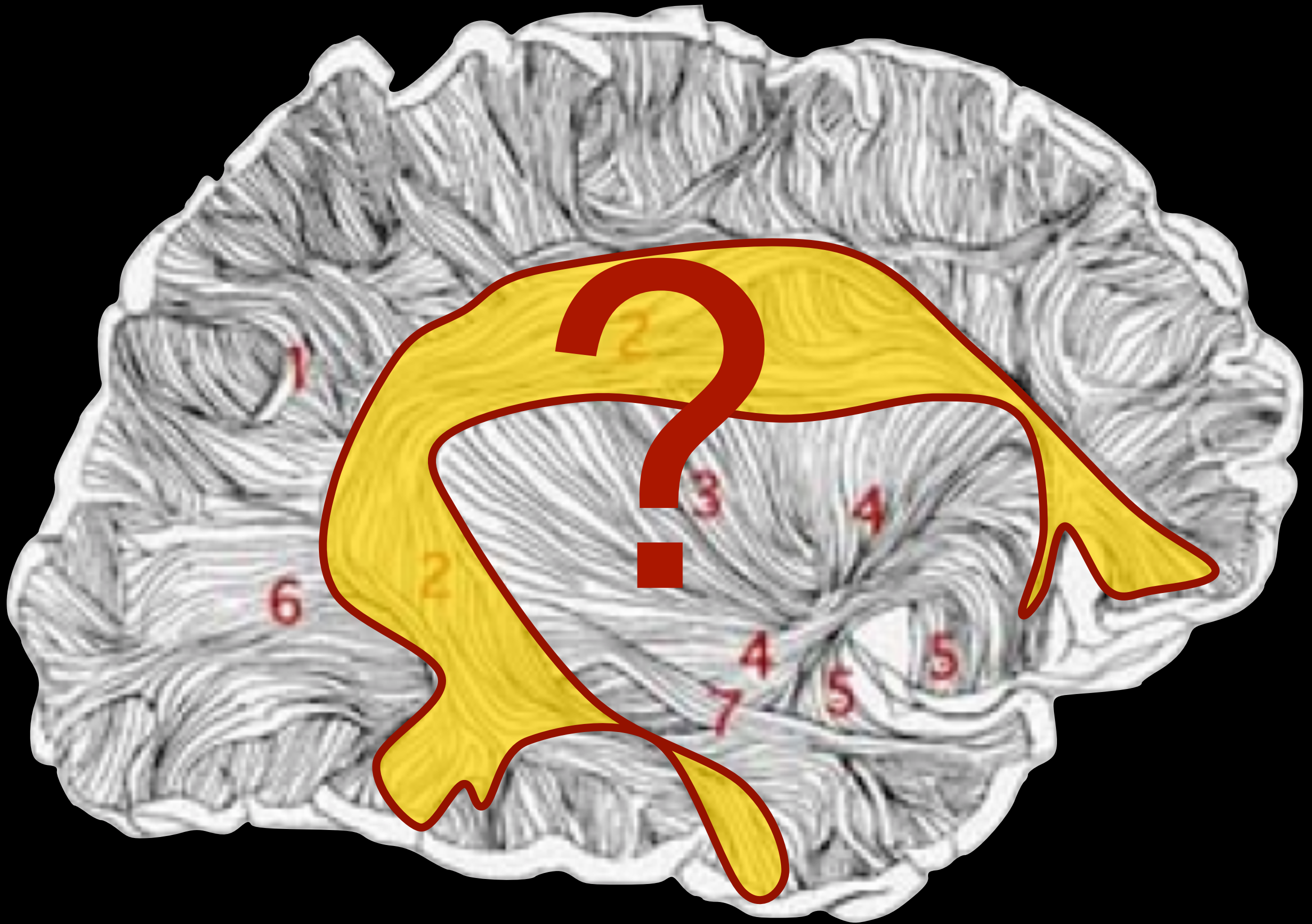

Images from [Williams-etal97]

Key idea:
Modeling of
diffusion tensors distribution

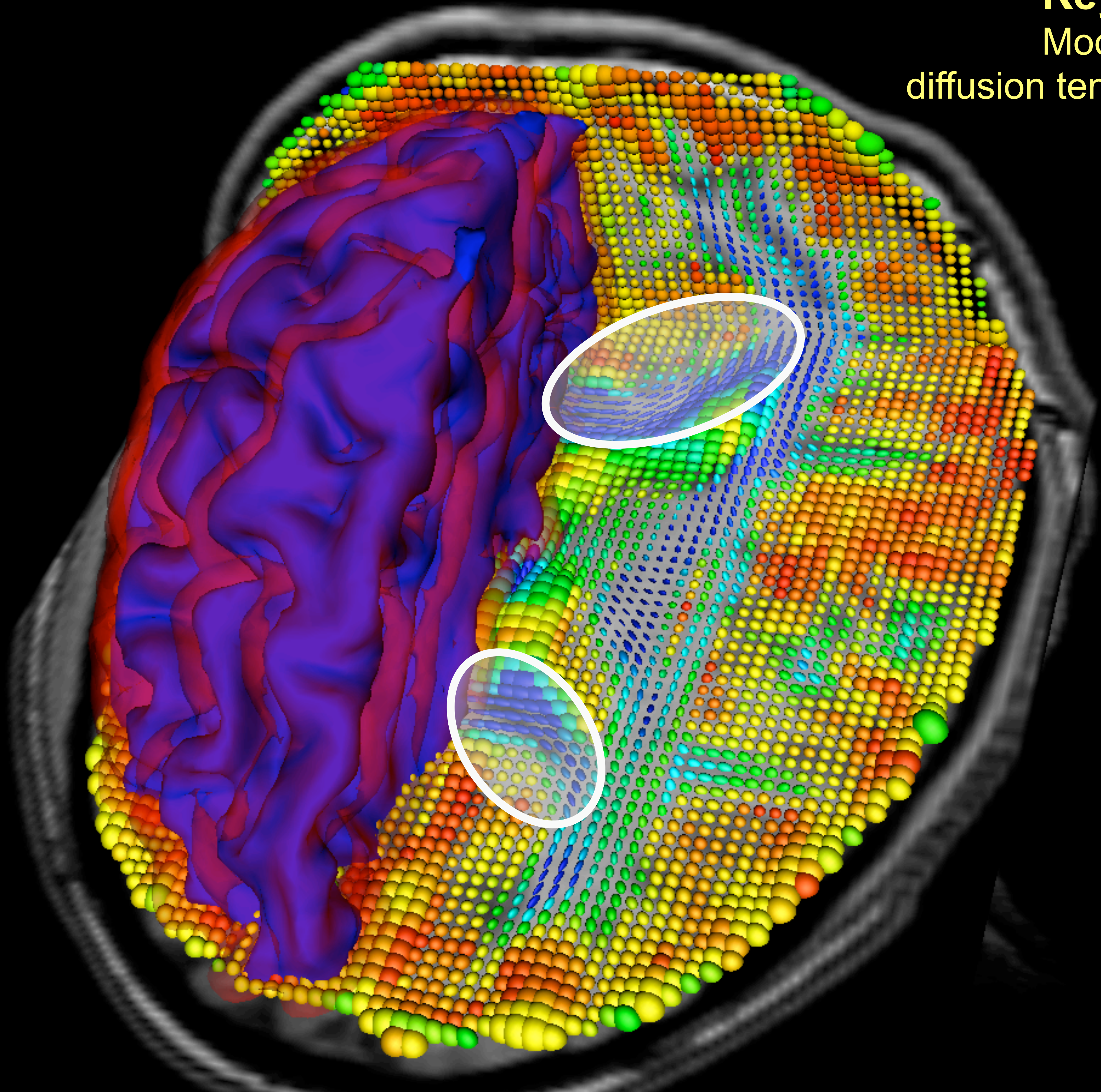

Key idea:
Modeling of
diffusion tensors distribution

Evolve a 3D surface
to maximize the
partition likelihood

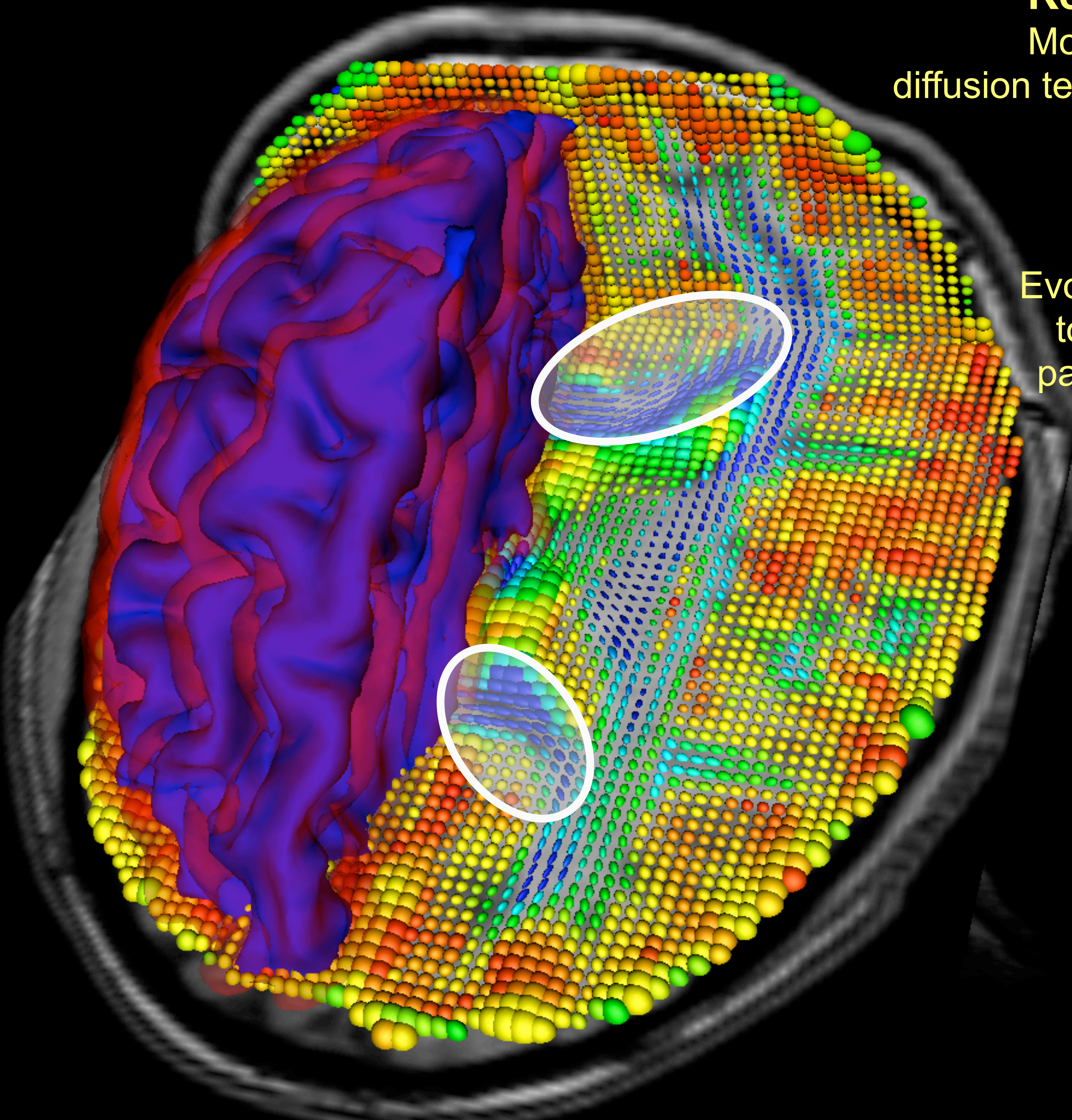

Statistical Surface Evolution

- $\mathcal{B}$: Evolving surface (implicitly represented by ψ)
- $\Sigma(x)$: Diffusion tensor at voxel x

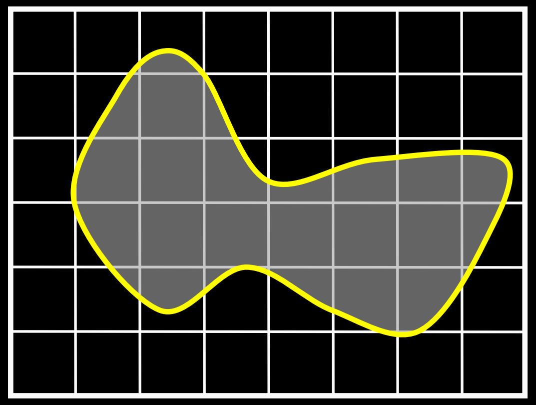

$$\begin{cases} \psi(x) = 0, & \text{if } x \in \mathcal{B} \\ \psi(x) = \mathcal{D}(x, \mathcal{B}), & \text{if } x \in \Omega_1 \\ \psi(x) = -\mathcal{D}(x, \mathcal{B}), & \text{if } x \in \Omega_2 \end{cases}$$

- The structure of interest is extracted by minimizing:

$$E(\psi, \Sigma_{1,2}, \Lambda_{1,2}) =$$

$$\nu \int_\Omega \delta(\psi) \|\nabla\psi\| \, dx + \int_\Omega \delta(\psi) \|\nabla\psi\| g_\alpha(\Sigma(x)) \, dx$$

$$- \int_{\Omega_1} \log p(\Sigma(x)|\overline{\Sigma}_1, \Lambda_1) dx - \int_{\Omega_2} \log p(\Sigma(x)|\overline{\Sigma}_2, \Lambda_2) dx$$

Statistical Surface Evolution

- $\mathcal{B}$: Evolving surface (implicitly represented by ψ)
- $\Sigma(x)$: Diffusion tensor at voxel x

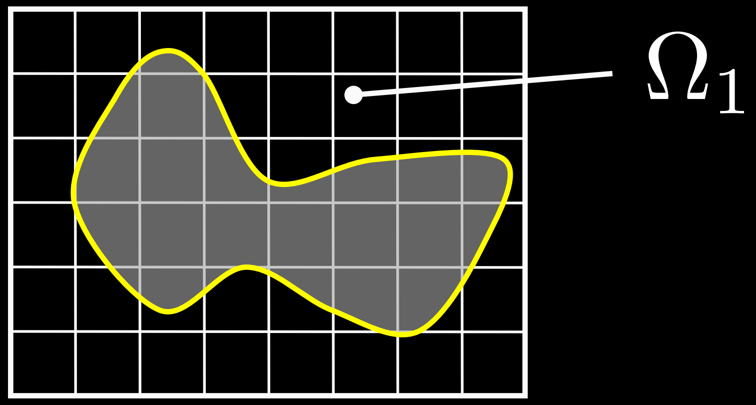

$$\begin{cases} \psi(x) = 0, & \text{if } x \in \mathcal{B} \\ \psi(x) = \mathcal{D}(x, \mathcal{B}), & \text{if } x \in \Omega_1 \\ \psi(x) = -\mathcal{D}(x, \mathcal{B}), & \text{if } x \in \Omega_2 \end{cases}$$

- The structure of interest is extracted by minimizing:

$$E(\psi, \Sigma_{1,2}, \Lambda_{1,2}) =$$
$$\nu \int_\Omega \delta(\psi) \|\nabla \psi\| \, dx + \int_\Omega \delta(\psi) \|\nabla \psi\| g_\alpha(\Sigma(x)) \, dx$$
$$- \int_{\Omega_1} \log p(\Sigma(x) | \overline{\Sigma}_1, \Lambda_1) dx - \int_{\Omega_2} \log p(\Sigma(x) | \overline{\Sigma}_2, \Lambda_2) dx$$

Statistical Surface Evolution

- $\mathcal{B}$: Evolving surface (implicitly represented by ψ)
- $\Sigma(x)$: Diffusion tensor at voxel x

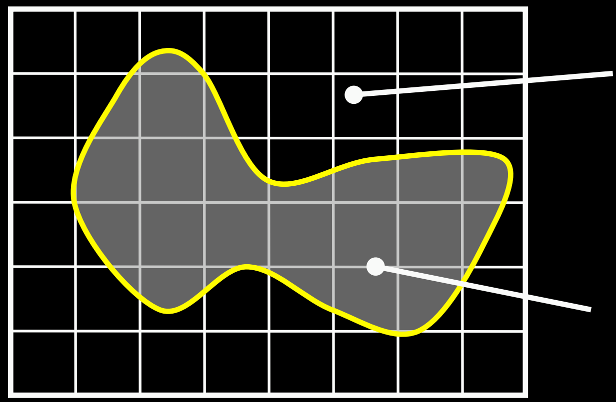

Ω_1

Ω_2

$$\begin{cases} \psi(x) = 0, & \text{if } x \in \mathcal{B} \\ \psi(x) = \mathcal{D}(x, \mathcal{B}), & \text{if } x \in \Omega_1 \\ \psi(x) = -\mathcal{D}(x, \mathcal{B}), & \text{if } x \in \Omega_2 \end{cases}$$

- The structure of interest is extracted by minimizing:

$$E(\psi, \Sigma_{1,2}, \Lambda_{1,2}) = \nu \int_\Omega \delta(\psi)\|\nabla\psi\| \, dx + \int_\Omega \delta(\psi)\|\nabla\psi\| g_\alpha(\Sigma(x)) \, dx - \int_{\Omega_1} \log p(\Sigma(x)|\overline{\Sigma}_1, \Lambda_1) dx - \int_{\Omega_2} \log p(\Sigma(x)|\overline{\Sigma}_2, \Lambda_2) dx$$

Statistical Surface Evolution

- $\mathcal{B}$: Evolving surface (implicitly represented by ψ)
- $\Sigma(x)$: Diffusion tensor at voxel x

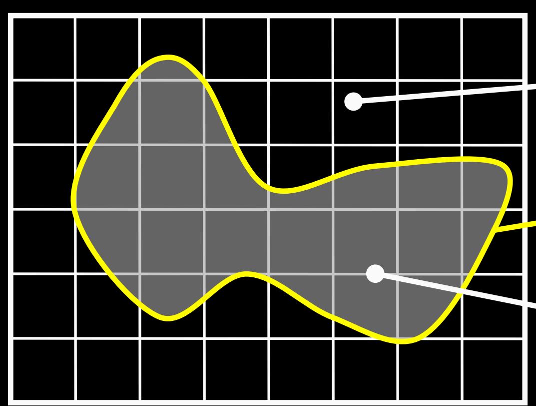

$$\begin{cases} \psi(x) = 0, & \text{if } x \in \mathcal{B} \\ \psi(x) = \mathcal{D}(x, \mathcal{B}), & \text{if } x \in \Omega_1 \\ \psi(x) = -\mathcal{D}(x, \mathcal{B}), & \text{if } x \in \Omega_2 \end{cases}$$

- The structure of interest is extracted by minimizing:

$$E(\psi, \Sigma_{1,2}, \Lambda_{1,2}) = \nu \int_\Omega \delta(\psi) \|\nabla\psi\| \, dx + \int_\Omega \delta(\psi) \|\nabla\psi\| g_\alpha(\Sigma(x)) \, dx - \int_{\Omega_1} \log p(\Sigma(x)|\overline{\Sigma}_1, \Lambda_1) dx - \int_{\Omega_2} \log p(\Sigma(x)|\overline{\Sigma}_2, \Lambda_2) dx$$

Statistical Surface Evolution

- Energy comes from the fact that, if tensors are *iid*, we have

$$p(\Sigma|\psi) = \prod_{x\in\Omega_1} p_1(\Sigma(x)). \prod_{x\in\Omega_2} p_2(\Sigma(x)). \prod_{x\in\mathcal{B}} p_b(\Sigma(x))$$

with

$$p_b(\Sigma(x)) = \exp\left(-g_\alpha(\|\nabla\Sigma(x)\|)\right)$$

and typically

$$g_\alpha(y) = \frac{1}{1+y^\alpha}$$

- Evolution equation:

$$\frac{\partial\psi}{\partial t} = \delta(\psi)\left((\nu + g_\alpha(\Sigma))\,\mathrm{div}\left(\frac{\nabla\psi}{\|\nabla\psi\|}\right) + \frac{\nabla\phi}{\|\nabla\phi\|}\cdot\nabla g_\alpha(\Sigma) + \log\frac{p(\Sigma|\overline{\Sigma}_1,\Lambda_1)}{p(\Sigma|\overline{\Sigma}_2,\Lambda_2)}\right)$$

Statistical Surface Evolution

- Energy comes from the fact that, if tensors are *iid*, we have

$$p(\Sigma|\psi) = \prod_{x \in \Omega_1} p_1(\Sigma(x)). \prod_{x \in \Omega_2} p_2(\Sigma(x)). \prod_{x \in \mathcal{B}} p_b(\Sigma(x))$$

with

$$p_b(\Sigma(x)) = \exp\left(-g_\alpha(\|\nabla\Sigma(x)\|)\right)$$

and typically

$$g_\alpha(y) = \frac{1}{1+y^\alpha}$$

- Evolution equation:

$$\frac{\partial\psi}{\partial t} = \delta(\psi)\left((\nu + g_\alpha(\Sigma))\,\mathrm{div}\left(\frac{\nabla\psi}{\|\nabla\psi\|}\right) + \frac{\nabla\phi}{\|\nabla\phi\|}\cdot\nabla g_\alpha(\Sigma) + \log\frac{p(\Sigma|\overline{\Sigma}_1,\Lambda_1)}{p(\Sigma|\overline{\Sigma}_2,\Lambda_2)}\right)$$

Synthetic Results #1

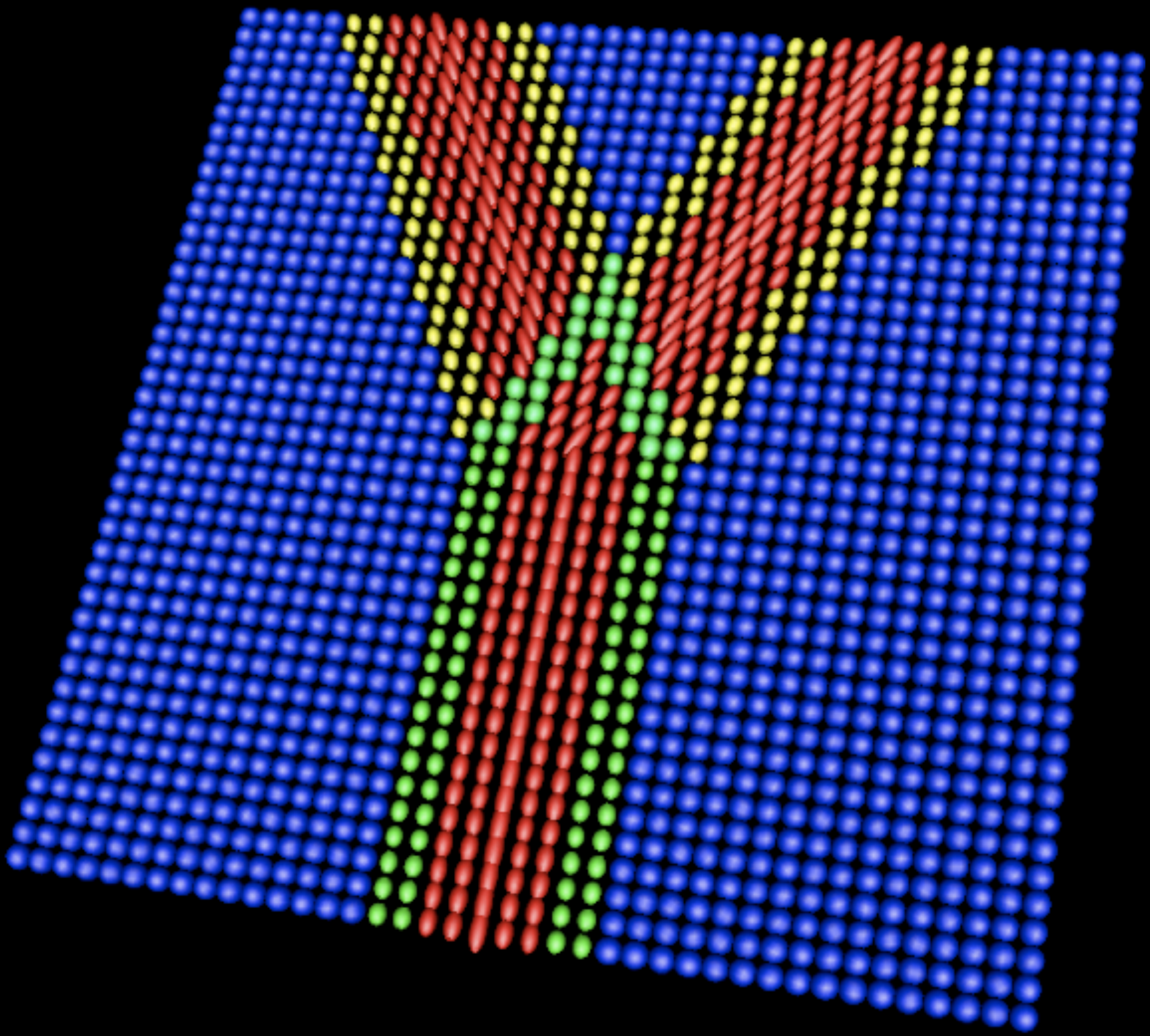

Euclidean (45) / J-divergence (30) / Riemannian (28)
probability metrics

Synthetic Results #1

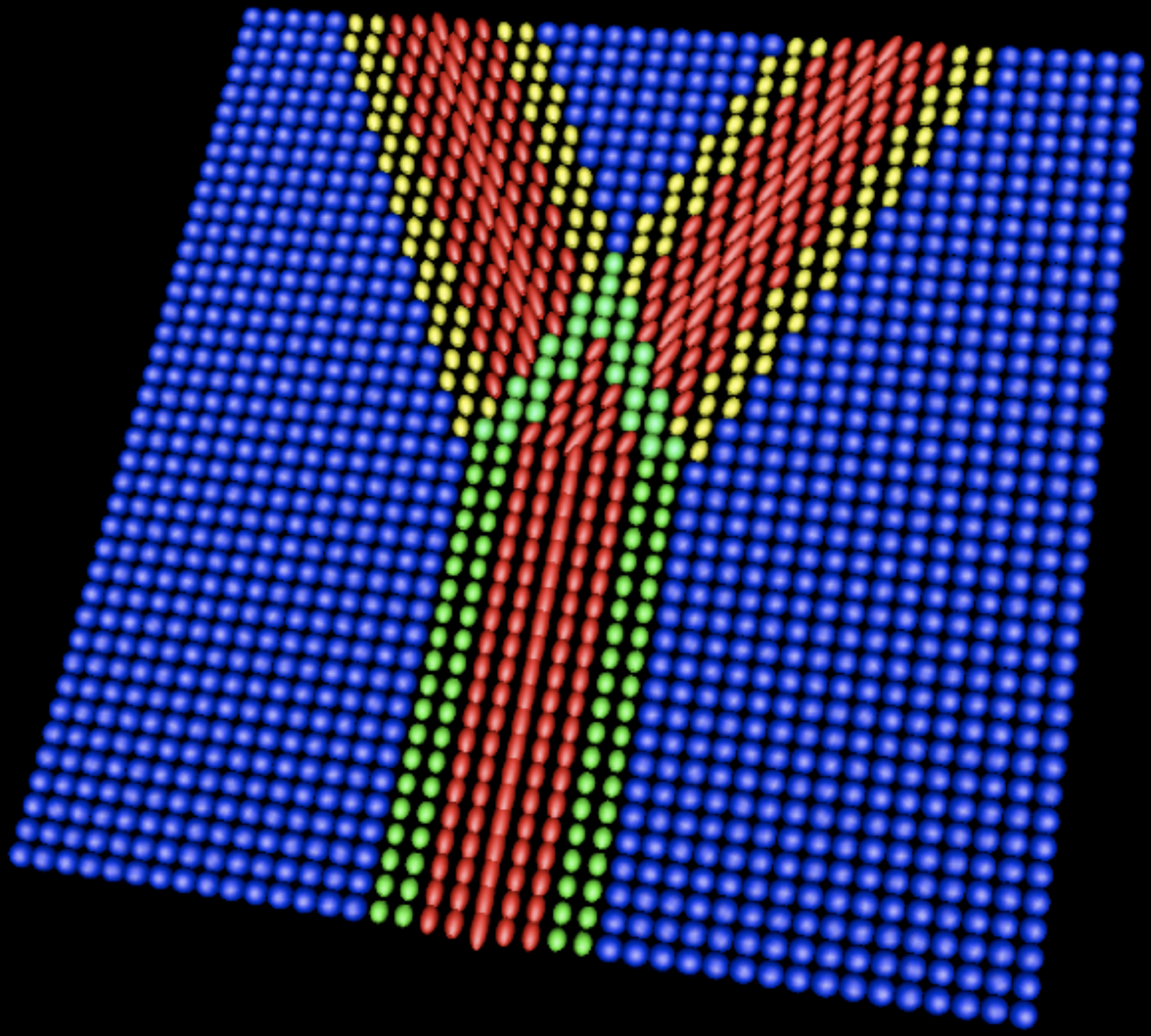

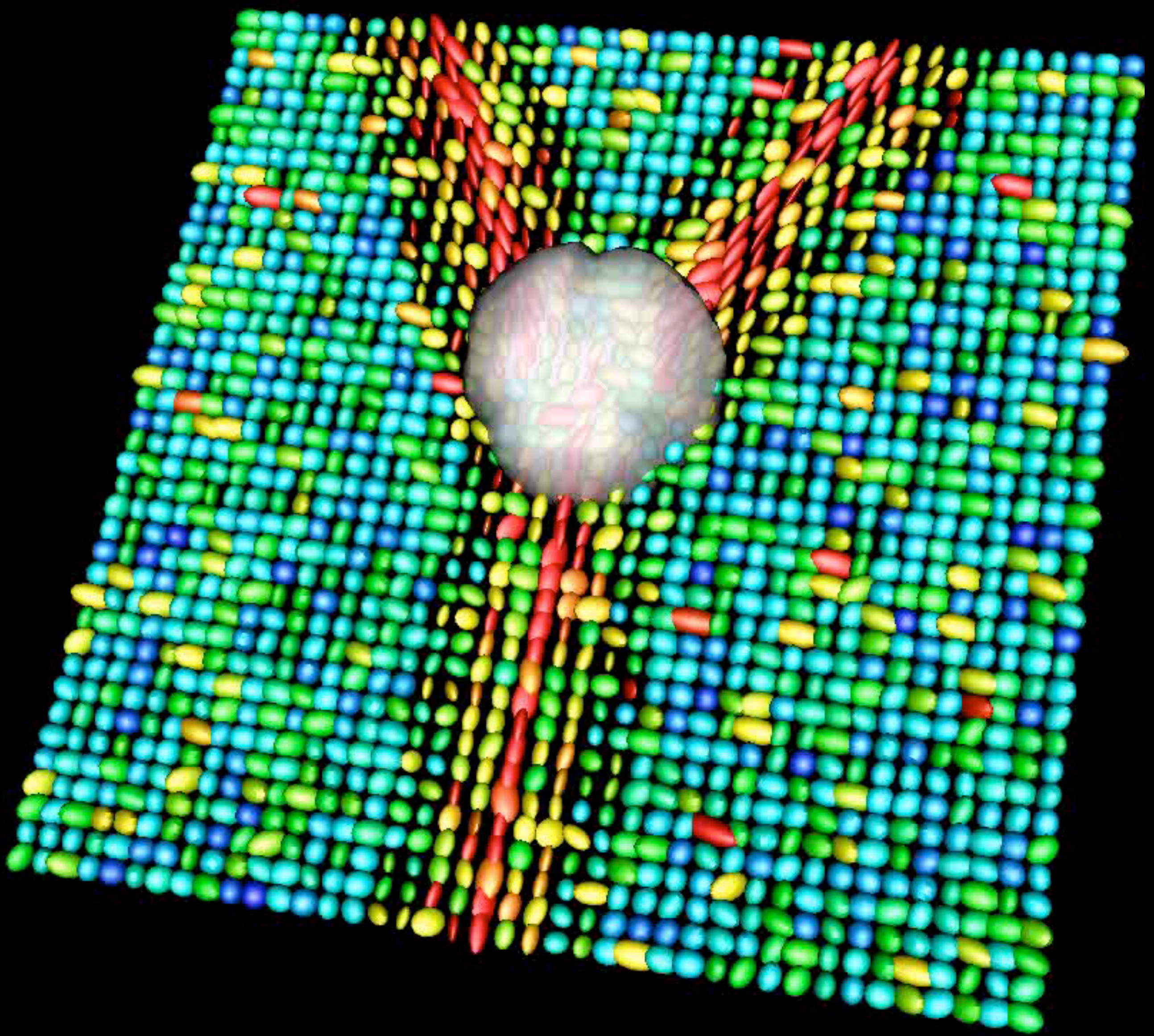

Euclidean (45) / J-divergence (30) / Riemannian (28)
probability metrics

Synthetic Results #2

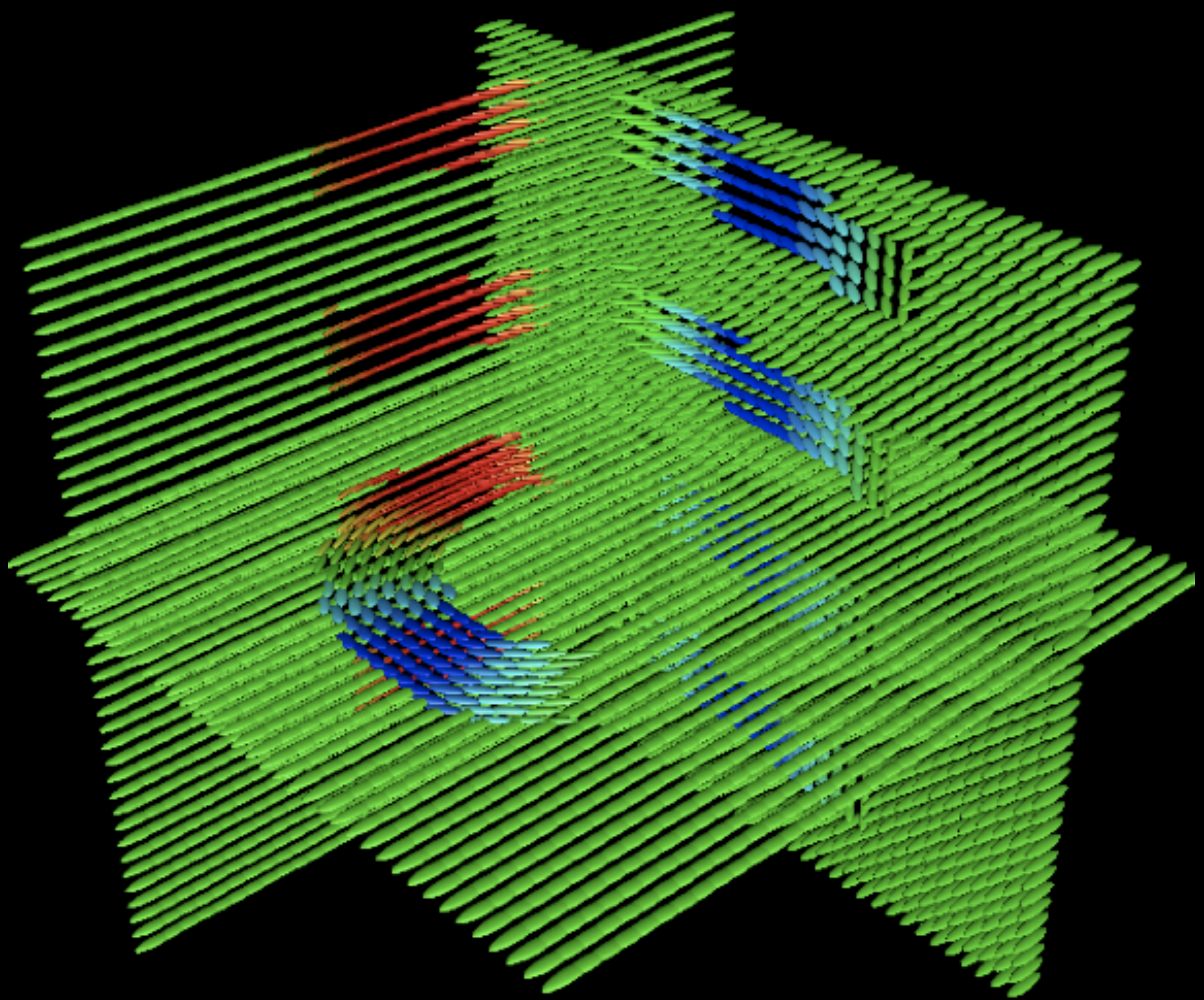

Euclidean metric (130)

J-divergence metric (80)

Riemannian metric (300)

Synthetic Results #2

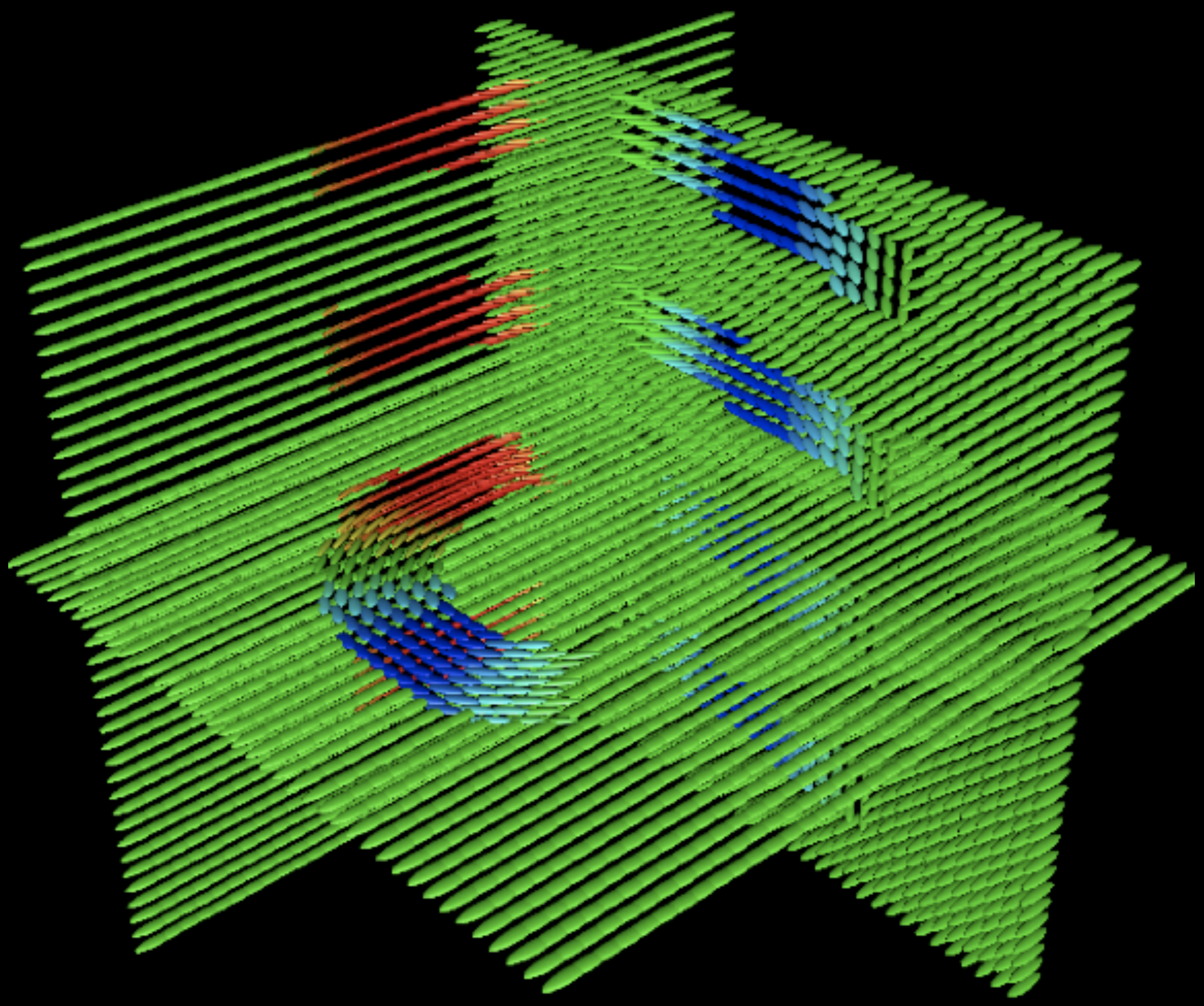

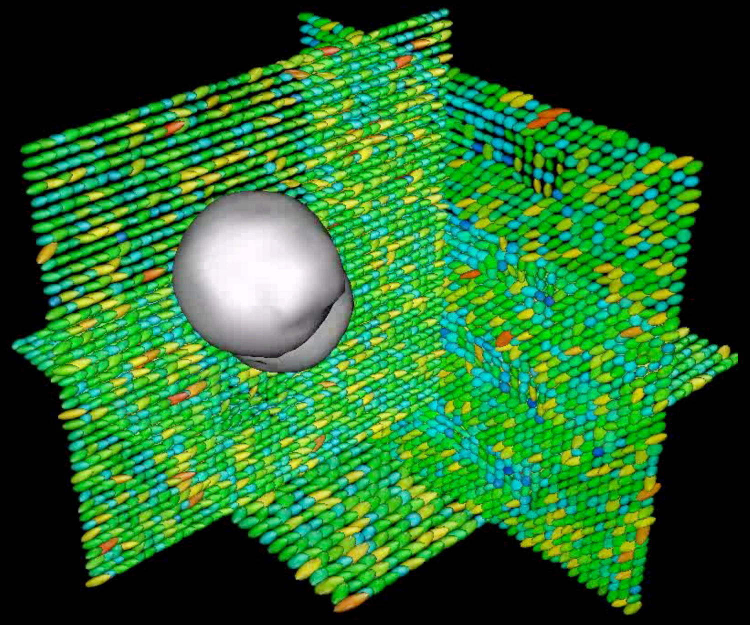

Euclidean metric (130)

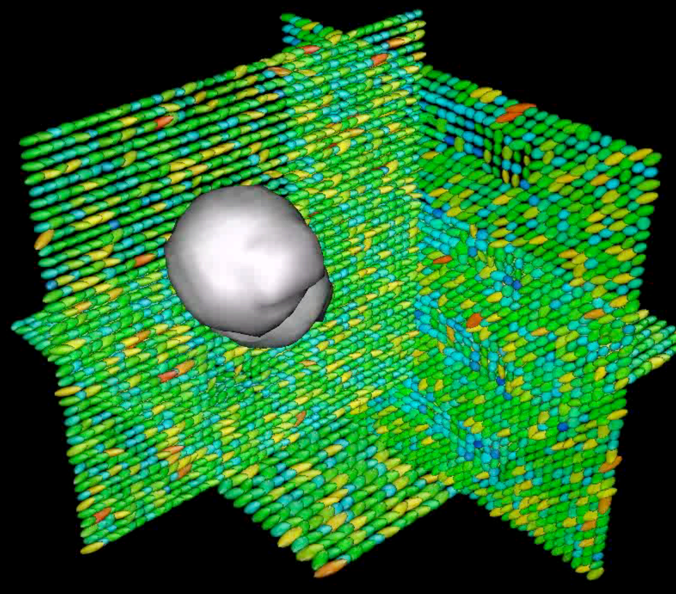

J-divergence metric (80)

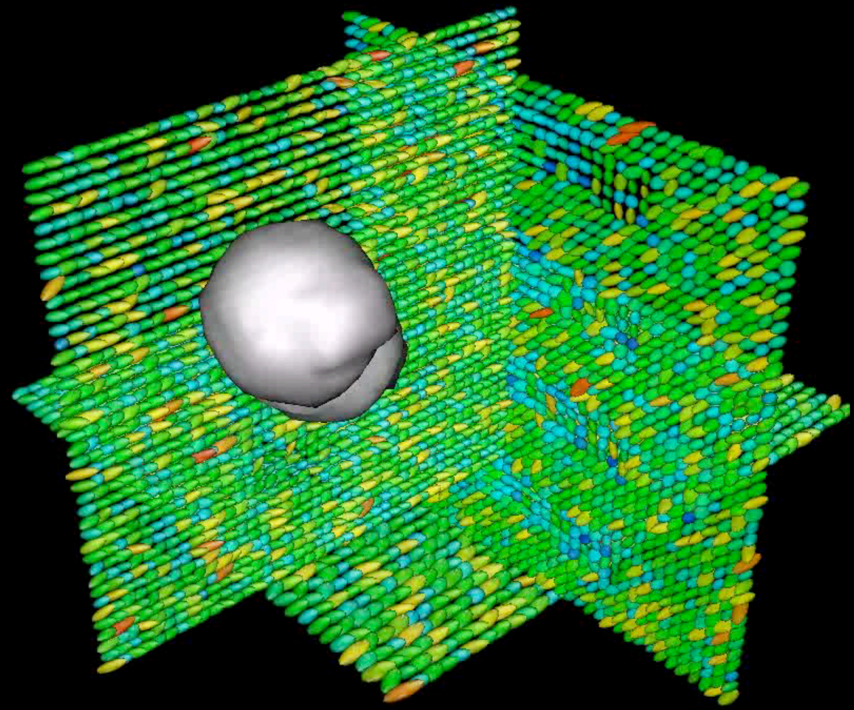

Riemannian metric (300)

Synthetic Results #2

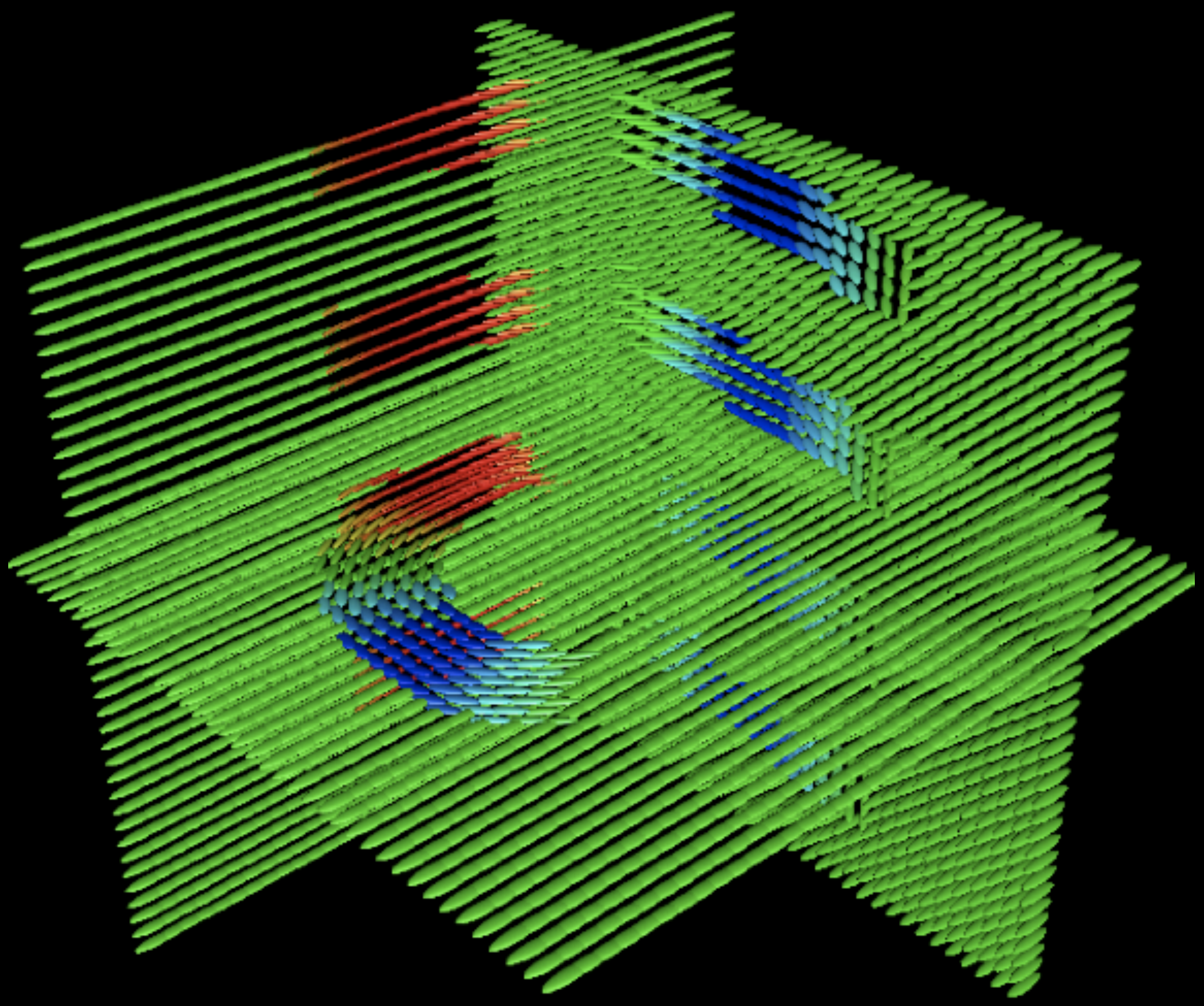

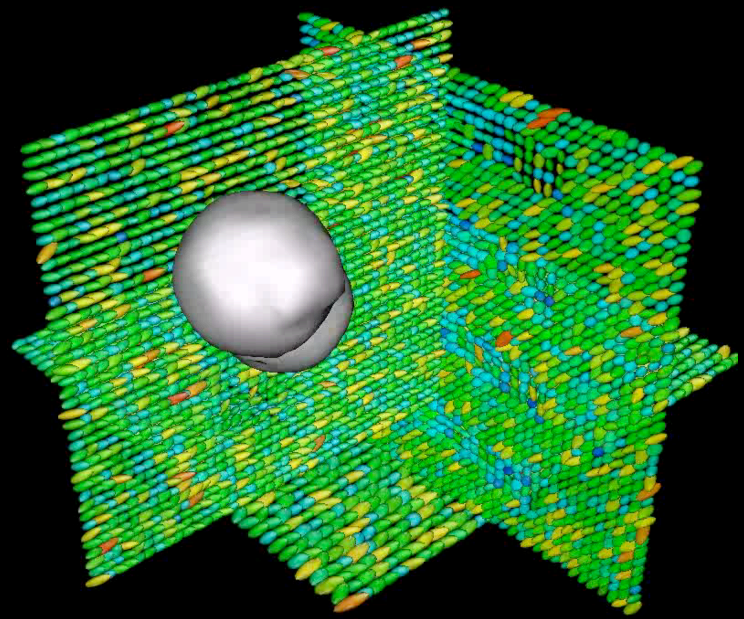

Euclidean metric (130)

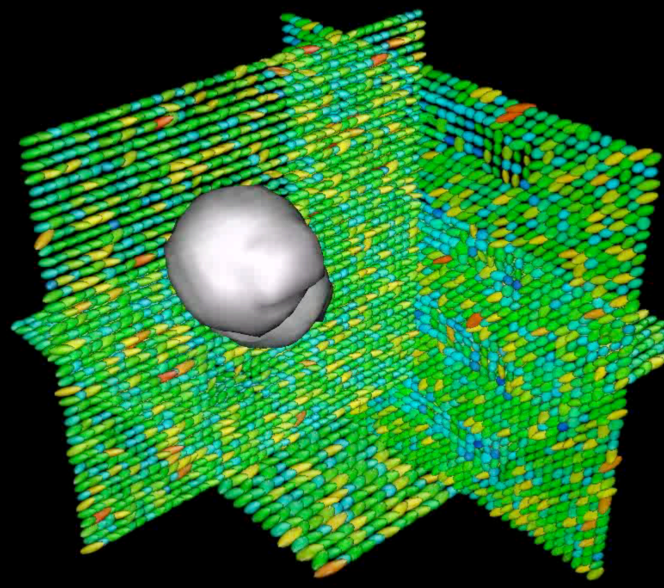

J-divergence metric (80)

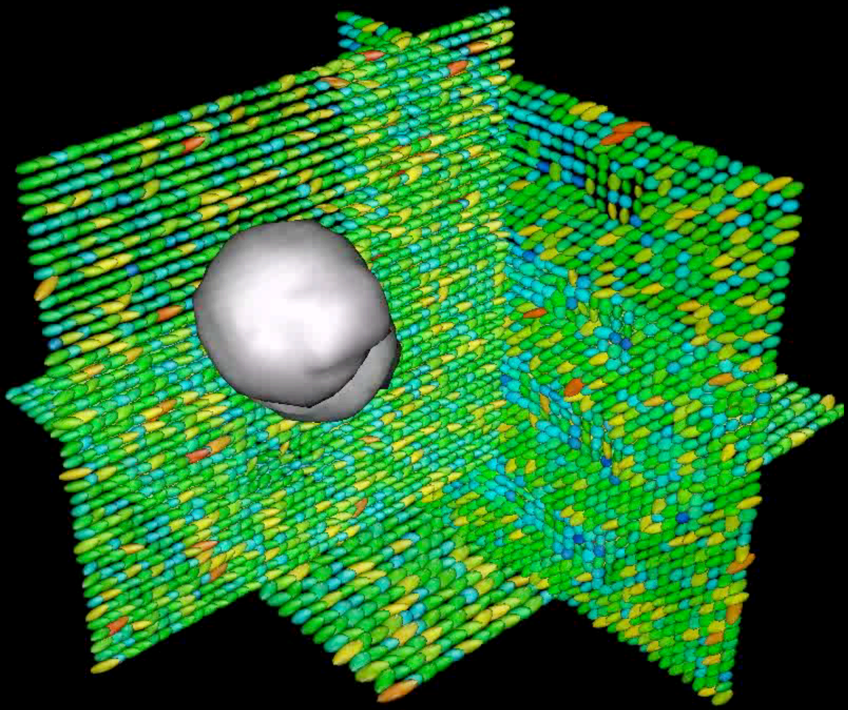

Riemannian metric (300)

Synthetic Results #2

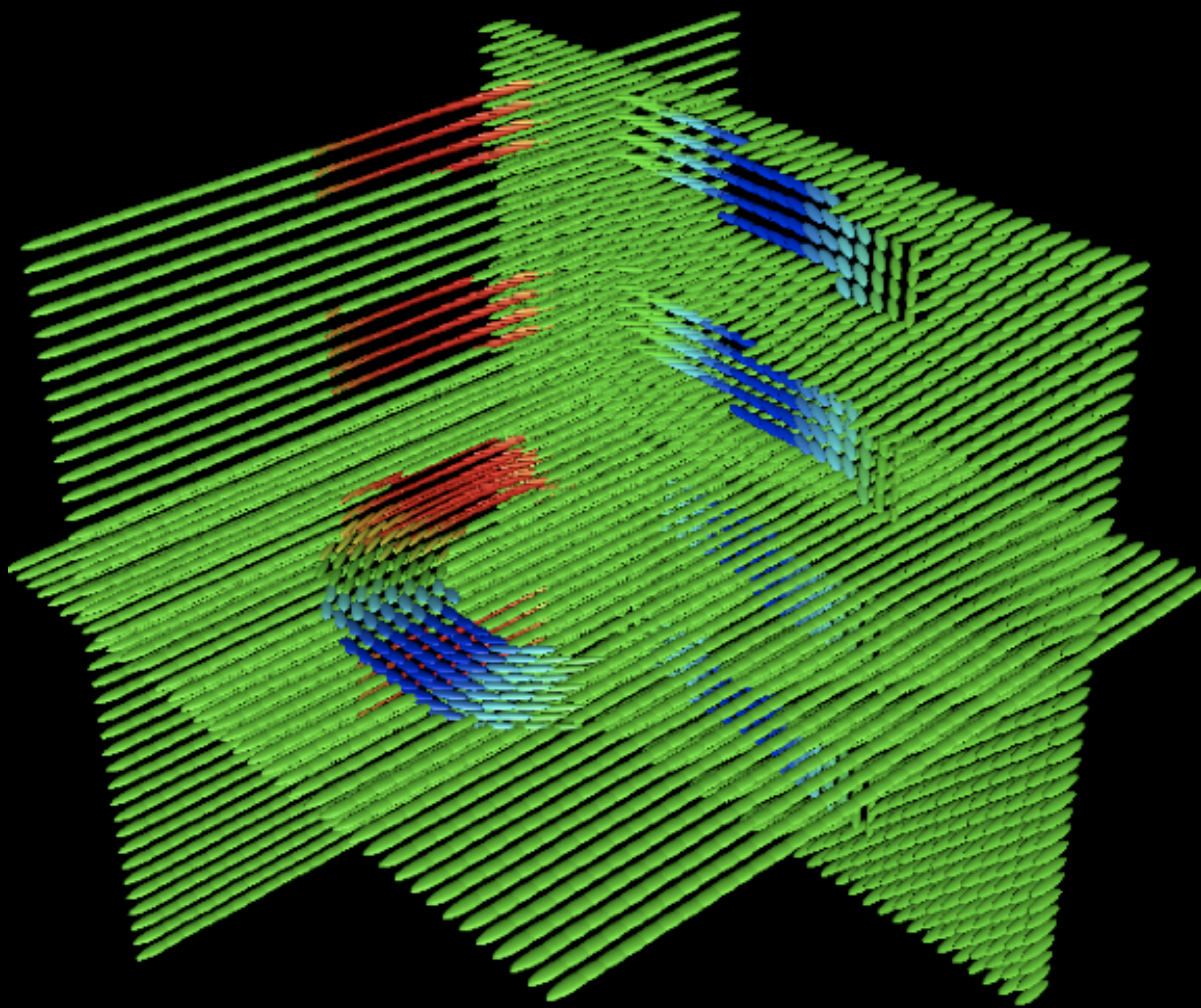

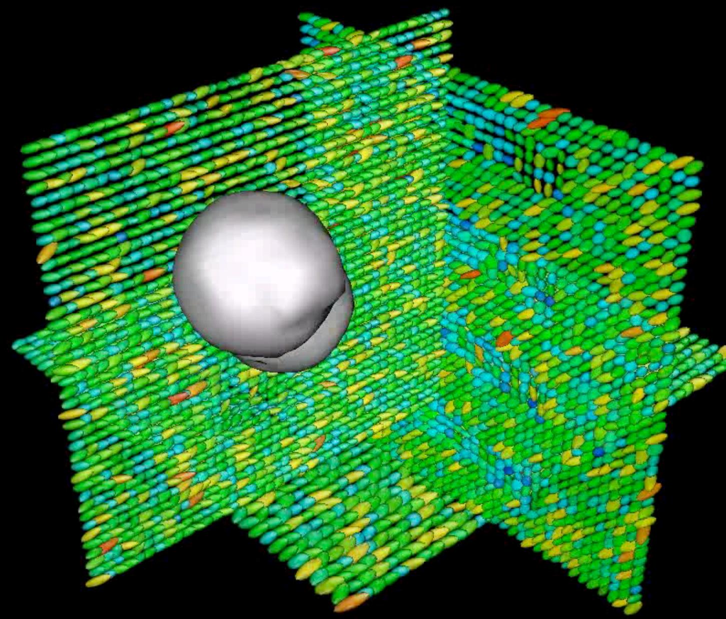

Euclidean metric (130)

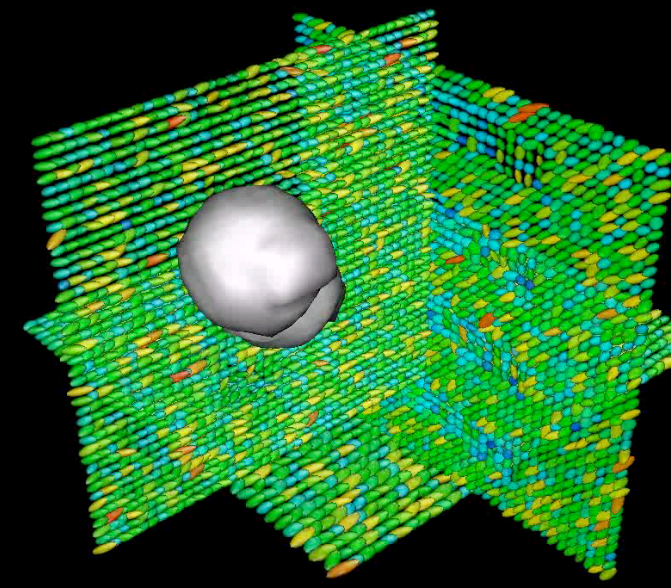

J-divergence metric (80)

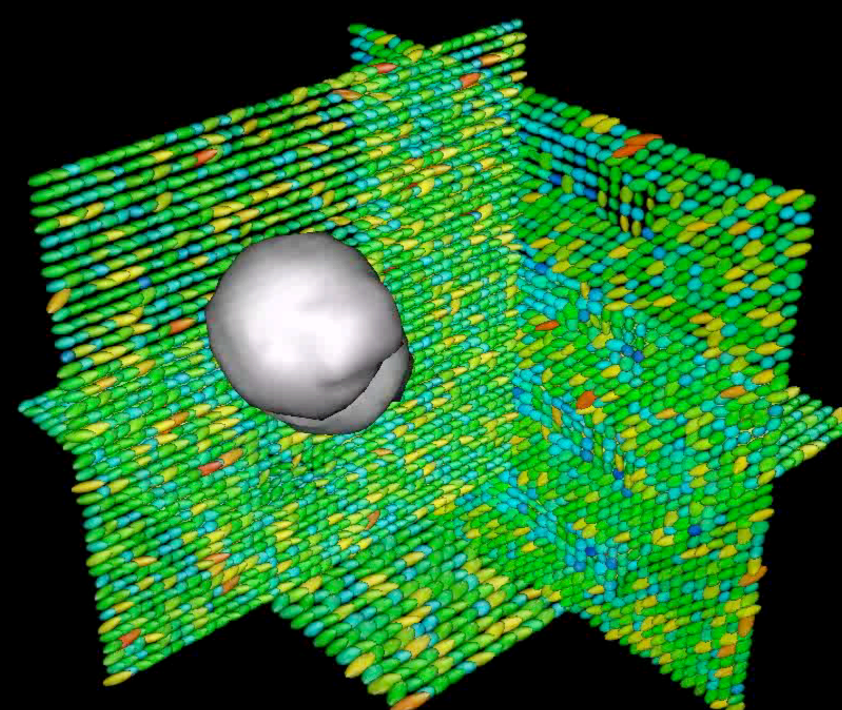

Riemannian metric (300)

Human Brain DTI: *Corpus Callosum*

Rough initialization in the genu and splenium

Euclidean metric

Riemannian metric

J-divergence metric

Data: Center for Magnetic Resonance Research, University of Minnesota

Human Brain DTI: *Corpus Callosum*

Rough initialization in the genu and splenium

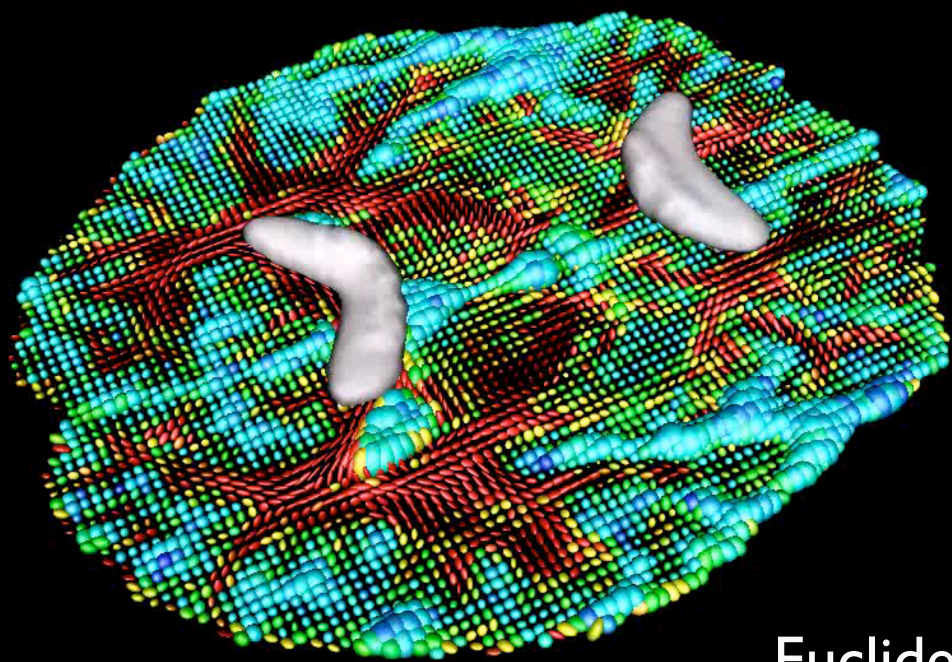

Euclidean metric

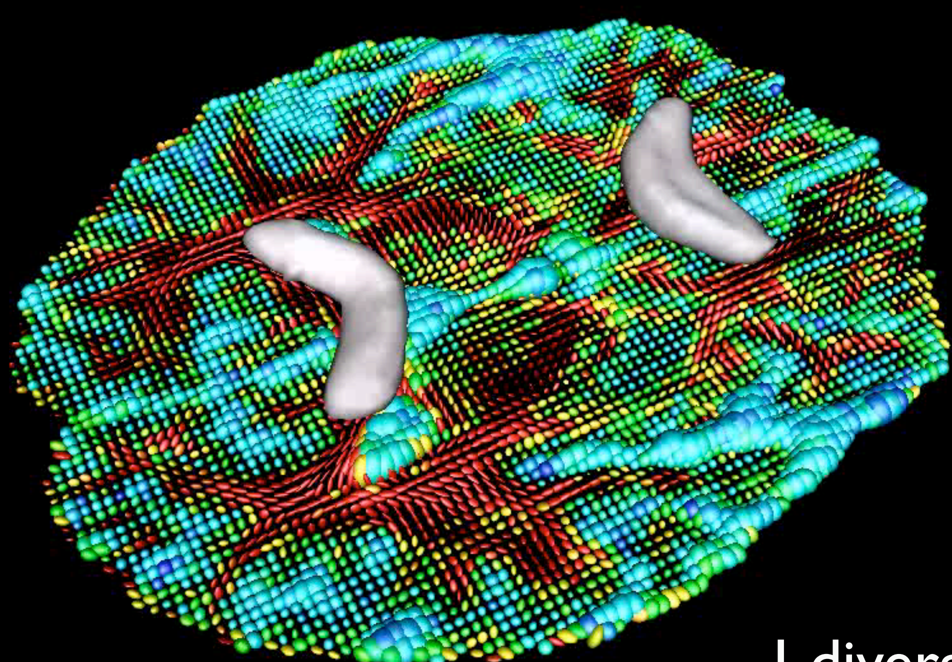

J-divergence metric

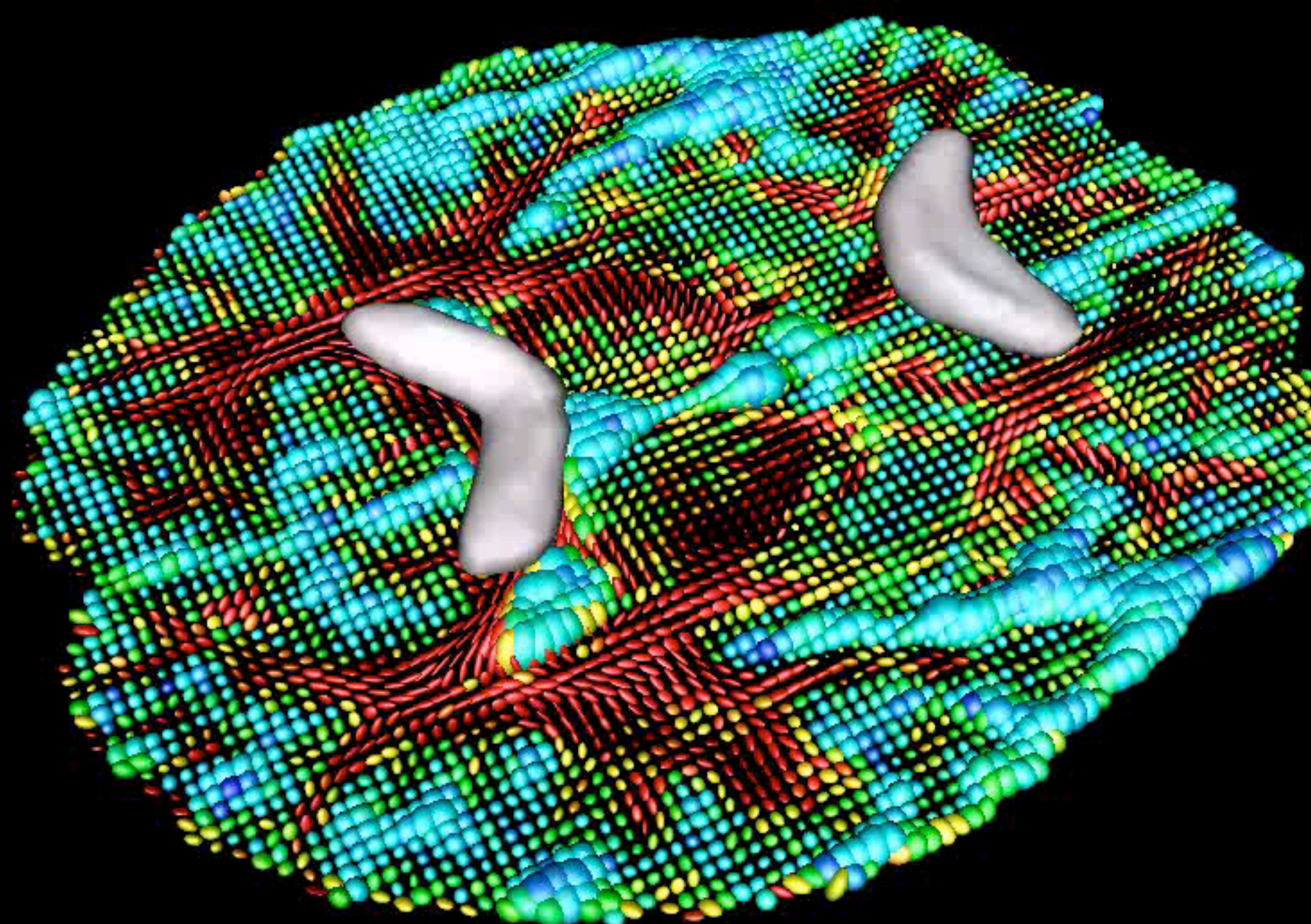

Riemannian metric

Data: Center for Magnetic Resonance Research, University of Minnesota

Human Brain DTI: *Corpus Callosum*

Rough initialization in the genu and splenium

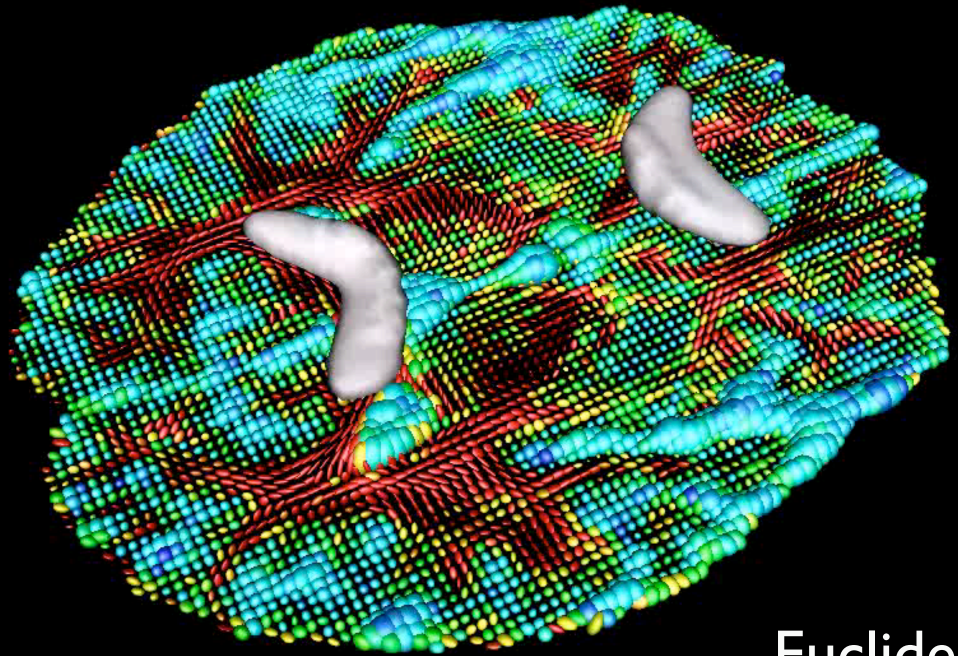

Euclidean metric

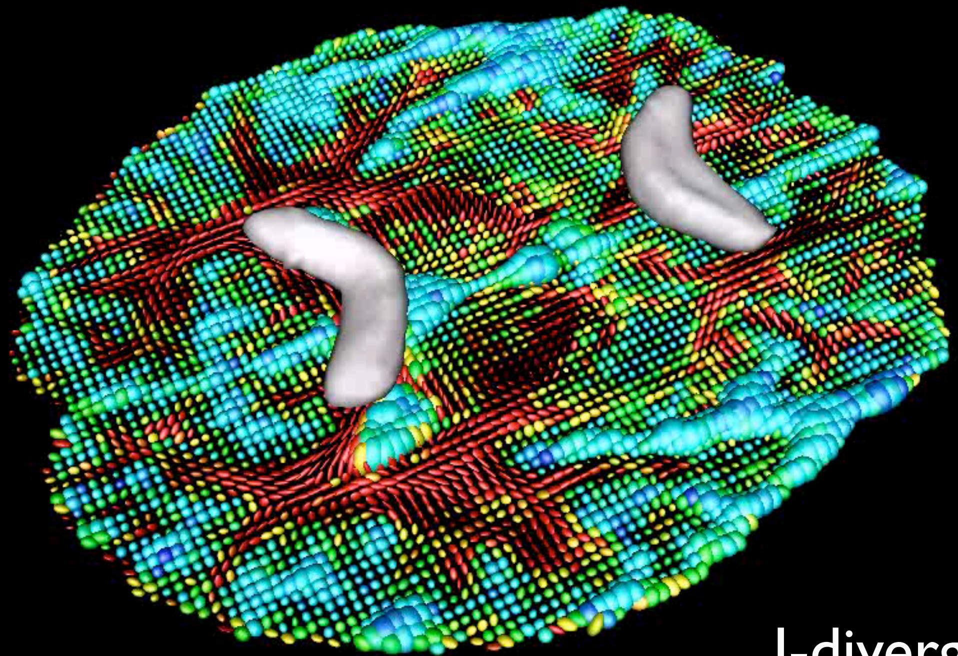

J-divergence metric

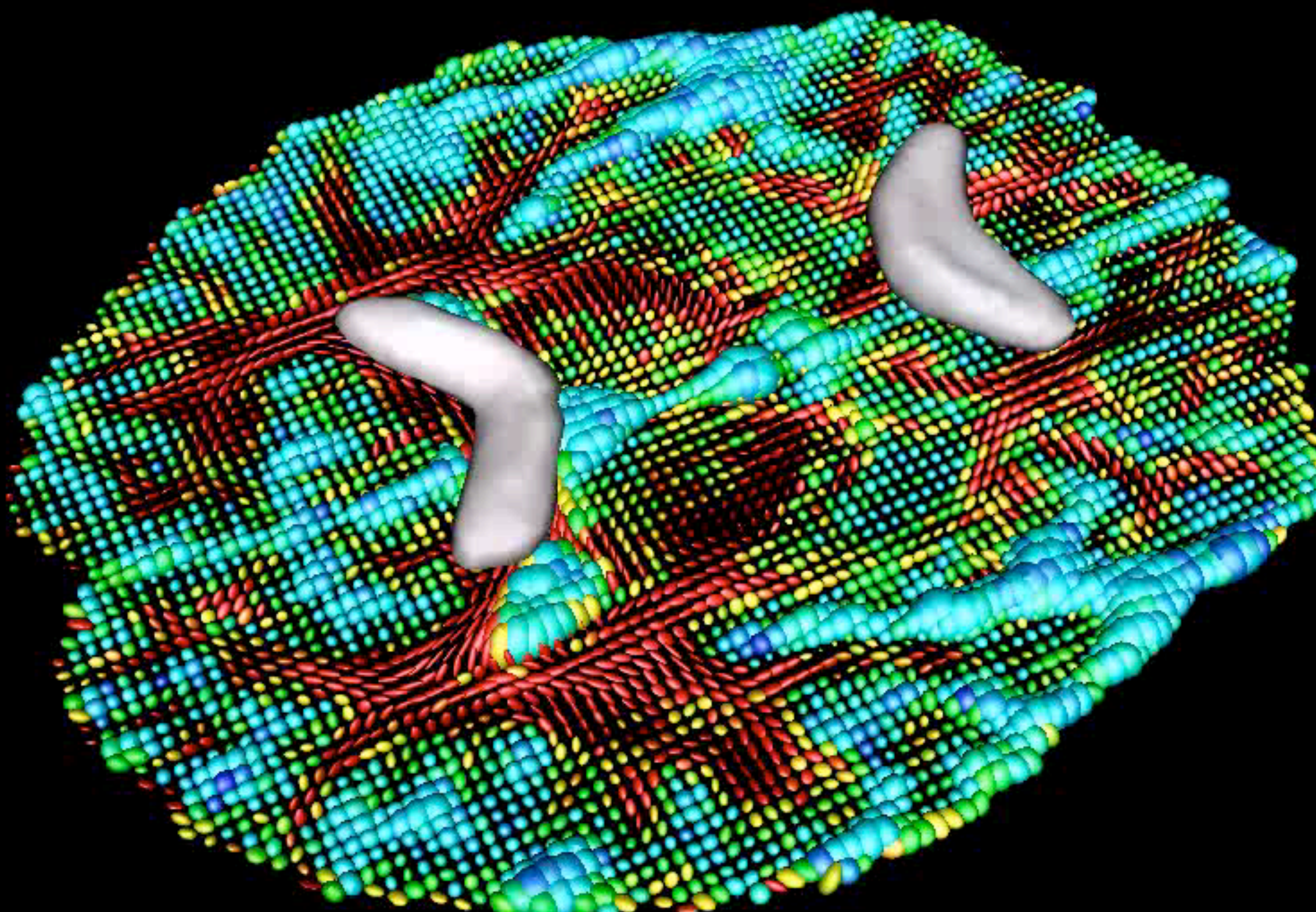

Riemannian metric

Data: Center for Magnetic Resonance Research, University of Minnesota

Human Brain DTI: *Corpus Callosum*

Rough initialization in the genu and splenium

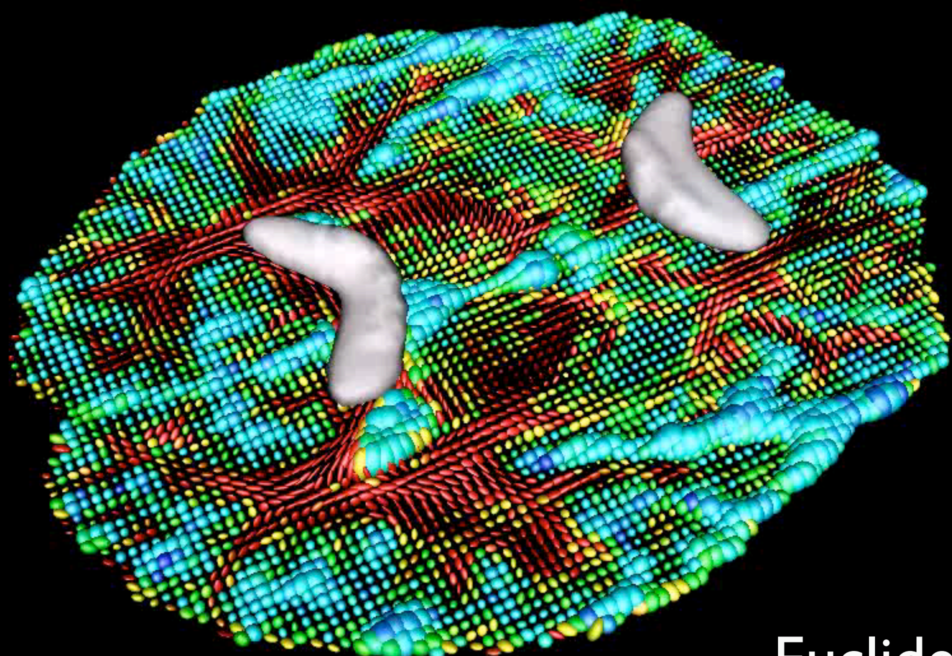

Euclidean metric

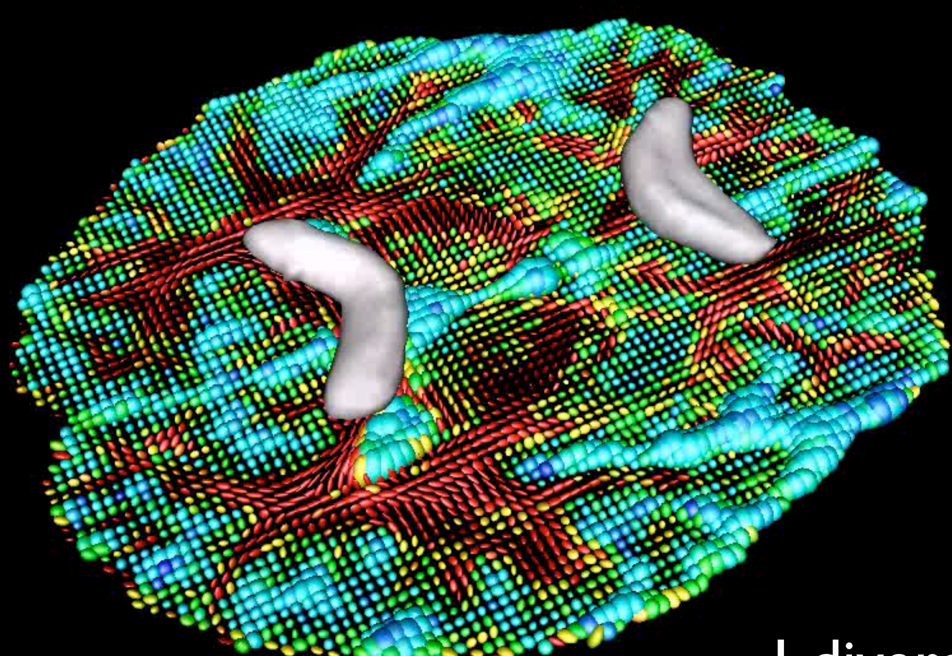

J-divergence metric

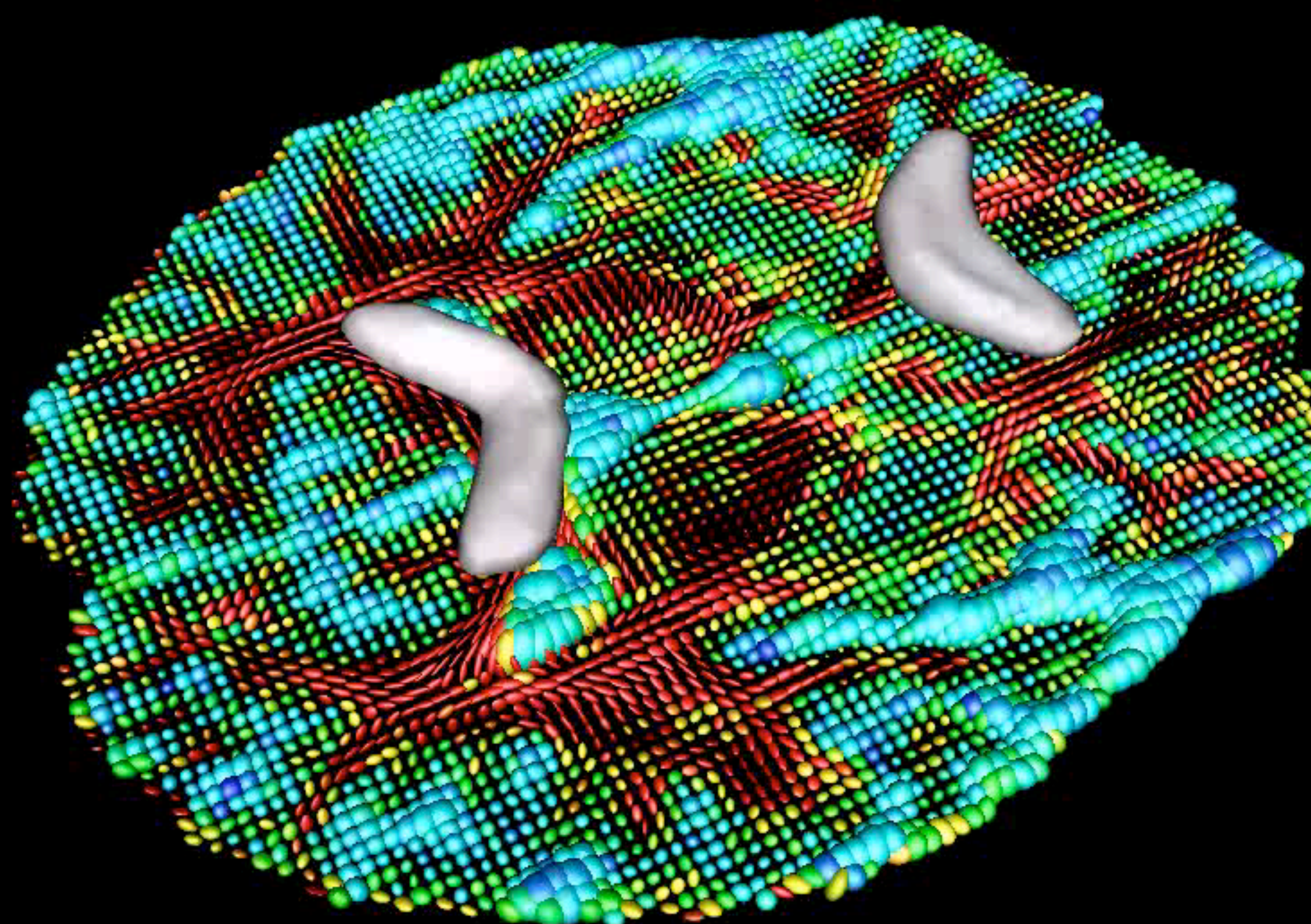

Riemannian metric

Data: Center for Magnetic Resonance Research, University of Minnesota

Corpus Callosum: Euclidean metric

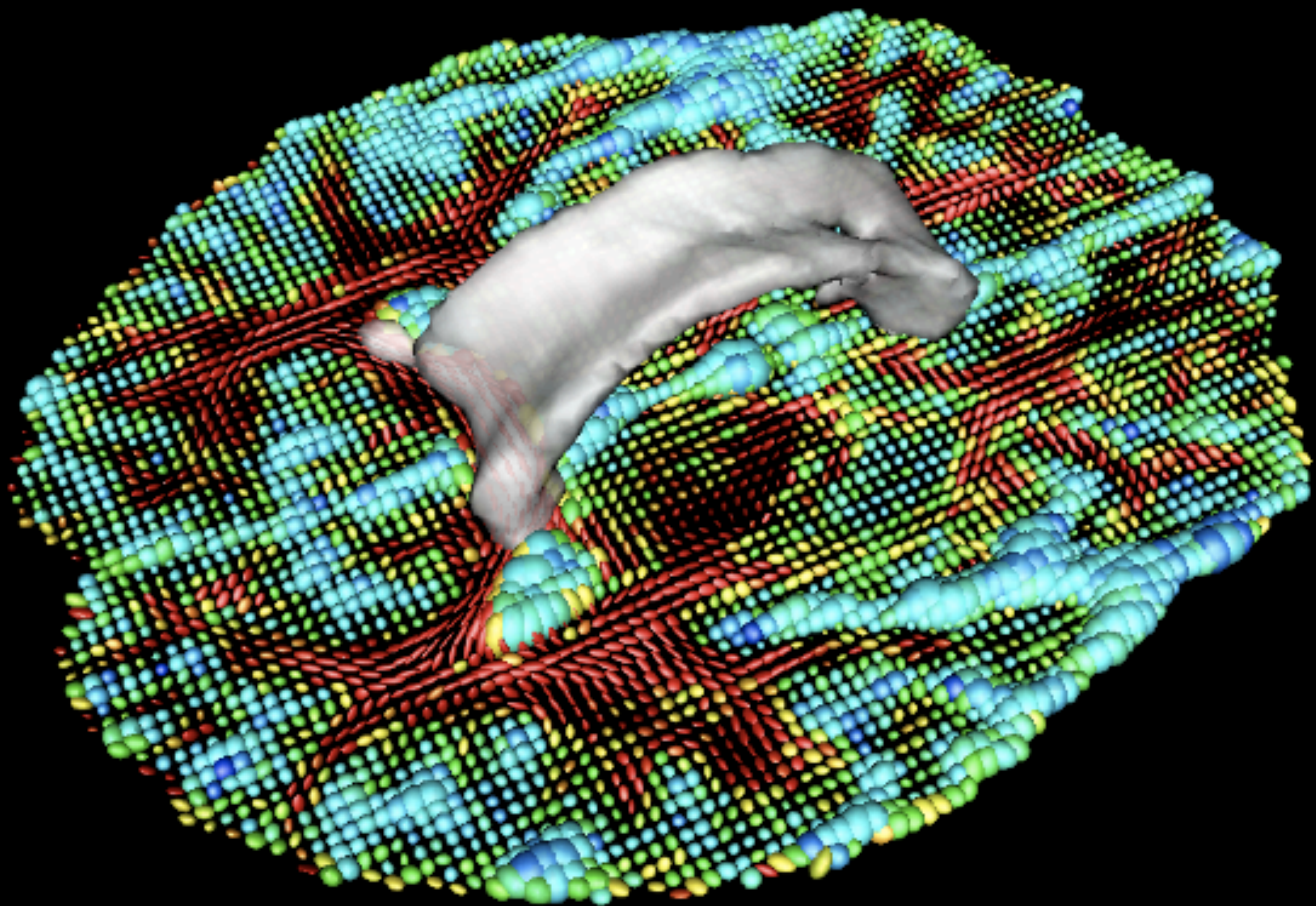

Corpus Callosum: J-divergence metric

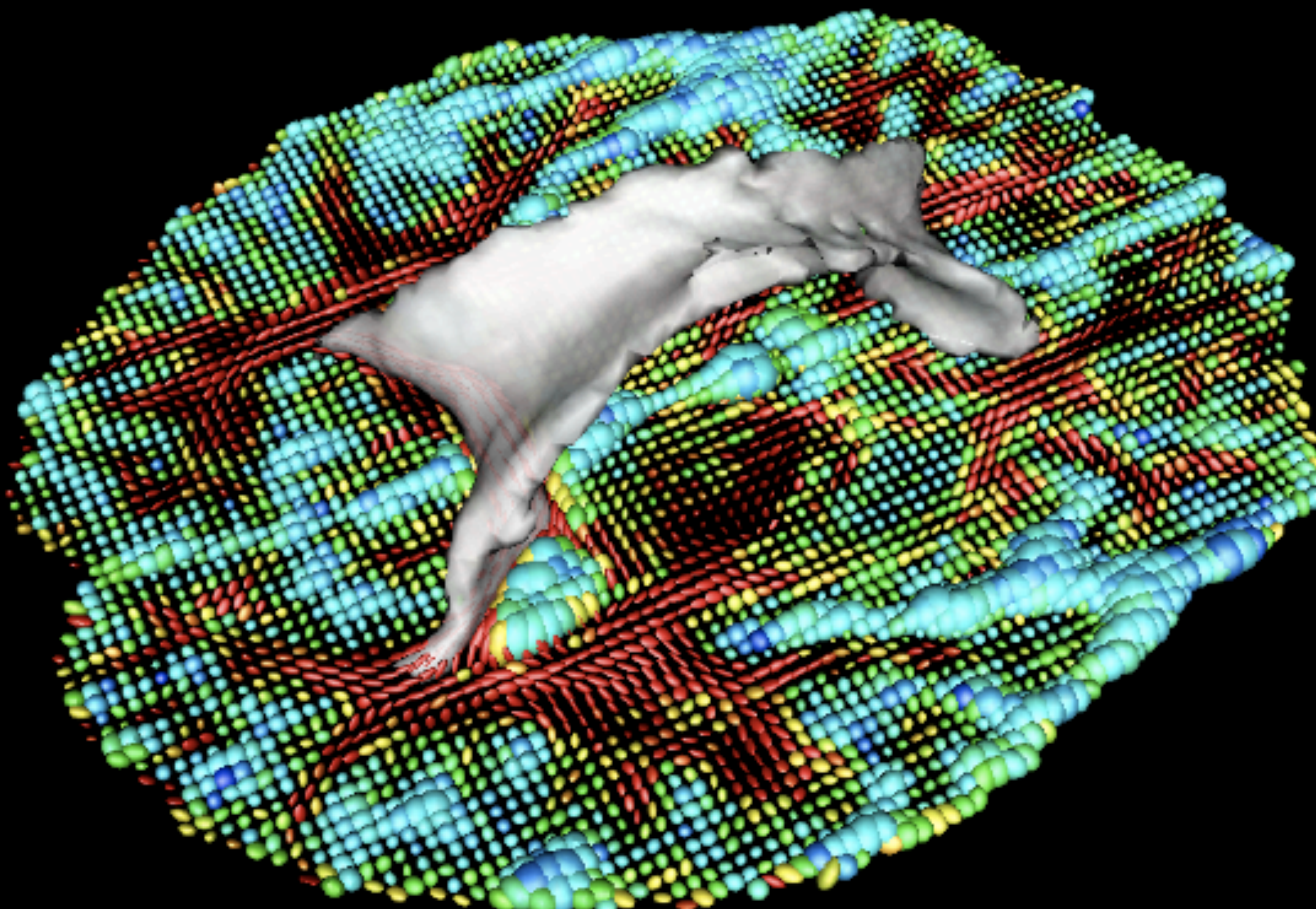

Corpus Callosum: Riemannian metric

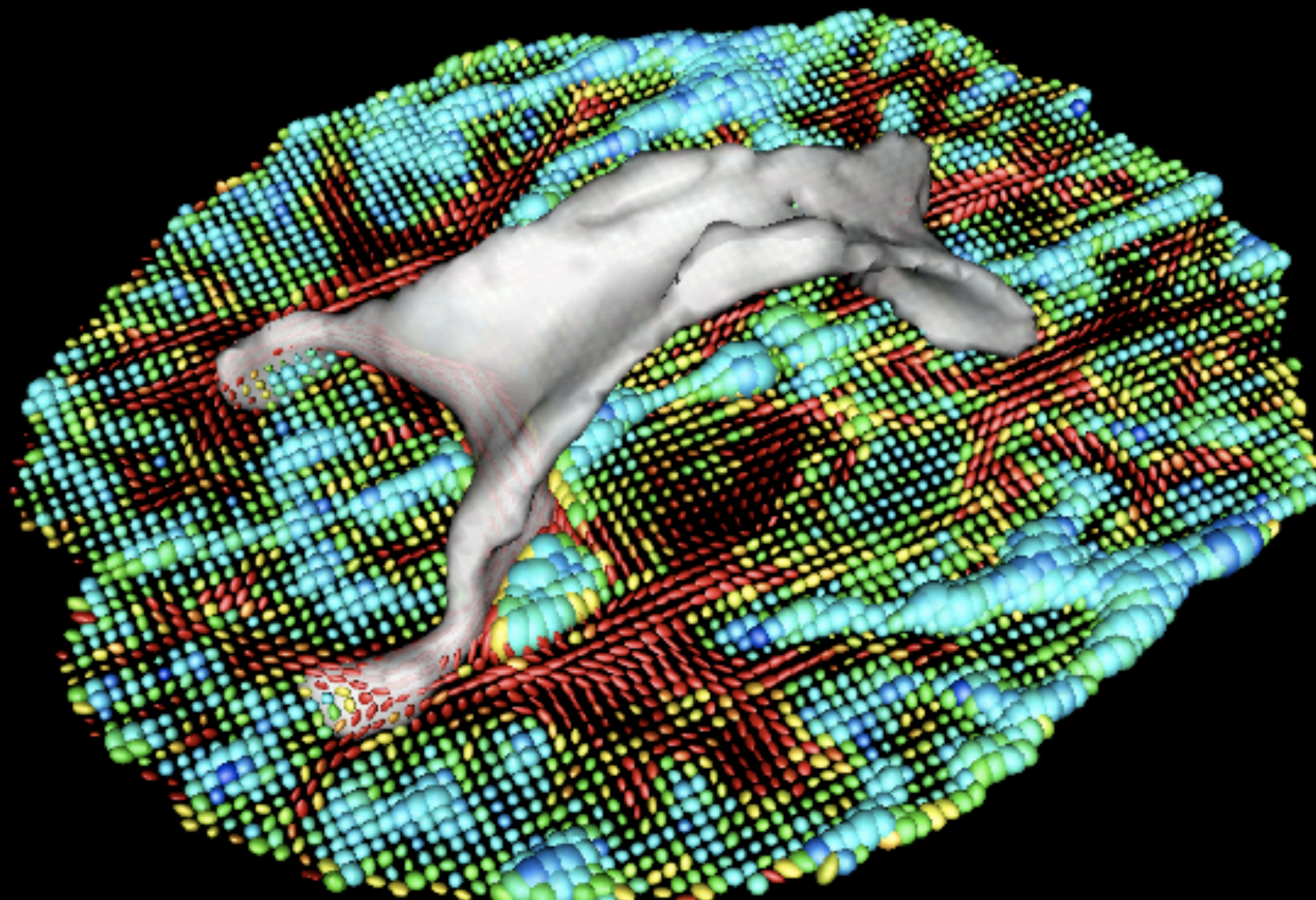

Metrics Comparison

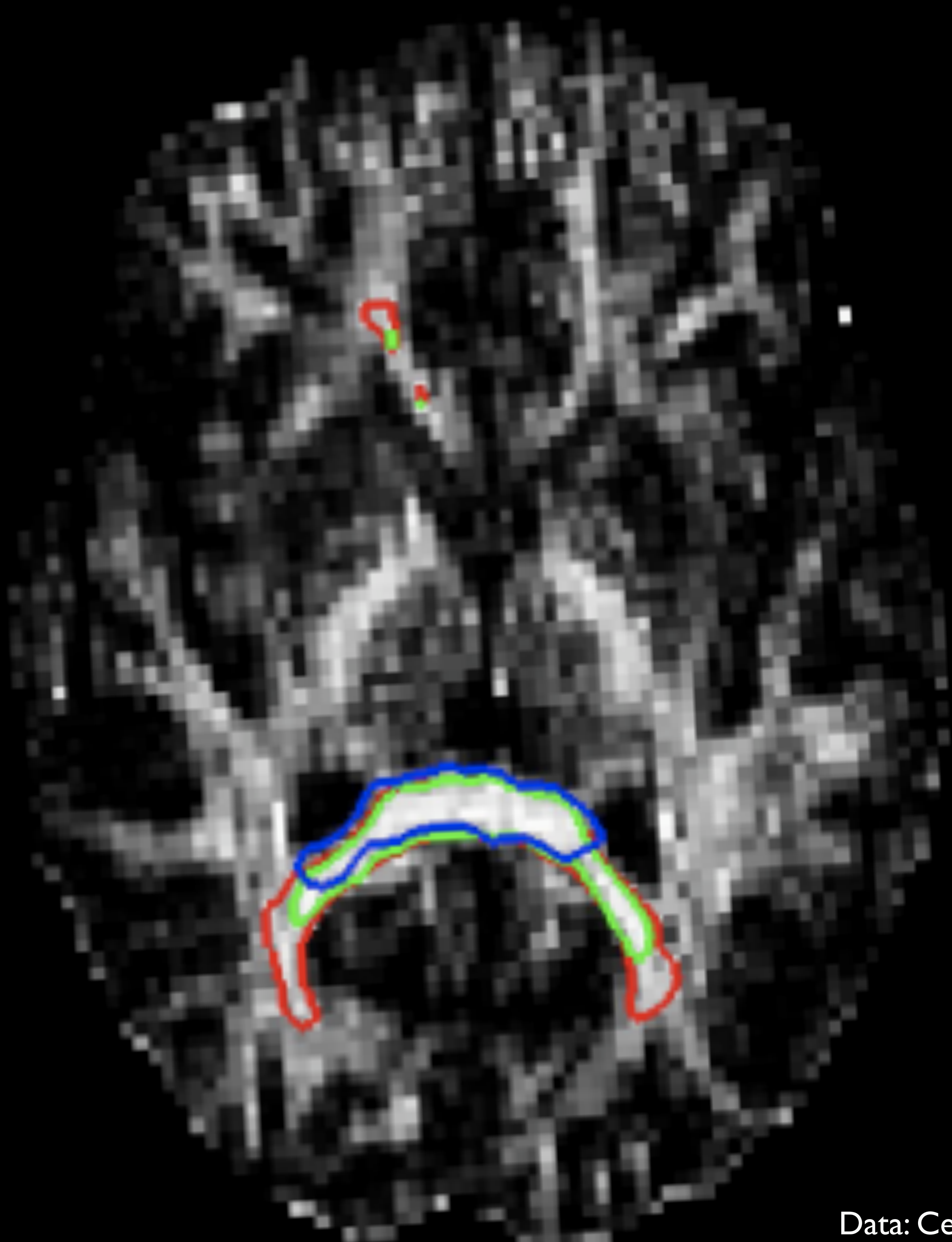

Data: Center for Magnetic Resonance Research, University of Minnesota

Human Brain DTI: *Corticospinal Tract*

Human Brain DTI: *Corticospinal Tract*

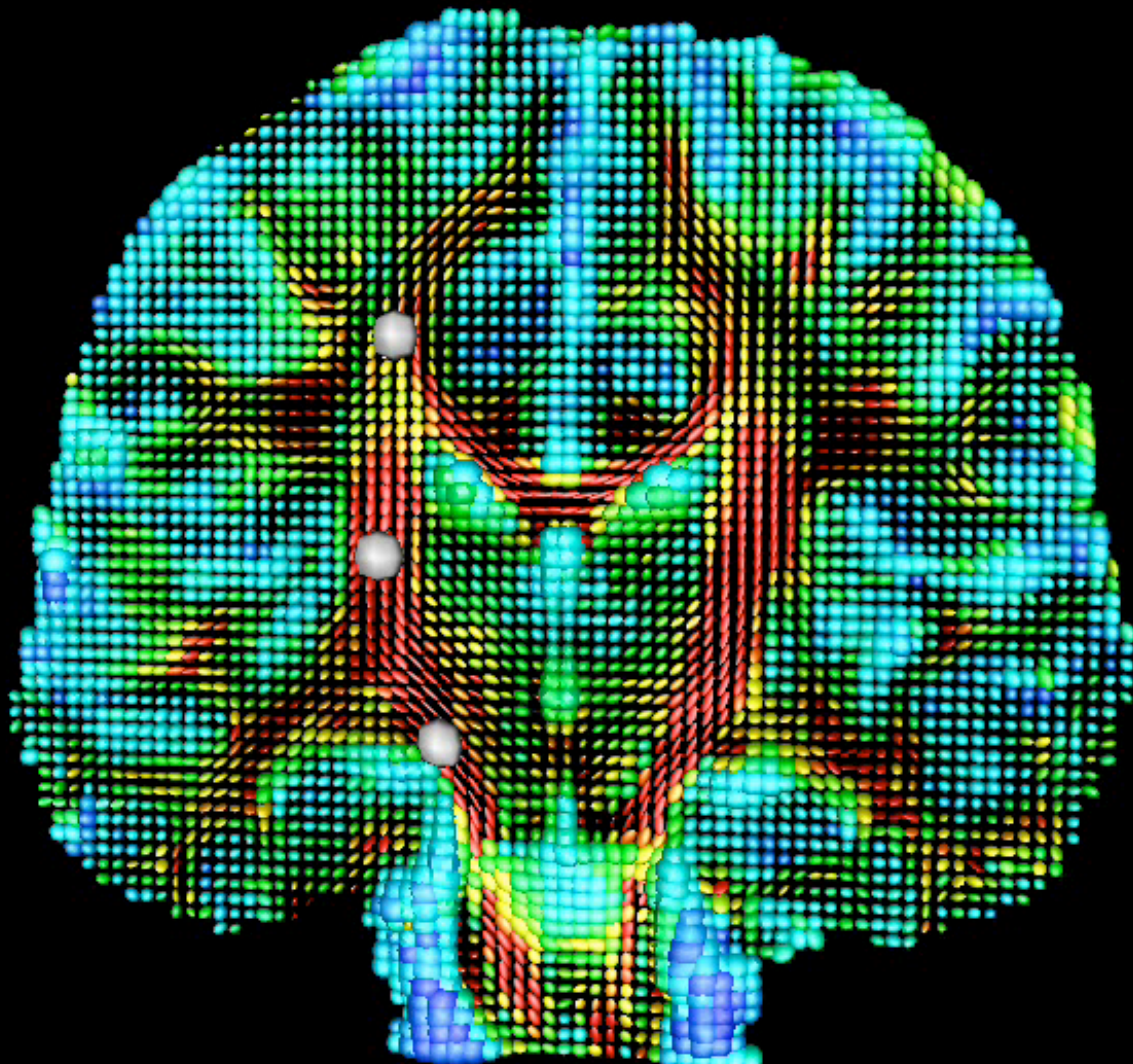

Biological Phantom

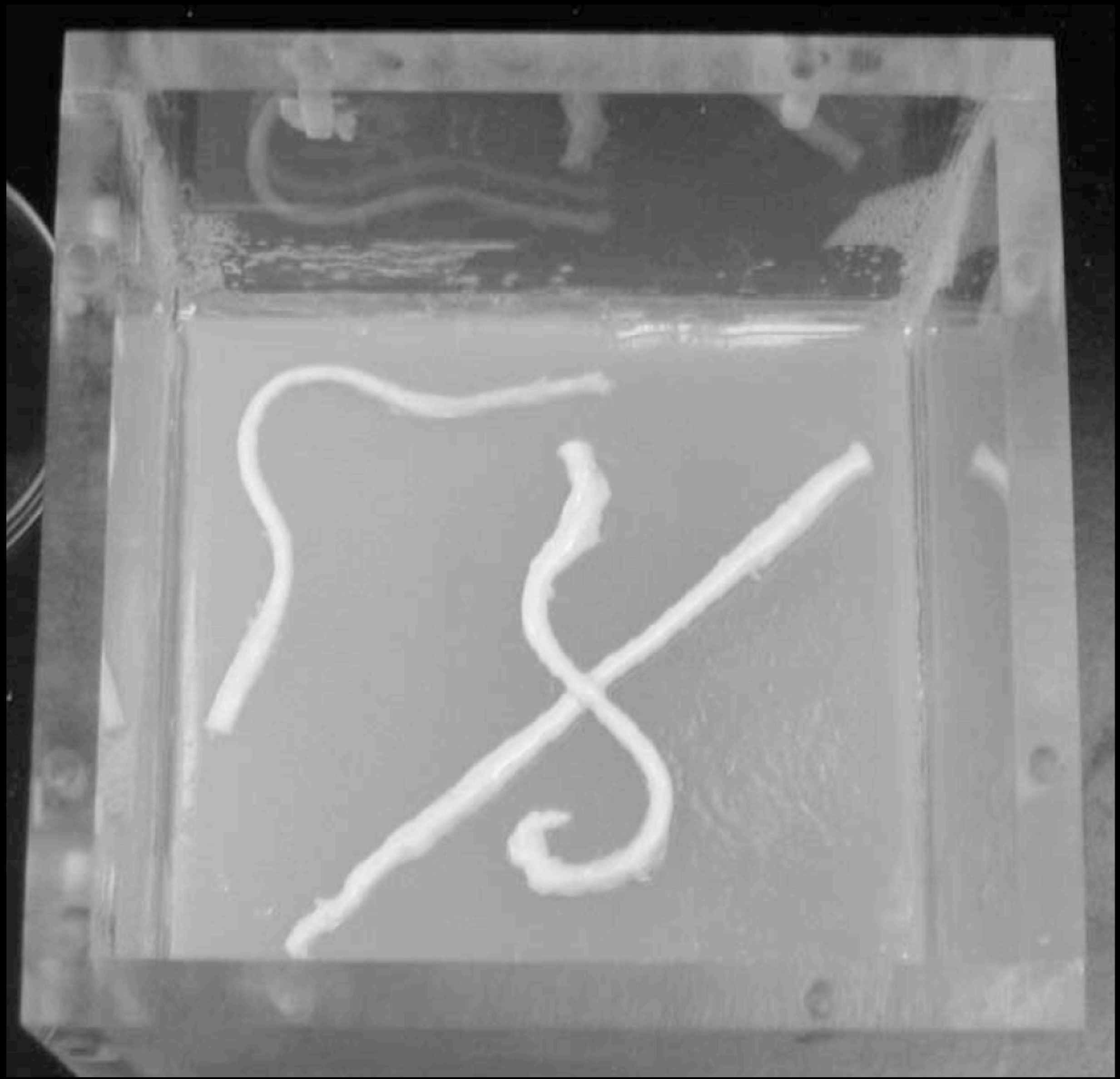

Scanned at 1.5T with a knee coil.

90 DW directions
b-value = 1300 s/mm^2
TR = 8s
TE = 110ms
40 slices, 2.5 mm isotropic
10 min scan.

Produced by J. Campbell et al. at the McConnel Brain Imaging Center and Montreal Neurological Institute.

From 2 excised Sprague-Dawley rat spinal cords embedded in 2% agar. Cords are 7-12 cm by 5 mm.

[Campbell-etal Neuroimage 2005]

Biological Phantom

Biological Phantom

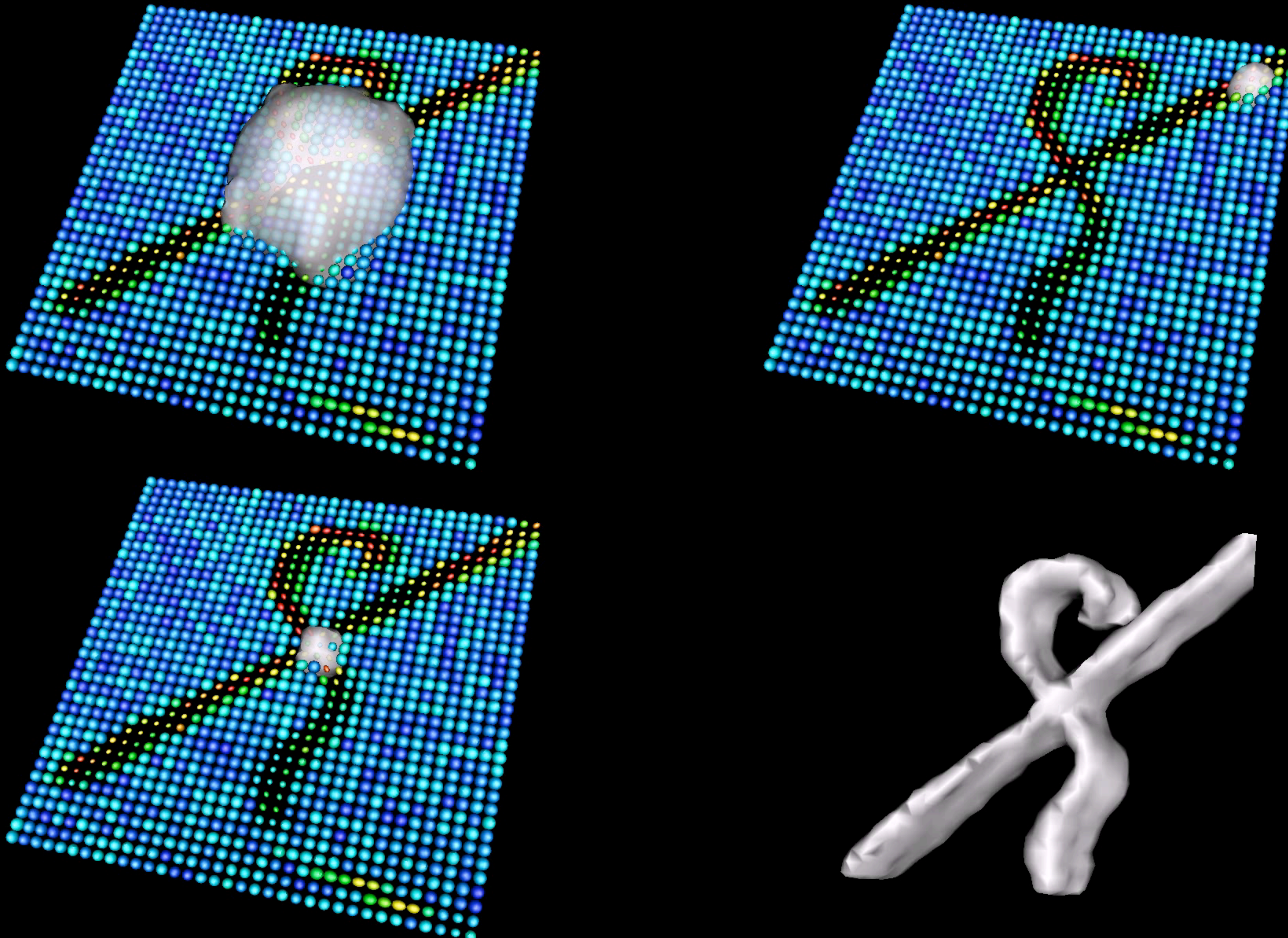

Biological Phantom

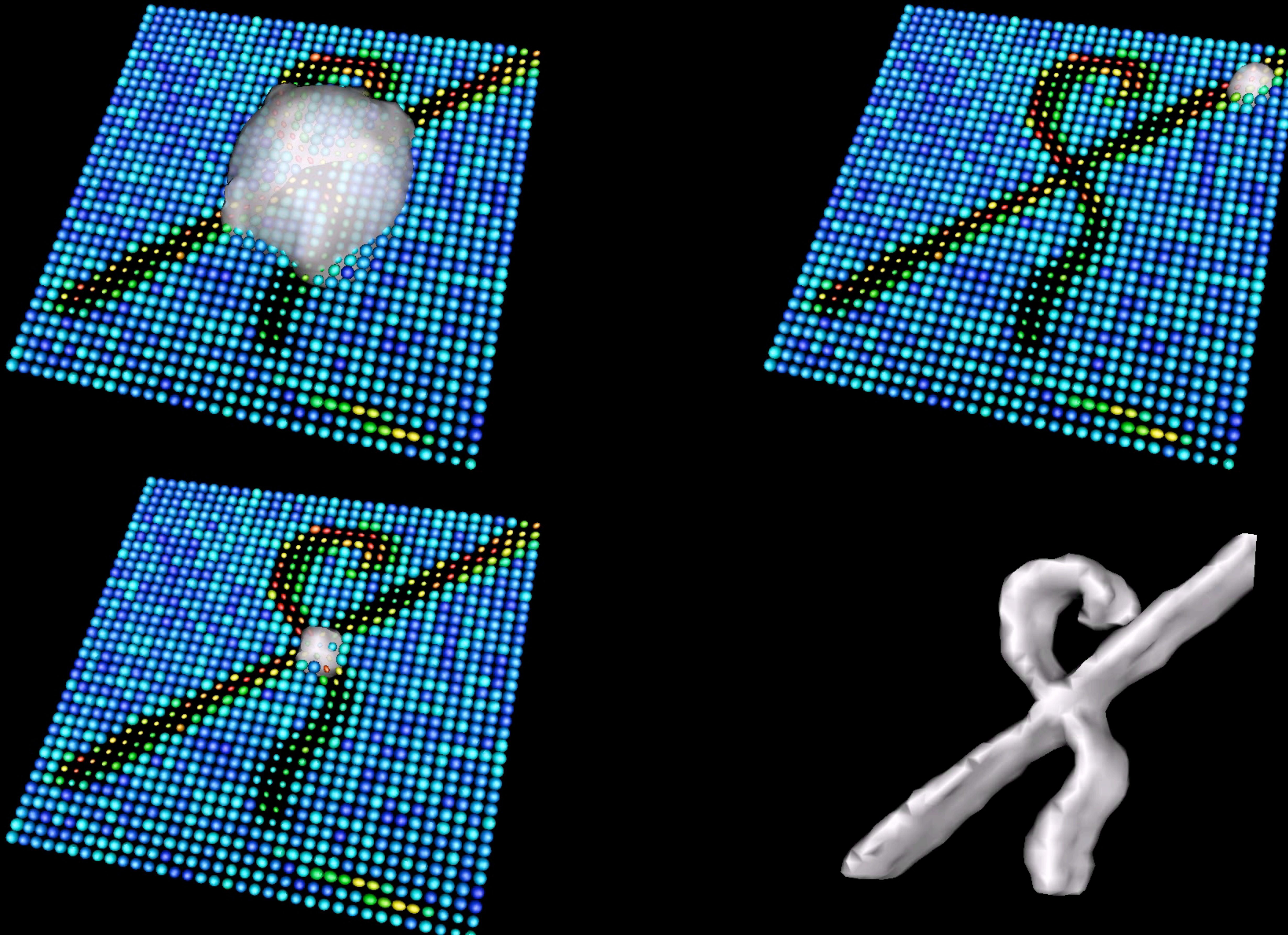

Biological Phantom

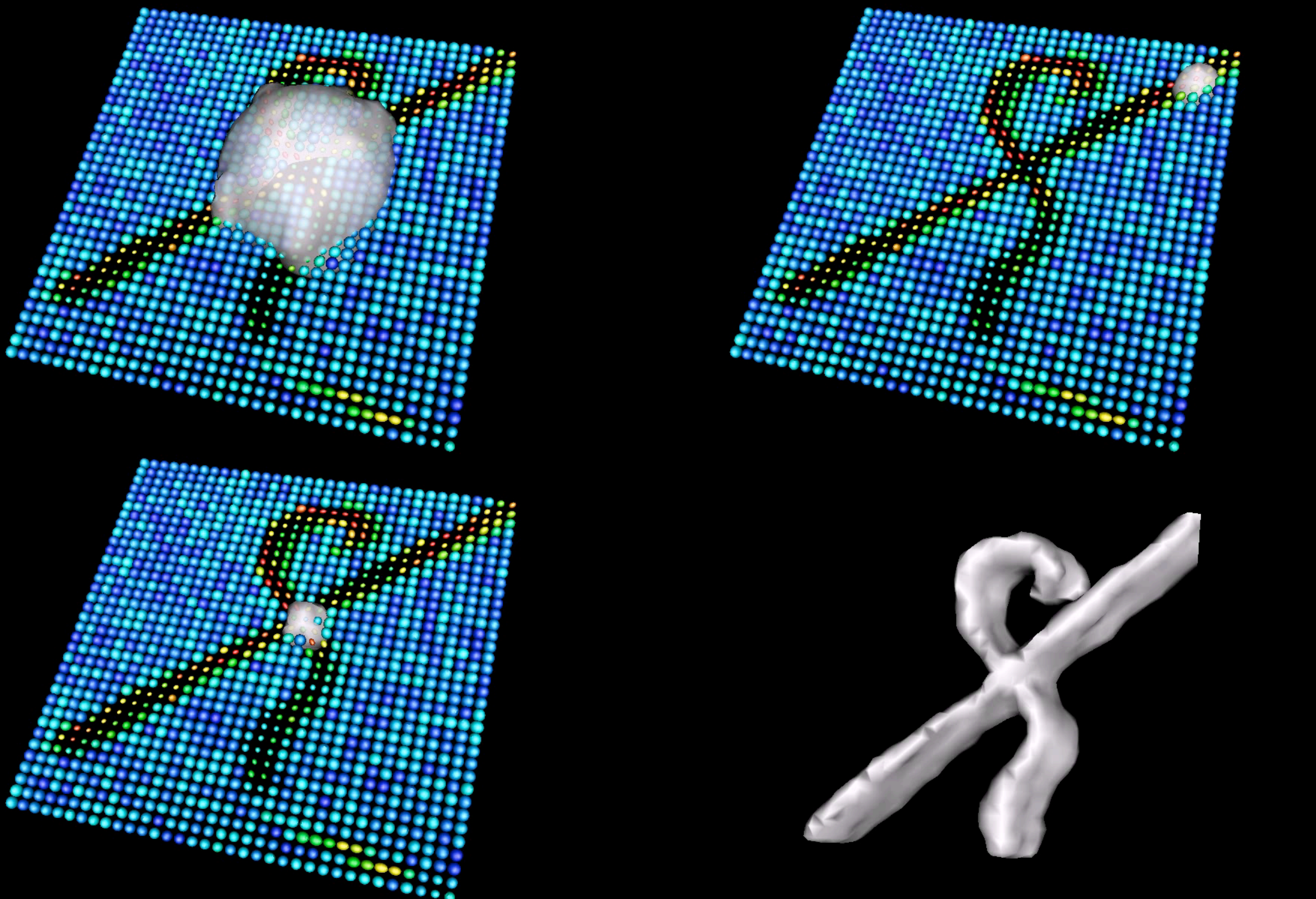

Biological Phantom

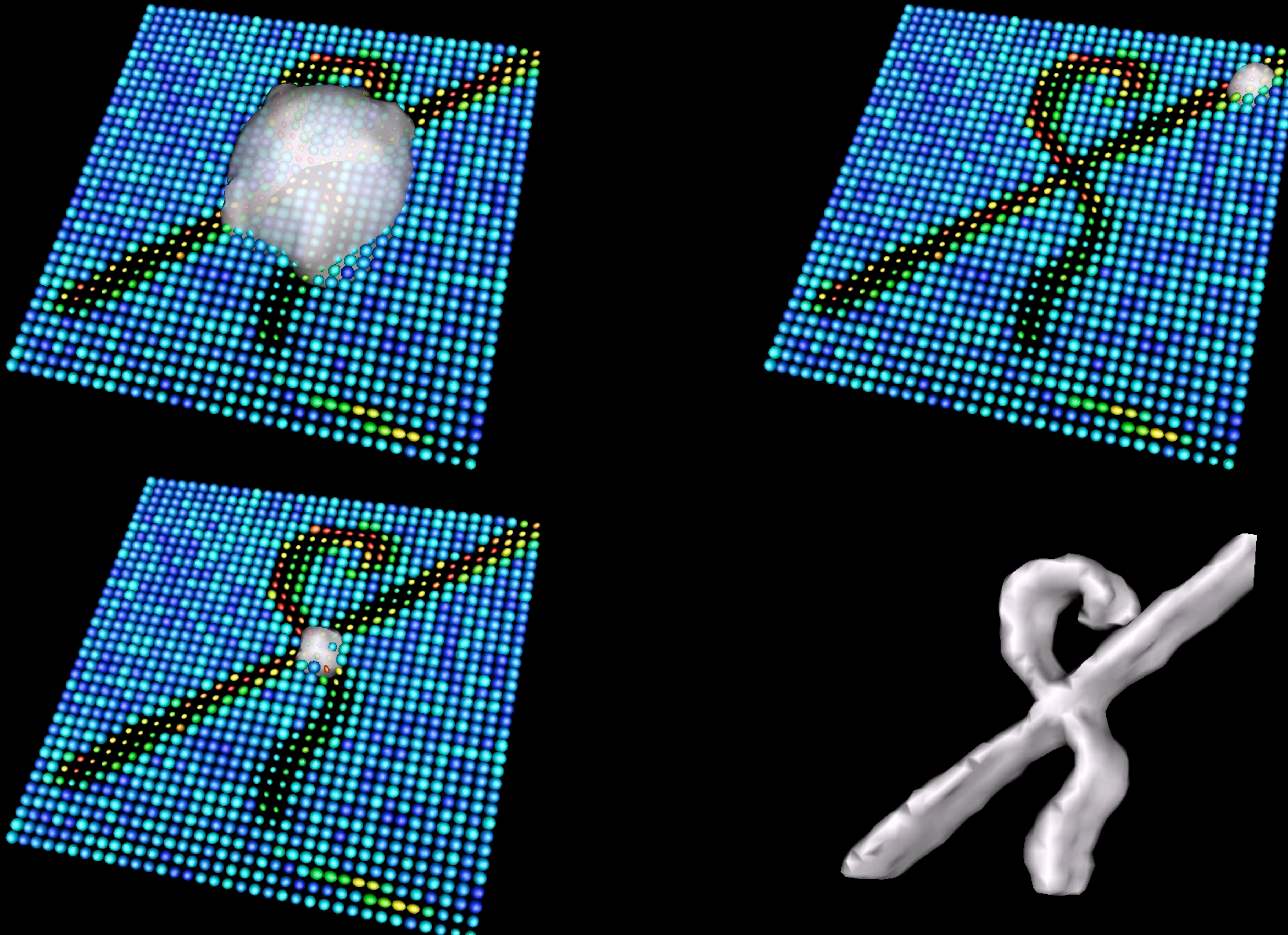

Biological Phantom

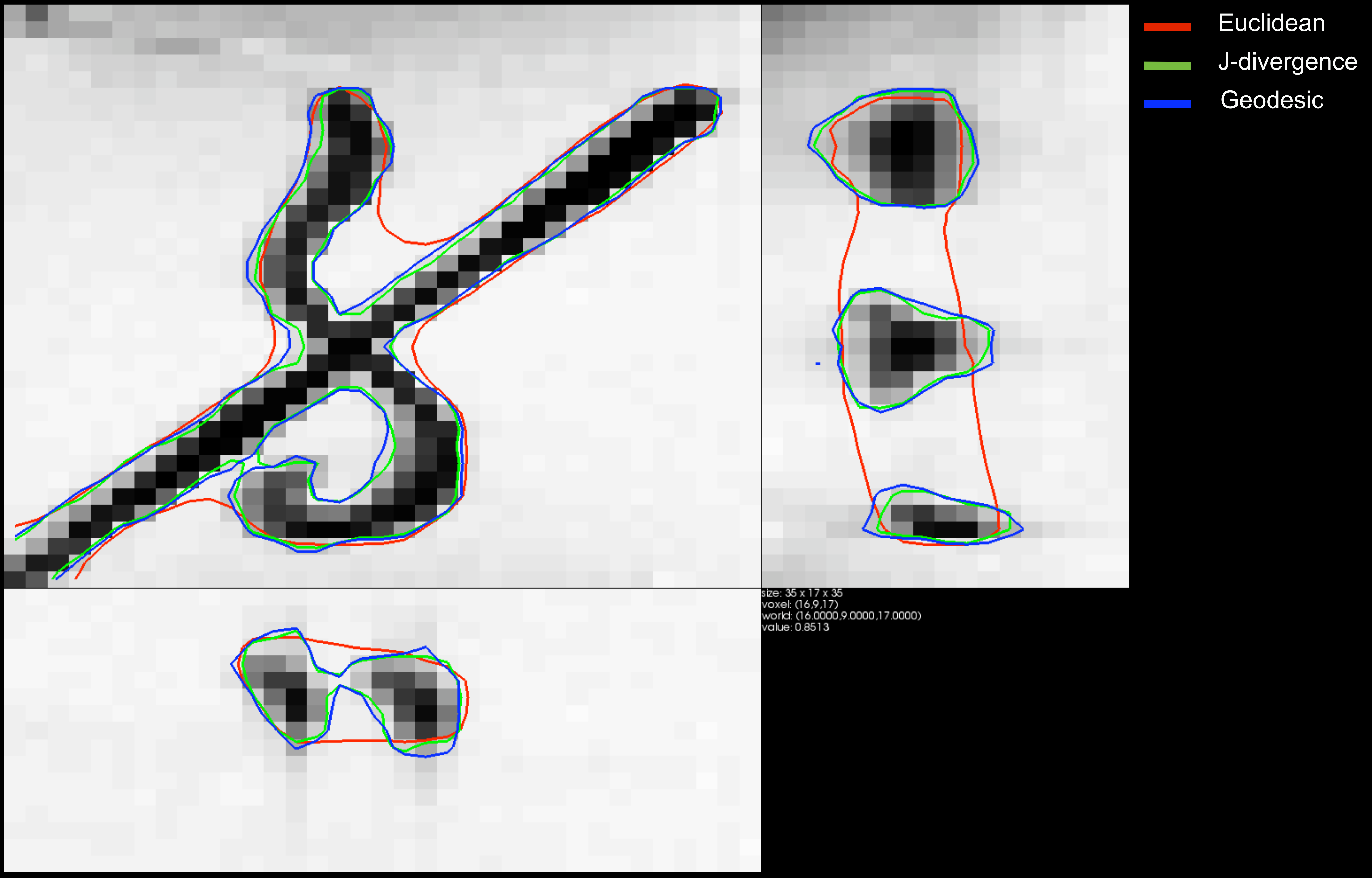

HARDI Segmentation

- Dissimilarity measure: L2 norm of SH coefficients difference

$$\langle \psi, \psi' \rangle = \int_{S^2} \psi(r).\psi'(r)dr = \int_{S^2} \left(\sum_{i=1}^{R} c_i Y_i(r) \right) \left(\sum_{i=1}^{R} c'_i Y_i(r) \right) dr = \sum_{i=1}^{R} c_i.c'_i$$

$$\Rightarrow \|\psi - \psi'\|^2 = \sum_{i=1}^{R} (c_i - c'_i)^2$$

- Assumption of Gaussian distribution for SH coefficients:

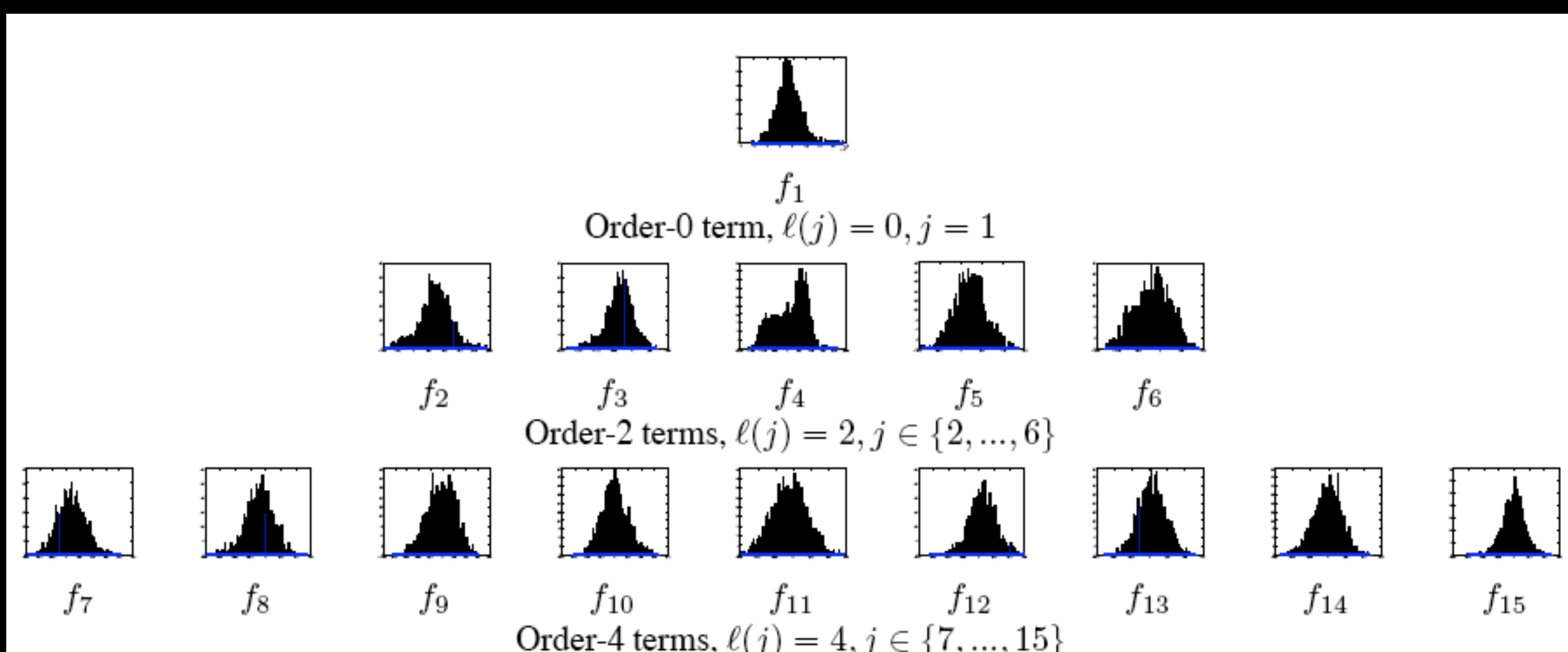

Distribution in manual segmentation of Corpus Callosum

[Descoteaux-etal JMIV 2008]

Synthetic Example

DTI

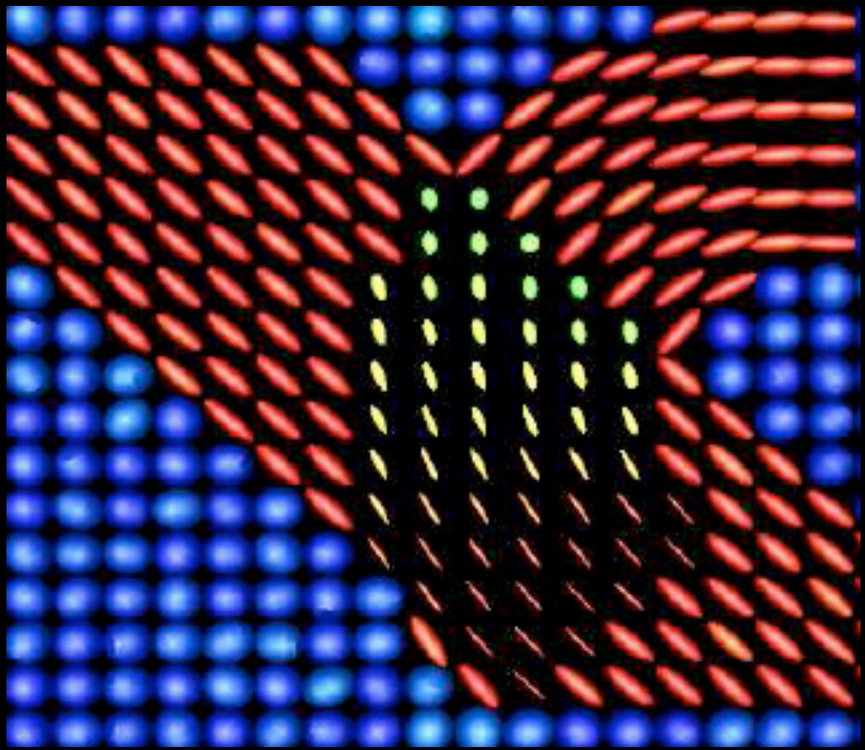

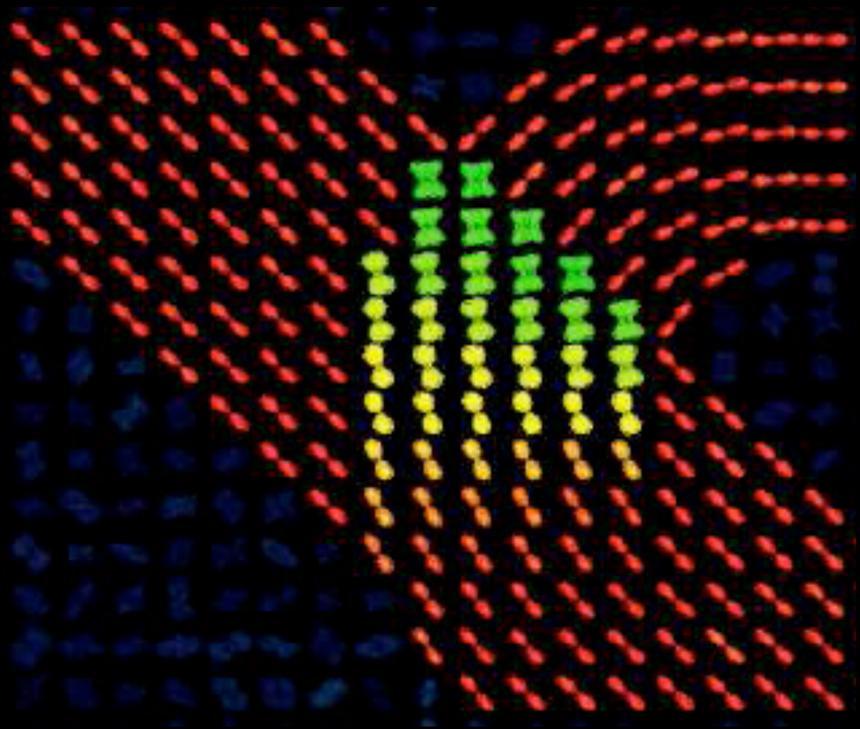

ODFs

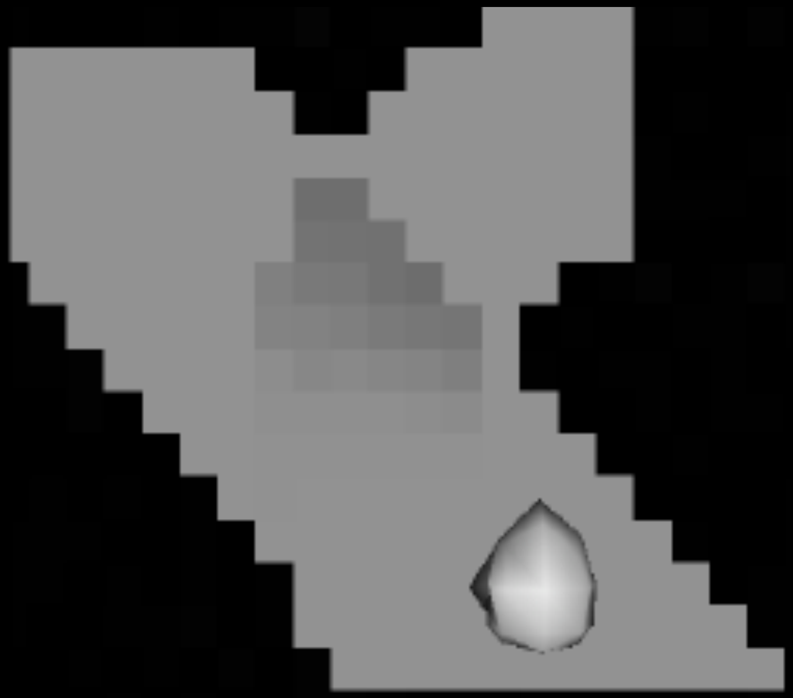

Initialization

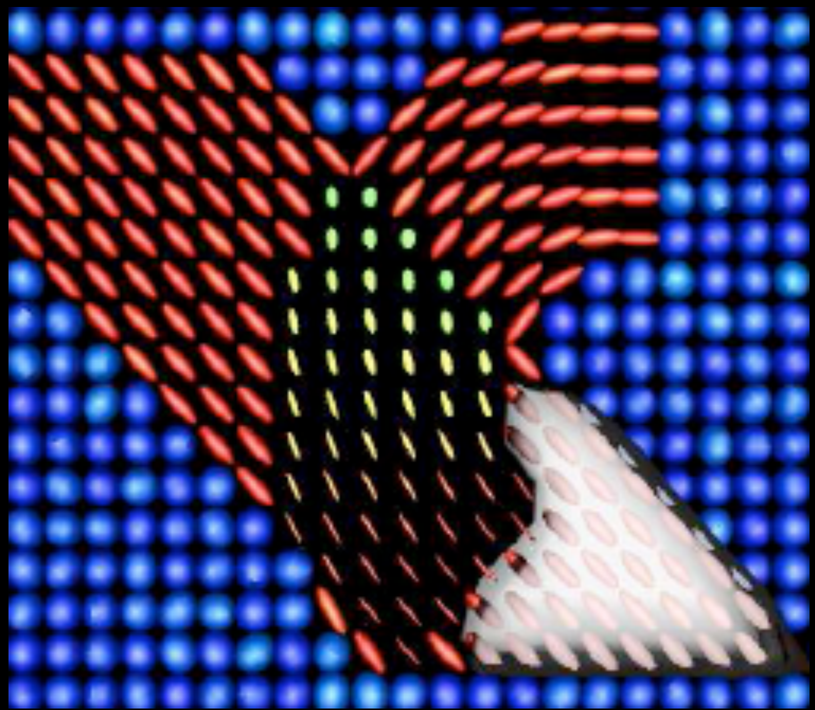

DTI Segmentation

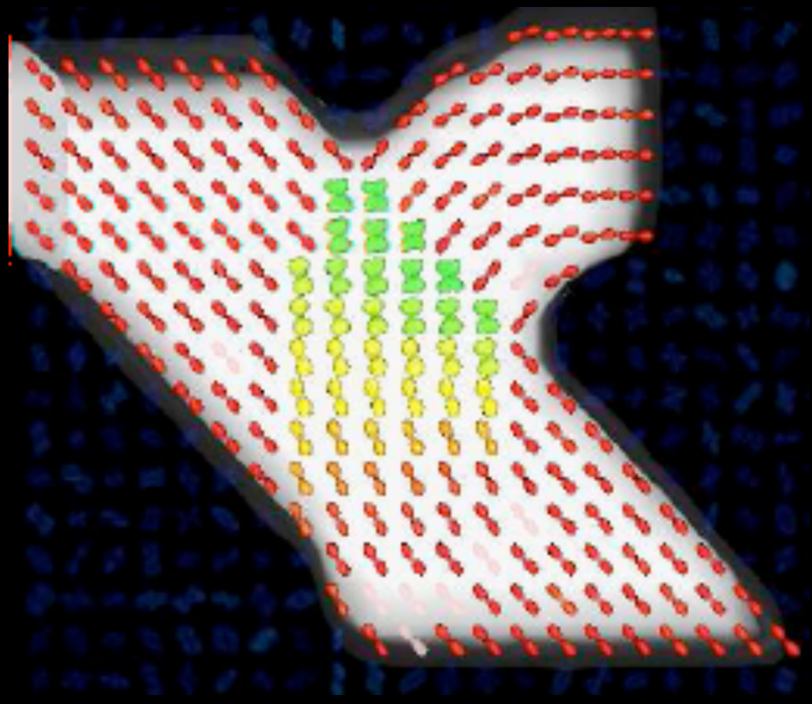

HARDI Segmentation

Synthetic Example

DTI

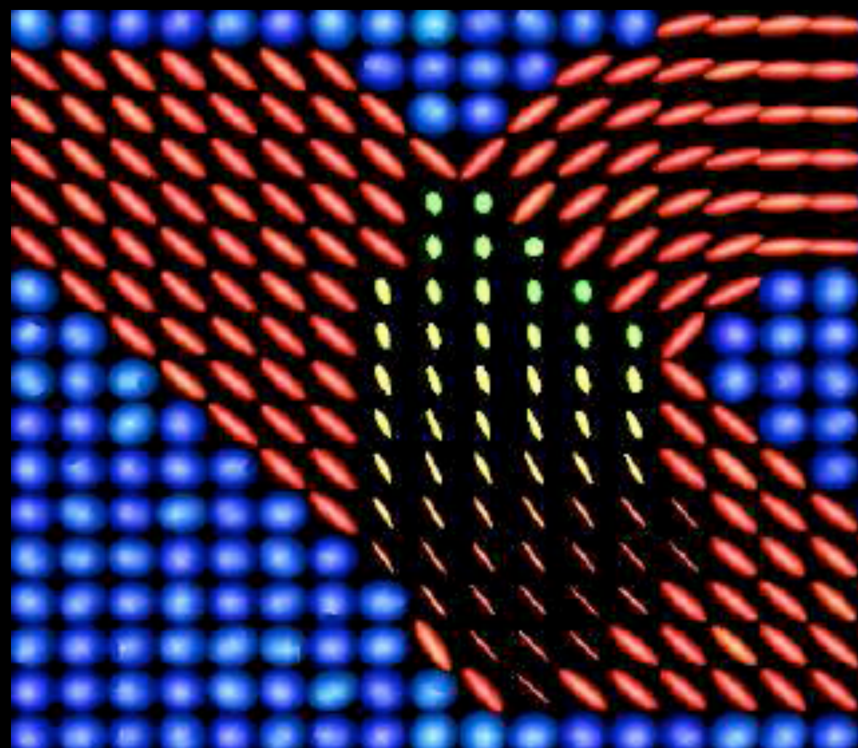

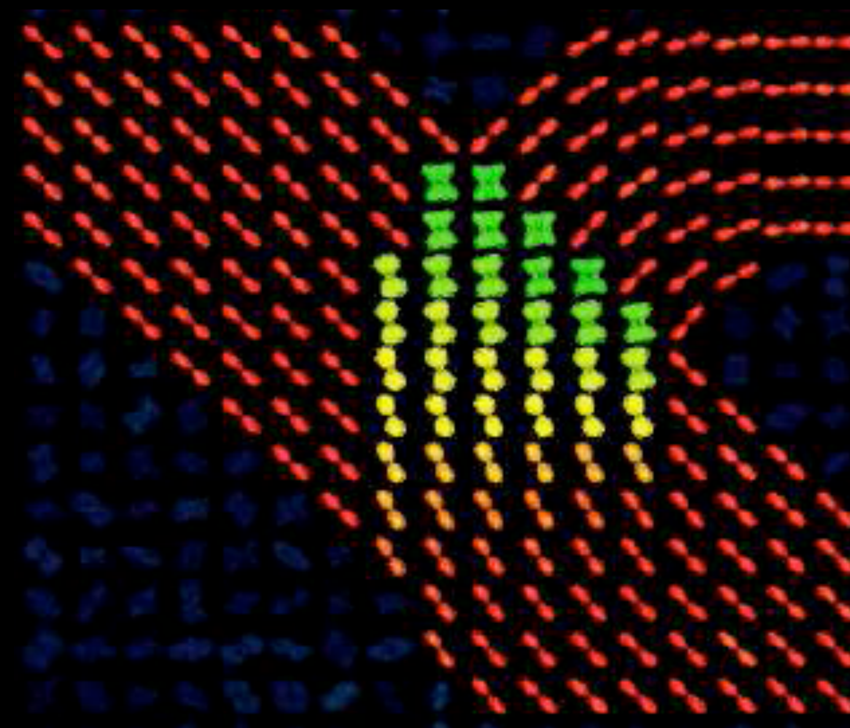

ODFs

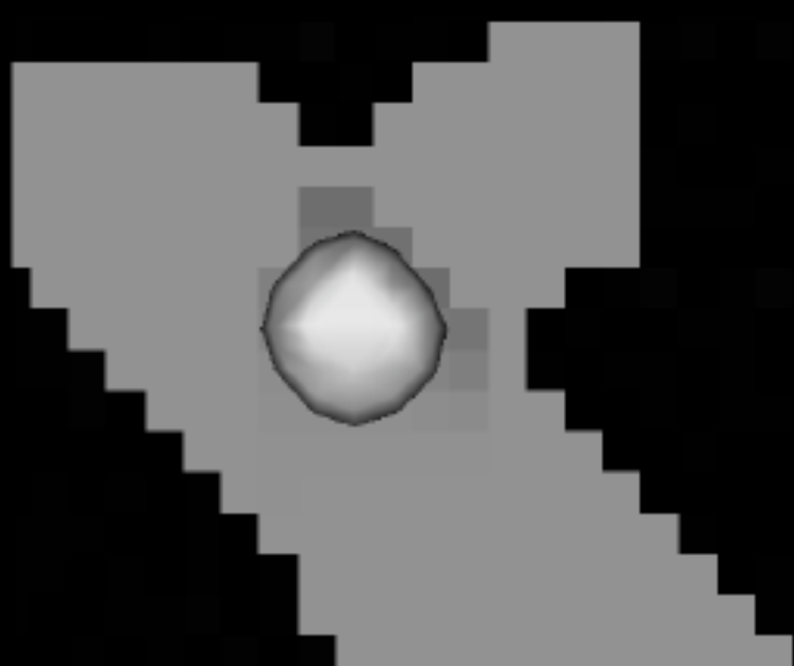

Initialization

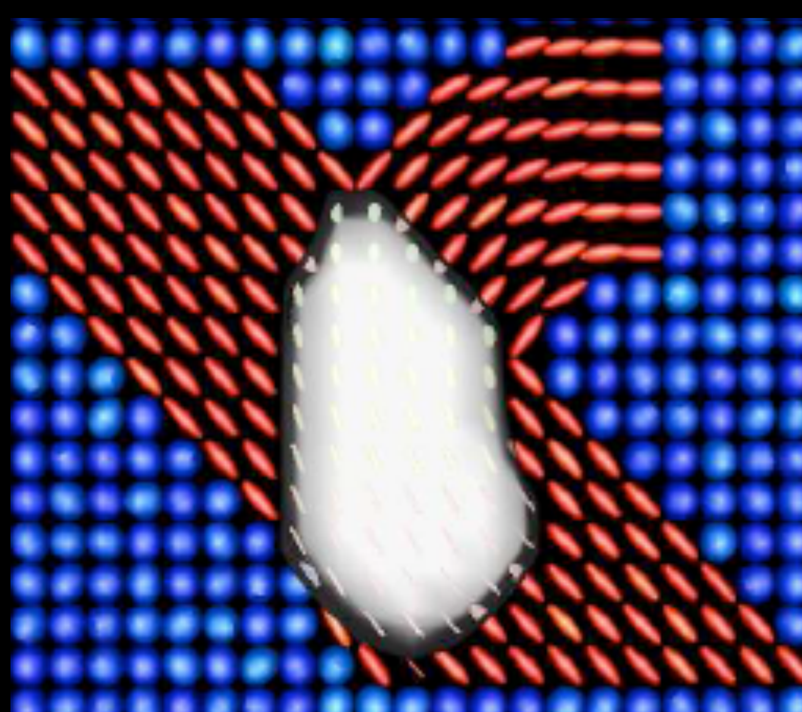

DTI Segmentation

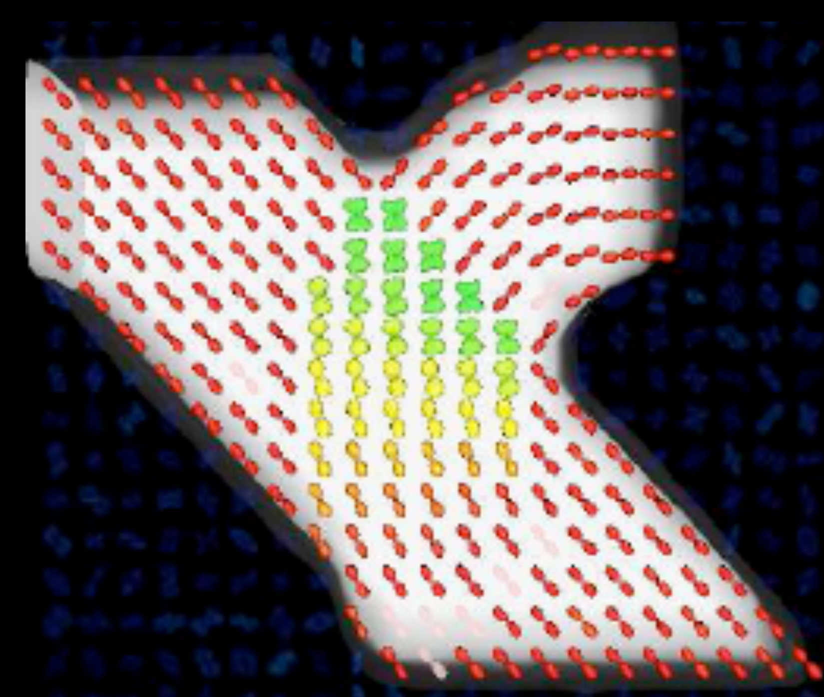

HARDI Segmentation

Human Brain DTI: *Corpus Callosum*

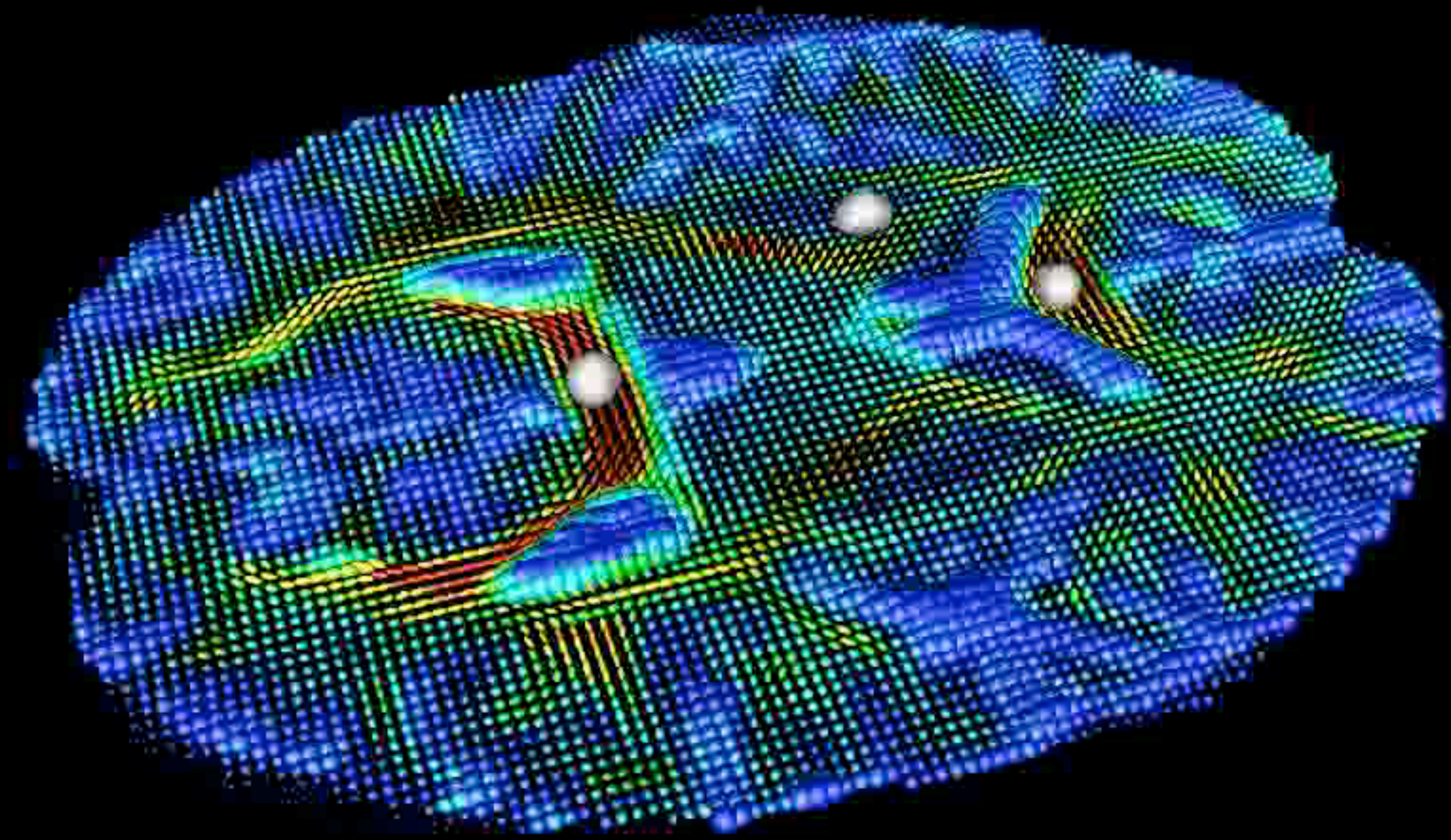

Data: Max Planck Institute, Leipzig, Germany

Human Brain DTI: *Corticospinal Tract*

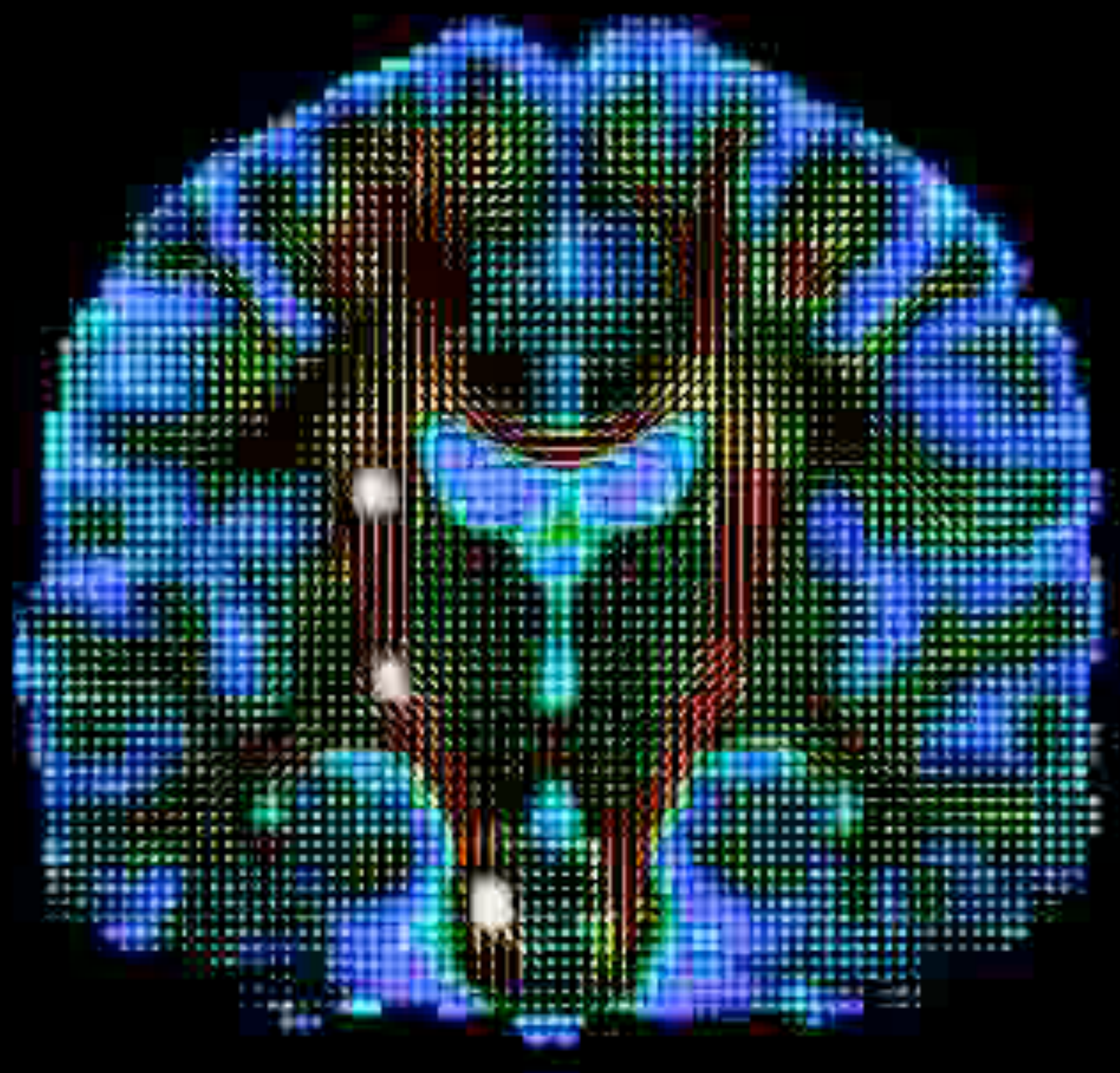

Data: Max Planck Institute, Leipzig, Germany

HARDI Mapping of White Matter Complexity

A manifold learning approach

(Joint work with G. Haro, G. Sapiro and P. Thompson)

Detecting Mixed Dimensionality and Density

Goal:

- Detect & estimate different dimensions and densities in the same noisy point cloud (stratifications)
- Cluster the points accordingly

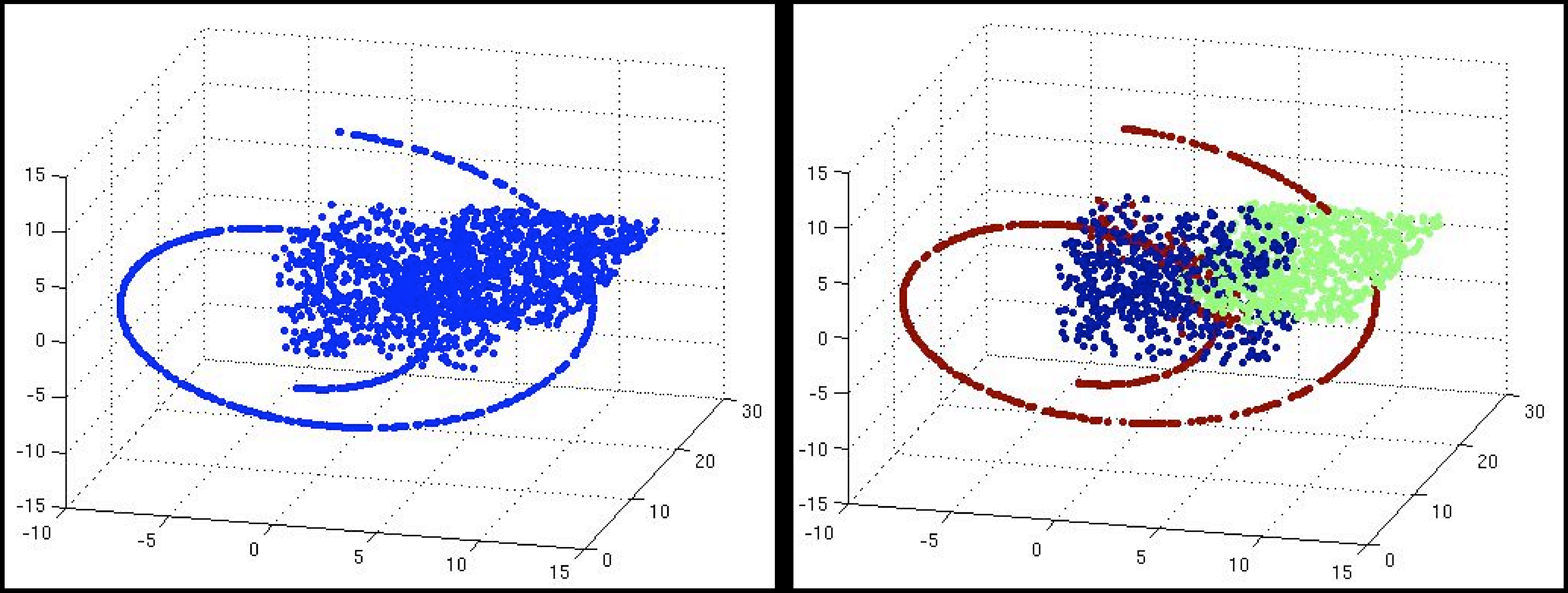

Haro, Randal & Sapiro's Approach

- Translated Poisson model to account for noise
- Local dimension and density estimator
- Translated Poisson mixture model to account for different sub-manifolds
- Clustering algorithm algorithm using EM based on mixture model

Numerical Experiments

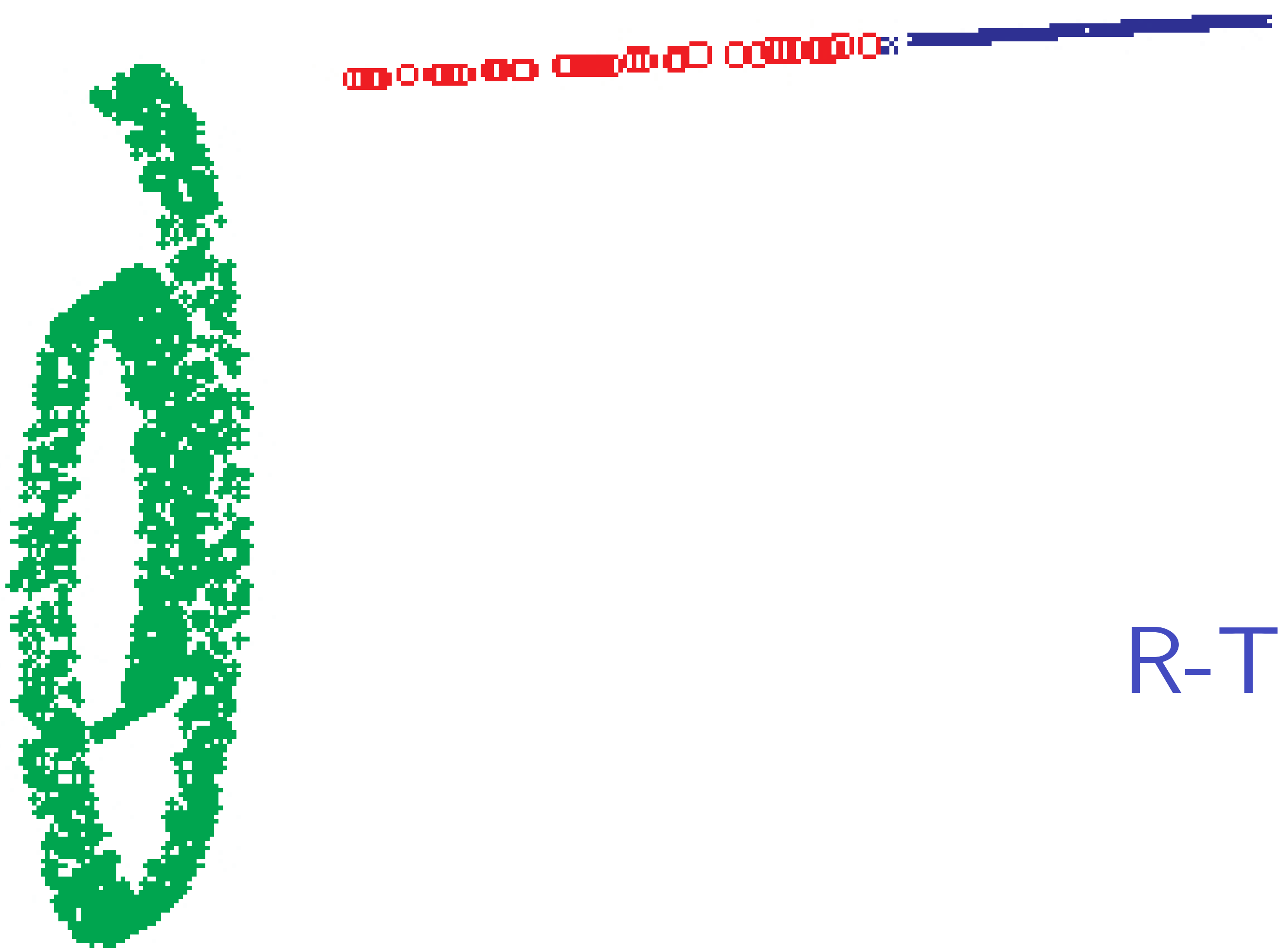

m: 1.98, 1.02, 0.99.
θ: 0.49, 0.53, 6.89.

R-TPMM ($k = 20$, $J = 3$, $\alpha = 2$).

Swiss roll and line with 2 different densities

Clustering from HARDI

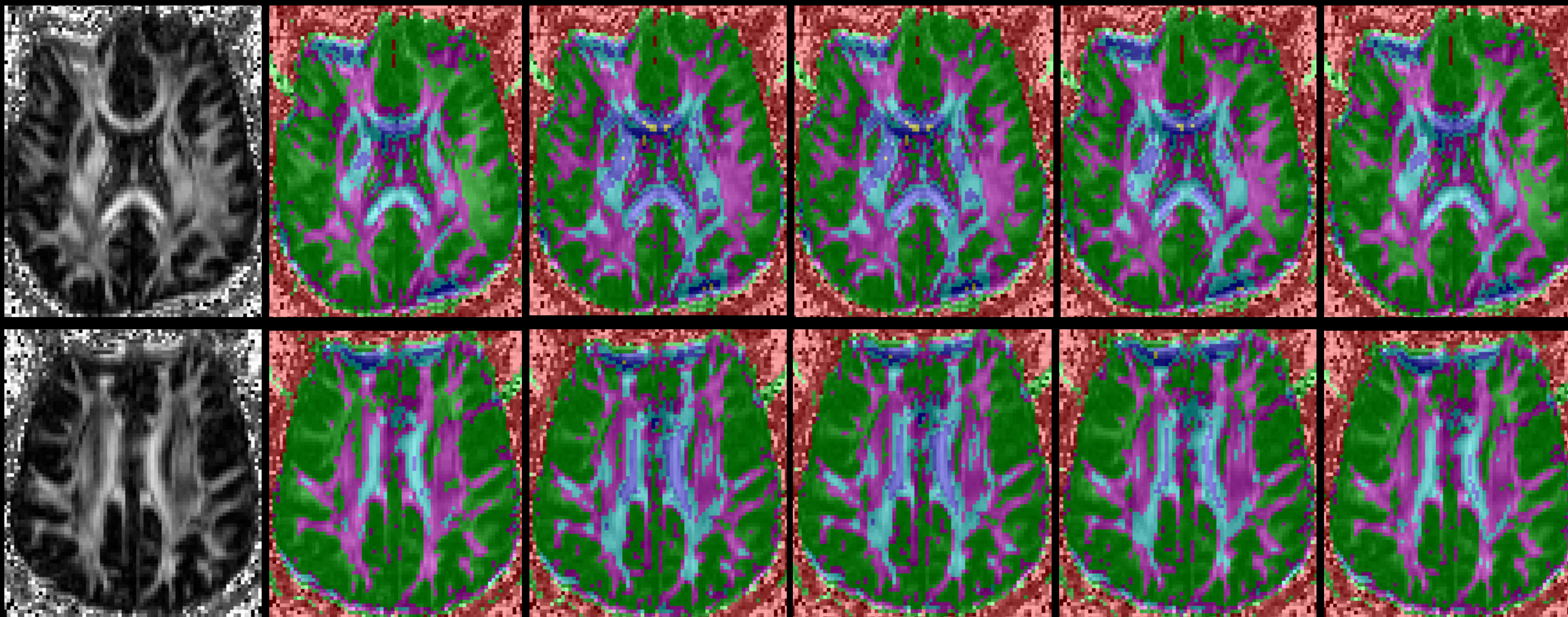

FA | Raw HARDI signal | 4^{th} order ODFs | 6^{th} order ODFs | 4^{th} order ODFs with sharpening | 6^{th} order ODFs with sharpening

Raw HARDI signal

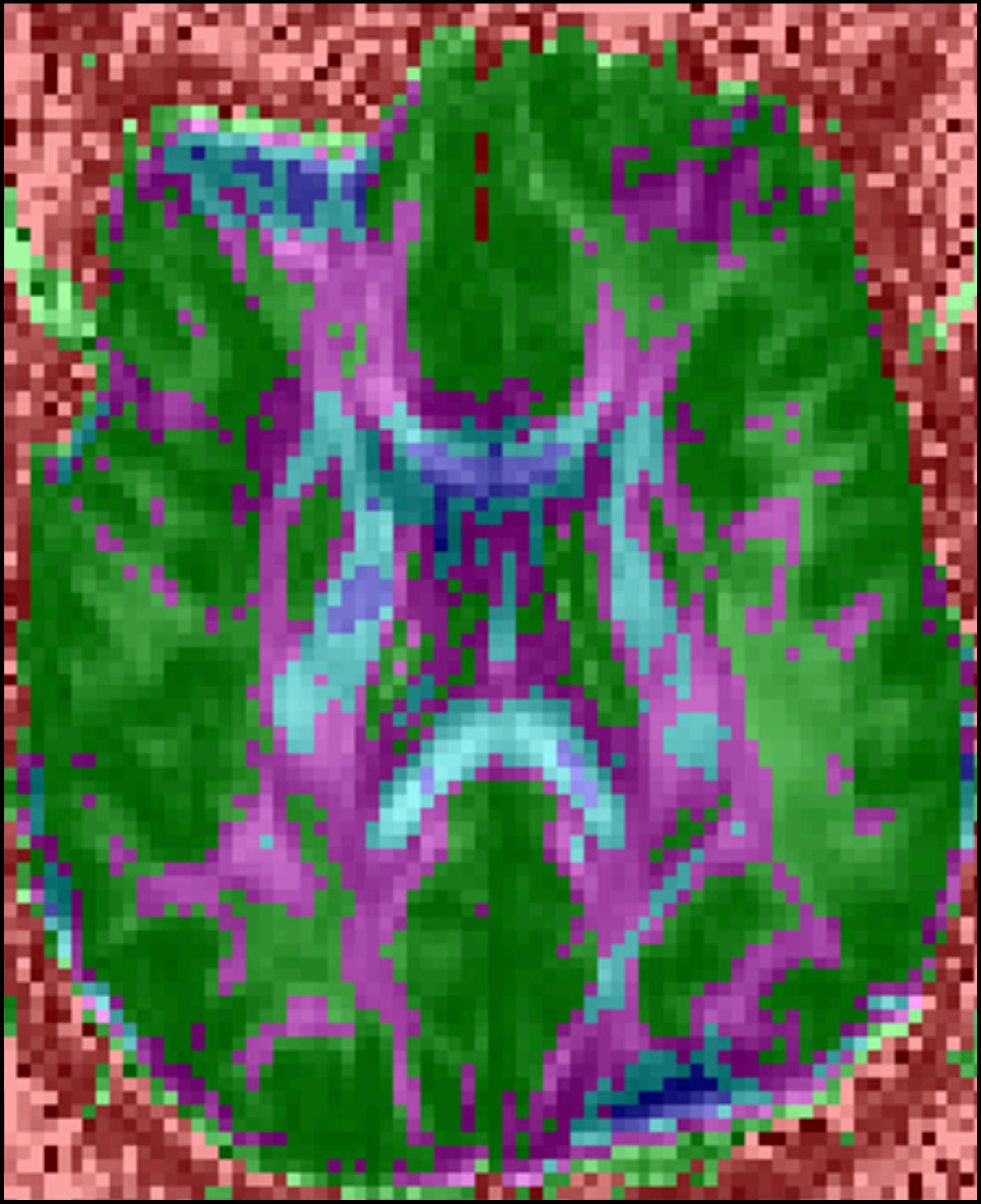

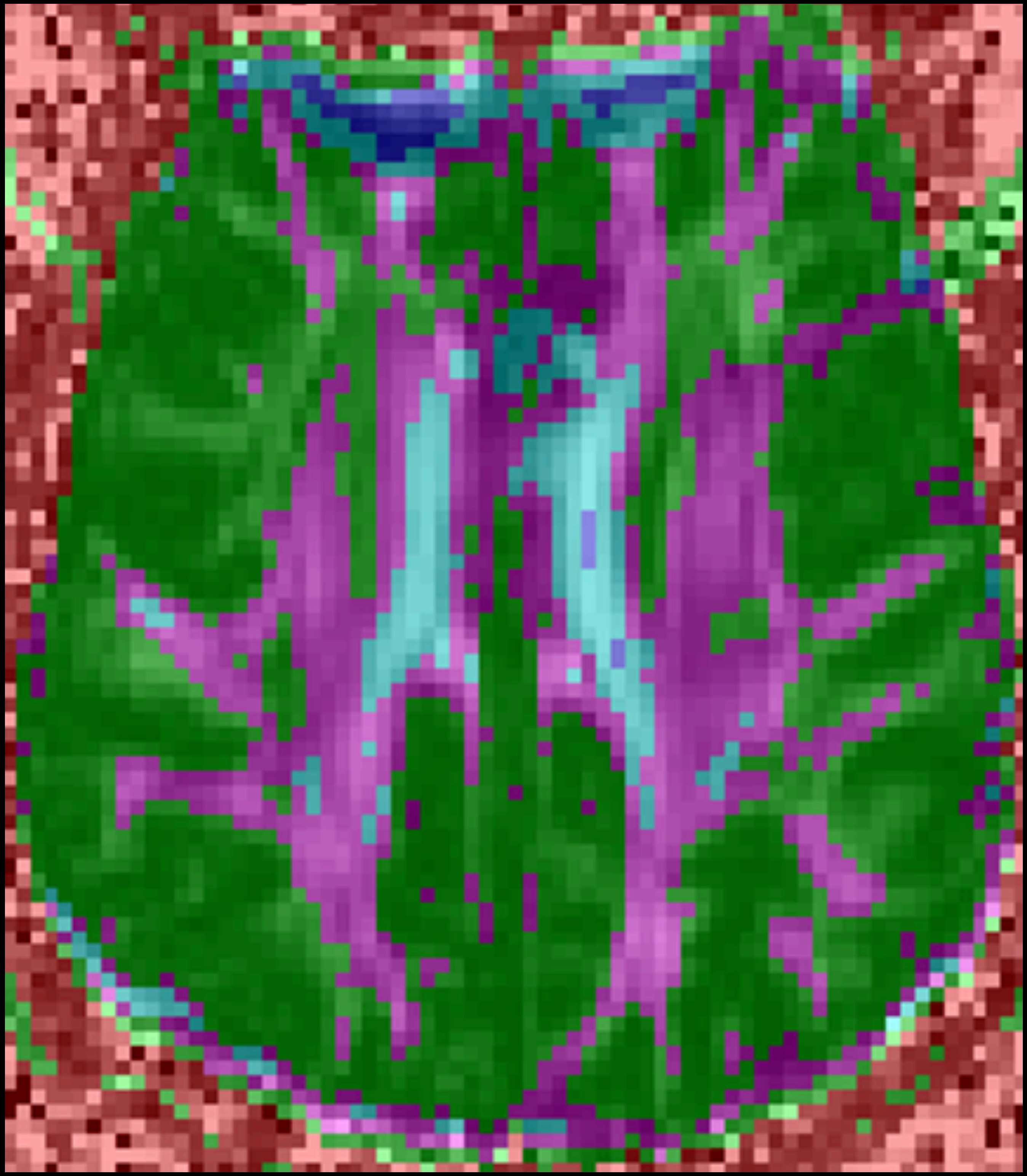

4^{th} order ODFs

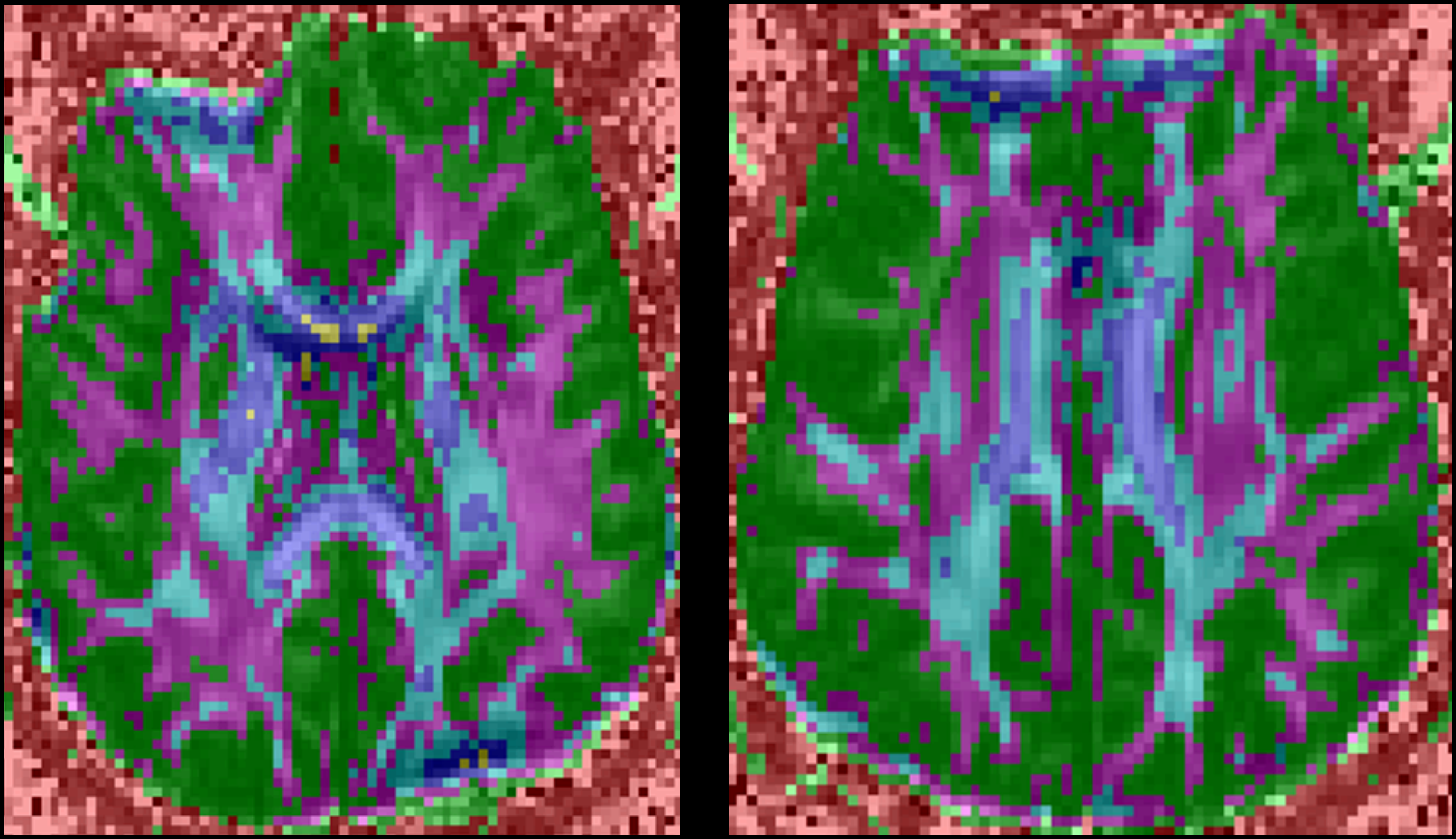

4th order ODFs with Sharpening

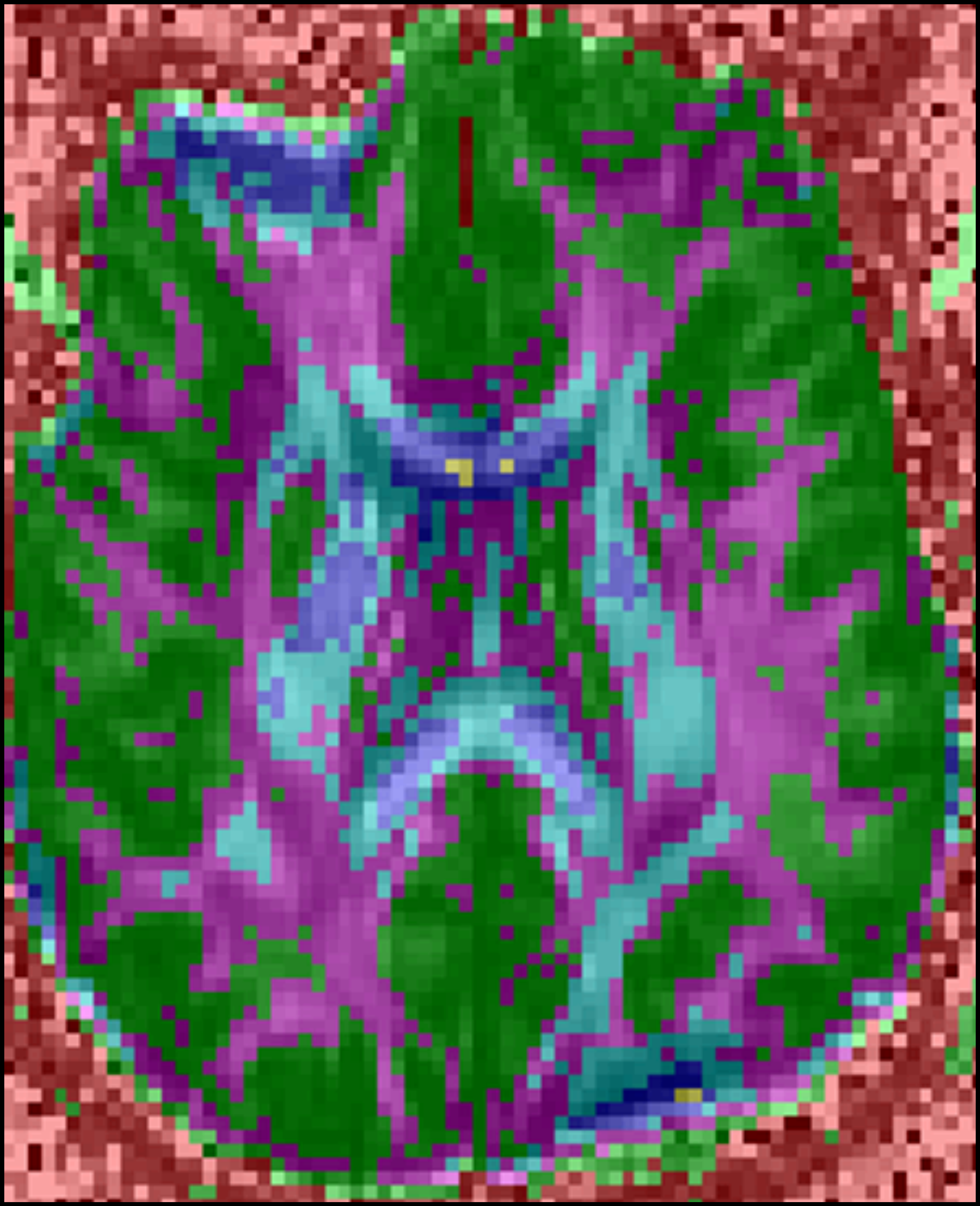

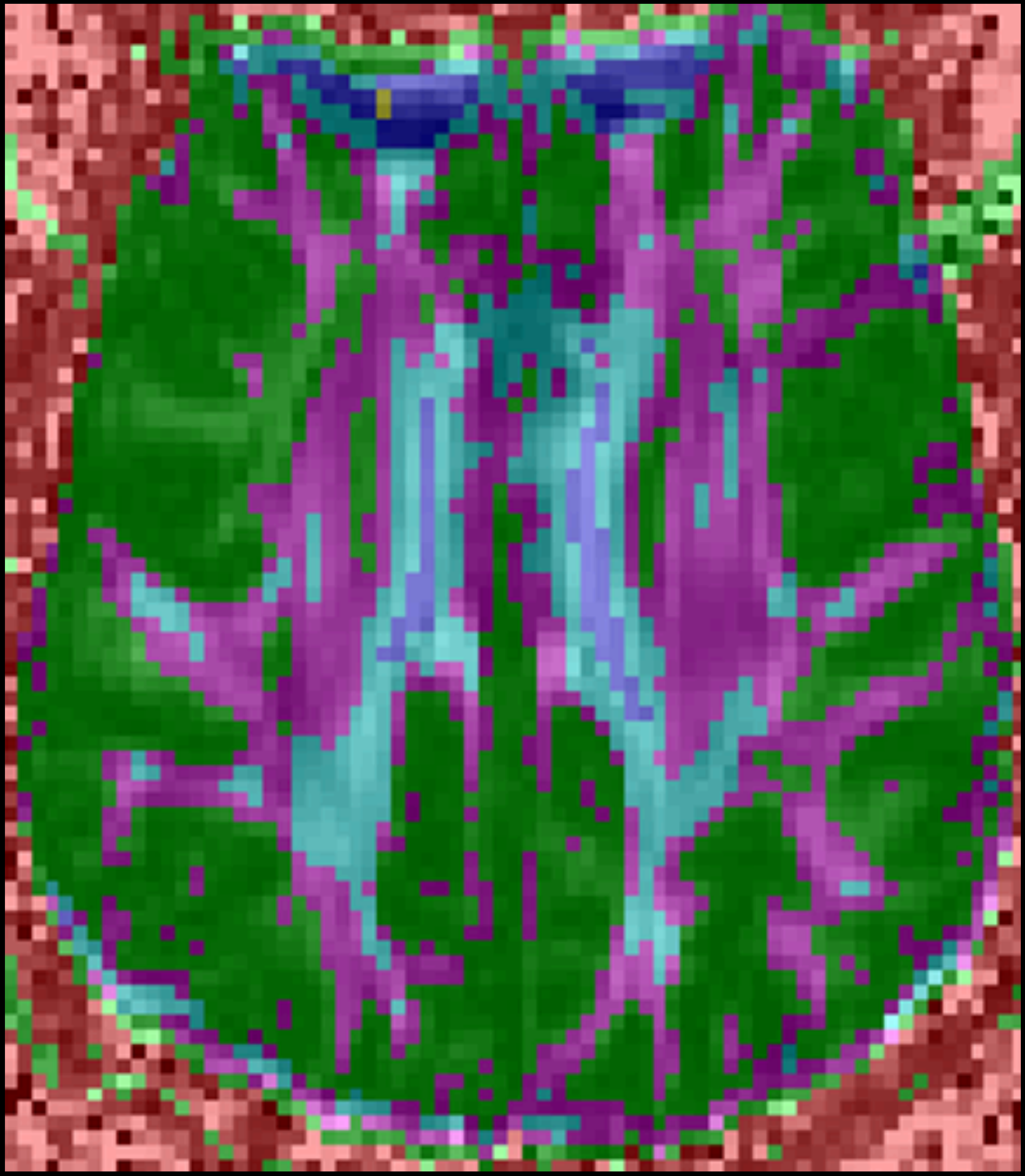

4^{th} order ODFs with Sharpening

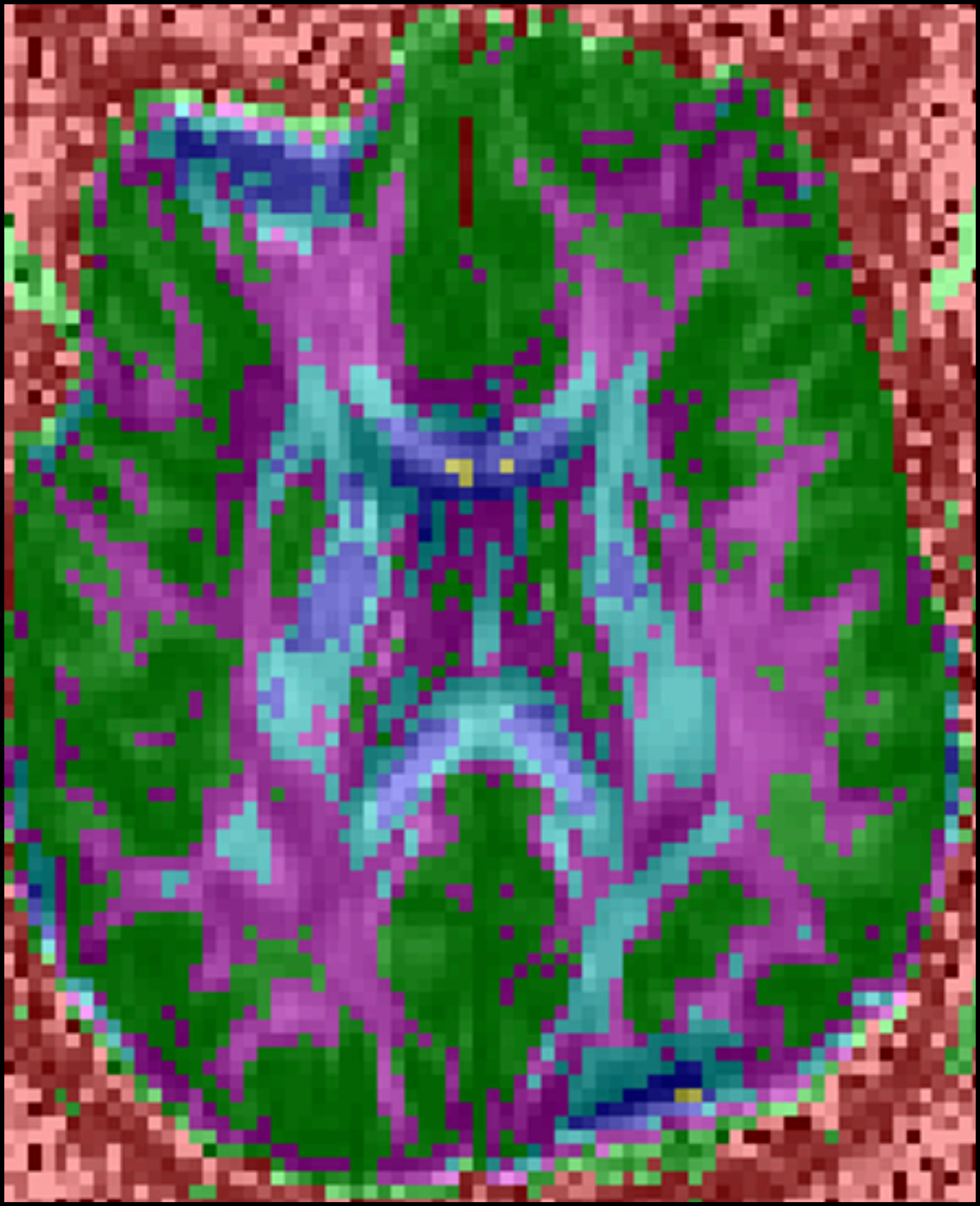

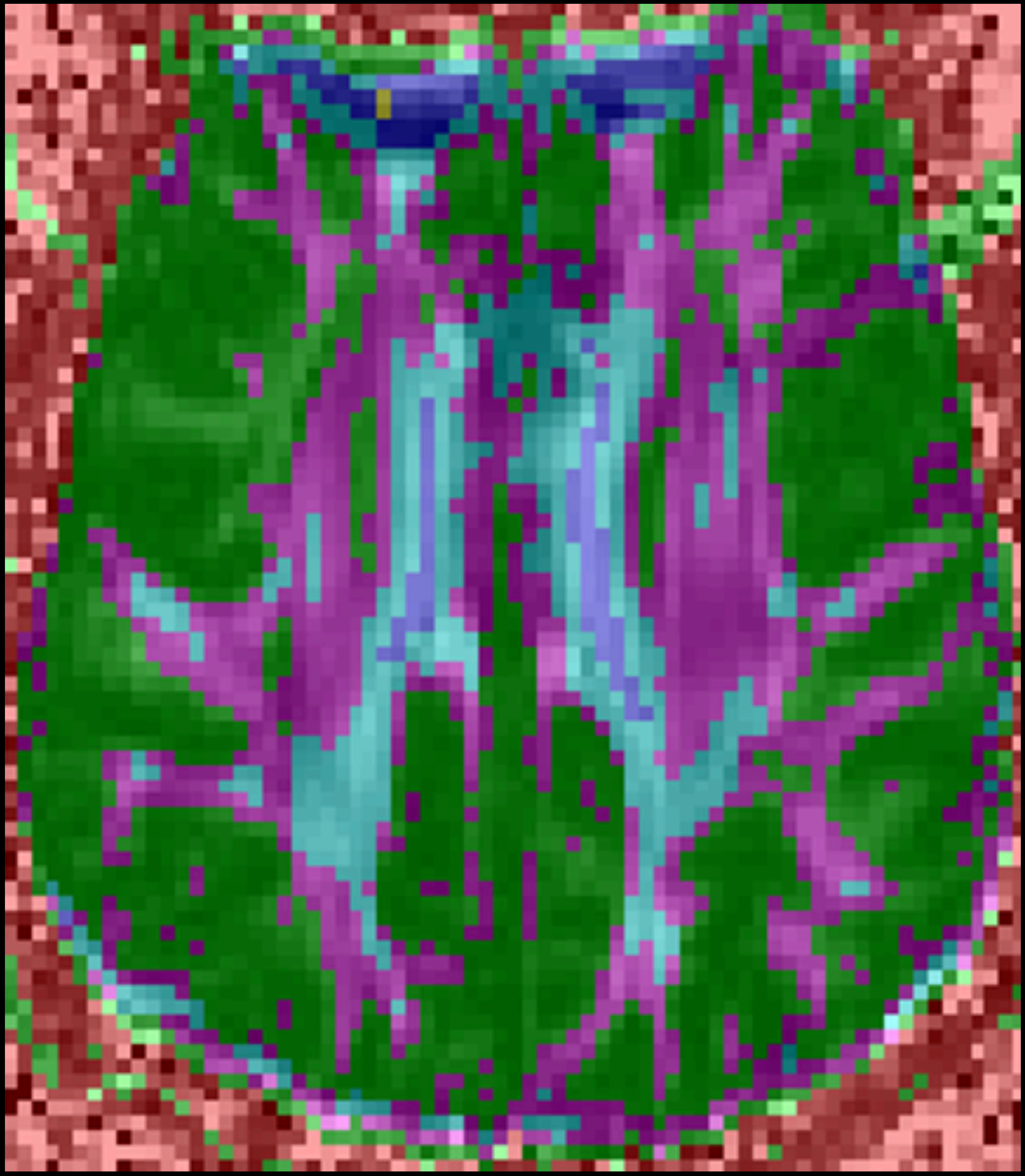

5.41 5.32 4.64 4.53 2.56 1.33

Complexity

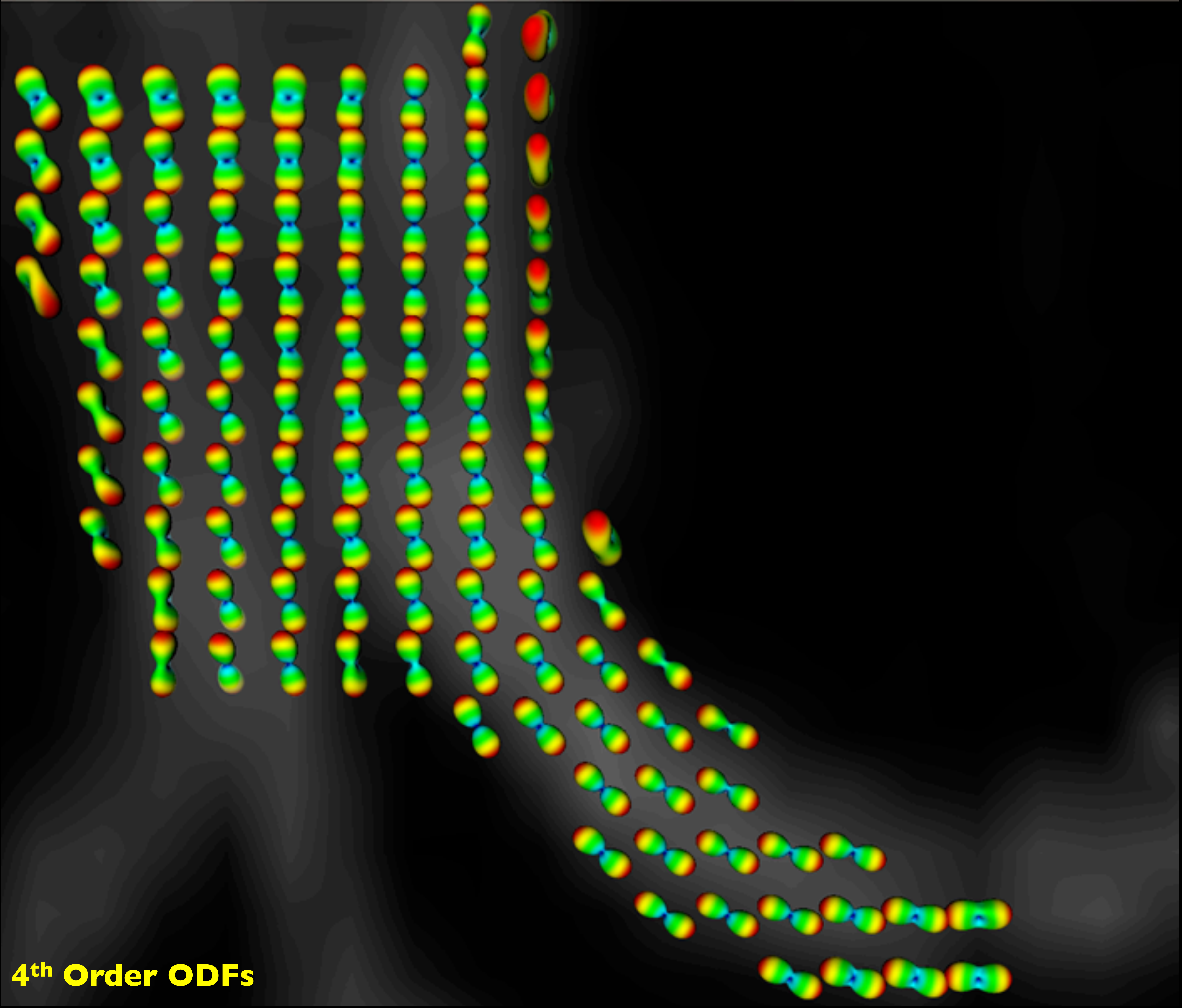
4th Order ODFs

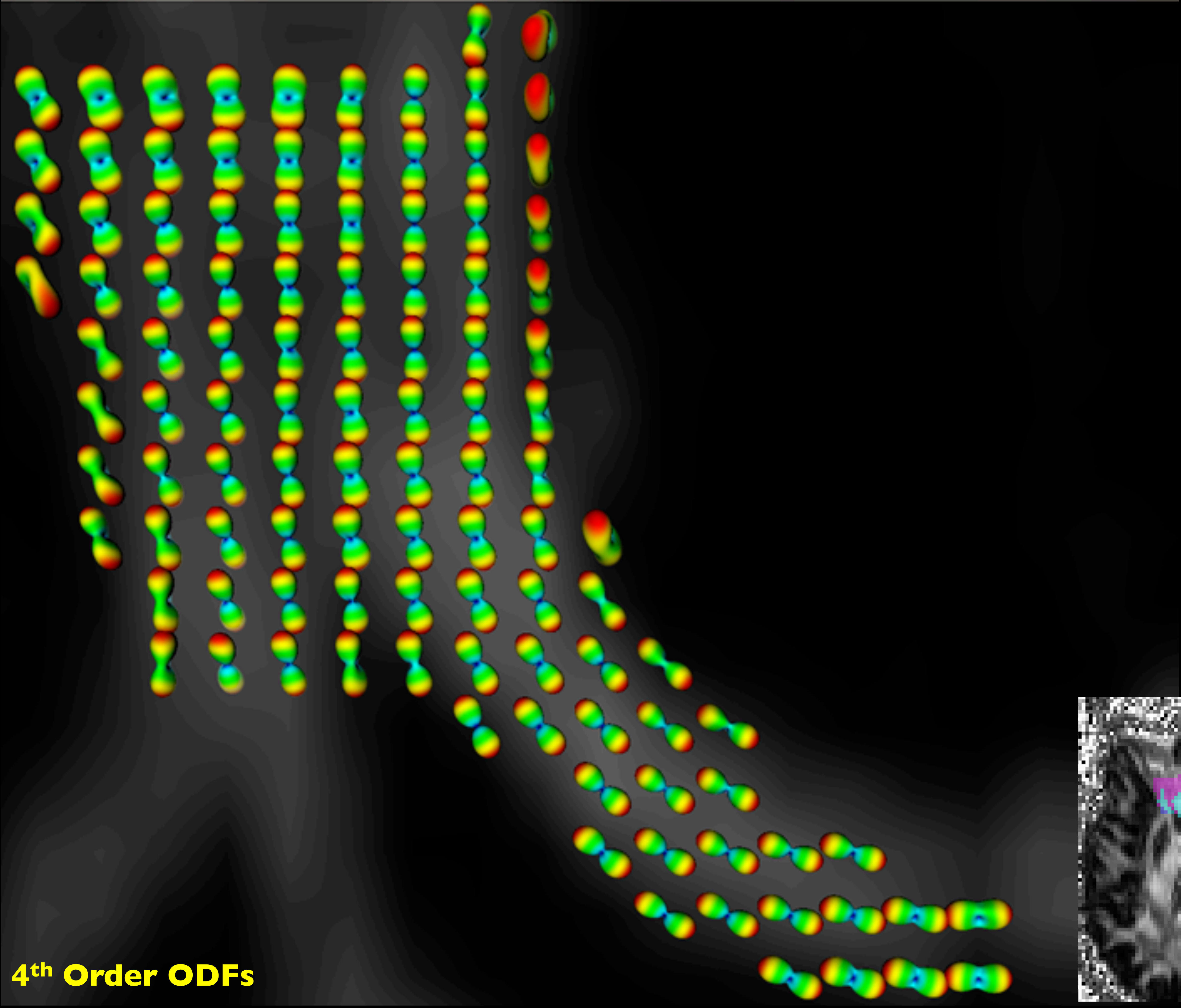

4^{th} Order ODFs

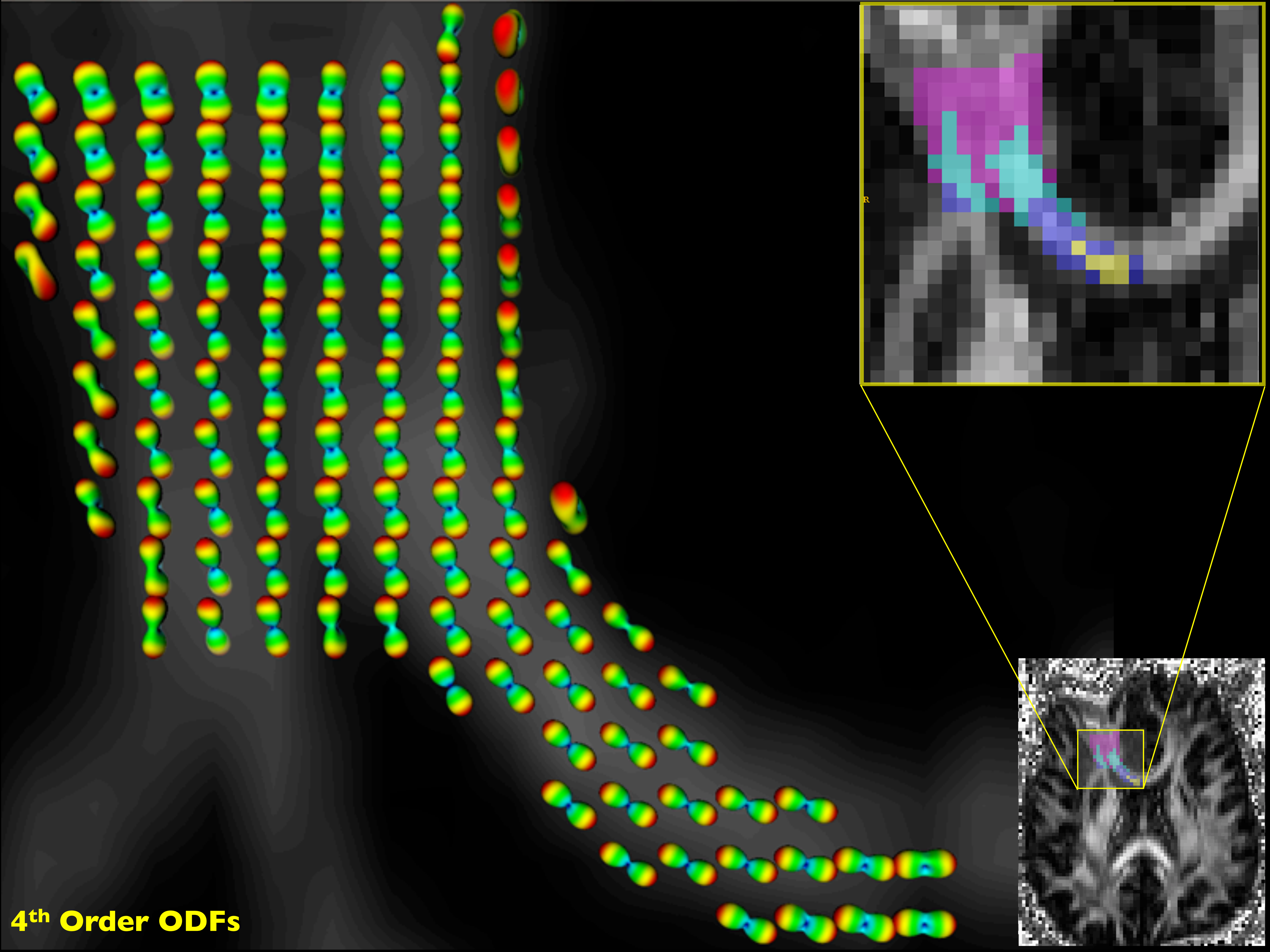
4th Order ODFs
R

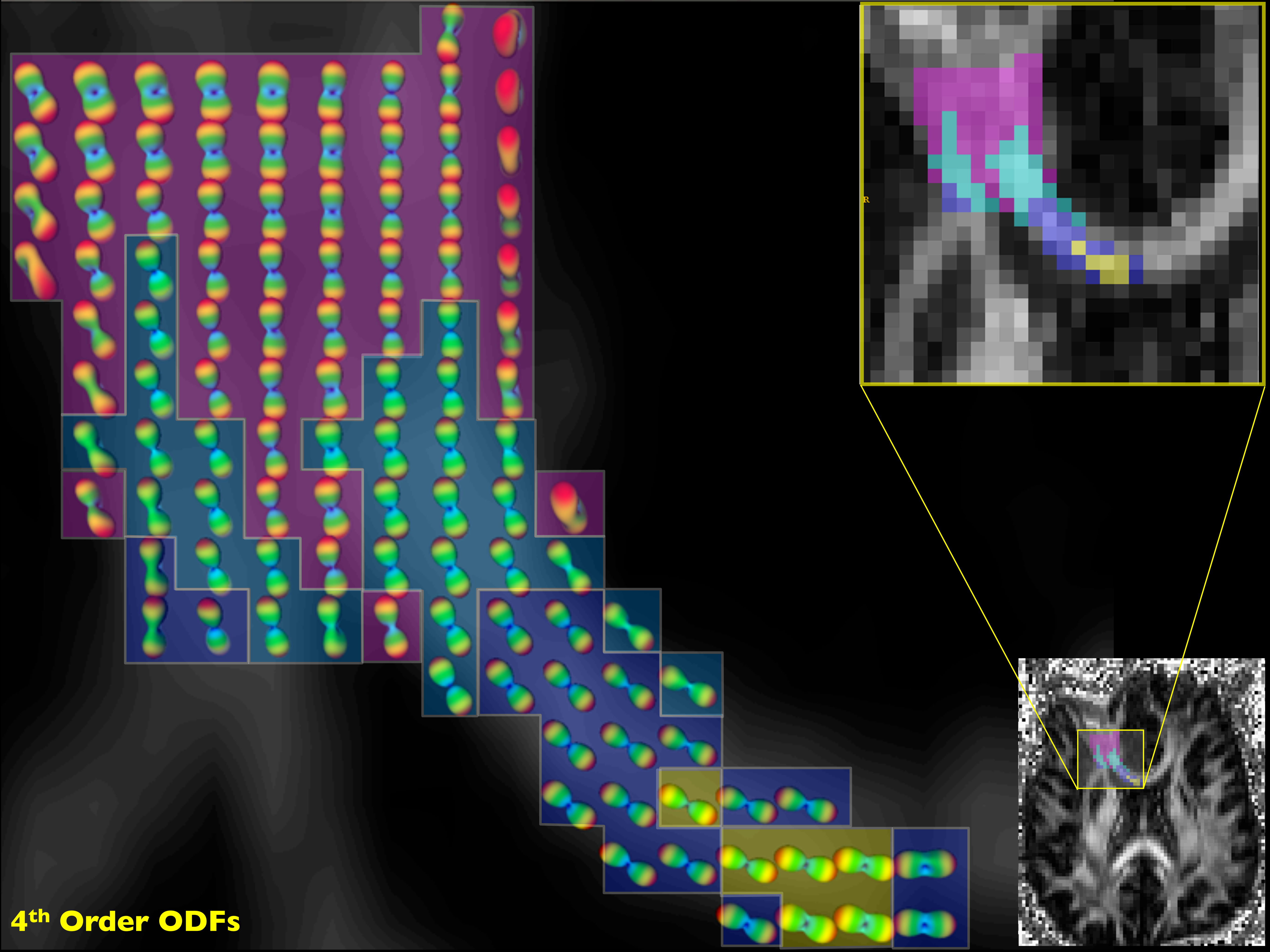
R
4th Order ODFs

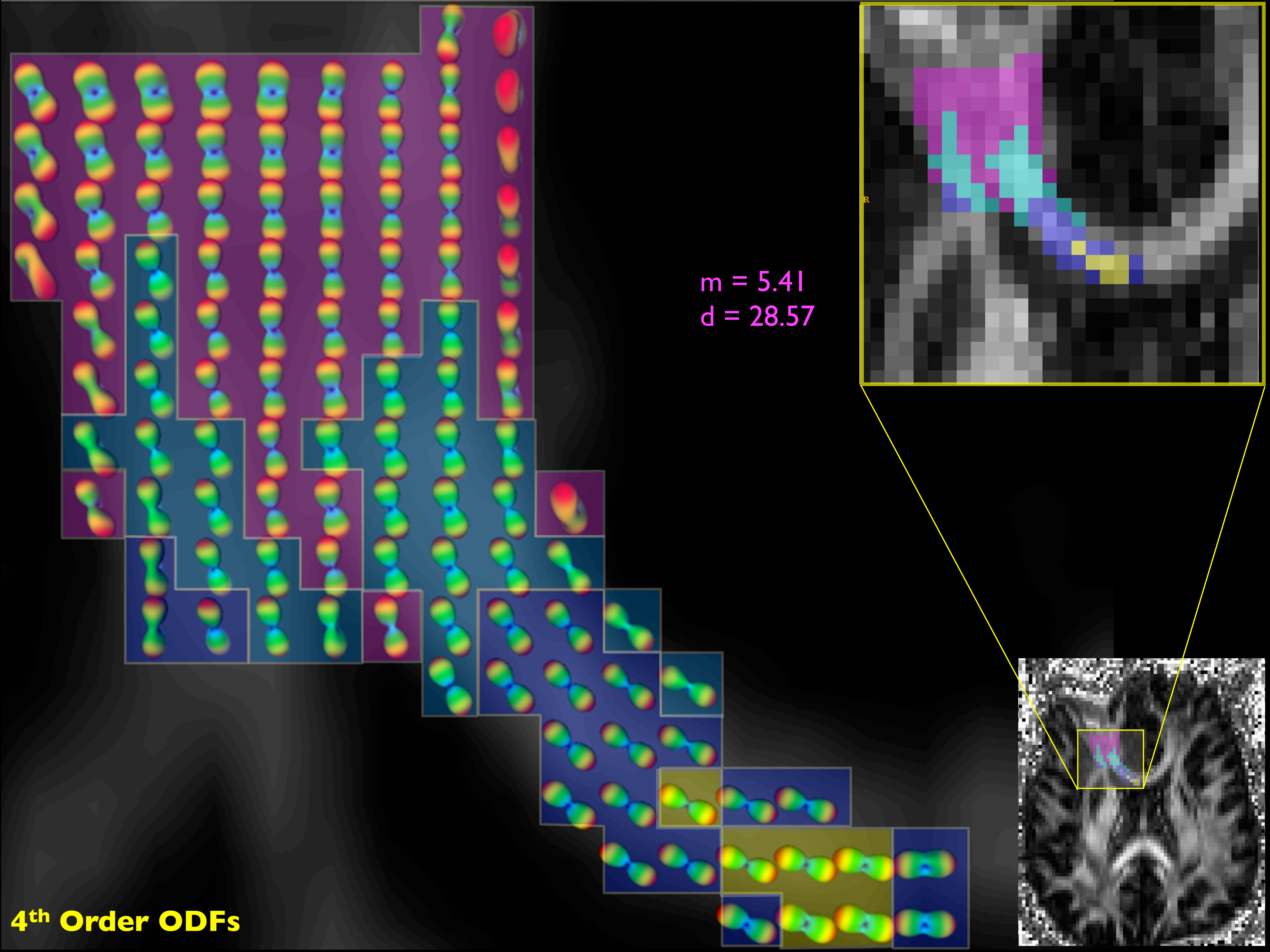
m = 5.41
d = 28.57
R
4th Order ODFs

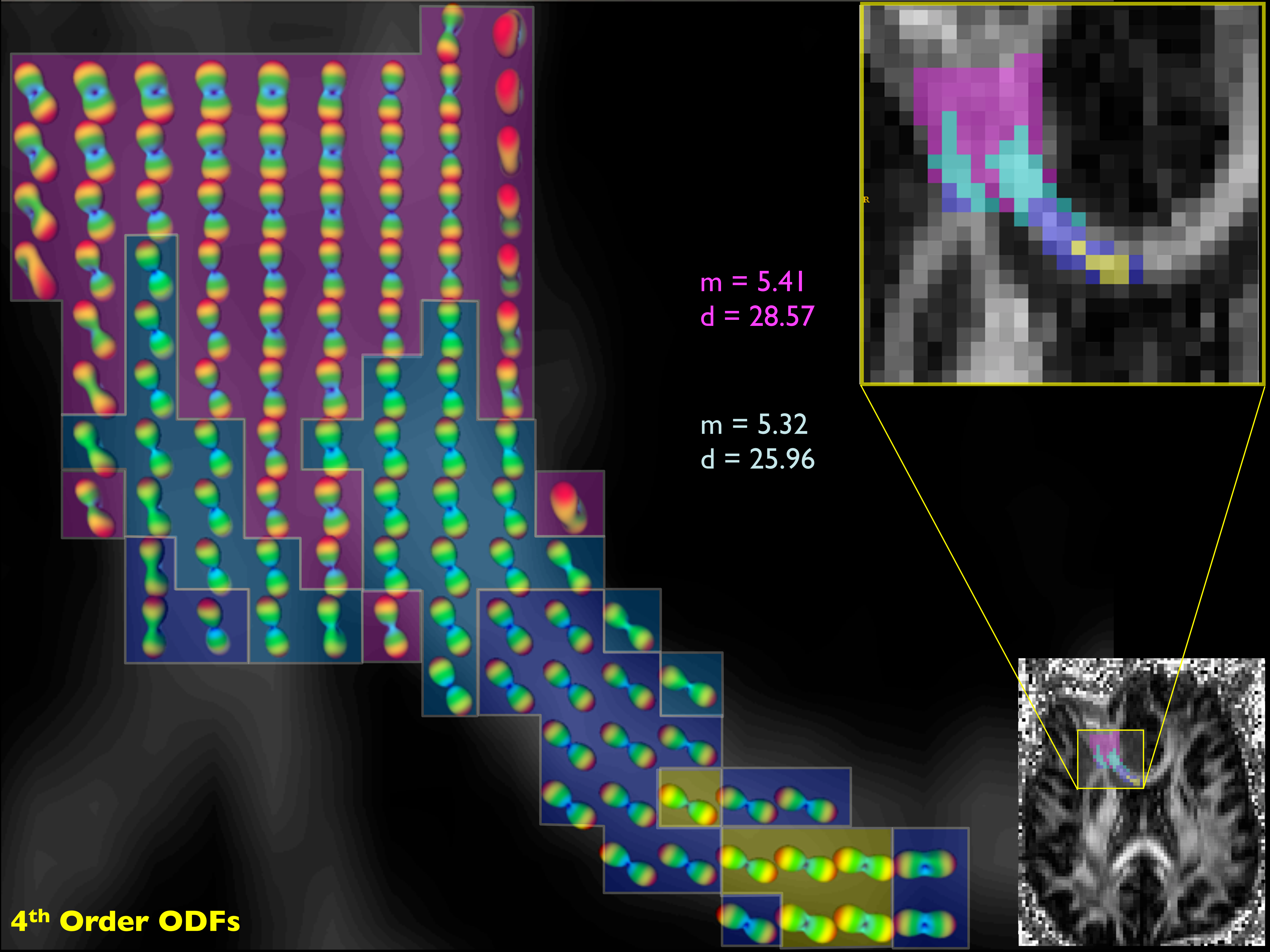
m = 5.41
d = 28.57
m = 5.32
d = 25.96
R
4th Order ODFs

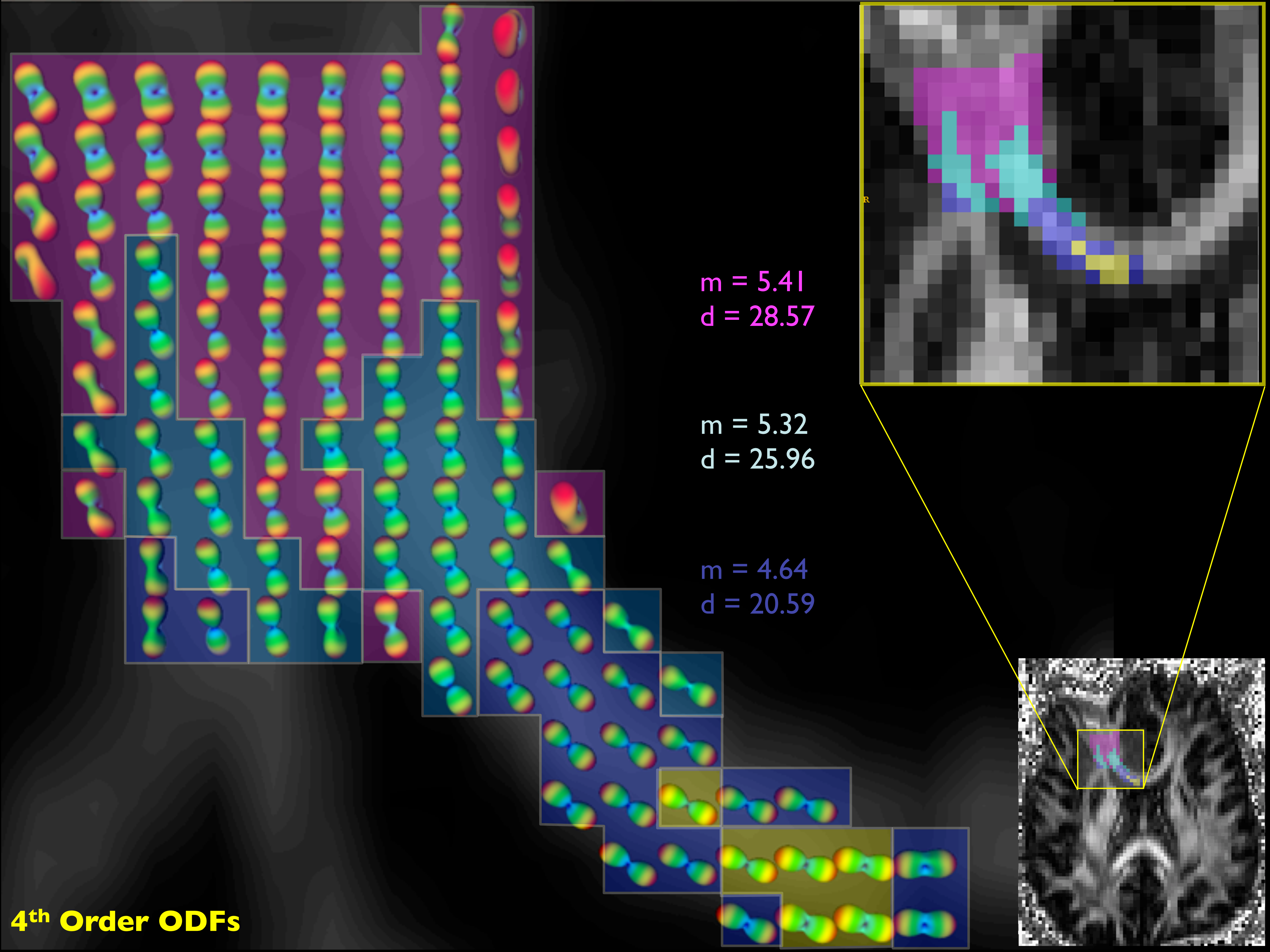
m = 5.41
d = 28.57
m = 5.32
d = 25.96
m = 4.64
d = 20.59
4th Order ODFs

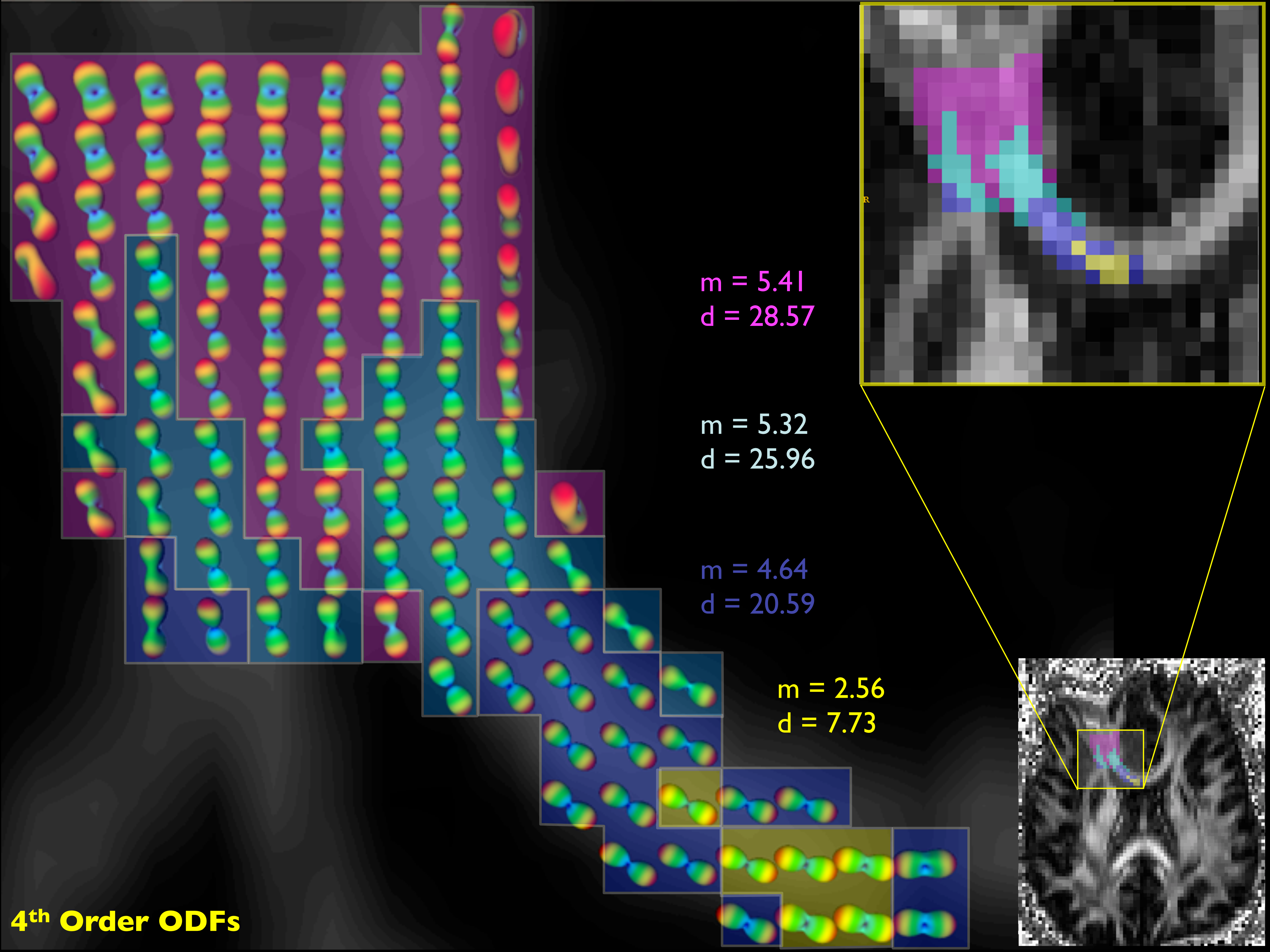
m = 5.41
d = 28.57
m = 5.32
d = 25.96
m = 4.64
d = 20.59
m = 2.56
d = 7.73
4th Order ODFs

Acknowledgments

G. Sapiro	ECE, University of Minnesota, Minneapolis
K. Ugurbil	CMRR, University of Minnesota, Minneapolis
G. Haro	Univ. Polytècnica de Catalunya, Barcelona
P. Thompson	LONI, UCLA, Los Angeles
M. Descoteaux	CEA/Neurospin, Paris
E. Prados	Perception Lab. INRIA Rhône-Alpes
N. Wotatwa	Odyssée Lab. INRIA, Sophia Antipolis
R. Deriche	Odyssée Lab. INRIA, Sophia Antipolis
O. Faugeras	Odyssée Lab. INRIA, Sophia Antipolis
S. Lehéricy	Hospital La Pitié-Salpêtrière, Paris
J. Campbell	BIC / CIM, McGill University, Montréal
K. Siddiqi	CIM, McGill University, Montréal
J.L. Anton	Centre IRMf, Hospital la Timone, Marseille
M. Roth	Centre IRMf, Hospital la Timone, Marseille
A. Anwander	Max Planck Institute - CBS, Leipzig

Questions?